



**Load Frequency Control for Multi-Area Interconnected
Power System Using Artificial Intelligent Controllers**

By

Mokhtar Shouran

**Thesis submitted in fulfilment of the requirement for the degree of
Doctor of Philosophy**

Wolfson Centre for Magnetics
School of Engineering
Cardiff University

October. 2022

ABSTRACT

Power system control and stability have been an area with different and continuous challenges in order to reach the desired operation that satisfies consumers and suppliers. To accomplish the purpose of stable operation in power systems, different loops have been equipped to control different parameters. For example, Load Frequency Control (LFC) is introduced to maintain the frequency at or near its nominal values, this loop is also responsible for maintaining the interchanged power between control areas interconnected via tie-lines at scheduled values. Other loops are also employed within power systems such as the Automatic Voltage Regulator (AVR). This thesis focuses on the problem of frequency deviation in power systems and proposes different solutions based on different theories. The proposed methods are implemented in two different power systems namely: unequal two-area interconnected thermal power system and the simplified Great Britain (GB) power system.

Artificial intelligence-based controllers have recently dominated the field of control engineering as they are practicable with relatively low solution costs, this is in addition to providing a stable, reliable and robust dynamic performance of the controlled plant. They professionally can handle different technical issues resulting from nonlinearities and uncertainties. In order to achieve the best possible control and dynamic system behaviour, a soft computing technique based on the Bees Algorithm (BA) is suggested for tuning the parameters of the proposed controllers for LFC purposes.

Fuzzy PID controller with filtered derivative action (Fuzzy PIDF) optimized by the BA is designed and implemented to improve the frequency performance in the two different systems under study during and after load disturbance. Further, three different fuzzy control configurations that offer higher reliability, namely Fuzzy Cascade PI – PD, Fuzzy PI plus Fuzzy PD, and Fuzzy (PI + PD), optimized by the BA have also been implemented in the two-area interconnected power system. The robustness of these fuzzy configurations has been evidenced against parametric uncertainties of the controlled power systems

Sliding Mode Control (SMC) design, modelling and implementation have also been conducted for LFC in the investigated systems where the parameters are tuned by the BA. The mathematical model design of the SMC is derived based on the parameters of the testbed systems. The robustness analysis of the proposed SMC against the controlled systems' parametric uncertainties has been carried out considering different scenarios.

Furthermore, to authenticate the excellence of the proposed controllers, a comparative study is carried out based on the obtained results and those from previously introduced works based on classical PID tuned by the Losi Map-Based Chaotic Optimization Algorithm (LCOA), Fuzzy PID Optimized by Teaching Learning-Based Optimization (TLBO).

DEDICATION

To the soul of my Father, may Allah Almighty have mercy upon him

To my blessed Mother

The priceless woman who is lighting my life

To my beloved Wife and Children

The beauty, happiness, and shiny part of my life

To my Brothers, Sisters, and family

The great and blessed persons who accompanying my success

To my beloved Country ... 'Libya'

To all others who love me

ACKNOWLEDGEMENTS

I am deeply thankful to God for the amazing graces, without his blessing and help this endeavour would not have been possible.

I would like to express my immense gratitude to my supervisors, Dr Fatih Anayi and Dr Michael Packianather, for providing me with the opportunity to carry out this highly interesting and relevant research, as well as for their continued supervision and support. Their vision and understanding of the key research challenges in this area have been invaluable for guiding my work.

I am eternally grateful for the financial support from the Ministry of Higher Education and Scientific Research in Libya throughout all my years of PhD study.

My thanks also go out to all my colleagues in the Wolfson Centre for Magnetics for their support, encouragement and fruitful discussions during meetings and seminars.

TABLE OF CONTENTS

ABSTRACT	ii
DEDICATION	iv
ACKNOWLEDGEMENTS	v
TABLE OF CONTENTS	vi
TABLE OF FIGURES	ix
TABLE OF TABLES	xiv
LIST OF ABBREVIATIONS	xvi
Chapter 1	1
Introduction	1
1.1 Control of frequency in the Great Britain power system	1
1.2 Control of frequency in multi-area power systems	2
1.3 Research motivation	4
1.4 Problem statement	4
1.5 Thesis structure	5
1.6 Research aim, objectives and Contributions	6
1.7 Publications	7
1.7 References:	8
Chapter 2	10
Literature Review	10
2.1 Abstract	10
2.2 Introduction	10
2.3 Frequency response modelling	11
2.3.1 Frequency control in the GB power system	14
2.3.2 Frequency control in an interconnected power system	15
2.4 LFC-based different Power System Models	18
2.4.1 Conventional (Traditional) Power Systems	18
2.4.2 Modern Power Systems	19
2.5 Control Strategies	23
2.5.1 Centralized Control Approach	23
2.5.2 Decentralized Control Approach	23
2.6 Classifications of LFC According to Various Control Techniques	24
2.6.1 Classical Control Methods	24
2.6.2 Optimal and Suboptimal Control	25
2.6.3 Adaptive Control	26

2.6.4 Robust Control	26
2.6.5 Sliding Mode Control (SMC).....	27
2.6.6 Artificial Intelligence Techniques	27
2.6.7 Other Control Approaches for LFC	30
2.7 Summary	31
2.8 References	32
Chapter 3	48
The Bees Algorithm: Mechanism and applications	48
3.1 Abstract	48
3.2 Introduction	48
3.3 Background.....	50
3.4 The Mechanism of the Bees Algorithm	52
3.5 The Applications of The Bees Algorithm	55
3.5.1 Bees Algorithm in Control Engineering	55
3.5.2 Applications of the Bees Algorithm to Intelligent Production and Manufacturing	55
3.5.3 Optimisation of classifiers / clustering systems.....	56
3.6 Summary	57
3.7 References	57
Chapter 4	63
LFC based Fuzzy Logic Control.....	63
4.1 Abstract	63
4.2 Introduction	63
4.3 LFC based Fuzzy Logic control for the simplified Great Britain power system. 64	
4.3.1 The simplified Great Britain power system	66
4.3.2 Control Strategies and Objective Functions	67
4.3.3 Results and Discussion	71
4.3.4 Robustness Analysis	79
4.4 LFC Based Different Fuzzy Logic control Structures for Two-area Interconnected Power System.....	84
4.4.1 Two-area Power System-model Understudy.....	85
4.4.3 Results and Discussions.....	88
4.4.5 Different Configurations of Fuzzy Control Tuned by BA	96
4.6 Summary	120
4.7 References	121

Chapter 5	124
LFC based Sliding Mode Control.....	124
5.1 Abstract.....	124
5.2 Introduction.....	124
5.3 Sliding Mode Control Optimised by the Bees Algorithm for LFC in the Great Britain Power System.....	125
5.3.1 Simplified GB Power System Model.....	125
5.3.2 SMC Design based GB power system parameters	126
5.3.3 Implementation, Results and Discussion.....	128
5.4 The Bees Algorithm Tuned Sliding Mode Control for Load Frequency Control in Two-Area Power System	135
5.4.1 The Investigated Two-area Interconnected Power System	136
5.4.2 Design and Implementation of the Proposed SMC System	137
5.4.3 Results and Discussion	140
5.5 Summary.....	161
5.6 References:.....	161
Chapter 6	165
Conclusions and Recommendations for Future Work.....	165
6.1. Conclusions.....	165
6.2. Recommendations for Future Work	167
Appendixes.....	169
Appendix A	169
Appendix B	169
Appendix C	172

TABLE OF FIGURES

Figure 1.1 Frequency fluctuations following the loss of generation up to 1800MW [3].	2
Figure 2.1. Frequency control loops in a power system	11
Figure 2.2. Schematic block diagram of a synchronous generator with basic frequency control loops [3].	12
Figure 2.3. Block diagram representation of generator-load model [3].	13
Figure 2.4. reduced block diagram of figure 2.2 [3].	13
Figure 2.5. GB power system primary frequency control model [10] [11].	14
Figure 2. 6. Steady-state frequency-power relationship of a turbine-governor control [8].	15
Figure 2.7. A schematic diagram of an N-area interconnected power system [3].	16
Figure 2.8. A simplified interconnected power system with LFC controller [3].	17
Figure 3.1. The pseudo-code of the basic Bees Algorithm.	52
Figure 3.2 The flow chart of the basic Bees Algorithm.	53
Figure 3.3 (a) The initially selected n patches and their evaluated fitness values; (b) Selection of elite and non-elite best patches; (c) Recruitment of forager bees to the elite and non-elite best locations; (d) Results from basic Bees-inspired Algorithm (BA) after local and global search.	54
Figure. 4.1. Typical structure of fuzzy logic controller.	64
Figure 4.2. GB simplified power system	67
Figure 4.3. Structural diagram of fuzzy PIDF controller.	69
Figure 4.4. Membership functions of the two inputs and output.	69
Figure 4.5. Change in frequency in the GB power system for 0.035 pu load disturbance with tuned PID-based ISE.	73
On the other hand, when ITAE is used as an objective function to design the PID controller a slight further drop in the frequency with a very small overshoot and a quicker response is observed. As demonstrated in Figure 4.6 and Table 4.7, the drop in the frequency was -0.1840 Hz, -0.1859 Hz and -0.1870 Hz based on PID optimized by BA, PSO and TLBO, respectively. Furthermore, the transient response of the system has been slightly improved with a better settling time and less overshoot observed.	74
Figure 4.6. Change in frequency in the GB power system for 0.035 pu load disturbance with tuned PID-based ITAE.	74
Figure 4.7. Change in frequency in the GB power system for 0.035 pu load disturbance with tuned FOPID-based ISE.	75
As shown in Figure 4.7 and Table 4.8, FOPID designed by minimizing ISE is found to be less effective in eliminating the steady-state error which made this technique less preferable option for this system. Furthermore, the performance of this controller as tuned by different optimization techniques is similar.	75

Figure 4.8. Change in frequency in the GB power system for 0.035 pu load disturbance with tuned FOPID-based ITAE.....	76
Figure 4.9. Change in frequency in the GB power system for 0.035 pu load disturbance with tuned Fuzzy PIDF-based ISE.....	77
Figure 4.10. Change in frequency in the GB power system for 0.035 pu load disturbance with tuned Fuzzy PIDF-based ITAE.....	78
Figure 4.11. Comparison of the dynamic response of GB power model with parameter uncertainties of scenarios 1 and 2 with no secondary control loop.	79
Figure 4.12. Comparison of three controllers tuned by BA based on ISE for scenario 2.....	81
Figure 4.13. Comparison of three controllers tuned by BA based on ITAE for scenario 2. ...	82
Figure 4.14. Comparison of three controllers tuned by BA based on ITAE for LFC of the GB system in the nominal scenario with 0.053 pu load disturbance.....	83
Figure 4.15. Comparison of three controllers tuned by BA based on ITAE for LFC of the GB system in scenario 2 with 0.053 pu load disturbance.....	84
Figure 4.16. Transfer function model of the testbed system.....	86
Figure 4.17. Frequency variation in area one ($\Delta F1$ in Hz).	89
Figure 4.18. Frequency variation in area two ($\Delta F2$ in Hz).	90
Figure 4.19. Tie line power variation (ΔP_{tie} in pu).	90
Figure 4.20. Percentage of improvement with different techniques.	92
Figure 4.21. Frequency deviation in area one ($\Delta F1$ in Hz) under parametric uncertainties of the testbed system.	93
Figure 4.22. Frequency deviation in area two ($\Delta F2$ in Hz) under parametric uncertainties of the testbed system.	93
Figure 4.23. Tie line power deviation (ΔP_{tie} in pu) under parametric uncertainties of the testbed system.	94
Figure 4.24. Random load profile.	94
Figure 4.25. Frequency deviation in area one. (A) based on BA tuning; (B) based on TLBO and PSO tuning.	95
Figure 4.26. Frequency deviation in area two. (A) based on BA tuning; (B) based on TLBO and PSO tuning.	95
Figure 4.27. Tie line power deviation (ΔP_{tie} in pu). (A) based on BA tuning; (B) based on TLBO and PSO tuning.....	96
Figure 4.28. Block diagram of Fuzzy Cascade PI-PD controller configuration equipped in area one.	97
Figure 4.29. Block diagram of Fuzzy PI plus Fuzzy PD controller configuration equipped in area one.	97
Figure 4.30. Block diagram of Fuzzy (PI + PD) controller configuration equipped in area one.	98
Figure 4.31. Frequency deviation in area one ($\Delta F1$ in Hz).....	100

Figure 4.32. Frequency deviation in area two (ΔF_2 in Hz).	100
Figure 4.33. Tie line power deviation (ΔP_{tie} in pu).	101
Figure 4.34. Dynamic response of the testbed power system based on different fuzzy controllers under parametric uncertainty condition, case 1. (A) Frequency variation in area 1; (B) Frequency variation in area 2; (C) Tie line power variation.	104
Figure 4.35. Dynamic response of the testbed power system based on different fuzzy controllers under parametric uncertainty condition, case 2. (A) Frequency variation in area 1; (B) Frequency variation in area 2; (C) Tie line power variation.	105
Figure 4.36. Dynamic response of the testbed power system based on different fuzzy controllers under parametric uncertainty condition, case 3. (A) Frequency variation in area 1; (B) Frequency variation in area 2; (C) Tie line power variation.	106
Figure 4.37. Dynamic response of the testbed power system based on different fuzzy controllers under parametric uncertainty condition, case 4. (A) Frequency variation in area 1; (B) Frequency variation in area 2; (C) Tie line power variation.	107
Figure 4.38. Dynamic response of the testbed power system based on different fuzzy controllers under parametric uncertainty condition, case 5. (A) Frequency variation in area 1; (B) Frequency variation in area 2; (C) Tie line power variation.	108
Figure 4.39. Dynamic response of the testbed power system based on different fuzzy controllers under parametric uncertainty condition, case 6. (A) Frequency variation in area 1; (B) Frequency variation in area 2; (C) Tie line power variation.	109
Figure 4.40. Dynamic response of the testbed power system based on different fuzzy controllers under parametric uncertainty condition, case 7. (A) Frequency variation in area 1; (B) Frequency variation in area 2; (C) Tie line power variation.	110
Figure 4.41. Dynamic response of the testbed power system based on different fuzzy controllers under parametric uncertainty condition, case 8. (A) Frequency variation in area 1; (B) Frequency variation in area 2; (C) Tie line power variation.	111
Figure 4.42. Dynamic response of the testbed power system based on different fuzzy controllers under parametric uncertainty condition, case 9. (A) Frequency variation in area 1; (B) Frequency variation in area 2; (C) Tie line power variation.	112
Figure 4.43. Dynamic response of the testbed power system based on different fuzzy controllers under parametric uncertainty condition, case 10. (A) Frequency variation in area 1; (B) Frequency variation in area 2; (C) Tie line power variation.	113
Figure 4.44. Dynamic response of the testbed power system based on different fuzzy controllers under parametric uncertainty condition, case 11. (A) Frequency variation in area 1; (B) Frequency variation in area 2; (C) Tie line power variation.	114
Figure 4.45. Dynamic response of the testbed power system based on different fuzzy controllers under parametric uncertainty condition, case 12. (A) Frequency variation in area 1; (B) Frequency variation in area 2; (C) Tie line power variation.	115
Figure 4.46. Dynamic response of the testbed power system based on different fuzzy controllers under parametric uncertainty condition, case 13. (A) Frequency variation in area 1; (B) Frequency variation in area 2; (C) Tie line power variation.	116

Figure. 5.1. GB simplified model with primary/ secondary control loops.	126
Figure. 5.2. Convergence characteristics of the BA and PSO tuned the proposed SMC design.	130
Figure. 5.3. The frequency deviation of the GB power system for 0.0395 pu load disturbance without LFC / with PID controller.....	130
Figure. 5.4. The frequency deviation of the GB power system for 0.0395 pu load disturbance with the proposed SMC.	131
Figure. 5.5. Percentage of improvement in different criteria with SMC tuned by BA and PSO.	132
Figure. 5.6. Comparison of the dynamic response of GB power model with parameter uncertainties case 1, 2, nominal, 3, and 4 with no secondary control loop employed.....	133
Figure. 5.7. The dynamic performance of the GB power system under parameter uncertainties conditions when BA-SMC is employed for LFC.	134
Figure. 5.8. The dynamic response of the GB power system under parametric uncertainties case 4 with SMC tuned by BA is employed for LFC when 0.053 pu load disturbance is applied.....	135
Figure 5.9. Transfer function model of the testbed system.....	137
Figure 5.10. The convergence characteristic of BA algorithm based on several runs.....	141
Figure 5.11. Frequency deviation in area one (ΔF_1 in Hz).....	143
Figure 5.12. Frequency deviation in area two (ΔF_2 in Hz).	143
Figure 5.13. Tie line power deviation (ΔP_{tie} in pu).	144
Figure 5.14. Percentage of improvement in undershoot, settling time and ITAE with different controllers	145
Figure 5.15. Dynamic response of the system with different controllers under parametric uncertainties, case 1. (A) Frequency deviation in area 1; (B) Frequency deviation in area 2; (C) Tie line power deviation.	148
Figure 5.16. Dynamic response of the system with different controllers under parametric uncertainties, case 2. (A) Frequency deviation in area 1; (B) Frequency deviation in area 2; (C) Tie line power deviation.	149
Figure 5.17. Dynamic response of the system with different controllers under parametric uncertainties, case 3. (A) Frequency deviation in area 1; (B) Frequency deviation in area 2; (C) Tie line power deviation.	150
Figure 5.18. Dynamic response of the system with different controllers under parametric uncertainties, case 4. (A) Frequency deviation in area 1; (B) Frequency deviation in area 2; (C) Tie line power deviation.	151
Figure 5.19. Dynamic response of the system with different controllers under parametric uncertainties, case 5. (A) Frequency deviation in area 1; (B) Frequency deviation in area 2; (C) Tie line power deviation.	152

Figure 5.20. Dynamic response of the system with different controllers under parametric uncertainties, case 6. (A) Frequency deviation in area 1; (B) Frequency deviation in area 2; (C) Tie line power deviation.	153
Figure 5.21. Dynamic response of the system with different controllers under parametric uncertainties, case 7. (A) Frequency deviation in area 1; (B) Frequency deviation in area 2; (C) Tie line power deviation.	154
Figure 5.22. Dynamic response of the system with different controllers under parametric uncertainties, case 8. (A) Frequency deviation in area 1; (B) Frequency deviation in area 2; (C) Tie line power deviation.	155
Figure 5.23. Dynamic response of the system with different controllers under parametric uncertainties, case 9. (A) Frequency deviation in area 1; (B) Frequency deviation in area 2; (C) Tie line power deviation.	156
Figure 5.24. Dynamic response of the system with different controllers under parametric uncertainties, case 10. (A) Frequency deviation in area 1; (B) Frequency deviation in area 2; (C) Tie line power deviation.	157
Figure 5.25. Dynamic response of the system with different controllers under parametric uncertainties, case 10 with a random load disturbance applied in area one. (A) Random load disturbance; (B) Frequency deviation in area 1; (C) Frequency deviation in area 2; (D) Tie line power deviation.	160
Figure A1.1 The primary frequency response of GB power system with and without the feedback gain of electrical vehicles.	169
Figure B.1 The primary frequency response of GB system with various values of T_g	169
Figure B.2 The primary frequency response of GB system with various values of H	170
Figure B.3 The primary frequency response of GB system with various values of D	170
Figure B.4 The primary frequency response of GB system with various values of R	171

TABLE OF TABLES

Table 1.1 The frequency containment policy of the GB power system [5].	2
Table 1.2 The structure of the thesis.	5
Table 2.1 Parameters of the Simplified Power System.	14
Table 4.1. Parameters for the simplified model of the power system.	67
Table 4.2. Fuzzy rule base of the proposed controller.	70
Table 4.3. The BA parameters.	71
Table 4.4. The PSO parameters.	71
Table 4.5. Optimal gains of PID and FOPID with different algorithms for GB power system.	72
Table 4.6. Frequency response performances with PID tuned by different algorithms and designed by minimizing ISE.	73
Table 4.7. Frequency response performances with PID tuned by different algorithms and designed by minimizing ITAE.	74
Table 4.8. Frequency response performances with FOPID tuned by different algorithms and designed by minimizing ISE.	75
Table 4.9. Frequency response performances with FOPID tuned by different algorithms and designed by minimizing ITAE.	76
Table 4.10. Optimal gains of Fuzzy PIDF with different algorithms for GB power system.	77
Table 4.11. Frequency response performance with Fuzzy PIDF controllers designed via ISE.	78
Table 4.12. Frequency response performance with Fuzzy PIDF controllers designed via ITAE.	78
Table 4.13. The variation range of the parameters in the two scenarios.	80
Table 4.14. Frequency response performances with different BA-tuned controllers designed via ISE for scenario 2.	80
Table 4.15. Frequency response performance with different BA-tuned controllers designed via ITAE for scenario 2.	81
Table 4.16. Frequency response performance with BA tuned different controllers designed via ITAE for scenario 2.	83
Table 4.17. Frequency response performances with BA-tuned controllers designed via minimizing ITAE in scenario 2 with 0.053 pu load disturbance.	83
Table 4.18. The parameter of the testbed system.	86
Table 4.19. The BA and PSO parameters.	88
Table 4.20. Gains of Fuzzy PIDF Controllers Tuned by BA, TLBO and PSO	88
Table 4.21. Gains of Fuzzy PID tuned by TLBO and PID tuned by LCOA.	89
Table 4.22. characteristics of the testbed system with several controllers.	91

Table 4.23. Frequency response performances with different controllers for parametric uncertainties analysis.	92
Table 4.24. The optimum values of the proposed Fuzzy C PI-PD and Fuzzy (PI + PD) controllers obtained by the BA.	98
Table 4.25. The optimum Fuzzy PI + Fuzzy PD gains optimised by BA.....	99
Table 4.26. Frequency response performances of different fuzzy structures tuned by BA.....	99
Table 4.27. Investigated scenarios of system parametric variations.....	103
Table 4.28. Performance of the system under different scenarios with different controllers.	117
Table 5.1 The simplified GB power system parameters.....	126
Table 5.2. The BA parameters.	128
Table 5.3. The PSO parameters.	128
Table 5.4. The SMC optimum parameters obtained by BA and PSO.	129
Table 5.5. Dynamic performance of the GB System with different controllers.	131
Table 5.6. Improvement percentage in Ush, Osh, Ts, ITAE, and ISE with the proposed SMC.	132
Table 5.7. The variation range of the parameters in the GB power system.....	133
Table 5.8. The dynamic performance of the GB power system under parameter uncertainties conditions when BA-SMC is employed for LFC.	134
Table 5.9. The parameter of the testbed system [22].....	136
Table 5.10. The parameters of the proposed BA.	140
Table 5.11. The optimum SMC gains obtained by BA.....	140
Table 5.12. The optimum gains of the controllers proposed in [21] and [22].	142
Table 5.13. Frequency response performances with different controllers.	142
Table 5.14. Different investigated scenarios of system parametric uncertainties.....	147
Table C.1. Dynamic response of the system under different parametric uncertainties scenarios.....	172

LIST OF ABBREVIATIONS

LFC	Load Frequency Control
AVR	Automatic Voltage Regulator
BA	the Bees Algorithm
AI	Artificial Intelligence
Fuzzy PIDF	Fuzzy Proportional Integral Derivative with filtered derivative action
SMC	Sliding Mode Control
AGC	Automatic Generation Control
LCOA	Losi Map-Based Chaotic Optimization Algorithm
TLBO	Teaching Learning-Based Optimization
FSM	Frequency Sensitive Mode
LFMS	limited frequency sensitive mode
SAPS _s	Single-Area Power Systems
MPC	Model Predictive Control
VIU	Vertically Integrated Utility
ISO	Independent System Operator
UPFC	Unified Power Flow Controller
DE-PS	Differential Evolution and Pattern Search
GA	Genetic Algorithm
DG	Distributed Generation
RER _s	Renewable Energy Resources
ESS _s	Energy Storage Systems
PV	Photovoltaic
BESS	Battery Energy Storage System
CES	Capacitive Energy Storage
EV _s	Electric Vehicles
IMC	Internal Model Control
MFO	Moth Flame Optimization
MRAC	Model Reference Adaptive Control
STR	Self-Tuning Regulator
LSM	Least Square Method
ANN	Artificial Neural Network

LMI	Linear Matrix Inequality
MG	Micro-Grid
VSC	Variable Structure Control
PSO	Particle Swarm Optimization
GWO	Grey Wolf Optimization.
DFIG	Doubly Fed Induction Generator
TDE	Tribe-Differential Evolution
GCSC	Gate-Controlled Series Capacitors
FA	Firefly Algorithm
MOP	Multi-objective Optimization Problem
F2DOFPID	Fuzzy Logic-Based Two-Degree-Of-Freedom Proportional–Integral–Derivative
MID	Modified Integral Derivative
LUS	Local Unimodal Sampling
LQR	Linear Quadratic Regulator
CDM	Coefficient Diagram Method
ACO	Ant Colony Optimization
CI	Computational Intelligence
SA	Simulated Annealing
ILS	Iterated Local Search
MBO	Marriage in Honey-Bees
HBMO	Honey-Bees Mating Optimization
BS	Bee System
BCO	Bee Colony Optimization
SVM	Support Vector Machine
MSF	Membership Function
GB-SQSS	Great Britain Security and Quality of Supply Standard
GDB	Governor Dead Band
GRC	Generation Rate Constrain
ACE	Area Control Error
NB	Negative Big
NS	Negative Small
Z	Zero

PS	Positive Small
PB	Positive Big
ISE	Integral of Square Error
ITAE	Integral Time Absolute Error
FOPID	Fractional Order PID
Fuzzy C PI-PD	Fuzzy Cascade PI-PD
DSFR	Demand Side Frequency Response

Chapter 1

Introduction

Modern power systems are highly nonlinear with increasing complexity in their structure. This is because of the obvious increase in capacity with wide dependence on different energy sources. Consequently, many issues are associated with this nonlinearity and complexity in which frequency deviation in power systems is one of the most serious problems in this field. The problem of frequency deviation is a persistent issue presented from the continuous change in the demand which accordingly requires changing the generated power in order to keep the frequency at its rated value. In power systems, this process is termed Load Frequency Control (LFC) [1]. Based on the basic role of the LFC loop, the principal tasks of this service in power systems are providing the necessitated power from the generation plants operating in the system to meet the load demand variation and maintaining the interchanged power among interconnected control areas at pre-rated values. The objectives of the LFC loop which contribute to enhancing the power system stability are to assure zero steady-state error in frequency variation and the tie-line power fluctuation. This loop is also responsible for damping the overshoot and undershoot of the oscillation in frequency and exchanged power within a specified time; this depends on the capacity of the power system and the disturbance size [2].

1.1 Control of frequency in the Great Britain power system

A secure supply of power energy is the main concern in power system operation, i.e., reliable electricity with appropriate quality is supplied to the customers at all times. Thus, it is essential that energy production is continuously balanced with demand. In order to control the frequency in power systems, various control loops are involved: primary, secondary, tertiary and emergency in specified conditions. In the GB power system where the nominal value of the frequency is 50Hz, the primary loop is known as dynamic power generation reaches its maximum in ten seconds, while the secondary control takes thirty seconds to reach its maximum operative capacity. Frequency reserve services are classified into dynamic service which respond automatically to any frequency alternation and non-dynamic which is triggered via load frequency relays. When the generated power and the demand is imbalanced, the system will experience frequency deviations; this frequency fluctuation is required by the Great Britain-Security and Quality of Supply Standard (GB-SQSS) to remain within acceptable ranges as demonstrated in Table 1.1. However, under a significant drop in the

frequency (i.e. below 49.2 Hz), a disconnection by low-frequency relays is provided for frequency control of both the generators and demand. Figure 1.1. shows the acceptable frequency deviations in the normal operating conditions and when a generation loss of up to 1800MW (representing a substantial nuclear generator) or less suddenly occurs [3]–[5].

Table 1.1 The frequency containment policy of the GB power system [5].

Frequency limits	Case description
± 0.2 Hz	System frequency in normal operating conditions and the acceptable frequency deviation following a generation loss or connecting demand to ± 300 MW.
± 0.5 Hz	The maximum deviation in frequency when generation units over 300 MW and of up to 1320 MW is lost.
-0.8 Hz	The maximum deviation in frequency following a generation loss over 1320 MW and up to 1800 MW, requires restoration of frequency to a minimum of 49.5 Hz in 60 s.

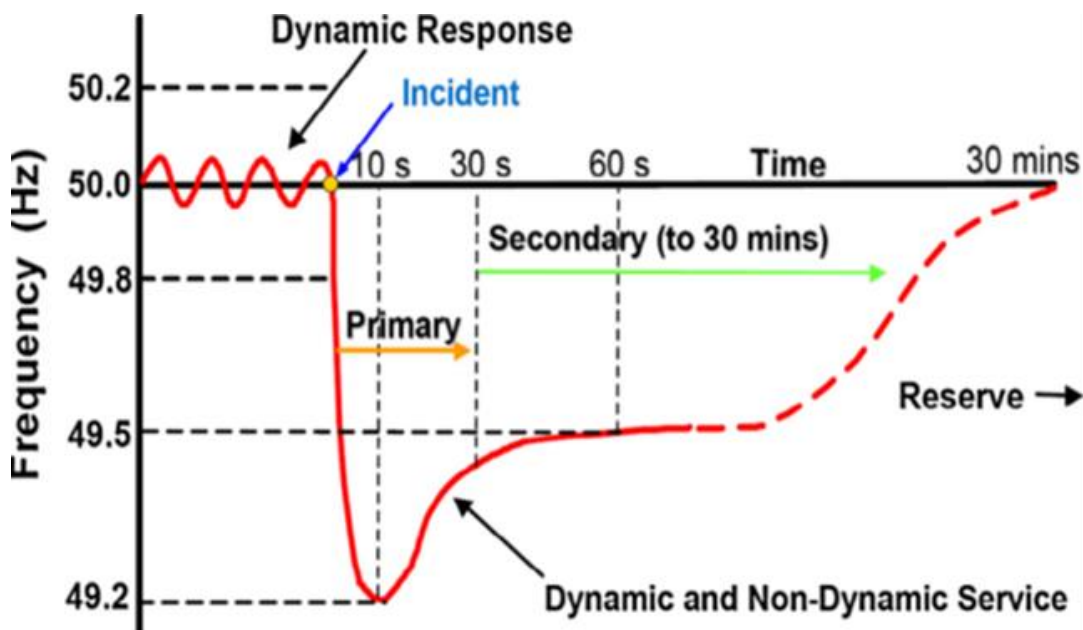


Figure 1.1 Frequency fluctuations following the loss of generation up to 1800MW [3].

1.2 Control of frequency in multi-area power systems

The interconnected power system is often referred to as the largest and most complex system ever built by humankind. This may be hyperbole, but it does emphasize an inherent truth: there is a complex interdependency between different parts of the system. That is, events in geographically distant parts of the system may interact strongly and in unexpected

ways. Earlier electric power systems were usually operated as individual units. However, in general, electrical energy generation and utilization (load centres) are far away from each other. Power grid interconnection and control of power flow are necessary to supply power to the load centres. Further, interconnections of electric power networks enable the decarbonization of the electricity system by harnessing and sharing large amounts of renewable energy. The highest potential renewable energy areas are often far from load centres, integrated through long-distance transmission interconnections. The transmission interconnection mitigates the variability of renewable energy sources by importing and exporting electricity between neighbouring regions.

The interconnected power system consists of multi-areas that are connected to each other by high voltage AC (and sometimes DC) transmission tie-lines. Each control area is considered as a coherent system consisting of a group of generators and loads, where all generators respond to the changes in load or speed changer settings [6]. The change of frequency measured in each area is an indicator of the change in the power mismatch between generation and demand in the same area and other interconnected areas. In an interconnected power system, LFC systems have their dominant function in which in addition to providing the desired real power output from the generators to meet the change in load (Controlling the frequency), they maintain the interchange of power between control areas connected through tie-lines at pre-specified values [7]. Further, the term multi-source power system is the interconnection of several lower-order subsystems in each area.

In addition to the economic, resource and environmental benefits, the main technological benefits of large-scale power network interconnections are [6] :

1. Balancing mismatches in supply and demand: Connecting summer peak-demand regions with winter peak-demand regions. For example, regions of different time zones, get large benefits by balancing seasonal and daily peak-load variability.
2. Incorporating intermittent renewable power: Transmission interconnection is a tool to facilitate the incorporation of variable renewable resources. The evolution of high and ultra-high voltage transmission technology opens up entirely new transportation corridors and interconnection possibilities.
3. Accessing remote energy resources: Electricity utilization is concentrated in major cities having large energy demand. This large demand will not be fulfilled by the local energy

resources. Even renewable energy sources such as wind, hydro, and solar are often located in remote regions far away from the demand centres.

The only possible disadvantage of having interconnected systems are; in some cases, faults may get propagated throughout the whole system causing the entire system instability also these systems require proper management.

1.3 Research motivation

For satisfactory operation of a power system, frequency should be maintained constant. Frequency variations can negatively impact power system operation, system reliability and efficiency. Large frequency variations can damage equipment, degrade load performance, overload transmission lines and interfere with system protection schemes. Variation in frequency adversely affects the operation and speed control of induction and synchronous machines. The reduced speed of motor-driven generating station auxiliaries, associated with the fuel, the feed-water and the combustion air supply systems, such as fans, pumps, and mills, will bring down plant output. A considerable drop in frequency could result in high magnetizing currents in induction motors and transformers thereby increasing reactive power consumption. In domestic appliances, where refrigerators' efficiency goes down, television and air conditioners reactive power consumption increases considerably with a reduction in power supply frequency [8]. Significant-frequency deviation can ultimately lead to cascading failure and system collapse.

Furthermore, the increasing number of major power grid blackouts that has been experienced recently, for example, Libyan black out of January 2017, Thailand blackout of May 2013, and Indian blackout of July 2012 shows that today's power system operations require more careful consideration of all forms of system instability and control issues. Importantly, it has been reported that violation of frequency control requirements was known as a main reason for numerous power grid blackouts [6] [9]. Therefore, this thesis is focused to propose two control techniques based on different control theories to regulate the frequency in two power systems as demonstrated in the following sections.

1.4 Problem statement

Controlling large-interconnected power systems with the consideration of increasing size, complexity, and numerous disturbances occurring unpredictably during the operation time is certainly one of the most challenging issues faced in electric power system control. Further, power consumption from the demand side is continually/ unexpectedly fluctuating

and this alteration in load demand in any control area(s) results in transient deviation in frequency, generation and tie-line power flow throughout the whole system. Thus, the mismatch between the abrupt demanded power and generation is the primary cause of these deviations. In stable, reliable and secured power systems, frequency and tie-line power flowing between interconnected areas are required to bring back to their scheduled values quickly following a load disturbance. This is accomplished by matching the generated power to the demand plus losses. This control mechanism is known as Load Frequency Control (LFC) allows the synchronous generators to regulate their generations in response to the load demands, as a result of which area frequency and tie-line power oscillations/errors are ensured to converge to zero. Inappropriate design of LFC may undermine the system performance causing unwanted large oscillations in the generation, area frequency and tie-line power flows which may enforce the system toward instability and loss of synchronism.

1.5 Thesis structure

Table 1.2 summarises the layout and the main scope of each chapter in this thesis.

Table 1.2 The structure of the thesis.

Chapter No.	Description of content
1	This chapter provides a background of the topic, the aim, objectives, contributions, and published works.
2	This chapter provides a comprehensive and up-to-date literature review on LFC in power systems from different aspects, the size of power systems, the type, the proposed LFC techniques, and strategies. This chapter also gives an evaluation of each section in addition to a brief summary.
3	Discusses the suggested algorithm “the Bees Algorithm” and gives an overall state of the art on this algorithm. It provides an idea about the basic concept of BA, the theoretical analysis conducted on BA and its main applications. As a new application of BA, this algorithm is extensively used in this thesis to find the best possible values of the controllers proposed in chapters 4 and 5 in order to reach the best possible performance.
4	Design and implementation of new different structures of Fuzzy Logic Controllers equipped as LFC systems in the testbed systems is presented in

	<p>this chapter. The robustness of these configurations has been examined against a wide range of parametric uncertainties of the investigated systems. Furthermore, the supremacy of the proposed fuzzy structures is investigated by comparing the results with those of other controllers.</p>
5	<p>In this chapter, a novel-simple design of Sliding Mode Control (SMC) is proposed and implemented for LFC in a dual-area interconnected power system and the simplified GB power system. Conducts many case studies to investigate the robustness and performance of SMC in comparison with other methods.</p>
6	<p>This chapter concisely summarises the thesis and provides a clear pathway for future works.</p>

1.6 Research aim, objectives and Contributions

This thesis aims to investigate the potentiality of developing new robust load frequency control systems to improve the dynamic performance of power systems by maintaining the frequency and tie-line power deviation within their acceptable limits even during a case of disturbance.

The contributions of this work are as following:

1. To develop four new fuzzy configurations and implement them for LFC in the investigated power models.
2. To achieve a novel design and implementation of Sliding Mode Control (SMC) derived based on the mathematical models of the investigated systems.
3. To implement the Bees Algorithm (BA) for the first time in the area of LFC to tune the parameters of the proposed controllers (no attempt has been made to utilize the bees algorithm in designing the secondary frequency control of a power system).

To investigate the validity and applicability of the proposed LFC systems, the suggested methods are implemented in two different power systems under several operating conditions. To achieve the above-mentioned aim, the following steps are taken:

1. To conduct a comprehensive review on load frequency control, investigate the key findings, ongoing studied topics, and the possible issues with the potential solutions for frequency variation in modern power systems.
2. To design and implement an optimal Fuzzy PID with filtered derivative action for LFC in the simplified GB power system and dual area interconnected power system.
3. To develop three different fuzzy control configurations namely Fuzzy Cascade PI – PD, Fuzzy PI plus Fuzzy PD, and Fuzzy (PI + PD), to efficiently control the frequency in the testbed two-area power system and maintain the power interchanges within pre-defined values.
4. To propose Sliding Mode Control (SMC) design with full mathematical deriving is proposed for third and fourth-order system models representing the two-area power system and the simplified GB power system, respectively.
5. To boost/enhance the performance of the proposed controllers, a simple and powerful optimization method called the Bees Algorithm (BA) is employed to attain the best possible values of the suggested controllers' parameters.
6. To carry out a comprehensive analysis of the robustness and superiority of the proposed control methods. This is done by testing the dynamic performance of the system under different operating conditions and comparing the obtained results with previously suggested control techniques.

1.7 Publications

Author publications:

A. Journal Publications:

1. **Shouran M;** Anayi F; Packianather M; Habil M. Different Fuzzy Control Configurations Tuned by the Bees Algorithm for LFC of Two-Area Power System. *Energies*. 2022; 15(2):657. <https://doi.org/10.3390/en15020657>
2. **Shouran, M.;** Anayi, F.; Packianather, M. Design of sliding mode control optimised by the Bees algorithm for LFC in the Great Britain power system. *Mater. Today Proc.* 2021. <https://doi.org/10.1016/j.matpr.2021.10.322>
3. **Shouran M,** Anayi F; Packianather M. The Bees Algorithm Tuned Sliding Mode Control for Load Frequency Control in Two-Area Power System. *Energies*. 2021; 14(18):5701. <https://doi.org/10.3390/en14185701>

4. **Shouran, M**, Anayi F; Packianather M; Habil M. Load Frequency Control Based on the Bees Algorithm for the Great Britain Power System. *Designs*. 2021; 5(3):50. <https://doi.org/10.3390/designs5030050>

B. Conference Publications:

1. **Shouran, M.**; Anayi, F.; Packianather, M. A State-of-the-Art Review on LFC Strategies in Conventional and Modern Power Systems. In Proceedings of the 2021 International Conference on Advance Computing and Innovative Technologies in Engineering (ICACITE), Greater Noida, India, 4–5 March 2021; pp. 268–277.
2. **Shouran, M.**; Anayi, F.; Packianather, M. Fuzzy PID with Filtered Derivative Mode Based Load Frequency Control of Two-Area Power System. In Proceedings of the 2021 56th International Universities Power Engineering Conference (UPEC), Virtuell, UK, 31 August–3 September 2021; pp. 1–6.

Collaborative published work:

1. **Shouran M**; Alseid A. Particle Swarm Optimization Algorithm-Tuned Fuzzy Cascade Fractional Order PI-Fractional Order PD for Frequency Regulation of Dual-Area Power System. *Processes*. 2022; 10(3):477. <https://doi.org/10.3390/pr10030477>
2. **Shouran, M.**; Alseid, A.M. Cascade of Fractional Order PID based PSO Algorithm for LFC in Two-Area Power System. In Proceedings of the 2021 3rd International Conference on Electronics Representation and Algorithm (ICERA), Yogyakarta, Indonesia, 29–30 July 2021; pp. 1–6.
3. **Shouran, M.**; Habil M. Tuning of PID Controller Using Different Optimization Algorithms for Industrial DC Motor. In Proceedings of the 2021 International Conference on Advance Computing and Innovative Technologies in Engineering (ICACITE), Greater Noida, India, 4–5 March 2021; pp. 756-759.
4. Mansour S, Badr AO, Attia MA, Sameh MA, Kotb H, Elgamli E, **Shouran M**. Fuzzy Logic Controller Equilibrium Base to Enhance AGC System Performance with Renewable Energy Disturbances. *Energies*. 2022; 15(18):6709. <https://doi.org/10.3390/en15186709>.
5. **Shouran, M**, and Fatih Anayi. 2022. "TLBO Tuned a Novel Robust Fuzzy Control Structure for LFC of a Hybrid Power System with Photovoltaic Source" *Engineering Proceedings* 19, no. 1: 1. <https://doi.org/10.3390/ECP2022-12684>

1.7 References:

- [1] B. Mohanty, S. Panda, and P. K. Hota, "Controller parameters tuning of differential evolution algorithm and its application to load frequency control of multi-source power

system,” *Int. J. Electr. Power Energy Syst.*, vol. 54, pp. 77–85, Jan. 2014, doi: 10.1016/j.ijepes.2013.06.029.

- [2] B. K. Sahu, T. K. Pati, J. R. Nayak, S. Panda, and S. K. Kar, “A novel hybrid LUS–TLBO optimized fuzzy-PID controller for load frequency control of multi-source power system,” *Int. J. Electr. Power Energy Syst.*, vol. 74, pp. 58–69, Jan. 2016, doi: 10.1016/j.ijepes.2015.07.020.
- [3] F. Teng, Y. Mu, H. Jia, J. Wu, P. Zeng, and G. Strbac, “Challenges on primary frequency control and potential solution from EVs in the future GB electricity system,” *Appl. Energy*, vol. 194, pp. 353–362, May 2017, doi: 10.1016/j.apenergy.2016.05.123.
- [4] Y. Mu, J. Wu, J. Ekanayake, N. Jenkins, and H. Jia, “Primary Frequency Response From Electric Vehicles in the Great Britain Power System,” *IEEE Trans. Smart Grid*, vol. 4, no. 2, pp. 1142–1150, Jun. 2013, doi: 10.1109/TSG.2012.2220867.
- [5] Z. A. OBAID, L. M. CIPCIGAN, L. ABRAHIM, and M. T. MUHSSIN, “Frequency control of future power systems: reviewing and evaluating challenges and new control methods,” *J. Mod. Power Syst. Clean Energy*, vol. 7, no. 1, pp. 9–25, Jan. 2019, doi: 10.1007/s40565-018-0441-1.
- [6] H. Bevrani, *Robust Power System Frequency Control*. Cham: Springer International Publishing, 2014.
- [7] P. M. Anderson and A. . A. Fouad, *Power system control and stability*, Second. New York: Institute of Electrical and Electronics, 2008.
- [8] S. K. Jain, S. Chakrabarti and S. N. Singh, "Review of Load Frequency Control methods, Part-I: Introduction and Pre-deregulation Scenario," *2013 International Conference on Control, Automation, Robotics and Embedded Systems (CARE)*, 2013, pp. 1-5, doi: 10.1109/CARE.2013.6733736.
- [9] K. M. Alkar, M. Meto, M. Jamjum and K. Amar, "Performance Evaluation of The Blackout and Power Outages in Libyan Power Grid - Al-Zawia Combined Cycle Power Plant Case Study," *2019 1st International Conference on Sustainable Renewable Energy Systems and Applications (ICSRESA)*, 2019, pp. 1-6, doi: 10.1109/ICSRESA49121.2019.9182337.

Chapter 2

Literature Review

2.1 Abstract

This chapter reflects a detailed and up-to-date review of Load Frequency Control (LFC) in traditional and modern power systems. A general overview of LFC is provided, followed by a discussion of different configurations of power systems and their features. Various control strategies concerning the LFC problem, such as centralized and decentralized are also highlighted. Then, LFC techniques based on classical, optimal, adaptive, robust, and artificial intelligence based on soft computing are identified.

2.2 Introduction

In large power systems comprising several interconnected control areas, the successful operation is to generate and distribute power as reliably as possible whilst preserving different parameters such as frequency and voltage within an acceptable limits [1]. This necessitates balancing the generated power and the demand at the load side. As load demand is unpredictable and uncertain with respect to time, this affects various operating points of the whole power system, which results in variations in frequency and scheduled power exchange of the system. This yields undesirable consequences, which may cause instability in the system that might lead to a whole system blackout [2].

The most prevalent solution for frequency fluctuation is hierarchical control, which is usually categorized into three levels, primary, secondary, and tertiary control levels [3]. Based on the deviation of the frequency from its nominal, an emergency control loop may also be needed to restore the frequency of the power system [4]. Under regular (normal) operating conditions, the slight frequency fluctuation is attenuated by the primary control (time action from several seconds). Depending on the available quantity of the reserved power, the secondary control loop, also known as an LFC is installed to restore the frequency for more significant frequency deviations (off-normal operation), this action may take up to 10 minutes. However, if an extreme imbalance between the generation and load demand caused by major fault is experienced, restoring the frequency to its nominal through the LFC loop may not be achievable. In this case, tertiary control will take the reaction. Emergency control services are also employed to reduce the possibility of cascade defects (see Figure 2.1) [5].

Based on the above statement, LFC or Automatic Generation Control (AGC) is a key service that has an essential function in power systems to assure a successful operation [6].

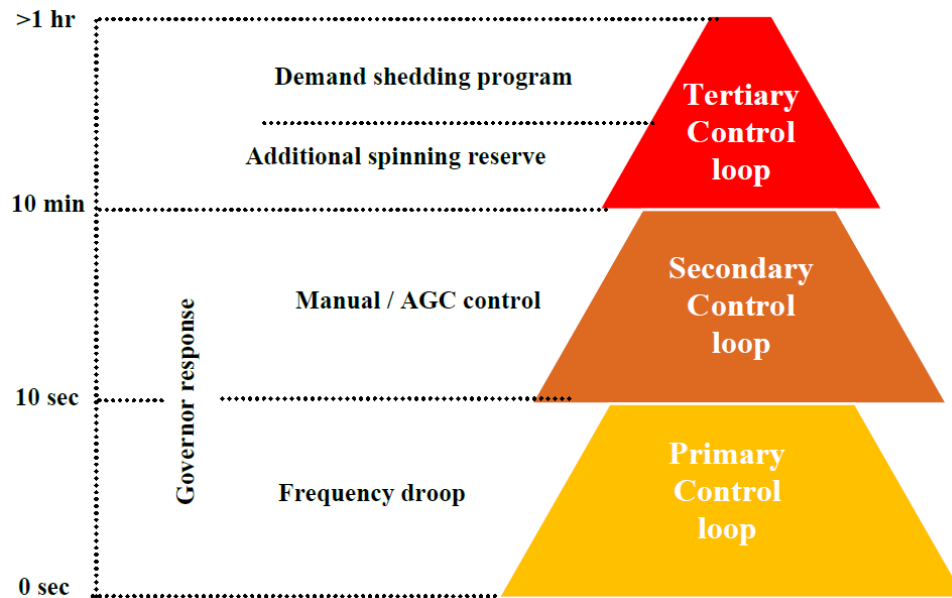


Figure 2.1. Frequency control loops in a power system

2.3 Frequency response modelling

The frequency of a power system is dependent on real power balance. A change in real power demand at one point of a network is reflected throughout the system by a change in frequency. Therefore, system frequency provides a useful index to indicate system generation and load imbalance. Any short-term energy imbalance results in an instantaneous change in system frequency as the disturbance is initially offset by the kinetic energy of the rotating plant. Significant loss in the generation without an adequate system response can produce extreme frequency excursions outside the working range of the plant [7] [8].

Depending on the type of generation, the real power delivered by a generator is controlled by the mechanical power output of the prime mover such as a steam turbine, gas turbine, hydro turbine, or diesel engine. In the case of a steam or hydro turbine, mechanical power is controlled by the opening or closing of valves regulating the input of steam or water flow into the turbine. Steam (or water) input to generators must be continuously regulated to match real power demand, failing which the machine speed will vary with consequent change in frequency. For satisfactory operation of a power system, the frequency should remain nearly constant [3] [9].

In addition to the primary frequency control, most large synchronous generators are equipped with a secondary frequency control loop. A schematic block diagram of a synchronous generator equipped with frequency control loops is shown in Figure. 2.2.

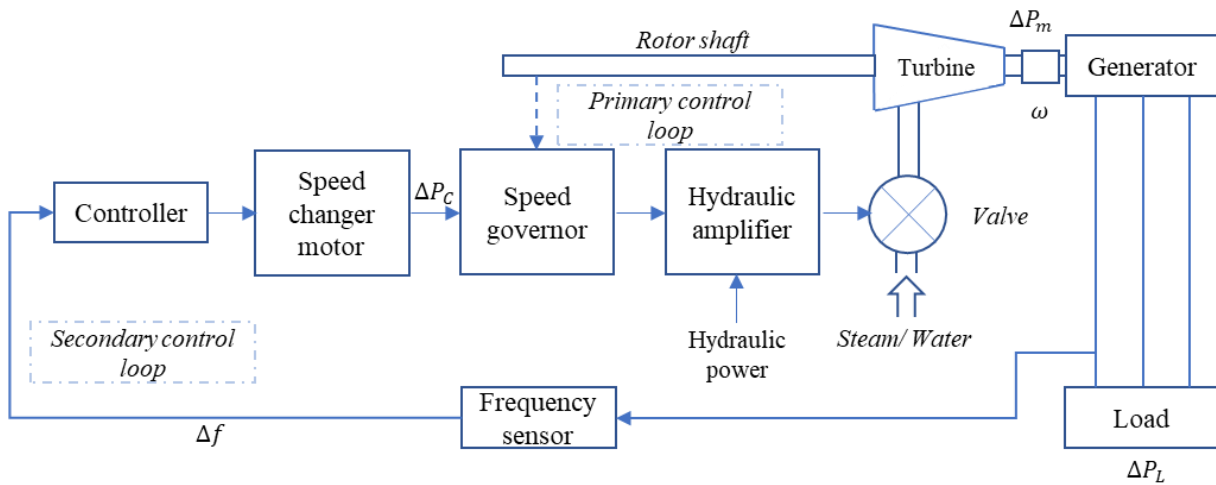


Figure 2.2. Schematic block diagram of a synchronous generator with basic frequency control loops [3].

In Figure. 2.2, the speed governor senses the change in speed (frequency) via the primary and secondary control loops. The hydraulic amplifier provides the necessary mechanical forces to position the main valve against the high steam (or hydro) pressure and the speed changer provides a steady-state power output setting for the turbine.

The speed governor on each generating unit provides a primary speed control function, and all generating units contribute to the overall change in generation, irrespective of the location of the load change, using their speed governing. However, primary control action is not usually sufficient to restore the system frequency, especially in an interconnected power system and the secondary control loop is required to adjust the load reference set point through the speed changer motor.

The secondary loop performs a feedback via the frequency deviation and adds it to the primary control loop through a dynamic controller. The resulting signal (ΔP_C) is used to regulate the system frequency.

According to Figure. 2.2, the frequency experiences a transient change (Δf) following a change in load (ΔP_L). Thus, the feedback mechanism comes into play and generates an appropriate signal for the turbine to make generation (ΔP_m) track the load and restore the system frequency [3].

In this subsection, a simplified frequency response model for the described schematic block diagram in Figure. 2.2 with one generator unit is described, and then the resulting model is generalized for an interconnected multimachine power system in subsection. 2.3.2. The overall generator-load dynamic relationship between the incremental mismatch power ($\Delta P_m - \Delta P_L$) and the frequency deviation (Δf) can be expressed by a swing differential equation as

$$\Delta P_m(t) - \Delta P_L(t) = 2H_{eq} \frac{d\Delta f(t)}{dt} + D \Delta f(t) \quad (2.1)$$

where Δf is the frequency deviation, ΔP_m the mechanical power change, ΔP_L the load change, H_{eq} the inertia constant, and D is the load damping coefficient. The damping coefficient is usually expressed as a percent change in load for a 1% change in frequency. For example, a typical value of 1.5 for D means that a 1 % change in frequency would cause a 1.5 % change in load [3]. Using the Laplace transform, Equation. (2.1) can be written as:

$$\Delta P_m(s) - \Delta P_L(s) = 2 H_{eq} s \Delta f(s) + D \Delta f(s) \quad (2.2)$$

Equation (2.2) can be represented in a block diagram as shown in Figure. 2.3. This generator-load model can simply reduce the schematic block diagram of a closed loop synchronous generator (Figure. 2.2) as shown in Figure. 2.4

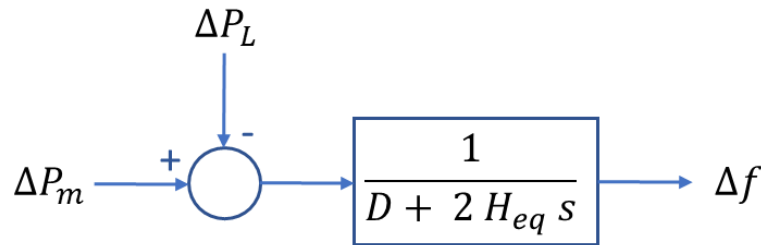


Figure 2.3. Block diagram representation of generator-load model [3].

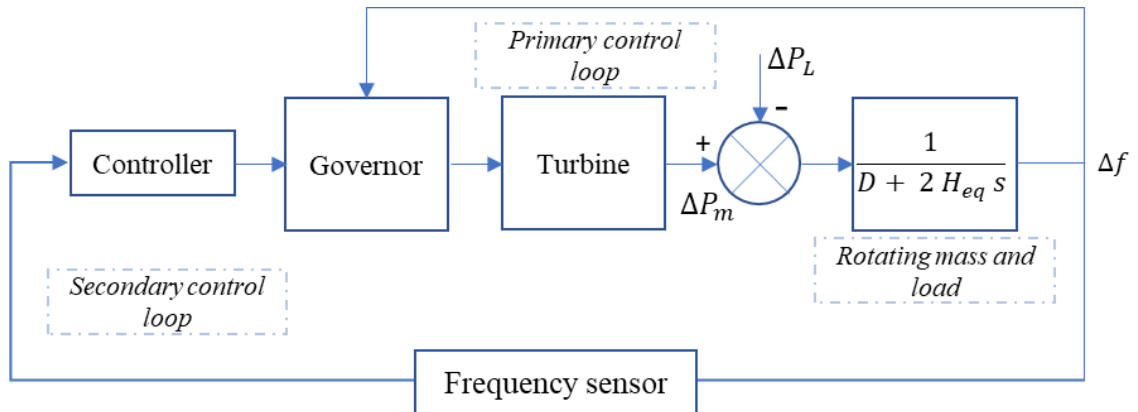


Figure 2.4. reduced block diagram of figure 2.2 [3].

2.3.1 Frequency control in the GB power system

A simplified governor-generator model of the GB power system was developed in [10] [11] and is shown in Figure 2.5. This model is used for power system frequency analysis and control design. First-order transfer functions are used to model the governor-turbine.

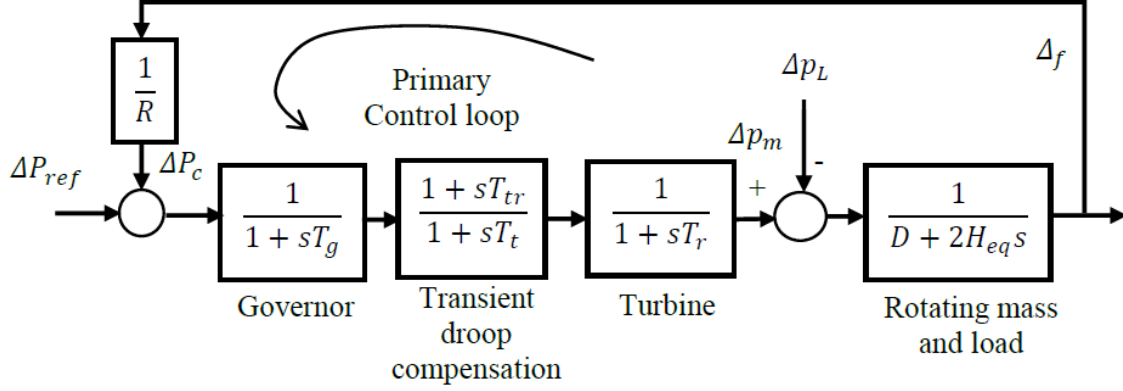


Figure 2.5. GB power system primary frequency control model [10] [11].

The governor and turbine time constants (T_g , T_t , T_{tr} , and T_r) are tabulated in Table 2.1 [11] [12]. The droop gain (R) is defined by the ratio of frequency change Δf to the change of generator power output ΔP , as shown in Figure 2.6. The purpose of the turbine-governor control is to maintain the desired system frequency by adjusting the mechanical output power of the turbine ΔP_m .

Table 2.1 Parameters of the Simplified Power System.

$1/R$	T_g	T_{tr}	T_t	T_r	H_{eq}	D
-0.09 pu	0.2 s	2 s	12 s	0.3 s	4.44 s	1 pu

The frequency-power relationship of turbine-governor control is shown in Equation (2.3):

$$\Delta P_c = \Delta P_{ref} - \frac{1}{R} \times \Delta f \quad (2.3)$$

The term $\Delta P_c - \Delta P_{ref}$ is denoted by ΔP , and the droop gain is defined as

$$-R = \text{Slope} = \frac{\Delta f}{\Delta P} \quad (2.4)$$

The governors use droop control to regulate the power output of the generators in response to frequency deviations. This is referred to the primary frequency control, which is provided automatically by governors. For example, if the demand power is increased (or the generation power is decreased) and this causes a drop in frequency, then the low-frequency

response is provided automatically by the governors. Similarly, for a loss in demand (causing a frequency rise), a high-frequency response service is provided by the governors [13].

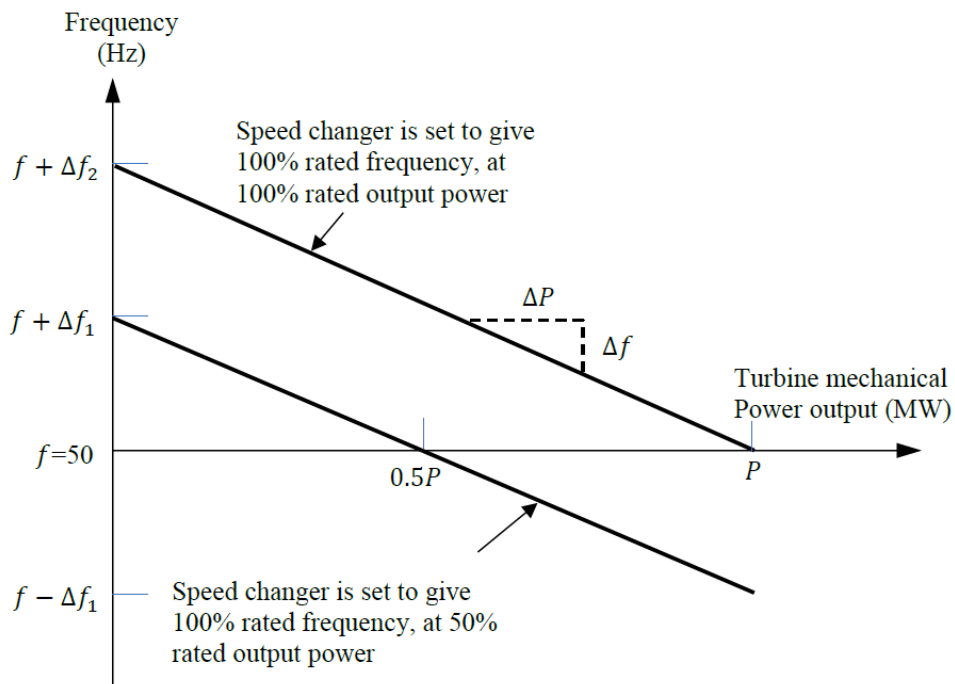


Figure 2. 6. Steady-state frequency-power relationship of a turbine-governor control [8].

2.3.2 Frequency control in an interconnected power system

A multiarea power system comprises areas that are interconnected by high-voltage transmission lines or tie-lines. The trend of frequency measured in each control area is an indicator of the trend of the mismatch power in the interconnection and not in the control area alone. The secondary frequency control (LFC) system in each control area of an interconnected (multiarea) power system should control the interchange power with the other control areas as well as its local frequency. For this purpose, consider Figure. 2.7 which shows a power system with N-control areas

The power flow through the tie-line from area 1 to area 2 is expressed in Equation (2.5).

$$P_{\text{tie},12} = \frac{V_1 V_2}{X_{12}} \sin (\delta_1 - \delta_2) \quad (2.5)$$

Where V_1 , V_2 are the voltages (in p.u.) at equivalent machine's terminals of area 1 and 2; δ_1 , δ_2 are the power angles of equivalent machines of the areas one and two; and X_{12} is the tie line reactance between area 1 and 2.

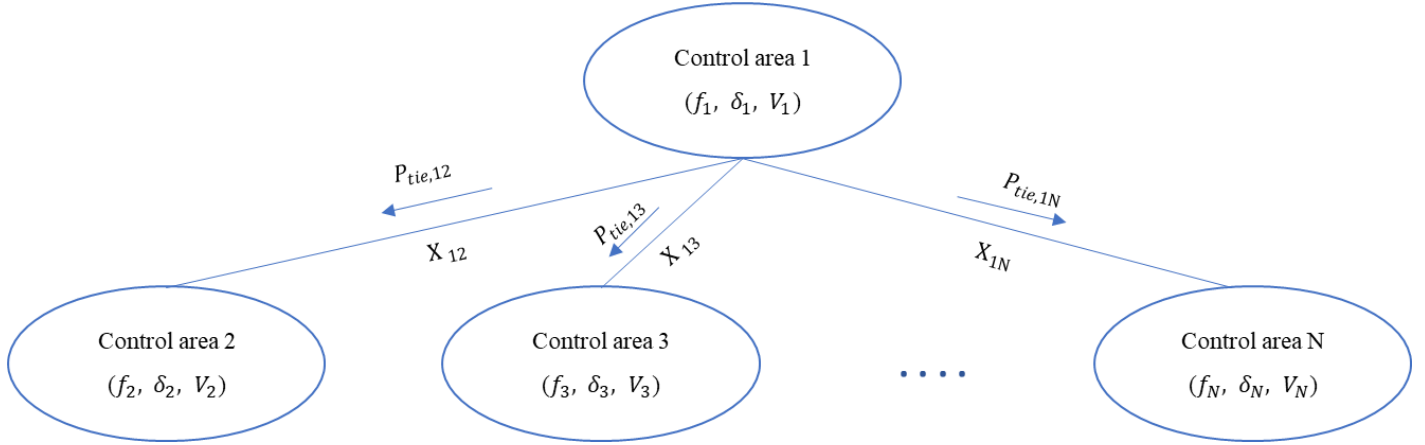


Figure 2.7. A schematic diagram of an N-area interconnected power system [3].

By linearizing (2.5) about an equilibrium point (δ_1^0, δ_2^0)

$$\Delta P_{tie,12} = T_{12} (\Delta \delta_1 - \Delta \delta_2) \quad (2.6)$$

where T_{12} represents the synchronizing torque coefficient presented by

$$T_{12} = \frac{|V_1||V_2|}{X_{12}} \cos(\delta_1^0 - \delta_2^0) \quad (2.7)$$

By considering the relationship between the area power angle and frequency, Equation (2.6) is rewritten as follows, where Δf_1 and Δf_2 are frequency changes in area one and 2, respectively. The Laplace transform of (2.8) results Equation (2.9)

$$\Delta P_{tie,12} = 2\pi T_{12} \left(\int \Delta f_1 - \int \Delta f_2 \right) \quad (2.8)$$

$$\Delta P_{tie,12}(s) = \frac{2\pi}{s} T_{12} (\Delta f_1(s) - \Delta f_2(s)) \quad (2.9)$$

Similarly, the net power interchange between A1 and A3 is given in Equation (2.10):

$$\Delta P_{tie,13}(s) = \frac{2\pi}{s} T_{13} (\Delta f_1(s) - \Delta f_3(s)) \quad (2.10)$$

Considering (2.9) and (2.10), the total tie-line power change between area 1 and the other areas can be calculated as expressed in (2.11):

$$\Delta P_{tie,1} = \Delta P_{tie,12} + \Delta P_{tie,13} = \frac{2\pi}{s} \left[\sum_{j=2,3} T_{1j} \Delta f_1 - \sum_{j=2,3} T_{1j} \Delta f_j \right] \quad (2.11)$$

Similarly, for N-control areas (Figure 2.7), the total tie-line power change between area 1 and other areas is

$$\Delta P_{tie,i} = \sum_{\substack{j=1 \\ j \neq i}}^N \Delta P_{tie,ij} = \frac{2\pi}{s} \left[\sum_{\substack{j=1 \\ j \neq i}}^N T_{ij} \Delta f_i - \sum_{\substack{j=1 \\ j \neq i}}^N T_{ij} \Delta f_j \right] \quad (2.12)$$

Equation (2.12) can be represented by a block diagram, which can be added to the mechanical power mismatch ($\Delta P_m - \Delta P_L$) that was described in Figure 2.5. Hence, the simplified block diagram of the interconnected power system is shown in Figure 2.8.

The shaded block in Figure 2.8 represents the secondary control loop in a presence of a tie-line. The tie-line power flow change ($\Delta p_{tie,i}$) is added to the frequency change (Δf_i) through a secondary feedback loop. The area control error (ACE_i) signal is then computed as shown in Equation (2.13) and applied to the controller $K(s)$:

$$ACE_i = \Delta P_{tie,i} + \beta_i \Delta f_i \quad (2.13)$$

where β_i is a bias factor, which can be obtained according to Equation (2.14) [3]:

$$\beta_i = \frac{1}{R_i} + D_i \quad (2.14)$$

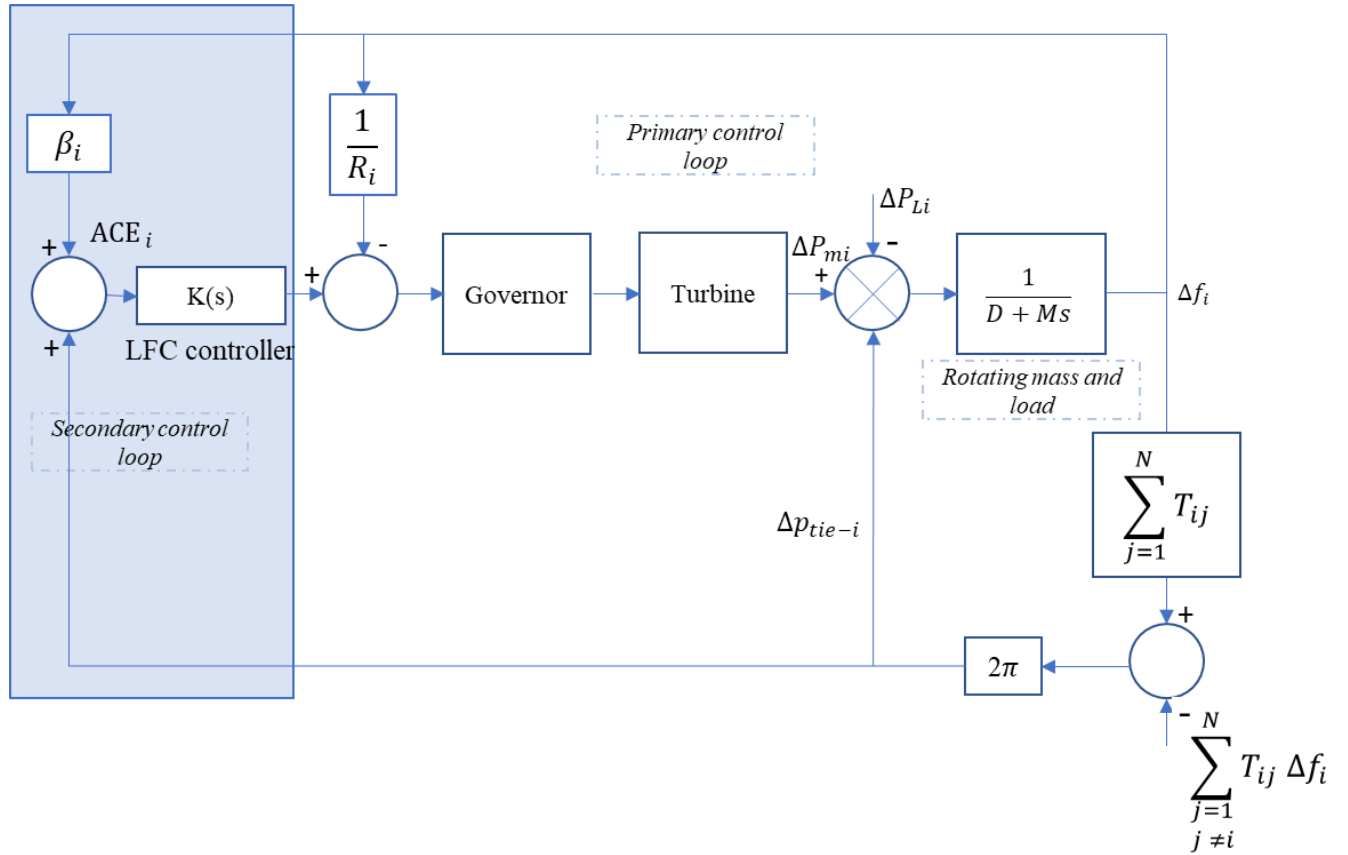


Figure 2.8. A simplified interconnected power system with LFC controller [3]

In the case of area frequency drop occurrence, the LFC controller $K(s)$ will correct the value of ACE_i (drive it back to zero) and send the control signal to the governor. That is, to regulate the area frequency and maintain the net-interchange power at the scheduled level.

2.4 LFC-based different Power System Models

2.4.1 Conventional (Traditional) Power Systems

This type of power system has been used for decades and is mainly based on thermal, hydro, and nuclear power resources. Based on their scale, they are generally divided into four groups: single-area, dual-area which is the most investigated, three-area, and four-area power systems. It is worth mentioning that several studies have considered larger power systems that comprise more than four control areas. However, this kind of power system is not widely investigated.

LFC in Single-Area Power Systems (SAPSs) has been investigated by many researchers. LFC of a single-area power model incorporating thermal power plants is studied in [14]. A single-area hydropower system is considered in [15] to test the usefulness of a new LFC technique based on reducing the size of the dump load using an ON/OFF control valve. Frequency control of a single-area multi-source power system based on several classical controllers is marked out in [16]. In [17], a combined model is investigated to show the relationship between the Automatic Voltage Regulator (AVR) and LFC loops, which represent the association between controlling the reactive/active power in a single-area power system.

The challenges associated with LFC incorporating dual-area power system models are widely discussed. Reference [18] demonstrates the design and implementation of LFC-based Fuzzy Logic Control (FLC) and Integral (I) for a two-area interconnected system. Based on many-objective optimization algorithms used to find the optimal gains of the Proportional Integral and Derivative (PID) controller, LFC for an identical dual-area power system with several power plants equipped in each area is reviewed in [19]. Different optimization techniques are used to optimize the parameters of PID controller-based LFC equipped in a dual-area power system under wave energy disturbance is investigated in [20]. LFC for a dual-area power system considering nonlinearities, based on Fuzzy-PID controller is presented in [21]. A design of LFC using an Internal Model Control-PID controller for a dual-area reheat hydro-thermal power system is marked out in [22]. The performance of AGC for

a dual-area interconnected power network with nonlinearities using Differential Evolution (DE) algorithm-based PI and PID controllers is studied in [23].

The issues related to LFC in three-area power systems are reviewed in [24-27]. The dynamic performance of LFC-based fuzzy intelligence of a three-area interconnected power network is presented in [24]. A design of LFC robust fractional order $PI^\lambda D$ (λ is the order of integration) controller with derivative filter action for a three-area reheat thermal power system is investigated in [25]. Implementation of a neuro-fuzzy controller-based LFC in a three-area hydrothermal system is tested in [26] under different load conditions. An efficient Model Predictive Control (MPC) design to control the frequency in a three-area power system comprising nine power plants is proposed in [27].

To maintain the fluctuation in frequency within a permissible limit, large power systems interconnected via tie lines are commonly partitioned into several areas. The first LFC work proposed for a four-area hydropower system based on a generalized approach combines the concepts of dual-mode control, discontinuous control, and variable structure systems is presented in [28], the proposed design takes into consideration the system nonlinearities. In reference [29], PI controller-based fuzzy gain scheduling is employed for LFC in a four-area power network is illustrated. The implementation of a modified version of Bat Algorithm (BA) along with fuzzy logic utilized to find the optimal gains of PI controllers employed for LFC in a four-area power network is addressed in [30].

2.4.2 Modern Power Systems

Owing to the depletion of fossil fuels, distributed generation from renewable energy sources has emerged as an effective solution to meet the rapid increase in demand. The control and stability of modern power systems have also been influenced by new conceptualizations such as smart grid, micro grid, and deregulation approach. Several new control methods are therefore proposed to mitigate the consequences of the uncertainty and complexity of modern power systems. Thus, concerns associated with modern power systems are discussed in this subsection.

2.4.2.1 Regulated and Deregulated Power Systems

The power sector is heading in a direction that helps to reduce generation and distribution costs, cope with inefficiencies, delegate obligations, and to offer more options for customers in a competitive market [31]. This direction is driven by the deregulation strategy, which was firstly introduced on 24 April 1996, when Order 888 was issued by the

United States federal energy regulatory commission, a ruling on open access transmission and then applied in different power systems around the world [32].

In traditional (regulated) power systems, the operating stages of the electric power run and are owned by a single unit called “Vertically Integrated Utility” (VIU), which supplies the electric power to the end-users at defined prices [33]. In the new configuration (deregulation), the former VIU is divided into independent companies; generation, transmission, and distribution companies each of which has its own tasks and is supervised by a unit called Independent System Operator (ISO). The following are the main benefits of this structure [34] [35] [36]:

- To provide more available choices for customers.
- To provide a suitable context to deliver better services.
- To offer the right pricing for customers.
- To provide a higher competitive quality.

LFC of the Norway and Sweden power system, which represents a real deregulated (restructured) environment is introduced in [37]. Based on the decentralized strategy, a hybrid Differential Evolution and Pattern Search (DE–PS) algorithm for load frequency control under deregulated power system with Unified Power Flow Controller (UPFC) and Redox Flow Batteries (RFB) is presented in [38]. A fuzzy logic controller is used to control the frequency in a deregulated two-area power system is presented in [39]. An implementation of LFC based optimal sliding mode controller equipped in a two-area restructured power system is proposed in [40].

2.4.2.2 Power Systems with HVDC Links

As High Voltage Direct Current (HVDC) links are preferable in a technical and economic point of view, this type of link is the most utilized to transfer the electric power a long distance in different power systems. In [41], an investigation of the influence of HVDC transmission on LFC in the interconnected south Mediterranean region is presented. LFC-based Genetic Algorithm (GA) tuned different controllers is used in a two-area power system connected by HVAC/HVDC is addressed in [42].

2.4.2.3 Distributed Generation (DG), Renewable Energy, and Energy Storage Systems (ESSs)

Due to their characteristics of aiding in reducing the emission and greenhouse issues, Distributed Generation (DG), as well as Renewable Energy Resources (RERs) have recently attracted considerable attention. DG is an economic and affordable solution to supply regions

where electricity is not accessible from the grid. Although DG represents a relatively slight fraction of total power, its penetration level in modern power systems is to be increased in the future [43].

In the merged use of diesel, solar, and wind hybrid power systems, variations in the speed of wind power plants and alterations in the radiation intensity of solar power plants result in a wide variance in the amount of produced power and frequency of the system. In addition, the wide contribution of RERs in nowadays power systems plays a vital role in decreasing the total system inertia, which has a direct impact on the systems' capabilities to keep the frequency fluctuations within permissible limits when the system experiences a sudden disturbance. This brings about the challenges of LFC becoming more complex. Indeed, RERs are to be combined with energy storage systems to create a hybrid system for enhanced efficiency and better coordination, hence reducing individual operational limitations [44].

Particle swarm optimization algorithm-based H_{∞} controller is employed to damp the frequency variation in an isolated hybrid DG system comprising diverse energy plants along with an energy storage system is studied in [45]. The impact of the generated power by Photovoltaic (PV) on the required capacity for LFC is presented in [46]. An investigation is carried out in [47] to examine the impacts of small wind turbines on LFC. LFC based on two-level control approach is proposed for a wind farm with 37 variable speed wind turbines is demonstrated in [48]. The implementation of a Doubly Fed Induction Generator (DFIG) in coordination with a Linear Quadratic Regulator (LQR) for load frequency control in a dual-area power model is marked out in [49].

LFC for different power system models equipped with Energy Storage Systems (ESS) is extensively investigated. The influence of a Battery Energy Storage System (BESS) on LFC tasks employed in a dual-area power system considering nonlinearity aspects is demonstrated in [50]. A new approach using superconducting magnetic energy storage coordinated with flexible AC transmission system devices based on static synchronous series compensator for LFC in a dual area reheat thermal power network is marked out in [51]. LFC of a dual-area power system using Capacitive Energy Storage (CES) and a multi-stage controller based on fuzzy logic is investigated in [52]. The proposed design has asserted better results than the other investigated approaches and the use of CES units has contributed to alleviating system oscillations.

2.4.2.4 Micro Grid

The concept of micro grid was introduced to harmonize local electricity production and consumption. The considerable growth in using RERs and DG has caused the increased interest in micro grids [53]. Robust PI control for LFC in a remote micro grid with the contribution of water heater is discussed in [54]. Based on Model Predictive Control (MPC) with communication delay, LFC in multiple micro grids is presented in [55].

2.4.2.5 Smart Grid

In order to develop the concept of smart grids, a great deal has been accomplished in recent years. Several studies have concluded that, when viewed at a high level, smart grid's benefits outweigh its costs [56]. The key benefits and other potential issues concerning the smart grid are explained in [57]. LFC for a four-area smart grid power system considering the impact of RERs and Electric Vehicles (EVs) based on advanced control methods is presented in [58]. It is approved from the obtained results that the fractional-order PID tuned by fuzzy logic controller offers better performance than the other investigated approaches. An LFC structure of a smart grid power system is presented in [59], this approach is designed to overcome the drawback of intermittency. References [60] and [61] present potential challenges of cyber-attacks on LFC in future smart grids such as resonance and Denial-of-Service attacks.

2.4.2.6 Non linear elements and Time Delay impacts on LFC systems

The important constraints which affect the power system performance are time delay, Generation Rate Constraint (GRC), and Governor Dead Band nonlinearity (GDB). GDB is defined as the total amount of a continued speed change within which there is no change in valve position. The effect of GDB is to increase the apparent steady state speed regulation [3]. The effects of the GDB on power system dynamics and frequency control were studied in recent decades [62]–[64]. for example, study presented in [62] proposes a fractional order PID controller for LFC in a two-area power system with and without the consideration of GDB. The results indicate that the performance of the LFC system can be affected in the case of wide dead band. However, the FOPID controller showed a good performance in both cases. Generation rate constraint (GRC) is a physical constraint that means practical limit on the rate of the change in the generating power due to physical limitations of turbine [65]. Results of investigation of the impact of GRC on LFC performance are reported in [25][27][66][67]. Owing to the growing complexity of power systems in deregulated environment,

communication delays become a significant challenge in the LFC analysis. Time delays can degrade a system's performance and even cause system instability.

Owing to the restructuring, expanding of physical setups, functionality, and complexity of power systems, the communication delays in the LFC synthesis/analysis are becoming a more significant challenge. In the control systems, it is well known that time delays can degrade the system's performance and even causes system instability [68]. The time delays in a secondary control system mainly exist on the communication channels between the control center and operating stations; specifically on the measured frequency and power tie-line flow from remote terminal units to the control center and the delay on the produced rise/lower signal from control center to individual generation units. The introduction of time delays in the secondary control loop reduces the effectiveness of controlled system performance [3]. Recently, several papers have been published to address the LFC modeling/synthesis in the presence of communication delays [69][70]. The impact of GRC, GDB and time delay on LFC performance and power system stability still need to be investigated to minimize their impact and improve the overall system performance.

2.5 Control Strategies

2.5.1 Centralized Control Approach

Several LFC techniques based on the centralized strategy in different power system models are reported in many studies. Elgerd and Fosha [71] proposed a feedback and loop gain to damp the frequency fluctuations. This technique was based on a state variable model and a state regulator problem of optimal control theory which also reported in [72]. A centralized LFC-based PID controller equipped in a dual-area multi-source power system is studied in [73]. The main limitation of this approach is the necessity to send and receive information between different control areas which may not be applicable.

2.5.2 Decentralized Control Approach

The decentralized concept for LFC in power systems was introduced as a solution to overcome the limitation of the centralized approach. Due to its simplicity and applicability, the decentralized control method is the best option for LFC in wide power systems as it decreases the computational burden and communication elaboration. In this approach, complex large power systems are divided into several subsystems where every subsystem has its own controller. In the case of a multi-area multi-source power system, there are two options for decentralization; a controller regulates each area, or each source has its own controller. Dong in [74] presented a decentralized LFC for a two-area interconnected power

system with nonlinearities using sliding mode control applied in each area of the system. A decentralized design based on integer and non-integer Internal Model Control (IMC) controllers using the simplified decoupling technique is proposed in [75] for LFC in a dual-area power system. A new decentralized LFC design based on switching control theory in a dual-area power system is studied in [76]. In [77], a decentralized adaptive deadbeat-based control for load frequency control in interconnected zones north and south of Scotland represents a part of the GB power system is presented.

Due to its advantages over the centralized, this approach is widely used and investigated. Notwithstanding its merits, one aspect should be highlighted; as the total power flow fluctuation through the tie lines linked the areas together is required to construct the control signal, and as this signal is not locally measured, this approach is not fully decentralized.

2.6 Classifications of LFC According to Various Control Techniques

In recent decades, different control techniques are proposed, various controllers are also developed and then successfully implemented to solve the problem of frequency deviation in an effective manner. With time, and as power systems are getting more complex, many control theories are proposed to meet the new challenges of modern power systems, thus several new hybrid techniques are introduced. An updated review of the suggested controllers for LFC is categorized and investigated in this subsection.

2.6.1 Classical Control Methods

Most research studies in the field of LFC are dedicated to the use of traditional controllers. In classical control methodologies, Bode, Nyquist, and root locus are typically used to obtain the optimal gains and phase margins. PID is the most widely used approach with 90% or more of the control loops in industries are based on traditional control models [78].

The classical PI is proposed for the LFC in a single-area electrical power system having a communication delay. The analytico-graphical criteria based on the stability boundary locus is used for obtaining the PI parameters [79]. Design and implementation of dual-mode PI controller tuned by Hooke-Jeeve's algorithm for LFC in a two-area power system is presented in [80]. The improvement impact on the delay margin when a fractional-order proportional-integral (PI^λ) controller is employed in a single-area-delayed LFC system is studied in [81]. PI controller parameters are optimized by different optimization techniques used for LFC in

a three-area interconnected system was illustrated in [82]. It is found that the integral gain must be precisely tuned to provide a balance between the desired transient response and the lowest possible overshoot in the dynamic performance of the investigated system.

LFC based on PID and fractional-order Proportional Integral Derivative ($PI^\lambda D^\mu$, where λ is the order of integration and μ is the order of differentiation) tuned by Moth Flame Optimization (MFO) of single and dual-area power systems is investigated in [83]. It is indicated that $PI^\lambda D^\mu$ has offered better performance than PID to damp the frequency oscillation and tie line power. A design and implementation of three degree-of-freedom PID controller is presented for LFC in a hybrid energy distributed power system [84]. A PID controller is utilized in a dual-area power system for LFC purposes, where a Losi Map-Based Chaotic Optimization Algorithm (LCOA) is suggested to optimally tune the values of the PID parameters [85]. Performances of Proportional Integral Double derivative (PIDD) and other classical controllers employed for LFC in a dual-area interconnected power network are studied in [86], it is revealed that PIDD controller offers a better dynamic response than the other investigated controllers.

Despite the wide range of its advantages, more realistic techniques to tune the parameters of this approach is required. It is also essential to improve the limitation of this approach against the systems' uncertainty.

2.6.2 Optimal and Suboptimal Control

Optimal control concepts are introduced as a simplified solution for large multivariable control issues. This type of controller is based on the state variable model and the minimization of the cost function. The first attempt in this approach for LFC was introduced in 1970 by Elgerd and Fosha, it was based on a state variable model to introduce new feedback control laws [71].

In order to design appropriate feedback control signals, the state variables of the investigated system should be known. An optimal output feedback technique, which utilizes only the measurable state variables is proposed to control the frequency deviation in a two-area thermal power system is proposed in [87]. An optimal approach combined the control methodologies of LFC and economic dispatch strategy in a 4-area interconnected power system with diverse energy sources in the presence of system constraints was presented in [88]; the simulation results reveal that the proposed design assures superior performance in comparison with the traditional approaches. Owing to the practical limitations of this

approach, suboptimal LFC was introduced to overcome these limitations. Suboptimal and near-optimal control for LFC in a dual-area power system is studied in [89].

Optimal controller approaches have proven many merits and might take a dominant role for LFC in the future if their design could include the dynamic states of the power system in real-time and potential cyber-attack challenges are considered.

2.6.3 Adaptive Control

Adaptive control has attracted many researchers in the recent four decades. This approach is classified into two groups: Self-Tuning Regulator (STR) as well as the most common adaptive type “Model Reference Adaptive Control (MRAC)”. The role of this approach is to reduce the sensitivity of the system under control to plant parameter changes and un-modelled plant dynamics. Several adaptive control techniques were investigated for LFC in different power systems. LFC relies on adaptive hierarchical control approach based on STR in a three-area power system is presented in [90]. The superiority of a multi-area adaptive LFC based on STR for a three-area interconnected power system is investigated in [91]. Reference [92] presents the implementation of adaptive LFC on the Hungarian power system. A design of adaptive LFC with dual-rate sampling for a two-area reheat thermal power system is marked out in [93]. In reference [94], an adaptive LFC based on Least Square Method (LSM) of a two-area interconnected power system is studied. MRAC with Neural Network (NN) for LFC of a hybrid micro grid power system under sudden load changes is proposed in [95], this scheme has successfully damped out the fluctuations and reduced the time response. A robust adaptive LFC considering system parametric uncertainties is investigated in [96], this study combined the standard robust control approach, Riccati equation approach and MRAC to achieve a good performance.

Notwithstanding the notable merits of this approach, they are complicated, and an ideal model following conditions of the controlled plant is essential to implement this type.

2.6.4 Robust Control

Researchers have investigated LFC approaches based on robust control design. This is due to their advantages, in terms of stability and robustness against plant uncertainties and changes in system parameters. Robust control problems including H_∞ control, multi-objective control problem via mixed H_2/H_∞ control technique and the μ synthesis are the main theories considered to design a robust control.

Robust LFC controller based on H_∞ methodologies enhanced with integral action and pole clustering is presented in [97]. H_∞ design is proposed in [98] to damp the frequency variations and tie-line power error in two and three- area interconnected power systems, Linear Matrix Inequality (LMI) approach is used to design of output-feedback H_∞ controller. The implementation of a robust μ -synthesis technique for LFC in a micro-grid power system is illustrated in [99]. H_∞ and μ -synthesis robust control techniques are used to develop the secondary frequency control loop in Islanded Micro Grid (IMG) [100], It is shown that the μ -synthesis approach due to considering structured/parametric uncertainties provides better performance than the H_∞ control method.

The advantages of this approach in handling parametric uncertainty are approved. However, robust controller design requires a good knowledge of the investigated system, which is unachievable in most power systems.

2.6.5 Sliding Mode Control (SMC)

The SMC follows the concept of Variable Structure Control (VSC). This approach was initially introduced at the beginning of the 1950s. Subsequently, this controller has received considerable attention from researchers, with the aim of employing it on different applications and benefiting from its numerous advantages. SMC was also considerably utilized to solve the problem of LFC in power systems. A design of sliding mode control for a single area power system is proposed in [101], this system comprises a wind turbine as a renewable energy resource. A discrete-SMC design for LFC in a four-area interconnected power system is presented in [102]. In [103], the authors have proposed SMC design for different power systems, the parameters of the controller are optimized by Particle Swarm Optimization (PSO) and Grey Wolf Optimization (GWO) algorithm. The author in [104] has proposed a new full-order SMC method for LFC in three different power systems. Furthermore, a sliding mode controller tuned by TLBO is suggested in [105] for LFC in an unequal dual-area multi-source power system. A design of second-order integral sliding mode control employed for LFC in a two-area power system is introduced in [106]. In [107], a highly robust observer sliding mode controller is proposed for LFC in a three-area power system integrated with two wind turbine plants. Second-order SMC combined with state estimator has recently been proposed for LFC in a two-area interconnected power system [108].

2.6.6 Artificial Intelligence Techniques

In the recent past, the integration of renewable energy sources has led to increasing the size and the structural complexity of power systems. The traditional or robust control may

not be sufficient to achieve the desired level of accurate operation. In order to address this issue, soft computing techniques such as Artificial Neural Network (ANN), fuzzy logic control, and soft computing based on optimization algorithms have been used to solve this problem to a great extent. A concise review of these approaches is provided in the following paragraphs.

Artificial Neural Network (ANN) is a concept motivated by biological nervous systems. The implementation of the ANN controller to enhance the dynamic performance of LFC in a three-area interconnected power system is studied in [109], ANN is utilized to tune the proportional and integral gains of PI controller. ANN observer-based nonlinear sliding mode control designed for load frequency control in a dual-area power system is presented in [110]; ANN observer is employed to estimate power plant unmeasured states and unmatched perturbations. A layered recurrent ANN based LFC in a dual-area interconnected power system with DFIG is illustrated in [111].

Due to its robustness and reliability, fuzzy logic control approach is applied to deal with complex and nonlinear control problems that cannot be addressed efficiently by traditional control methods. Fuzzy Logic Controllers (FLCs) can be designed and implemented without modelling the controlled process. This approach has widely been used for various LFC challenges in power systems. Design and implementation of fuzzy-based hierarchical approach to improve the frequency control performance in the Great Britain power system is investigated in [11]. Hence, the proposed design asserts its robustness against different load conditions and parameters uncertainty of the investigated system. In [112], PI controller incorporated with fuzzy logic gain scheduling technique based on two-level control strategy has been successfully employed for LFC in a dual-area power system. Using fuzzy self-tuning PID controller based on Tribe-Differential Evolution (TDE) algorithm, LFC for an interconnected two-area power system is proposed in [113]. The authors in [114] proposed a novel approach to enhance the frequency performance of a hybrid dual-area power system via coordination between an optimized fuzzy fine-tuning scheme and Gate-Controlled Series Capacitors (GCSC).

In order to guarantee reliable control and desirable dynamic system performances, soft computing based on optimization algorithms techniques has been considerably used in LFC loop to optimally tune the controllers' parameters. In the last decade, many researchers have investigated the control and stability of power systems using different algorithms such as

Genetic Algorithms (GA), Firefly Algorithm (FA), and Teaching-Learning-Based Optimization (TLBO).

Genetic Algorithm (GA) is one of the most widely utilized algorithms to address different issues in the field of power systems. The successful implementation of GA to optimize the parameters of a fuzzy controller used for LFC in a dual-area power system with a Photovoltaic Solar Power Plant (PV-SPP) connected is marked out in [115]. A combination of fuzzy logic, GA, and NNs for LFC in a single-area power system is presented in [116], the developed design is used to restore the frequency to its nominal value whenever there is any disturbance in load demand or losing a generation unit. In [117], the decentralized LFC synthesis is formulated as a multiobjective optimization problem (MOP) and is solved using GA to design well-tuned PI controllers in multi-area power system.

Particle swarm optimization (PSO) algorithm has attracted considerable attention since its introduction in 1995 by Kennedy and Eberhart. A design of adaptive deadbeat controller for LFC in the simplified Scottish power system is investigated in [77], in order to guarantee a robust performance of the proposed controller that meets the requirements of the national grid system operator, the controller's optimal gains are optimized using PSO. A design and implementation of Fuzzy PI controller based on a hybrid of GA and PSO for LFC in a two-area interconnected power system is demonstrated in [118], the achieved results reveal the superiority of the proposed design over both GA and PSO.

Firefly algorithm (FA) [119] has also been used to solve the issues associated with LFC in several power systems. Firefly algorithm tuned Fuzzy logic based on Two-Degree Of Freedom PID (F2DOFPID) controller is employed to damp the frequency fluctuations and control the tie lines power flow in an interconnected diverse-sourced multi-area power system is considered in [120]. FA tuned PI controller-based LFC of a two-area system comprising a photovoltaic system is investigated in [121]. Hybridization of an improved version of FA and Pattern Search (hIFA-PS) tuned the optimal gains of fuzzy aided PID controller to damp out the frequency deviation in a five-area power system comprising ten power units taking into account the nonlinearity constraints of the investigated system is presented in [122]. In addition to the approved superiority of the proposed design over other previous suggested techniques, there is no need to retune the parameters of the proposed controller when the system experiences different load conditions or parameters uncertainties.

Many researchers have proposed several LFC techniques using Differential Evolution (DE) algorithm. In reference [123], design and implementation of DE tuned Proportional Integral controller for LFC equipped in a dual-area nonlinear hydro-thermal power system is investigated, load disturbance was applied in each area to examine the performance of the system. In reference [124], DE is used to find the optimal gains of fuzzy PID integrated with derivative Filter (PIDF) for LFC in a two-area six-unit interconnected deregulated power system. A hybrid DE and Pattern Search (PS) is used to tune the parameters of the Modified Integral Derivative (MID) controller for LFC in a dual-area six-source power system considering physical constraints is proposed in [38].

The first introduction of Teaching–Learning Based Optimization (TLBO) algorithm was in 2010. Since then, this algorithm is used in many engineering and science fields. This is due to its merits, such as simple concept, without algorithm-specific parameters and easy implementation [125]. The first use of TLBO algorithm for LFC is presented in [126], in this study, TLBO is used to obtain the optimal gains of fuzzy-PID controller equipped in a two-area interconnected thermal power system. In reference [105], output feedback sliding mode controller (SMC) in which its parameters are optimized by TLBO is investigated for LFC of a dual-area thermal power system. The implementation of TLBO in this work is to optimize the feedback gain and switching vector of output feedback SMC. In [127], a hybrid algorithm based on Local Unimodal Sampling (LUS) and TLBO is proposed to effectively optimize the gains of a decentralized fuzzy-PID controller equipped in a dual-area six-source power system to solve the problem of LFC.

Besides all these techniques, other algorithms such as Ant Lion Optimizer algorithm, Bacterial Foraging Optimization, Grey Wolf Optimizer algorithm, and Artificial Bee Colony, have also been implemented to tune several controllers' parameters to solve the challenges of LFC in different power systems [128]–[131].

LFC methods based on AI techniques have shown their strength to provide outstanding performance in handling the system nonlinearities and modelling uncertainties under various operating conditions as their noteworthy advantage is that an accurate model of the system is not required.

2.6.7 Other Control Approaches for LFC

Linear Quadratic Regulator (LQR) methodology based LFC in a restructured power system is marked out in [123][124]. Model Predictive Control strategy (MPC) is employed to control the frequency perturbation in the Egyptian power system equipped with renewable

energy resources with inherent nonlinearities, the obtained results assert the superior robustness of MPC scheme over the conventional PI controller tuned by PSO algorithm [134]. LFC based pole-placement controllers are studied in [126][127]. Linear matrix inequalities (LMI) approach based LFC equipped in a three-area power model is studied in [137], the robustness of this controller is investigated with respect to different types of communication delay. Coefficient Diagram Method (CDM) is one of several techniques that has attracted less attention to overcome LFC problems [138]. A combination of this approach with ecological optimal technique is introduced in [139] for LFC of a three-area power system.

2.7 Summary

In power systems, LFC is an essential ancillary service to provide customers with sufficient and reliable electric power. In this chapter, a comprehensive and recent up to date literature survey on LFC for power systems is presented. Owing to their scale, LFC for conventional power system models are surveyed. In addition, this work highlighted the recent development of LFC methodologies for different features of modern power systems such as deregulated power systems, smart grids, micro grids, and modern power systems equipped with renewable energy resources are investigated. Moreover, various control strategies have been discussed in a very concise way. Finally, several control approaches are reviewed for LFC in different power systems. The advantages and potential drawbacks of each approach are also elaborated. It is revealed that LFC based on the decentralized approach using soft computing techniques in coordination with renewable energy resources is the most investigated challenge that needs more improvement as it is the most widely used in modern power systems.

From this literature review, it is concluded that potential improvement in LFC systems based on soft computing techniques is a research gap to be further investigated. Therefore, to the best of my knowledge, no attempt has been made to utilize the Bees Algorithm (BA) in designing the secondary frequency control of a power system. Since this algorithm has demonstrated a high level of superiority and effectiveness as an optimization tool in many different fields, this promising achievement motivated the author to make use of this very powerful optimization technique to determine the optimum parameters' gains of the PID, FOPID and SMC and different fuzzy logic control structures for LFC in different power systems. The following chapter summarizes the mechanism and application of the BA. To prove the validity of the proposed techniques, these controllers are equipped in two different widely investigated power systems, namely, the simplified GB power system and a two-area

interconnected power system. Further, due to its wide merits, the decentralized strategy is considered.

2.8 References

- [1] H. Haes Alhelou, M. E. Hamedani-Golshan, R. Zamani, E. Heydarian-Forushani, and P. Siano, “Challenges and opportunities of load frequency control in conventional, modern and future smart power systems: A comprehensive review,” *Energies*, vol. 11, no. 10, 2018, doi: 10.3390/en11102497.
- [2] J. A. Momoh, *Electric Power System Applications of Optimization*. CRC Press, 2000.
- [3] H. Bevrani, *Robust Power System Frequency Control*. Cham: Springer International Publishing, 2014.
- [4] F. M. Gonzalez-Longatt and J. Luis Rueda, Eds., *PowerFactory Applications for Power System Analysis*. Cham: Springer International Publishing, 2014.
- [5] H. Bevrani and T. Hiyama, *Intelligent Automatic Generation Control*. CRC Press, 2017.
- [6] X.-F. Wang, Y. Song, and M. Irving, *Modern Power Systems Analysis*. Boston, MA: Springer US, 2008.
- [7] B. M. Weedy, B. J. Cory, N. Jenkins, J. B. Ekanayake, and G. Strbac, *Electric Power Systems Fifth Edition*, 5th ed. West Sussex: John Wiley & Sons Ltd, 2015.
- [8] J. D. Glover, M. S. Sarma, and T. Overbye, *Power Systems Analysis and Design*. Australia: Thomson, 2008.
- [9] P. M. Anderson and A. A. Fouad, *Power system control and stability*, Second. New York: Institute of Electrical and Electronics, 2008.
- [10] P. Kundur, N. Balu, and M. Lauby, *Power system stability and control*. New York: McGraw-Hill, 1994.
- [11] Z. A. Obaid, L. M. Cipcigan, and M. T. Muhssin, “Fuzzy hierarchal approach-based optimal frequency control in the Great Britain power system,” *Electr. Power Syst. Res.*, vol. 141, pp. 529–537, Dec. 2016, doi: 10.1016/j.epsr.2016.08.032.
- [12] A. J. Wood and Bruce F. Wollenberg Gerald B. Sheblé, *Power Generation, Operation, and Control*. New Jersey: Wiley, 2014.

- [13] M. T. Muhssin, “Adaptive Control and Dynamic Demand Response for the Stabilization of Grid Frequency,” Cardiff University, 2018.
- [14] C. Ismayil, K. R. Sreerama, and T. K. Sindhu, “Automatic Generation Control of Single Area Thermal Power System with Fractional Order PID ($PI\lambda D\mu$) Controllers,” *IFAC Proc. Vol.*, vol. 47, no. 1, pp. 552–557, 2014, doi: 10.3182/20140313-3-IN-3024.00025.
- [15] S. Doolla and T. S. Bhatti, “Load Frequency Control of an Isolated Small-Hydro Power Plant With Reduced Dump Load,” *IEEE Trans. Power Syst.*, vol. 21, no. 4, pp. 1912–1919, Nov. 2006, doi: 10.1109/TPWRS.2006.881157.
- [16] B. Mohanty, S. Panda, and P. K. Hota, “Controller parameters tuning of differential evolution algorithm and its application to load frequency control of multi-source power system,” *Int. J. Electr. Power Energy Syst.*, vol. 54, pp. 77–85, Jan. 2014, doi: 10.1016/j.ijepes.2013.06.029.
- [17] E. Rakhshani, K. Rouzbehi, and S. Sadeh, “A New Combined Model for Simulation of Mutual Effects between LFC and AVR Loops,” in *2009 Asia-Pacific Power and Energy Engineering Conference*, Mar. 2009, pp. 1–5, doi: 10.1109/APPEEC.2009.4918066.
- [18] S. A. Rahim, S. Ahmed, and M. Nawari, “A Study of Load Frequency Control for Two Area Power System Using Two Controllers,” in *2018 International Conference on Computer, Control, Electrical, and Electronics Engineering (ICCCEEE)*, Aug. 2018, pp. 1–6, doi: 10.1109/ICCCEEE.2018.8515892.
- [19] M. Hajjakerbari Fini, G. R. Yousefi, and H. Haes Alhelou, “Comparative study on the performance of many-objective and single-objective optimisation algorithms in tuning load frequency controllers of multi-area power systems,” *IET Gener. Transm. Distrib.*, vol. 10, no. 12, pp. 2915–2923, Sep. 2016, doi: 10.1049/iet-gtd.2015.1334.
- [20] M. Mostafa Elsaied, M. Abdallah Attia, M. Abdelhamed Mostafa, and S. Fouad Mekhamer, “Application of Different Optimization Techniques to Load Frequency Control with WECS in a Multi-Area System,” *Electr. Power Components Syst.*, vol. 46, no. 7, pp. 739–756, Apr. 2018, doi: 10.1080/15325008.2018.1509913.
- [21] R. Ramjug-Ballgobin, S. Z. Sayed Hassen, and S. Veerapen, “Load frequency control

- of a nonlinear two-area power system,” in *2015 International Conference on Computing, Communication and Security (ICCCS)*, Dec. 2015, pp. 1–6, doi: 10.1109/CCCS.2015.7374172.
- [22] J. Singh, K. Chatterjee, and C. B. Vishwakarma, “Two degree of freedom internal model control-PID design for LFC of power systems via logarithmic approximations,” *ISA Trans.*, vol. 72, pp. 185–196, Jan. 2018, doi: 10.1016/j.isatra.2017.12.002.
- [23] B. Mohanty, S. Panda, and P. K. Hota, “Differential evolution algorithm based automatic generation control for interconnected power systems with non-linearity,” *Alexandria Eng. J.*, vol. 53, no. 3, pp. 537–552, Sep. 2014, doi: 10.1016/j.aej.2014.06.006.
- [24] S. K. Jain, A. Bhargava, and R. K. Pal, “Three area power system load frequency control using fuzzy logic controller,” in *2015 International Conference on Computer, Communication and Control (IC4)*, Sep. 2015, pp. 1–6, doi: 10.1109/IC4.2015.7375614.
- [25] A. Delassi, S. Arif, and L. Mokrani, “Load frequency control problem in interconnected power systems using robust fractional PI λ D controller,” *Ain Shams Eng. J.*, vol. 9, no. 1, pp. 77–88, Mar. 2018, doi: 10.1016/j.asej.2015.10.004.
- [26] L. C. Saikia, A. Paul, P. Dash, and N. B. Dev Choudhury, “AGC of an interconnected multi-area hydrothermal system using a neuro-fuzzy controller,” in *Proceedings of The 2014 International Conference on Control, Instrumentation, Energy and Communication (CIEC)*, Jan. 2014, pp. 407–411, doi: 10.1109/CIEC.2014.6959120.
- [27] M. Shiroei, M. R. Toulabi, and A. M. Ranjbar, “Robust multivariable predictive based load frequency control considering generation rate constraint,” *Int. J. Electr. Power Energy Syst.*, vol. 46, pp. 405–413, Mar. 2013, doi: 10.1016/j.ijepes.2012.10.039.
- [28] O. P. Malik, A. Kumar, and G. S. Hope, “A load frequency control algorithm based on a generalized approach,” *IEEE Trans. Power Syst.*, vol. 3, no. 2, pp. 375–382, May 1988, doi: 10.1109/59.192887.
- [29] C. S. Chang and W. Fu, “Area load frequency control using fuzzy gain scheduling of PI controllers,” *Electr. Power Syst. Res.*, vol. 42, no. 2, pp. 145–152, Aug. 1997, doi: 10.1016/S0378-7796(96)01199-6.

- [30] M. H. Khooban and T. Niknam, “A new intelligent online fuzzy tuning approach for multi-area load frequency control: Self Adaptive Modified Bat Algorithm,” *Int. J. Electr. Power Energy Syst.*, vol. 71, pp. 254–261, Oct. 2015, doi: 10.1016/j.ijepes.2015.03.017.
- [31] S. H. Shahalami and D. Farsi, “Analysis of Load Frequency Control in a restructured multi-area power system with the Kalman filter and the LQR controller,” *AEU - Int. J. Electron. Commun.*, vol. 86, pp. 25–46, Mar. 2018, doi: 10.1016/j.aeue.2018.01.011.
- [32] W. Tan, “Load frequency control: Problems and solutions,” in *Proceedings of the 30th Chinese Control Conference, CCC 2011*, 2011, pp. 6281–6286.
- [33] A. Pappachen and A. Peer Fathima, “Critical research areas on load frequency control issues in a deregulated power system: A state-of-the-art-of-review,” *Renew. Sustain. Energy Rev.*, vol. 72, pp. 163–177, May 2017, doi: 10.1016/j.rser.2017.01.053.
- [34] R. D. Christie and A. Bose, “Load frequency control issues in power system operations after deregulation,” *IEEE Trans. Power Syst.*, vol. 11, no. 3, pp. 1191–1200, 1996, doi: 10.1109/59.535590.
- [35] M. Esmail, R. Tzoneva, and S. Krishnamurthy, “Review of Automatic Generation Control in Deregulated Environment,” *IFAC-PapersOnLine*, vol. 50, no. 2, pp. 88–93, Dec. 2017, doi: 10.1016/j.ifacol.2017.12.016.
- [36] K. L. Lo and Y. S. Yuen, *Power System Restructuring and Deregulation*. Chichester, UK: John Wiley & Sons, Ltd, 2001.
- [37] B. H. Bakken and O. S. Grande, “Automatic generation control in a deregulated power system,” *IEEE Trans. Power Syst.*, vol. 13, no. 4, pp. 1401–1406, 1998, doi: 10.1109/59.736283.
- [38] R. K. Sahu, T. S. Gorripotu, and S. Panda, “A hybrid DE–PS algorithm for load frequency control under deregulated power system with UPFC and RFB,” *Ain Shams Eng. J.*, vol. 6, no. 3, pp. 893–911, Sep. 2015, doi: 10.1016/j.asej.2015.03.011.
- [39] Y. P. Verma and A. Kumar, “Load frequency control in deregulated power system with wind integrated system using fuzzy controller,” *Front. Energy*, vol. 7, no. 2, pp. 245–254, Jun. 2013, doi: 10.1007/s11708-012-0218-6.
- [40] T. A. Kumar and N. V. Ramana, “Design of optimal sliding mode controller for load

- frequency control in multi-area deregulated thermal system,” in *2012 International Conference on Emerging Trends in Electrical Engineering and Energy Management (ICETEEEM)*, Dec. 2012, pp. 44–51, doi: 10.1109/ICETEEEM.2012.6494442.
- [41] A. Haj Hamida, K. Ben-Kilani, and M. Elleuch, “HVDC transmission in the interconnected south mediterranean region - LFC control analysis,” in *2014 IEEE 11th International Multi-Conference on Systems, Signals & Devices (SSD14)*, Feb. 2014, pp. 1–7, doi: 10.1109/SSD.2014.6808833.
- [42] M. Mahdavian *et al.*, “Load frequency control for a two-area HVAC/HVDC power system using hybrid Genetic Algorithm controller,” in *2012 9th International Conference on Electrical Engineering/Electronics, Computer, Telecommunications and Information Technology*, May 2012, pp. 1–4, doi: 10.1109/ECTICon.2012.6254306.
- [43] T. Ackermann, G. Andersson, and L. Söder, “Distributed generation: a definition,” *Electr. Power Syst. Res.*, vol. 57, no. 3, pp. 195–204, Apr. 2001, doi: 10.1016/S0378-7796(01)00101-8.
- [44] D. B. Nelson, M. H. Nehrir, and C. Wang, “Unit sizing and cost analysis of stand-alone hybrid wind/PV/fuel cell power generation systems,” *Renew. Energy*, vol. 31, no. 10, pp. 1641–1656, Aug. 2006, doi: 10.1016/j.renene.2005.08.031.
- [45] V. P. Singh, S. R. Mohanty, N. Kishor, and P. K. Ray, “Robust H-infinity load frequency control in hybrid distributed generation system,” *Int. J. Electr. Power Energy Syst.*, vol. 46, pp. 294–305, Mar. 2013, doi: 10.1016/j.ijepes.2012.10.015.
- [46] H. Asano, K. Yajima, and Y. Kaya, “Influence of photovoltaic power generation on required capacity for load frequency control,” *IEEE Trans. Energy Convers.*, vol. 11, no. 1, pp. 188–193, Mar. 1996, doi: 10.1109/60.486595.
- [47] D. H. Curtice and T. W. Reddoch, “An Assessment of Load Frequency Control Impacts Caused by Small Wind Turbines,” *IEEE Trans. Power Appar. Syst.*, vol. PAS-102, no. 1, pp. 162–170, Jan. 1983, doi: 10.1109/TPAS.1983.318012.
- [48] J. L. Rodriguez-Amenedo, S. Arnalte, and J. C. Burgos, “Automatic generation control of a wind farm with variable speed wind turbines,” *IEEE Trans. Energy Convers.*, vol. 17, no. 2, pp. 279–284, Jun. 2002, doi: 10.1109/TEC.2002.1009481.

- [49] G. Pandey and S. Bhongade, "Participation of DFIG based wind turbine generator in Load Frequency Control with linear quadratic regulator," in *2014 Annual IEEE India Conference (INDICON)*, Dec. 2014, pp. 1–6, doi: 10.1109/INDICON.2014.7030610.
- [50] Chun-Feng Lu, Chun-Chang Liu, and Chi-Jui Wu, "Effect of battery energy storage system on load frequency control considering governor deadband and generation rate constraint," *IEEE Trans. Energy Convers.*, vol. 10, no. 3, pp. 555–561, 1995, doi: 10.1109/60.464882.
- [51] K. Chatterjee, R. Sankar, and T. K. Chatterjee, "SMES Coordinated with SSSC of an Interconnected Thermal System for Load Frequency Control," in *2012 Asia-Pacific Power and Energy Engineering Conference*, Mar. 2012, pp. 1–4, doi: 10.1109/APPEEC.2012.6307061.
- [52] Y. Arya, "AGC of PV-thermal and hydro-thermal power systems using CES and a new multi-stage FPIDF-(1+PI) controller," *Renew. Energy*, vol. 134, pp. 796–806, Apr. 2019, doi: 10.1016/j.renene.2018.11.071.
- [53] C. Yuen, A. Oudalov, and A. Timbus, "The Provision of Frequency Control Reserves From Multiple Microgrids," *IEEE Trans. Ind. Electron.*, vol. 58, no. 1, pp. 173–183, Jan. 2011, doi: 10.1109/TIE.2010.2041139.
- [54] C. S. Ali Nandar, "Robust PI control of smart controllable load for frequency stabilization of microgrid power system," *Renew. Energy*, vol. 56, pp. 16–23, Aug. 2013, doi: 10.1016/j.renene.2012.10.032.
- [55] X. Wang, Q. Zhao, B. He, Y. Wang, J. Yang, and X. Pan, "Load frequency control in multiple microgrids based on model predictive control with communication delay," *J. Eng.*, vol. 2017, no. 13, pp. 1851–1856, Jan. 2017, doi: 10.1049/joe.2017.0652.
- [56] S. Massoud Amin, "Smart Grid: Overview, Issues and Opportunities. Advances and Challenges in Sensing, Modeling, Simulation, Optimization and Control," *Eur. J. Control*, vol. 17, no. 5–6, pp. 547–567, Jan. 2011, doi: 10.3166/ejc.17.547-567.
- [57] A. Bari, J. Jiang, W. Saad, and A. Jaekel, "Challenges in the Smart Grid Applications: An Overview," *Int. J. Distrib. Sens. Networks*, vol. 10, no. 2, p. 974682, Feb. 2014, doi: 10.1155/2014/974682.
- [58] M. M. Ismail and A. F. Bendary, "Load Frequency Control for Multi Area Smart Grid

- based on Advanced Control Techniques,” *Alexandria Eng. J.*, vol. 57, no. 4, pp. 4021–4032, Dec. 2018, doi: 10.1016/j.aej.2018.11.004.
- [59] A. Keyhani and A. Chatterjee, “Automatic Generation Control Structure for Smart Power Grids,” *IEEE Trans. Smart Grid*, vol. 3, no. 3, pp. 1310–1316, Sep. 2012, doi: 10.1109/TSG.2012.2194794.
- [60] Y. Wu, Z. Wei, J. Weng, X. Li, and R. H. Deng, “Resonance Attacks on Load Frequency Control of Smart Grids,” *IEEE Trans. Smart Grid*, vol. 9, no. 5, pp. 4490–4502, Sep. 2018, doi: 10.1109/TSG.2017.2661307.
- [61] S. Liu, X. P. Liu, and A. El Saddik, “Denial-of-Service (dos) attacks on load frequency control in smart grids,” in *2013 IEEE PES Innovative Smart Grid Technologies Conference (ISGT)*, Feb. 2013, pp. 1–6, doi: 10.1109/ISGT.2013.6497846.
- [62] E. Çelik, “Design of new fractional order PI–fractional order PD cascade controller through dragonfly search algorithm for advanced load frequency control of power systems,” *Soft Comput.*, vol. 25, no. 2, pp. 1193–1217, Jan. 2021, doi: 10.1007/s00500-020-05215-w.
- [63] J. Morsali, K. Zare, and M. Tarafdar Hagh, “Comparative performance evaluation of fractional order controllers in LFC of two-area diverse-unit power system with considering GDB and GRC effects,” *J. Electr. Syst. Inf. Technol.*, vol. 5, no. 3, pp. 708–722, Dec. 2018, doi: 10.1016/j.jesit.2017.05.002.
- [64] S. M. Nosratabadi, M. Bornapour, and M. A. Gharaei, “Grasshopper optimization algorithm for optimal load frequency control considering Predictive Functional Modified PID controller in restructured multi-resource multi-area power system with Redox Flow Battery units,” *Control Eng. Pract.*, vol. 89, pp. 204–227, Aug. 2019, doi: 10.1016/j.conengprac.2019.06.002.
- [65] J. Morsali, K. Zare, and M. Tarafdar Hagh, “Appropriate generation rate constraint (GRC) modeling method for reheat thermal units to obtain optimal load frequency controller (LFC),” in *2014 5th Conference on Thermal Power Plants (CTPP)*, Jun. 2014, pp. 29–34, doi: 10.1109/CTPP.2014.7040611.
- [66] H. Shayeghi, A. Rahnama, R. Mohajery, N. Bizon, A. G. Mazare, and L. M. Ionescu, “Multi-Area Microgrid Load-Frequency Control Using Combined Fractional and

- Integer Order Master–Slave Controller Considering Electric Vehicle Aggregator Effects,” *Electronics*, vol. 11, no. 21, p. 3440, Oct. 2022, doi: 10.3390/electronics11213440.
- [67] A. A. Abou El-Ela, R. A. El-Sehiemy, A. M. Shaheen, and A. E.-G. Diab, “Design of cascaded controller based on coyote optimizer for load frequency control in multi-area power systems with renewable sources,” *Control Eng. Pract.*, vol. 121, p. 105058, Apr. 2022, doi: 10.1016/j.conengprac.2021.105058.
- [68] R. K. Sahu, S. Panda, and U. K. Rout, “DE optimized parallel 2-DOF PID controller for load frequency control of power system with governor dead-band nonlinearity,” *Int. J. Electr. Power Energy Syst.*, vol. 49, pp. 19–33, Jul. 2013, doi: 10.1016/j.ijepes.2012.12.009.
- [69] C. A. Macana, E. Mojica-Nava, and N. Quijano, “Time-delay effect on load frequency control for microgrids,” in *2013 10th IEEE INTERNATIONAL CONFERENCE ON NETWORKING, SENSING AND CONTROL (ICNSC)*, Apr. 2013, pp. 544–549, doi: 10.1109/ICNSC.2013.6548797.
- [70] X.-C. Shangguan, Y. He, C.-K. Zhang, L. Jiang, and M. Wu, “Load frequency control of time-delayed power system based on event-triggered communication scheme,” *Appl. Energy*, vol. 308, p. 118294, Feb. 2022, doi: 10.1016/j.apenergy.2021.118294.
- [71] O. Elgerd and C. Fosha, “Optimum Megawatt-Frequency Control of Multiarea Electric Energy Systems,” *IEEE Trans. Power Appar. Syst.*, vol. PAS-89, no. 4, pp. 556–563, Apr. 1970, doi: 10.1109/TPAS.1970.292602.
- [72] C. Fosha and O. Elgerd, “The Megawatt-Frequency Control Problem: A New Approach Via Optimal Control Theory,” *IEEE Trans. Power Appar. Syst.*, vol. PAS-89, no. 4, pp. 563–577, Apr. 1970, doi: 10.1109/TPAS.1970.292603.
- [73] N. Hakimuddin, A. Khosla, and J. K. Garg, “Centralized and decentralized AGC schemes in 2-area interconnected power system considering multi source power plants in each area,” *J. King Saud Univ. - Eng. Sci.*, vol. 32, no. 2, pp. 123–132, Feb. 2020, doi: 10.1016/j.jksues.2018.07.003.
- [74] L. Dong, “Decentralized load frequency control for an interconnected power system with nonlinearities,” in *2016 American Control Conference (ACC)*, Jul. 2016, pp.

- 5915–5920, doi: 10.1109/ACC.2016.7526597.
- [75] I. Kasireddy, A. W. Nasir, and A. K. Singh, “IMC based Controller Design for Automatic Generation Control of Multi Area Power System via Simplified Decoupling,” *Int. J. Control. Autom. Syst.*, vol. 16, no. 3, pp. 994–1010, Jun. 2018, doi: 10.1007/s12555-017-0362-1.
- [76] Y. Arya, “Automatic generation control of two-area electrical power systems via optimal fuzzy classical controller,” *J. Franklin Inst.*, vol. 355, no. 5, pp. 2662–2688, Mar. 2018, doi: 10.1016/j.jfranklin.2018.02.004.
- [77] M. T. Muhssin, L. M. Cipcigan, Z. A. Obaid, and W. F. AL-Ansari, “A novel adaptive deadbeat- based control for load frequency control of low inertia system in interconnected zones north and south of Scotland,” *Int. J. Electr. Power Energy Syst.*, vol. 89, pp. 52–61, Jul. 2017, doi: 10.1016/j.ijepes.2016.12.005.
- [78] Š. Kozák, “State-of-the-art in control engineering,” *J. Electr. Syst. Inf. Technol.*, vol. 1, no. 1, pp. 1–9, May 2014, doi: 10.1016/j.jesit.2014.03.002.
- [79] S. Saxena and Y. V. Hote, “PI Controller Based Load Frequency Control Approach for Single-Area Power System Having Communication Delay,” *IFAC-PapersOnLine*, vol. 51, no. 4, pp. 622–626, 2018, doi: 10.1016/j.ifacol.2018.06.165.
- [80] K. Chatterjee, “Design of Dual Mode PI Controller for Load Frequency Control,” *Int. J. Emerg. Electr. Power Syst.*, vol. 11, no. 4, Sep. 2010, doi: 10.2202/1553-779X.2452.
- [81] V. ÇELİK, M. T. ÖZDEMİR, and K. Y. LEE, “Effects of fractional-order PI controller on delay margin in single-area delayed load frequency control systems,” *J. Mod. Power Syst. Clean Energy*, vol. 7, no. 2, pp. 380–389, Mar. 2019, doi: 10.1007/s40565-018-0458-5.
- [82] N. Kumari, N. Malik, J. A. N., and G. Malleshham, “Design of PI Controller for Automatic Generation Control of Multi Area Interconnected Power System Using Bacterial Foraging Optimization,” *Int. J. Eng. Technol.*, vol. 8, no. 6, pp. 2779–2786, Dec. 2016, doi: 10.21817/ijet/2016/v8i6/160806236.
- [83] K. Saurabh, N. K. Gupta, and A. K. Singh, “Fractional Order Controller Design for Load Frequency Control of Single Area and Two Area System,” in *2020 7th International Conference on Signal Processing and Integrated Networks (SPIN)*, Feb.

- 2020, pp. 531–536, doi: 10.1109/SPIN48934.2020.9070993.
- [84] D. Guha, P. K. Roy, and S. Banerjee, “Optimal tuning of 3 degree-of-freedom proportional-integral-derivative controller for hybrid distributed power system using dragonfly algorithm,” *Comput. Electr. Eng.*, vol. 72, pp. 137–153, Nov. 2018, doi: 10.1016/j.compeleceng.2018.09.003.
- [85] S. Ganjefar, M. Alizadeh, and M. Farahani, “PID controller adjustment using chaotic optimisation algorithm for multi-area load frequency control,” *IET Control Theory Appl.*, vol. 6, no. 13, pp. 1984–1992, Sep. 2012, doi: 10.1049/iet-cta.2011.0405.
- [86] L. C. Saikia, S. Debbarma, M. Pathak, D. J. Borah, K. K. Kumar, and M. Kumar, “Automatic generation control of an interconnected thermal system using a new classical controller: A preliminary study,” in *2012 1st International Conference on Power and Energy in NERIST (ICPEN)*, Dec. 2012, pp. 1–6, doi: 10.1109/ICPEN.2012.6492327.
- [87] J. C. Geromel and P. L. D. Peres, “Decentralised load-frequency control,” *IEE Proc. D Control Theory Appl.*, vol. 132, no. 5, p. 225, 1985, doi: 10.1049/ip-d.1985.0039.
- [88] R. Patel, C. Li, L. Meegahapola, B. McGrath, and X. Yu, “Enhancing Optimal Automatic Generation Control in a Multi-Area Power System With Diverse Energy Resources,” *IEEE Trans. Power Syst.*, vol. 34, no. 5, pp. 3465–3475, Sep. 2019, doi: 10.1109/TPWRS.2019.2907614.
- [89] V. R. Moorthi and R. P. Aggarwal, “Suboptimal and near-optimal control of a load-frequency-control system,” *Proc. Inst. Electr. Eng.*, vol. 119, no. 11, p. 1653, 1972, doi: 10.1049/piee.1972.0329.
- [90] A. Rubaai, “Self-tuning load frequency control: multilevel adaptive approach,” *IEE Proc. - Gener. Transm. Distrib.*, vol. 141, no. 4, p. 285, 1994, doi: 10.1049/ip-gtd:19949964.
- [91] R. R. Shoults and J. A. Jativa Ibarra, “Multi-area adaptive LFC developed for a comprehensive AGC simulator,” *IEEE Trans. Power Syst.*, vol. 8, no. 2, pp. 541–547, May 1993, doi: 10.1109/59.260829.
- [92] I. Vajk, M. Vajta, L. Keviczky, R. Haber, J. Hetthéssy, and K. Kovács, “Adaptive load-frequency control of the hungarian power system,” *Automatica*, vol. 21, no. 2, pp.

- 129–137, Mar. 1985, doi: 10.1016/0005-1098(85)90108-6.
- [93] K. Yamashita, M. Hirayasu, K. Okafuji, and H. Mlyagi, “A design method of adaptive load frequency control with dual-rate sampling,” *Int. J. Adapt. Control Signal Process.*, vol. 9, no. 2, pp. 151–162, Mar. 1995, doi: 10.1002/acs.4480090204.
- [94] A. Beni Rehiara, N. Yorino, Y. Sasaki, and Y. Zoka, “An Adaptive Load Frequency Control Based on Least Square Method,” in *Advances in Modelling and Control of Wind and Hydrogenerators*, IntechOpen, 2020.
- [95] M. M. Mahdi, E. Mhawi Thajeel, and A. Z. Ahmad, “Load Frequency Control for Hybrid Micro-grid Using MRAC with ANN Under-sudden Load Changes,” in *2018 Third Scientific Conference of Electrical Engineering (SCEE)*, Dec. 2018, pp. 220–225, doi: 10.1109/SCEE.2018.8684061.
- [96] Y. Wang, “New robust adaptive load-frequency control with system parametric uncertainties,” *IEE Proc. - Gener. Transm. Distrib.*, vol. 141, no. 3, p. 184, 1994, doi: 10.1049/ip-gtd:19949757.
- [97] L. Dritsas, E. Kontouras, E. Vlahakis, I. Kitsios, G. Halikias, and A. Tzes, “Modelling issues and aggressive robust load frequency control of interconnected electric power systems,” *Int. J. Control*, vol. 95, no. 3, pp. 753–767, Mar. 2022, doi: 10.1080/00207179.2020.1821248.
- [98] F. U. A. Ahammad and S. Mandal, “Robust load frequency control in multi-area power system: An LMI approach,” in *2016 IEEE First International Conference on Control, Measurement and Instrumentation (CMI)*, Jan. 2016, pp. 136–140, doi: 10.1109/CMI.2016.7413726.
- [99] H. Li, X. Wang, and J. Xiao, “Differential Evolution-Based Load Frequency Robust Control for Micro-Grids with Energy Storage Systems,” *Energies*, vol. 11, no. 7, p. 1686, Jun. 2018, doi: 10.3390/en11071686.
- [100] H. Bevrani, M. R. Feizi, and S. Ataei, “Robust Frequency Control in an Islanded Microgrid: H_∞ and μ -Synthesis Approaches,” *IEEE Trans. Smart Grid*, pp. 1–1, 2015, doi: 10.1109/TSG.2015.2446984.
- [101] Y. Mi, Y. Fu, D. Li, C. Wang, P. C. Loh, and P. Wang, “The sliding mode load frequency control for hybrid power system based on disturbance observer,” *Int. J.*

- Electr. Power Energy Syst.*, vol. 74, pp. 446–452, Jan. 2016, doi: 10.1016/j.ijepes.2015.07.014.
- [102] K. Vrdoljak, N. Perić, and I. Petrović, “Sliding mode based load-frequency control in power systems,” *Electr. Power Syst. Res.*, vol. 80, no. 5, pp. 514–527, May 2010, doi: 10.1016/j.epsr.2009.10.026.
- [103] A. Kumar, M. N. Anwar, and S. Kumar, “Sliding mode controller design for frequency regulation in an interconnected power system,” *Prot. Control Mod. Power Syst.*, vol. 6, no. 1, p. 6, Dec. 2021, doi: 10.1186/s41601-021-00183-1.
- [104] J. Guo, “Application of full order sliding mode control based on different areas power system with load frequency control,” *ISA Trans.*, vol. 92, pp. 23–34, Sep. 2019, doi: 10.1016/j.isatra.2019.01.036.
- [105] B. Mohanty, “TLBO optimized sliding mode controller for multi-area multi-source nonlinear interconnected AGC system,” *Int. J. Electr. Power Energy Syst.*, vol. 73, pp. 872–881, Dec. 2015, doi: 10.1016/j.ijepes.2015.06.013.
- [106] V. Van Huynh *et al.*, “New Second-Order Sliding Mode Control Design for Load Frequency Control of a Power System,” *Energies*, vol. 13, no. 24, p. 6509, Dec. 2020, doi: 10.3390/en13246509.
- [107] V. Van Huynh, B. L. N. Minh, E. N. Amaefule, A.-T. Tran, and P. T. Tran, “Highly Robust Observer Sliding Mode Based Frequency Control for Multi Area Power Systems with Renewable Power Plants,” *Electronics*, vol. 10, no. 3, p. 274, Jan. 2021, doi: 10.3390/electronics10030274.
- [108] A.-T. Tran *et al.*, “Load Frequency Regulator in Interconnected Power System Using Second-Order Sliding Mode Control Combined with State Estimator,” *Energies*, vol. 14, no. 4, p. 863, Feb. 2021, doi: 10.3390/en14040863.
- [109] P. K. A. Kumar, R. Uthirasamy, G. Saravanan, and A. M. Ibrahim, “AGC performance enhancement using ANN,” in *2016 2nd International Conference on Contemporary Computing and Informatics (IC3I)*, Dec. 2016, pp. 452–456, doi: 10.1109/IC3I.2016.7918007.
- [110] S. Prasad and M. R. Ansari, “Frequency regulation using neural network observer based controller in power system,” *Control Eng. Pract.*, vol. 102, p. 104571, Sep.

- 2020, doi: 10.1016/j.conengprac.2020.104571.
- [111] G. Sharma, A. Panwar, Y. Arya, and M. Kumawat, "Integrating layered recurrent ANN with robust control strategy for diverse operating conditions of AGC of the power system," *IET Gener. Transm. Distrib.*, vol. 14, no. 18, pp. 3886–3895, Sep. 2020, doi: 10.1049/iet-gtd.2019.0935.
- [112] T. Hussein and A. Shamekh, "Design of PI Fuzzy Logic Gain Scheduling Load Frequency Control in Two-Area Power Systems," *Designs*, vol. 3, no. 2, p. 26, Jun. 2019, doi: 10.3390/designs3020026.
- [113] N. Jalali, H. Razmi, and H. Doagou-Mojarrad, "Optimized fuzzy self-tuning PID controller design based on Tribe-DE optimization algorithm and rule weight adjustment method for load frequency control of interconnected multi-area power systems," *Appl. Soft Comput.*, vol. 93, p. 106424, Aug. 2020, doi: 10.1016/j.asoc.2020.106424.
- [114] R. Khezri, A. Oshnoei, S. Oshnoei, H. Bevrani, and S. M. Muyeen, "An intelligent coordinator design for GCSC and AGC in a two-area hybrid power system," *Appl. Soft Comput.*, vol. 76, pp. 491–504, Mar. 2019, doi: 10.1016/j.asoc.2018.12.026.
- [115] E. Cam, G. Gorel, and H. Mamur, "Use of the Genetic Algorithm-Based Fuzzy Logic Controller for Load-Frequency Control in a Two Area Interconnected Power System," *Appl. Sci.*, vol. 7, no. 3, p. 308, Mar. 2017, doi: 10.3390/app7030308.
- [116] Y. L. Karnavas and D. P. Papadopoulos, "AGC for autonomous power system using combined intelligent techniques," *Electr. Power Syst. Res.*, vol. 62, no. 3, pp. 225–239, Jul. 2002, doi: 10.1016/S0378-7796(02)00082-2.
- [117] F. Daneshfar and H. Bevrani, "Multiobjective design of load frequency control using genetic algorithms," *Int. J. Electr. Power Energy Syst.*, vol. 42, no. 1, pp. 257–263, Nov. 2012, doi: 10.1016/j.ijepes.2012.04.024.
- [118] C.-F. Juang and C.-F. Lu, "Load-frequency control by hybrid evolutionary fuzzy PI controller," *IEE Proc. - Gener. Transm. Distrib.*, vol. 153, no. 2, p. 196, 2006, doi: 10.1049/ip-gtd:20050176.
- [119] X. S. Yang, "Firefly algorithm, stochastic test functions and design optimisation," *Int. J. Bio-Inspired Comput.*, vol. 2, no. 2, p. 78, 2010, doi: 10.1504/IJBIC.2010.032124.

- [120] M. Raju, U. Sarma, and L. C. Saikia, “Application of Firefly Algorithm Optimized Fuzzy 2DOFPID Controller for Diverse-Sourced Multi-area LFC,” 2020, pp. 261–267.
- [121] S. M. Abd-Elazim and E. S. Ali, “Firefly algorithm-based load frequency controller design of a two area system composing of PV grid and thermal generator,” *Electr. Eng.*, vol. 100, no. 2, pp. 1253–1262, Jun. 2018, doi: 10.1007/s00202-017-0576-5.
- [122] K. S. Rajesh, S. S. Dash, and R. Rajagopal, “Hybrid improved firefly-pattern search optimized fuzzy aided PID controller for automatic generation control of power systems with multi-type generations,” *Swarm Evol. Comput.*, vol. 44, pp. 200–211, Feb. 2019, doi: 10.1016/j.swevo.2018.03.005.
- [123] M. A. Zamee, K. K. Islam, A. Ahmed, and K. R. Zafreen, “Differential evolution algorithm based load frequency control in a two-area conventional and renewable energy based nonlinear power system,” in *2016 4th International Conference on the Development in the in Renewable Energy Technology (ICDRET)*, Jan. 2016, pp. 1–6, doi: 10.1109/ICDRET.2016.7421476.
- [124] R. K. Sahu, G. T. Chandra Sekhar, and S. Panda, “DE optimized fuzzy PID controller with derivative filter for LFC of multi source power system in deregulated environment,” *Ain Shams Eng. J.*, vol. 6, no. 2, pp. 511–530, Jun. 2015, doi: 10.1016/j.asej.2014.12.009.
- [125] F. Zou, D. Chen, and Q. Xu, “A survey of teaching–learning-based optimization,” *Neurocomputing*, vol. 335, pp. 366–383, Mar. 2019, doi: 10.1016/j.neucom.2018.06.076.
- [126] B. K. Sahu, S. Pati, P. K. Mohanty, and S. Panda, “Teaching–learning based optimization algorithm based fuzzy-PID controller for automatic generation control of multi-area power system,” *Appl. Soft Comput.*, vol. 27, pp. 240–249, Feb. 2015, doi: 10.1016/j.asoc.2014.11.027.
- [127] B. K. Sahu, T. K. Pati, J. R. Nayak, S. Panda, and S. K. Kar, “A novel hybrid LUS–TLBO optimized fuzzy-PID controller for load frequency control of multi-source power system,” *Int. J. Electr. Power Energy Syst.*, vol. 74, pp. 58–69, Jan. 2016, doi: 10.1016/j.ijepes.2015.07.020.
- [128] E. S. Ali and S. M. Abd-Elazim, “Bacteria foraging optimization algorithm based load

- frequency controller for interconnected power system,” *Int. J. Electr. Power Energy Syst.*, vol. 33, no. 3, pp. 633–638, Mar. 2011, doi: 10.1016/j.ijepes.2010.12.022.
- [129] N. El Yakine Kouba, M. Mena, M. Hasni, and M. Boudour, “Optimal load frequency control based on artificial bee colony optimization applied to single, two and multi-area interconnected power systems,” in *2015 3rd International Conference on Control, Engineering & Information Technology (CEIT)*, May 2015, pp. 1–6, doi: 10.1109/CEIT.2015.7233027.
- [130] D. Guha, P. K. Roy, and S. Banerjee, “Load frequency control of large scale power system using quasi-oppositional grey wolf optimization algorithm,” *Eng. Sci. Technol. an Int. J.*, vol. 19, no. 4, pp. 1693–1713, Dec. 2016, doi: 10.1016/j.jestch.2016.07.004.
- [131] M. Raju, L. C. Saikia, and N. Sinha, “Automatic generation control of a multi-area system using ant lion optimizer algorithm based PID plus second order derivative controller,” *Int. J. Electr. Power Energy Syst.*, vol. 80, pp. 52–63, Sep. 2016, doi: 10.1016/j.ijepes.2016.01.037.
- [132] A. K. Thirukkovulur, H. Nandagopal, and V. Parivallal, “Decentralized control of multi-area power system restructuring for LFC optimization,” in *2012 IEEE International Conference on Power Electronics, Drives and Energy Systems (PEDES)*, Dec. 2012, pp. 1–6, doi: 10.1109/PEDES.2012.6484456.
- [133] H. Singla and A. Kumar, “LQR based load frequency control with SMES in deregulated environment,” in *2012 Annual IEEE India Conference (INDICON)*, Dec. 2012, pp. 286–292, doi: 10.1109/INDCON.2012.6420630.
- [134] G. Magdy, G. Shabib, A. A. Elbaset, and Y. Mitani, “Frequency Stabilization of Renewable Power Systems Based on MPC With Application to The Egyptian Grid,” *IFAC-PapersOnLine*, vol. 51, no. 28, pp. 280–285, 2018, doi: 10.1016/j.ifacol.2018.11.715.
- [135] Y. Tang, Y. Bai, C. Huang, and B. Du, “Linear active disturbance rejection-based load frequency control concerning high penetration of wind energy,” *Energy Convers. Manag.*, vol. 95, pp. 259–271, May 2015, doi: 10.1016/j.enconman.2015.02.005.
- [136] H. Badihi, Y. Zhang, and H. Hong, “Design of a Pole Placement Active Power Control System for Supporting Grid Frequency Regulation and Fault Tolerance in Wind

- Farms,” *IFAC Proc. Vol.*, vol. 47, no. 3, pp. 4328–4333, 2014, doi: 10.3182/20140824-6-ZA-1003.01379.
- [137] X. Yu and K. Tomsovic, “Application of Linear Matrix Inequalities for Load Frequency Control With Communication Delays,” *IEEE Trans. Power Syst.*, vol. 19, no. 3, pp. 1508–1515, Aug. 2004, doi: 10.1109/TPWRS.2004.831670.
- [138] M. Z. Bernard, T. H. Mohamed, Y. Mitani, and Y. S. Qudaih, “CDM application on power system as a load frequency controller,” in *2013 IEEE Electrical Power & Energy Conference*, Aug. 2013, pp. 1–5, doi: 10.1109/EPEC.2013.6802920.
- [139] T. H. Mohamed, G. Shabib, and H. Ali, “Distributed load frequency control in an interconnected power system using ecological technique and coefficient diagram method,” *Int. J. Electr. Power Energy Syst.*, vol. 82, pp. 496–507, Nov. 2016, doi: 10.1016/j.ijepes.2016.04.023.

Chapter 3

The Bees Algorithm: Mechanism and applications

3.1 Abstract

Optimization is a mathematical technique for finding the fittest / best solution to a problem. Optimization has been utilized in many fields such as engineering, physics, chemistry, manufacturing, energy, economy, computer science, logistics, robotics, finance, and medicine. Several types of optimization techniques have been proposed. However, there is not a single optimization technique that can claim to be suitable for all types of problems. One of the most recent proposed optimisation bee-based algorithms is the Bees Algorithm (BA). The BA is a population-based metaheuristic algorithm that was proposed by Pham in 2006, and it is based on the behaviour of honeybees as they are observed when they are foraging for food. This chapter details the mechanism of the utilized Bees Algorithm and its main application as an excellent optimisation tool.

3.2 Introduction

Global optimization is a branch of numerical analysis and applied mathematics that focuses on optimization [1]. The optimization can be defined as the process of obtaining the best configuration among a set of alternative configurations in terms of some quality or performance criterion [2]. The meaning of the ‘best’ varies depending on the problem. In some of the problems, ‘best’ means the ‘maximum’, and these problems are called maximization optimization problems. On the other hand, in other problems, ‘best’ means the ‘minimum’, and these problems are called minimization optimization problems. Technically, the word ‘optimum’ is used instead of ‘best’, which is more appropriate for daily use. Therefore, in general, optimization means achieving the optimum. Theoretically, optimization is a branch of mathematics that is concerned with the study of optima quantitatively and with the methods of finding those optima. On the other hand, in practice, optimization includes all of the techniques, methods, and algorithms that can be used to find the optima [3].

Many optimization algorithms and methods have been developed to solve various optimization problems. In general, these algorithms can be divided into two basic classes: deterministic and stochastic algorithms [4]. Most conventional optimization algorithms are deterministic algorithms in which the objective function values alone (direct deterministic or gradient-free algorithms) or the objective function values with their derivatives (indirect

deterministic or gradient-based algorithms) are required to find the optimum. Deterministic algorithms guarantee finding the optimal solution. Gradient based methods can be considered to be efficient methods for solving optimization problems. However, the derivative of an objective function might be unreliable, unavailable, or time consuming to calculate [5]. For free-gradient algorithms, although they are free of derivatives, the use of function values alone is not a practical method because of the exhaustive search. In an exhaustive search, every combination of solutions must be examined, and the time required for this examination is unacceptable and could even be impossible to accomplish. As a result, many researchers started to think of other approaches that can locate acceptable solutions in a reasonable amount of time while occupying a reasonable amount of space. Hence, stochastic algorithms have come into play. Stochastic optimization algorithms can be defined as algorithms that employ random rules to find high-quality solutions within a reasonable amount of time [6]. An important class of stochastic algorithms is the class of metaheuristic algorithms.

A metaheuristic algorithm can be defined as a higher-level algorithm that combines one or more heuristic procedures and guides them in an intelligent way to solve a wide variety of general classes of optimization problems [1]. A metaheuristic algorithm can be adapted to solve a specific problem with a small number of modifications [7]. The main goal is to overcome the drawbacks of local search heuristics, especially the problem of solutions becoming trapped in local optima, by exploring the search space globally [8].

Metaheuristic algorithms can be classified in many ways. The most common way to classify metaheuristic algorithms is based on the number of solutions that are manipulated simultaneously. In this way, metaheuristic algorithms can be classified into trajectory-based and population-based algorithms. Trajectory-based algorithms work on a single solution and describe a trajectory through the search space such as a Tabu Search (TS) [9], Simulated Annealing (SA) [10], and Iterated Local Search (ILS) [11]. On the other hand, population-based algorithms use a population and set of solutions that are refined iteratively through the search space, such as the Genetic Algorithm (GA) [12], Particle Swarm Optimization (PSO) [13] and Ant Colony Optimization (ACO) [14]. These population-based algorithms constitute a part of the Computational Intelligence (CI) field, which is a subfield of the Artificial Intelligence (AI) field.

Most population-based metaheuristic algorithms, especially in recent years, have been inspired by the collective intelligent behaviors of swarms of animals and insects, such as fish, birds, bacteria, ants, termites, wasps, and fireflies. Biological studies have shown that a swarm

of such animals has impressive abilities to achieve fascinating complex collective behaviors despite the simple behavior of each individual [15]. It was found that the explanation of this amazing observation is the feature of self-organization that social animals have. Self-organization can be considered to be organization without an organizer, in which no guidance from an external or internal controller is needed [16]. Instead, decentralized control mechanisms are required for these social beings to update their activities by themselves based on some limited and local information. These intelligent collective behaviors and the incredible capabilities of social animals to solve their daily life problems interested researchers in modeling their behaviors when solving real-world optimization problems. Then, the model can be used as a base for developing artificial versions, either by tuning the model parameters using values outside the biological range or by assuming additional non-biological characteristics in the model design [8]. As a result, swarm intelligence in nature has been transferred from biological systems to artificial systems, and thus, a new field called Swarm Intelligence (SI) has emerged under the field of AI, especially under the domain of CI. Consequently, algorithms such as ACO [14], PSO [13], and the Firefly Algorithm (FA) [17] have been developed.

One of the most recent bee-based algorithms is the Bees Algorithm (BA). The BA is a population-based metaheuristic algorithm that was proposed by Pham [18], and it is a bee swarm intelligence-based metaheuristic algorithm that is inspired by the natural behavior of honeybees when foraging for food. Fundamentally, the algorithm performs a type of exploitative local or neighborhood search combined with an exploratory global search. Both types of search modes implement a uniform random search. In a global search, the scout bees are distributed uniformly at random to different areas of the search space to scout for potential solutions. In a local or neighborhood search, follower bees are recruited for patches that are found by scout bees to be more promising, to exploit those patches. BA has been successfully applied to problems in many fields, such as control engineering [19], [20], manufacturing [21], [22], classification / mining [23], [24], project scheduling problems [25], and many other applications [26]–[28].

3.3 Background

In nature, honey bees have several complicated behaviors such as mating, breeding and foraging. These behaviors have been mimicked for several honey bee based optimization algorithms.

One of the famous mating and breeding behavior of honey bees inspired algorithm is Marriage in Honey Bees Optimization (MBO). The algorithm starts from a single queen without family and passes on to the development of a colony with family having one or more queens. In the literature, several versions of MBO have been proposed such as Honey-Bees Mating Optimization (HBMO) [29], Fast Marriage in Honey Bees Optimization (FMHBO) [30] and The Honey-Bees Optimization (HBO) [31].

The other type of bee-inspired algorithms mimics the foraging behavior of the honey bees. These algorithms use standard evolutionary or random explorative search to locate promising locations. Then the algorithms utilize the exploitative search on the most promising locations to find the global optimum. The following algorithms were inspired from foraging behavior of honey bees; Bee System (BS), Bee Colony Optimization (BCO), Artificial Bee Colony (ABC) and The Bees Algorithm (BA). Bee System is an improved version of the Genetic Algorithm (GA) [32]. The main purpose of the algorithm is to improve local search while keeping the global search ability of GA.

Bee Colony Optimization (BCO) was proposed to solve combinatorial optimization problems by [33]. BCO has two phases called forward pass and backward pass. A partial solution is generated in the forward pass stage with individual exploration and collective experience, which will then be employed at the backward pass stage. In the backward pass stage the probability information is utilized to make the decision whether to continue to explore the current solution in the next forward pass or to start the neighborhood of the new selected ones. The new one is determined using probabilistic techniques such as the roulette wheel selection.

Artificial Bee Colony optimization (ABC) was proposed by [34]. The algorithm consists of the following bee groups: employed bees, onlooker bees and scout bees as in nature. Employed bees randomly explore and return to the hive with information about the landscape. This explorative search information is shared with onlooker bees. The onlooker bees evaluate this information with a probabilistic approach such as the roulette wheel method to start a neighborhood search. Meanwhile, the scout bees perform a random search to carry out the exploitation.

The Bees Algorithm was proposed by [18], which is very similar to the ABC in the sense of having local search and global search processes. However, there is a difference between both algorithms during the neighborhood search process. As mentioned above, ABC

has a probabilistic approach during the neighborhood stage; however, the Bees Algorithm does not use any probability approach, but instead uses fitness evaluation to drive the search.

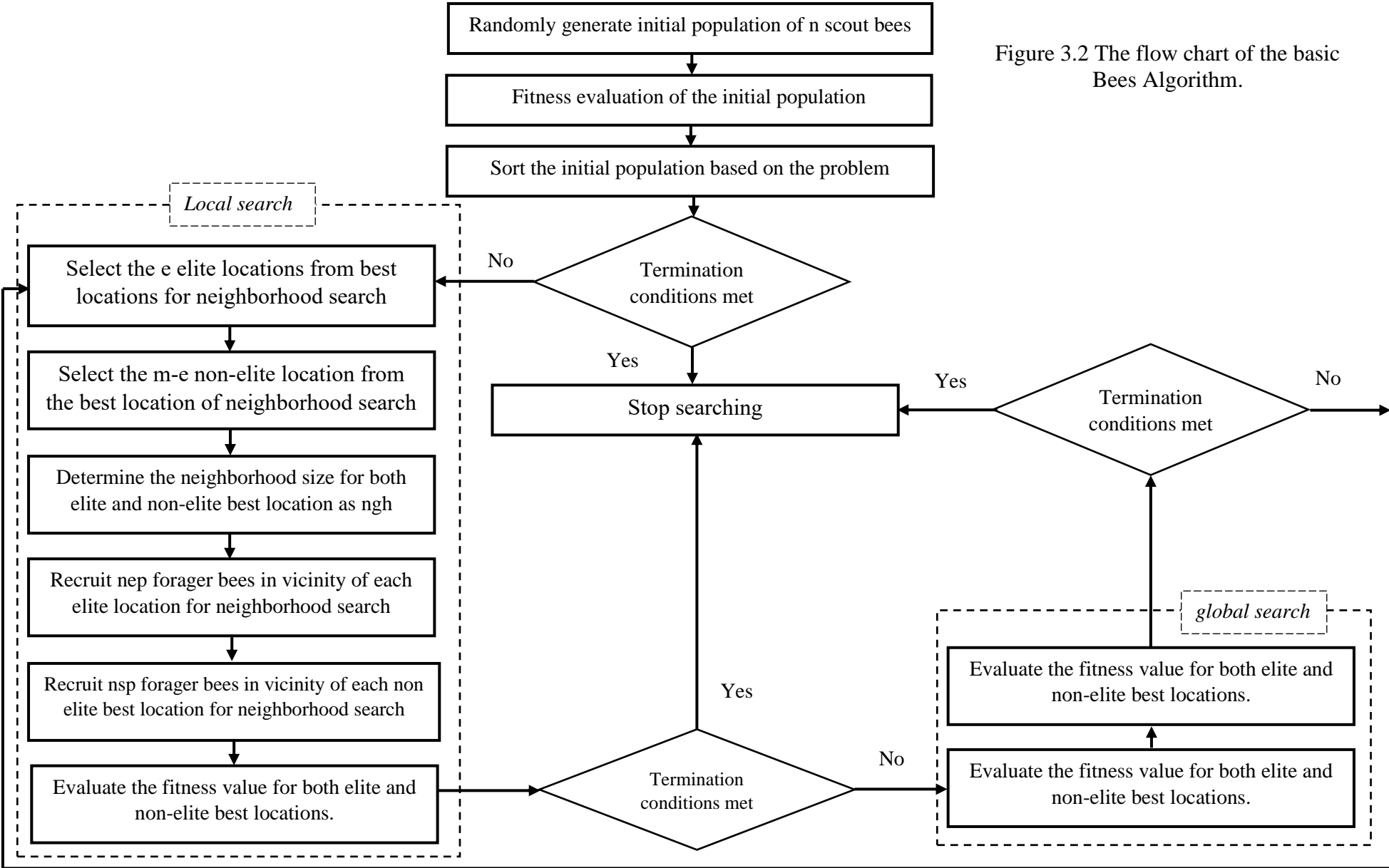
3.4 The Mechanism of the Bees Algorithm

The pseudo-code and flow chart of the algorithm is shown in Figure 3.1 and 3.2, respectively. The algorithm requires a number of parameters to be set, which are given as follow; the number of the sites (n), the number of sites selected for neighborhood search among n sites (m), the number of top-rated (elite) sites among m selected sites (e), the number of bees recruited for the best e sites (nep), the number of bees recruited for the other ($m-e$) selected sites (nsp), the neighborhood size of each selected patch for neighborhood (local) search (ngh), and the stopping criterion. The algorithm starts with the n scout bees being placed randomly in the search space Figure 3.3 (a). The fitness values of the sites visited by the scout bees are evaluated and sorted from the highest to the lowest (a maximization problem). Then the m fittest sites are designated as “selected sites” and chosen for neighborhood search. The algorithm conducts local search process around the selected sites by assigning more bees to the best e sites and fewer bees to the non-elite best sites Figure 3.3 (b-c). Selection of the best sites is made according to their associated fitness value. Finally, the remaining sites ($n-m$) will be searched randomly, which is the global search stage of the Bees Algorithm Figure 3.3 (d). During the global search stage one bee will be recruited for each ($n-m$) site. The algorithm was run until one of the three stopping criteria, which are arranged in the following order, is met. First, the solution found is equal to the real optimum value. Second, the numbers of iterations reach the pre-set value. Third, if there is no significant improvement in the consecutive solutions found [35].

<p><i>Generate initial population.</i></p> <p><i>Evaluate fitness value of initial population.</i></p> <p><i>Sort the initial population based on fitness result.</i></p> <p><i>While stopping criteria not met</i></p> <p><i>Select the elite patches and non-elite best patches for neighbourhood search.</i></p> <p><i> Recruit forager bees for selected sites.</i></p> <p><i>Evaluate the fitness value of each patch.</i></p> <p><i> Sort the results based on their fitness.</i></p> <p><i>Allocate the rest of the bees for global search to the non-best locations.</i></p> <p><i>Evaluate the fitness value of non-best patches.</i></p> <p><i>Sort the overall results based on their fitness.</i></p> <p><i>Run the algorithm until the termination criteria met</i></p> <p><i>End.</i></p>

Figure 3.1. The pseudo-code of the basic Bees Algorithm.

Figure 3.2 The flow chart of the basic Bees Algorithm.



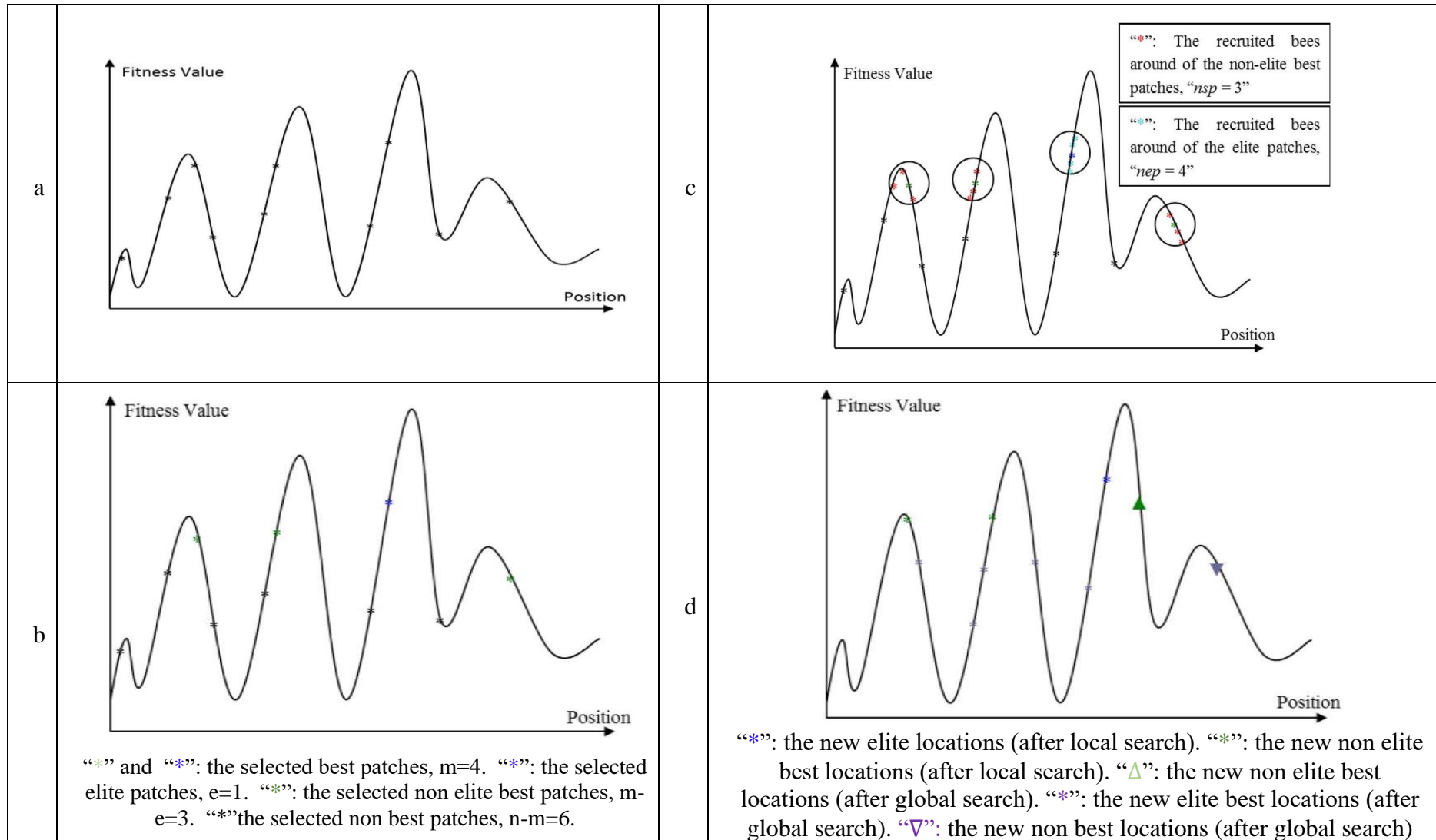


Figure 3.3 (a) The initially selected n patches and their evaluated fitness values; (b) Selection of elite and non-elite best patches; (c) Recruitment of forager bees to the elite and non-elite best locations; (d) Results from basic Bees-inspired Algorithm (BA) after local and global search.

3.5 The Applications of The Bees Algorithm

As a result and because of its simplicity and closeness to the actual behavior in nature, BA has garnered a significant amount of interest from researchers since its invention. It has been utilized in solving different problems in different fields. The first application of the Bees Algorithm was on the optimization of continuous type benchmark functions where the algorithm was applied on nine continuous type benchmark functions [36]. This section summarises the implementation of the bees algorithm in various applications.

3.5.1 Bees Algorithm in Control Engineering

In recent years, the BA has witnessed a considerable attention as an excellent tool to find the optimum values of different controllers in order to achieve the best possible performance. In [19], the BA was utilised to optimise the parameters of PID controller for a two-floor structure under earthquake excitation. In this study, the PID based BA has outperformed the same controller tuned by the Genetic Algorithm (GA). In [37], the BA was used for optimization of PID controller for one leg of a quadruped robot. The study carried out in [38] proves the capability of the bees algorithm to solve complex parameter optimization problems for robot manipulator control. Two applications are presented; the first case considers the modelling of the inverse kinematics of an articulated robot arm using neural networks. The second case considers the design of a hierarchical proportional–integral–derivative (PID) controller for a flexible single link robot manipulator. Further, a design of a PID controller based on the BA is implemented for a single-input multi-output (SIMO) inverted pendulum system [39]. In [40], a Linear Quadratic Regulator (LQR) controller was designed for an Inverted Pendulum (IP) system using BA to provide optimal parameters of the proposed LQR. Intelligent backstepping controller based on the BA for gyro system is proposed in [41], the parameters of the backstepping controller are tuned using the BA by minimizing the Integral of Time multiplied Absolute Error (ITAE). Furthermore, in order to enhance the dynamic performance of fuzzy control, the BA has widely been implemented as an optimisation tool to tune the scaling factors of different fuzzy control configurations. In [42], the BA was used to tune the parameters of fuzzy logic controller for positioning control of a flexible single-link robot arm. A novel design of a model predictive control (MPC) scheme based on the BA is proposed for a three tank system, the BA was utilized in order to solve the open loop optimization problem [20]. Optimization of MPC weights for control of permanent magnet synchronous motor by using the multi objective BA is studied in [43].

3.5.2 Applications of the Bees Algorithm to Intelligent Production and Manufacturing

The Bees algorithm has extensively implemented to solve various problems in manufacturing. For example, in [44], an application of BA to the problem of crack detection in beams is investigated. An improved version of the Bees Algorithm is proposed in [45] for computer-aided preliminary design. The algorithm has been adapted for discrete function optimisation and tested on a simple machine design task, preliminary gearbox design. Experimental results show that the proposed Bees Algorithm outperforms random search and a genetic optimisation algorithm. An integer quadratic programming model based on the Bees Algorithm is proposed in [46] for workload balancing in the examination job assignment problem. The obtained results show that the proposed BA algorithm is able to generate better solutions with much shorter computational times. The problem and efficiency improvement of the instrument factory in Thailand is studied in [47], the methods of production schedule are performed by the BA and other techniques. The BA has been employed in [48] for the first time to a strategic planning and design model for global supply chains. The algorithm was adapted for an existing model that involves facility location, market fulfilment and supplier selection decisions for multi-echelon and multi-product supply chains in dynamic environments. In this study, the Bees Algorithm performs better of 10% in quality of solution respect to the GA with equivalent calculation time.

3.5.3 Optimisation of classifiers / clustering systems

In [49], the Bees Algorithm and Kalman filter was used to train a radial basis function (RBF) neural network for pattern classification. The study presented in [50] proposed a novel application of the BA to the optimisation of neural networks for the identification of defects in wood veneer sheets. A novel tool named Bee for Mining (B4M) is proposed in [24] for classification tasks, which enables the Bees Algorithm (BA) to discover rules automatically. The proposed algorithm was implemented and tested using five different datasets, the results obtained using the proposed B4M show that it was capable of achieving better classification accuracy. This work presented in [51] describes another application of the Bees Algorithm to the optimization of a Support Vector Machine (SVM) for the problem of classifying defects in plywood.

Moreover, this algorithm has been used in many other fields to solve different problems. In [8], the Bees Algorithm variants and its wide use in various application are well explained, this paper summarises most of the research based on the Bees Algorithm.

3.6 Summary

This chapter summarised the background of the proposed Bess Algorithm, its mechanism and main applications. It is revealed from this chapter that, this algorithm has been implemented successfully in different application domains. Its merits made this algorithm favourable to the researchers to utilize it to solve a wide range of optimisation problems. Therefore, in this thesis, the BA is proposed to tune the parameters of different controllers suggested as load frequency Control systems in two different power networks which is detailed in the following chapters.

3.7 References

- [1] T. Weise, *Global optimization algorithms-theory and application*, 2nd editio. Thomas Weise, 2009.
- [2] A. Antoniou and W.-S. Lu, *Practical Optimization-Algorithms and Engineering Applications*. New York, NY: Springer US, 2021.
- [3] C. Blum and A. Roli, "Metaheuristics in combinatorial optimization: Overview and conceptual comparison," *ACM Comput. Surv.*, vol. 35, no. 3, pp. 268–308, Sep. 2003, doi: 10.1145/937503.937505.
- [4] X. S. Yang, "Review of meta-heuristics and generalised evolutionary walk algorithm," *Int. J. Bio-Inspired Comput.*, vol. 3, no. 2, p. 77, 2011, doi: 10.1504/IJBIC.2011.039907.
- [5] L. M. Rios and N. V. Sahinidis, "Derivative-free optimization: a review of algorithms and comparison of software implementations," *J. Glob. Optim.*, vol. 56, no. 3, pp. 1247–1293, Jul. 2013, doi: 10.1007/s10898-012-9951-y.
- [6] J. Brownlee, *Clever Algorithms: Nature-Inspired Programming Recipes*. Melbourne, 2011.
- [7] E.-G. Talbi, *Metaheuristics: From Design to Implementation*. Hoboken, NJ, USA: John Wiley & Sons, Inc., 2009.
- [8] W. A. Hussein, S. Sahran, and S. N. H. Sheikh Abdullah, "The variants of the Bees Algorithm (BA): a survey," *Artif. Intell. Rev.*, vol. 47, no. 1, pp. 67–121, Jan. 2017, doi: 10.1007/s10462-016-9476-8.
- [9] F. Glover, E. Taillard, and E. Taillard, "A user's guide to tabu search," *Ann. Oper. Res.*, vol. 41, no. 1, pp. 1–28, Mar. 1993, doi: 10.1007/BF02078647.
- [10] S. Kirkpatrick, "Optimization by simulated annealing: Quantitative studies," *J. Stat. Phys.*,

vol. 34, no. 5–6, pp. 975–986, Mar. 1984, doi: 10.1007/BF01009452.

- [11] H. R. Lourenço, O. C. Martin, and T. Stützle, “Iterated Local Search: Framework and Applications,” in *Handbook of Metaheuristics*, vol. 146, M. Gendreau and J.-Y. Potvin, Eds. Boston, MA: Springer US, 2010, pp. 363–397.
- [12] S. Katoch, S. S. Chauhan, and V. Kumar, “A review on genetic algorithm: past, present, and future,” *Multimed. Tools Appl.*, vol. 80, no. 5, pp. 8091–8126, Feb. 2021, doi: 10.1007/s11042-020-10139-6.
- [13] J. Kennedy and R. Eberhart, “Particle swarm optimization,” in *Proceedings of ICNN’95 - International Conference on Neural Networks*, vol. 4, pp. 1942–1948, doi: 10.1109/ICNN.1995.488968.
- [14] A. Prakasam and N. Savarimuthu, “Metaheuristic algorithms and probabilistic behaviour: a comprehensive analysis of Ant Colony Optimization and its variants,” *Artif. Intell. Rev.*, vol. 45, no. 1, pp. 97–130, Jan. 2016, doi: 10.1007/s10462-015-9441-y.
- [15] S. Garnier, J. Gautrais, and G. Theraulaz, “The biological principles of swarm intelligence,” *Swarm Intell.*, vol. 1, no. 1, pp. 3–31, Oct. 2007, doi: 10.1007/s11721-007-0004-y.
- [16] T. D. Seeley, “When Is Self-Organization Used in Biological Systems?,” *Biol. Bull.*, vol. 202, no. 3, pp. 314–318, Jun. 2002, doi: 10.2307/1543484.
- [17] X.-S. Yang, “Firefly Algorithms,” in *Nature-Inspired Optimization Algorithms*, Elsevier, 2021, pp. 123–139.
- [18] D. T. Pham, A. Ghanbarzadeh, E. Koç, S. Otri, S. Rahim, and M. Zaidi, “The Bees Algorithm — A Novel Tool for Complex Optimisation Problems,” in *Intelligent Production Machines and Systems*, Elsevier, 2006, pp. 454–459.
- [19] M. Arif Şen, M. Tinkir, and M. Kalyoncu, “Optimisation of a PID controller for a two-floor structure under earthquake excitation based on the bees algorithm,” *J. Low Freq. Noise, Vib. Act. Control*, vol. 37, no. 1, pp. 107–127, Mar. 2018, doi: 10.1177/1461348418757906.
- [20] M. Sarailoo, Z. Rahmani, and B. Rezaie, “A novel model predictive control scheme based on bees algorithm in a class of nonlinear systems: Application to a three tank system,” *Neurocomputing*, vol. 152, pp. 294–304, Mar. 2015, doi: 10.1016/j.neucom.2014.10.066.
- [21] N. Hartono, F. J. Ramírez, and D. T. Pham, “Optimisation of robotic disassembly plans

using the Bees Algorithm,” *Robot. Comput. Integr. Manuf.*, vol. 78, p. 102411, Dec. 2022, doi: 10.1016/j.rcim.2022.102411.

- [22] J. Liu, Z. Zhou, D. T. Pham, W. Xu, C. Ji, and Q. Liu, “Collaborative optimization of robotic disassembly sequence planning and robotic disassembly line balancing problem using improved discrete Bees algorithm in remanufacturing☆,” *Robot. Comput. Integr. Manuf.*, vol. 61, p. 101829, Feb. 2020, doi: 10.1016/j.rcim.2019.101829.
- [23] P. Tapkan, L. Özbakır, S. Kulluk, and A. Baykasoğlu, “A cost-sensitive classification algorithm: BEE-Miner,” *Knowledge-Based Syst.*, vol. 95, pp. 99–113, Mar. 2016, doi: 10.1016/j.knosys.2015.12.010.
- [24] M. S. Packianather, A. K. Al-Musawi, and F. Anayi, “Bee for mining (B4M) – A novel rule discovery method using the Bees algorithm with quality-weight and coverage-weight,” *Proc. Inst. Mech. Eng. Part C J. Mech. Eng. Sci.*, vol. 233, no. 14, pp. 5101–5112, Jul. 2019, doi: 10.1177/0954406219833719.
- [25] E. Oztemel and A. A. Selam, “Bees Algorithm for multi-mode, resource-constrained project scheduling in molding industry,” *Comput. Ind. Eng.*, vol. 112, pp. 187–196, Oct. 2017, doi: 10.1016/j.cie.2017.08.012.
- [26] S. Abdullah and M. Alzaqebah, “A hybrid self-adaptive bees algorithm for examination timetabling problems,” *Appl. Soft Comput.*, vol. 13, no. 8, pp. 3608–3620, Aug. 2013, doi: 10.1016/j.asoc.2013.04.010.
- [27] T. Mazitov, P. Božek, A. Abramov, Y. Nikitin, and I. Abramov, “Using Bee Algorithm in the Problem of Mapping,” *Procedia Eng.*, vol. 149, pp. 305–312, 2016, doi: 10.1016/j.proeng.2016.06.671.
- [28] G.-H. Luo, S.-K. Huang, Y.-S. Chang, and S.-M. Yuan, “A parallel Bees Algorithm implementation on GPU,” *J. Syst. Archit.*, vol. 60, no. 3, pp. 271–279, Mar. 2014, doi: 10.1016/j.sysarc.2013.09.007.
- [29] O. B. Haddad, A. Afshar, and M. A. Mariño, “Honey-Bees Mating Optimization (HBMO) Algorithm: A New Heuristic Approach for Water Resources Optimization,” *Water Resour. Manag.*, vol. 20, no. 5, pp. 661–680, Oct. 2006, doi: 10.1007/s11269-005-9001-3.
- [30] C. Yang, J. Chen, and X. Tu, “Algorithm of Fast Marriage in Honey Bees Optimization and Convergence Analysis,” in *2007 IEEE International Conference on Automation and*

Logistics, Aug. 2007, pp. 1794–1799, doi: 10.1109/ICAL.2007.4338865.

- [31] P. Curkovic, “Honey-bees optimization algorithm applied to path planning problem,” *Int. J. Simul. Model.*, vol. 6, no. 3, pp. 154–164, Sep. 2007, doi: 10.2507/IJSIMM06(3)2.087.
- [32] T. Sato and M. Hagiwara, “Bee System: finding solution by a concentrated search,” in *1997 IEEE International Conference on Systems, Man, and Cybernetics. Computational Cybernetics and Simulation*, vol. 4, pp. 3954–3959, doi: 10.1109/ICSMC.1997.633289.
- [33] D. Teodorović, “Bee Colony Optimization (BCO),” in *Innovations in Swarm Intelligence*, Berlin, Heidelberg: Springer Berlin Heidelberg, 2009, pp. 39–60.
- [34] D. Karaboga, B. Gorkemli, C. Ozturk, and N. Karaboga, “A comprehensive survey: artificial bee colony (ABC) algorithm and applications,” *Artif. Intell. Rev.*, vol. 42, no. 1, pp. 21–57, Jun. 2014, doi: 10.1007/s10462-012-9328-0.
- [35] B. Yuce, E. Mastrocinque, M. S. Packianather, A. Lambiase, and D. T. Pham, “The Bees Algorithm and Its Applications,” in *Handbook of Research on Artificial Intelligence Techniques and Algorithms (2 Volumes)*, Hershey, USA: IGI Global, 2015, pp. 122–151.
- [36] D. T. Pham, S. Otri, A. Ghanbarzadeh, and E. Koc, “Application of the Bees Algorithm to the Training of Learning Vector Quantisation Networks for Control Chart Pattern Recognition,” in *2006 2nd International Conference on Information & Communication Technologies*, vol. 1, pp. 1624–1629, doi: 10.1109/ICTTA.2006.1684627.
- [37] V. Bakırcıoğlu, M. Arif Şen, and M. Kalyoncu, “Optimization of PID controller based on The Bees Algorithm for one leg of a quadruped robot,” *MATEC Web Conf.*, vol. 42, p. 03004, Feb. 2016, doi: 10.1051/mateconf/20164203004.
- [38] A. A. Fahmy, M. Kalyoncu, and M. Castellani, “Automatic design of control systems for robot manipulators using the bees algorithm,” *Proc. Inst. Mech. Eng. Part I J. Syst. Control Eng.*, vol. 226, no. 4, pp. 497–508, Apr. 2012, doi: 10.1177/0959651811425312.
- [39] M. A. Sen and M. Kalyoncu, “Optimisation of a PID Controller for an Inverted Pendulum Using the Bees Algorithm,” *Appl. Mech. Mater.*, vol. 789–790, pp. 1039–1044, Sep. 2015, doi: 10.4028/www.scientific.net/AMM.789-790.1039.
- [40] M. A. Sen and M. Kalyoncu, “Optimal Tuning of a LQR Controller for an Inverted Pendulum Using the Bees Algorithm,” *J. Autom. Control Eng.*, pp. 384–387, 2016, doi: 10.18178/joace.4.5.384-387.

- [41] R. Gholipour, A. Khosravi, and H. Mojallali, “Bees Algorithm Based Intelligent Backstepping Controller Tuning For Gyro System,” *J. Math. Comput. Sci.*, vol. 05, no. 03, pp. 205–211, Oct. 2012, doi: 10.22436/jmcs.05.03.08.
- [42] D. T. Pham and M. Kalyoncu, “Optimisation of a fuzzy logic controller for a flexible single-link robot arm using the Bees Algorithm,” in *2009 7th IEEE International Conference on Industrial Informatics*, Jun. 2009, pp. 475–480, doi: 10.1109/INDIN.2009.5195850.
- [43] M. Sahin, “Optimization of Model Predictive Control Weights for Control of Permanent Magnet Synchronous Motor by Using the Multi Objective Bees Algorithm,” in *Model Predictive Control - Recent Design and Implementations for Varied Applications [Working Title]*, London: IntechOpen, 2021.
- [44] S. Moradi, P. Razi, and L. Fatahi, “On the application of bees algorithm to the problem of crack detection of beam-type structures,” *Comput. Struct.*, vol. 89, no. 23–24, pp. 2169–2175, Dec. 2011, doi: 10.1016/j.compstruc.2011.08.020.
- [45] D. Pham, M. Castellani, and A. Ghanbarzadeh, “Preliminary design using the bees algorithm,” in *Laser Metrology and Machine Performance VIII - 8th International Conference and Exhibition on Laser Metrology, Machine Tool, CMM and Robotic Performance, LAMDAMAP*, 2007, pp. 420–429.
- [46] A. Baykasoglu, L. Ozbakir, and P. Tapkan, “The bees algorithm for workload balancing in examination job assignment,” *Eur. J. Ind. Eng.*, vol. 3, no. 4, p. 424, 2009, doi: 10.1504/EJIE.2009.027035.
- [47] P. Aungkulanon, “Comparison of Bee Algorithm and Scheduling Methodologies: A Case Study of Manufacturing in Thailand,” *Appl. Mech. Mater.*, vol. 835, pp. 864–868, May 2016, doi: 10.4028/www.scientific.net/AMM.835.864.
- [48] A. Lambiase, R. Iannone, S. Miranda, A. Lambiase, and D. Pham, “Bees algorithm for effective supply chains configuration,” *Int. J. Eng. Bus. Manag.*, vol. 8, p. 184797901667530, Jan. 2016, doi: 10.1177/1847979016675301.
- [49] D. T. Pham and H. A. Darwish, “Using the Bees Algorithm with Kalman Filtering to Train an Artificial Neural Network for Pattern Classification,” *Proc. Inst. Mech. Eng. Part I J. Syst. Control Eng.*, vol. 224, no. 7, pp. 885–892, Nov. 2010, doi:

10.1243/09596518JSCE1004.

- [50] D. . Pham, A. Soroka, A. Ghanbarzadeh, E. Koc, S. Otri, and M. Packianather, “Optimising Neural Networks for Identification of Wood Defects Using the Bees Algorithm,” in *2006 IEEE International Conference on Industrial Informatics*, Aug. 2006, pp. 1346–1351, doi: 10.1109/INDIN.2006.275855.

- [51] D. T. Pham, M. Zaidi, M. Mahmuddin, A. Ghanbarzadeh, E. Koc, and S. Otri, “Using the bees algorithm to optimise a support vector machine for wooddefect classification,” in *IPROMS 2007 Innovative Production Machines andSystems Virtual Conference*, 2007, pp. 454–461.

Chapter 4

LFC based Fuzzy Logic Control

4.1 Abstract

In this chapter, different structures of Fuzzy Logic Control (FLC) are proposed and successfully implemented for LFC purposes in two different power systems. Firstly, the proposed Fuzzy Proportional–Integral–Derivative with Filtered derivative (Fuzzy PIDF) is employed for LFC in the simplified Great Britain power system to keep the frequency within acceptable limits under different load conditions. A comparative study is conducted to investigate the superiority of the proposed controller. Then, the same control structure is tested for LFC in a two-area power system. Furthermore, an extensive robustness analysis of the controller is illustrated against parametric uncertainty of the investigated systems. Moreover, further three novel configurations of fuzzy control are proposed and examined for LFC in the testbed two area power system. The Bees Algorithm (BA) is used to tune the parameters of the proposed controller in both systems.

4.2 Introduction

Classical control algorithms have some limitation in power systems such as parameter uncertainties, changing the operation point which is used in deriving the model, and the collapse of these parameters. Intelligent methods such as Fuzzy Logic has been widely used in research due to high robustness and stability, offering better control performance than classical methods. Prof. A Zadeh proposed the idea of a fuzzy system in 1965. A typical fuzzy controller shown in Figure 4.1 which is a one-input-one-output controller. This structure can be modified into multi-input/multi-output fuzzy controller by adding an extra Fuzzy Membership Function (MSF) at each additional input or output [1].

There are four main stages in a fuzzy system: the fuzzifier, the inference engine, the knowledge base, and the defuzzifier. The first stage in the fuzzy system computations is to transform the numeric into fuzzy sets, this operation is called fuzzification. From the point of view of fuzzy set theory, the inference engine is the heart of the fuzzy system that performs all logic manipulations in a fuzzy system. A fuzzy system knowledge base consists of fuzzy IF–THEN rules and membership functions characterizing the fuzzy sets [2]. The result of the inference process is an output represented by a fuzzy set, but the output of the fuzzy system should be a numeric value. The transformation of a fuzzy set into a numeric value is called defuzzification. In addition, input and output scaling factors are needed to modify the universe

of discourse of the MSF. Their role is to tune the fuzzy controller to obtain the desired dynamic properties of the process-controller closed loop. These values are very important to get better control performance [3].

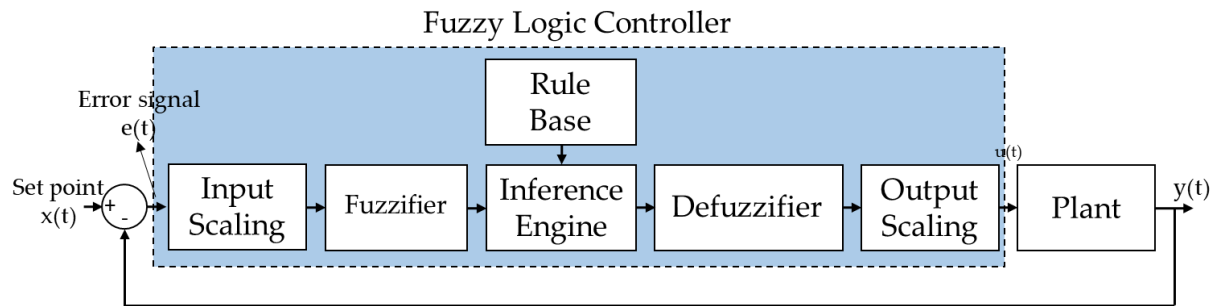


Figure. 4.1. Typical structure of fuzzy logic controller.

Due to its merits, FLC has recently been widely addressed as a potential solution for LFC based on different structures. It is revealed that FLC can successfully handle the problem of load frequency control. However, there was no identified rule to be utilised in order to find the fuzzy parameters i.e., scaling factors of the inputs and outputs as well as the membership functions and rule base [4]. Therefore, soft computing methods have been emerged to deal with this issue. In [3], a fuzzy hierarchal scheme tuned by Particle Swarm Optimization (PSO) is proposed for LFC in a single area power system. Differential Evolution (DE) was employed to optimise the parameters of a new fuzzy PID structure for LFC in a deregulated power system having multi-sources [5]. An optimized fuzzy self-tuning PID controller is proposed for LFC in two and three area interconnected power systems [6], to ameliorate the proposed controller, a Tribe-DE optimization algorithm was utilized to find the optimum values of scaling factor and membership function parameters of fuzzy PID controllers. Fuzzy PID tuned by Teaching Learning Based Optimization (TLBO) for dual area power system is studied in [7]. A novel hybrid DE and Pattern Search (PS) has been used to tune the scaling factor gains of fuzzy PI/PID controllers employed for LFC in a two-area power system [8]. The most recent controllers based on different strategies employed for LFC in power systems is concluded in [9], [10]. In view of the above, this chapter proposes different fuzzy control configurations for LFC implemented in two different power systems as detailed in the following subsections.

4.3 LFC based Fuzzy Logic control for the simplified Great Britain power system.

This subsection focuses on implementing the proposed Fuzzy Proportional–Integral–Derivative with Filtered derivative (Fuzzy PIDF), Fractional Order PID (FOPID) controller and classical PID controller developed to stabilize and balance the frequency in the Great

Britain (GB) power system at rated value. The Bees Algorithm (BA) is utilized to tune the parameters of these controllers proposed to meet the requirements of the GB Security and Quality of Supply Standard (GB-SQSS), which requires frequency to be brought back to its nominal value after a disturbance within a specified time. In comparison with controllers tuned by Particle Swarm Optimization (PSO) and Teaching Learning-Based Optimization (TLBO) used for the same system, simulation results show that the Fuzzy PIDF tuned by BA is able to significantly reduce the deviation in the frequency when a sudden disturbance is applied. Furthermore, the applied controllers tuned by BA including the Fuzzy PIDF prove their high robustness against a wide range of system parametric uncertainties and different load disturbances. The main investigations of this subsection are:

- To propose a metaheuristic algorithm _ the Bees Algorithm (BA), inspired by the natural behaviour of honeybees, for LFC of the GB power system.
- To optimize PID and FOPID controllers' gains and study their dynamic performance for the GB power system.
- To design and optimize a fuzzy logic controller structure scaling factor gains and study its dynamic performance for GB power system.
- To compare the dynamic performance of BA-based PID, FOPID and Fuzzy PIDF controllers with the same controllers tuned by PSO and TLBO for the same system.
- To investigate the effects of parametric uncertainties of the system with different load disturbances when the proposed controllers are implemented for LFC.

It may be worth mentioning that the reason behind choosing PSO and TLBO for comparison with BA is due to their wide use in the area of LFC and their superior performance as a tool of optimization. Therefore, if the proposed algorithm provides a frequency response similar to or better than these two algorithms, this will be another successful use of BA in engineering applications.

Another bee-based optimisation algorithm called Artificial Bee Colony (ABC) optimization algorithm has been implemented in LFC applications [11][12]. There are some similarities in the mechanism of the Artificial Bee Colony (ABC) and the Bees Algorithm (BA) used in this work. However, in [13], the BA has outperformed the ABC algorithm as an optimization tool, this was investigated on eight well-known benchmark problems (unimodal/multimodal functions).

A new study to further investigate the differences and the superiority between these algorithms for LFC applications is a good research topic for future work.

4.3.1 The simplified Great Britain power system

A simplified model of the GB power system shown in Figure 4.2 was developed using MATLAB Simulink; this model is utilized to analyse the power system frequency and then design an appropriate controller. The characteristics of the generators employed in the system are considered in this simplified model, as well as damping from the loads depending on frequency. Within this, synchronous coal-powered, gas-powered, hydro-power and nuclear plants are responsive to any decline in frequency and increase their generated output power correspondingly. In the model, such synchronous generators are represented by first-order transfer function blocks used to model the governor and the turbine. The governor droop gain R represents the turbine velocity control; this gain is the combined value of all droops of generator speed governors in the system. T_g is the typical time constant of the governor. Stable performance of the speed control is guaranteed by introducing transient droop compensation represented as lead-lag between the governor and turbine. The output mechanical power following the response of the governor which defines the turbine model is characterized in this simulation by the time constant T_t . The system inertia in this simplified model is represented by the time constant H_{eq} , which was considered to represent the current scenario of the GB power system with the high penetration of RERs. The damping obtained from frequency-dependent loads is represented by an equivalent gain value D . The effect of charging Electrical Vehicle (EV) was also considered in this design, which was modeled as an aggregated value represented by a feedback gain in the primary loop, with an estimated aggregated load equal to 2.16 GW. The value of this load was considered to be $=1.35$ pu ($EV \text{ load} \times f / (\text{Network base})$), where the network base value is equal to 79.2 GW [3]; the effect of EV gain on the primary loop response is provided in Appendix A. The secondary control applied in this model is the main study of this work, which will be examined via different controllers tuned by proposed algorithms including the Bees Algorithm, which represents the main contribution of this work. The parameters applied in this simplified model are tabulated in Table 4.1 [3], [14], [15]. It should be noted that the model used in this study to examine the frequency response of the GB power system is simplified; accordingly, the small effects of nonlinearities such as governor dead band (GDB) and generation rate constrain (GRC) are neglected.

Table 4.1. Parameters for the simplified model of the power system.

R	T_g	T_{ld}	T_{lg}	T_t	H_{eq}	D	E_v
-0.09 pu	0.2 s	2 s	12 s	0.3 s	8.88 s	1 pu	1.35 pu

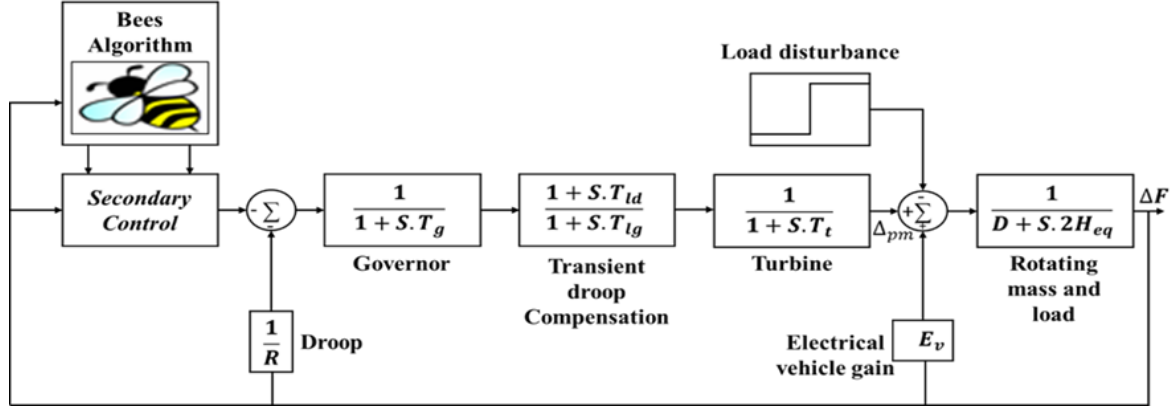


Figure 4.2. GB simplified power system

4.3.2 Control Strategies and Objective Functions

4.3.2.1 Classical Controllers

PID controllers are the most widely applied feedback controller in the process sector. Easy to understand and offering robustness, strong performance and the low cost are the main merits of this controller. The PID controller essentially includes proportional, integral and derivative modes. While a proportional controller decreases the rise time, it cannot completely remove the steady-state error. Integral controls, on the other hand, eliminate steady-state error, yet they can worsen transient responses. Derivative controls improve the system stability, decrease the overshoot/undershoot and enhance transient responses. Current industrial applications most frequently rely upon the Proportional–Integral (PI) controller. Controls without derivative action are applied in the following circumstances: when it is not important for the system to respond rapidly, when significant noise and disturbance are experienced during the system operation. The overall stability of the system can be improved by adding the derivative mode as it enables an increase in the proportional gain and decrease in the integral, thus increasing the speed response of the controller. Accordingly, PID controllers are frequently applied in systems that require stability with a fast response. Considering these points, this study investigates the effectiveness of a PID controller for the LFC of the GB power system. Equation (4.1) illustrates the transfer function of this controller, where K_P is the proportional gain, K_I the integral gain, and K_D is the derivative gain.

$$TF_{PID} = K_P + \frac{K_I}{S} + K_D S \quad (4.1)$$

Generally, for LFC, conventional methods of control remain the main approach, but in more complex systems, such approaches can become inadequate. A recently introduced control approach used for LFC tasks is known as non-integer control, developed on the basis of fractional calculus, which is generalized from integer order calculus. Fractional calculus is a generalization of differentiation/integration to a non-integer order, and thus provides n degrees of additional freedom when designing controllers, which can make them more efficient, flexible and robust [16]. The Fractional Order PID (FOPID) controller's transfer function is shown in Equation (4.2), where λ is the order of integration, and μ is the order of the differentiator.

$$TF_{FOPID} = K_P + \frac{K_I}{S^\lambda} + K_D S^\mu \quad (4.2)$$

Fractional-Order Control (FOC) has emerged to address the problem of LFC. However, this is the first attempt to tune the parameters of this controller using the Bees Algorithm.

4.3.2.2 Fuzzy PID Logic Control

There has been a broad implementation of fuzzy PID controllers in different structures to solve the LFC problem and a significant enhancement in performance has been achieved. It is also proven that in order to gain further enhancement in the overall system performance and improve the stability, a simple filter for the derivative mode of the fuzzy PID controller can be applied [17], [18]. Moreover, the performance of these controllers mainly relies on the selection of the scaling factor gains of the input and output of the controller, but it is difficult to find the optimum values of these gains using the trial-and-error technique. In view of the above, a fuzzy PID controller with derivative filter (Fuzzy PIDF), in which the scaling factor gains are tuned by the Bees Algorithm, is proposed in this section for LFC purposes. The structural design of this controller is illustrated in Figure 4.3. As it is clear from the figure, the controller has two inputs, ΔF and the derivative of ΔF and one output; in the case of employing this controller in a multi-area power system, the two inputs are the Area Control Error (ACE) and the derivative of (ACE).

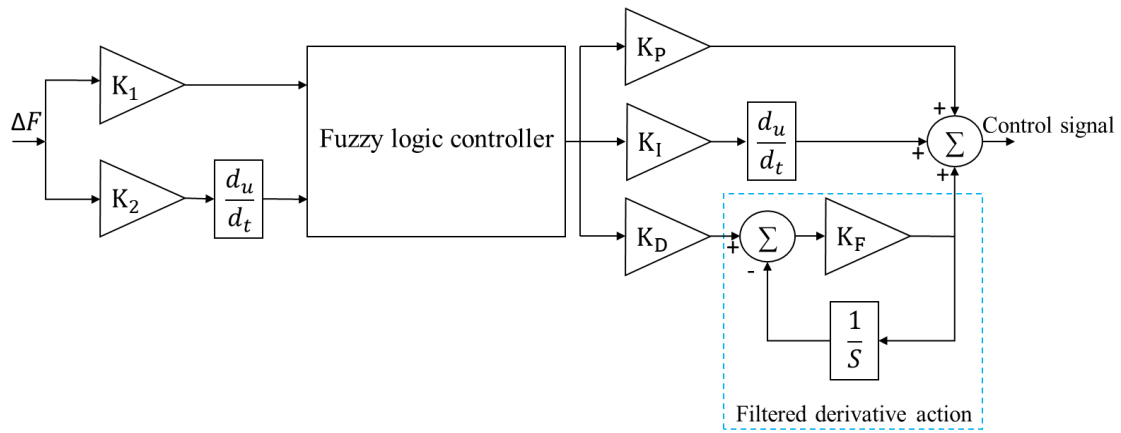


Figure 4.3. Structural diagram of fuzzy PIDF controller.

The scaling factor gains of the input are (K_1 and K_2) and four scaling factors in the output, namely K_P , K_I , K_D , and K_F is the filter gain. Due to its simplicity and the lower computation time needed for this type of membership, three triangular/two trapezoidal membership functions are used for the inputs and the output variables shown in Figure 4.4, namely Negative Big (NB), Negative Small (NS), Zero (Z), Positive Small (PS) and Positive Big (PB). Thus, 25 rules are required to generate the fuzzy output of the controller. Table 4.2 depicts the rule base of the proposed controller. Since the performance of the controller depends on these rules, the tabulated rules are generated by a comprehensive study of the dynamic behaviors of the testbed power system. The “Mamdani” interface tool is used in this controller for the fuzzification stage, while the “Centroid” method is used in the defuzzification stage to convert the fuzzy output value of the controller to a real value.

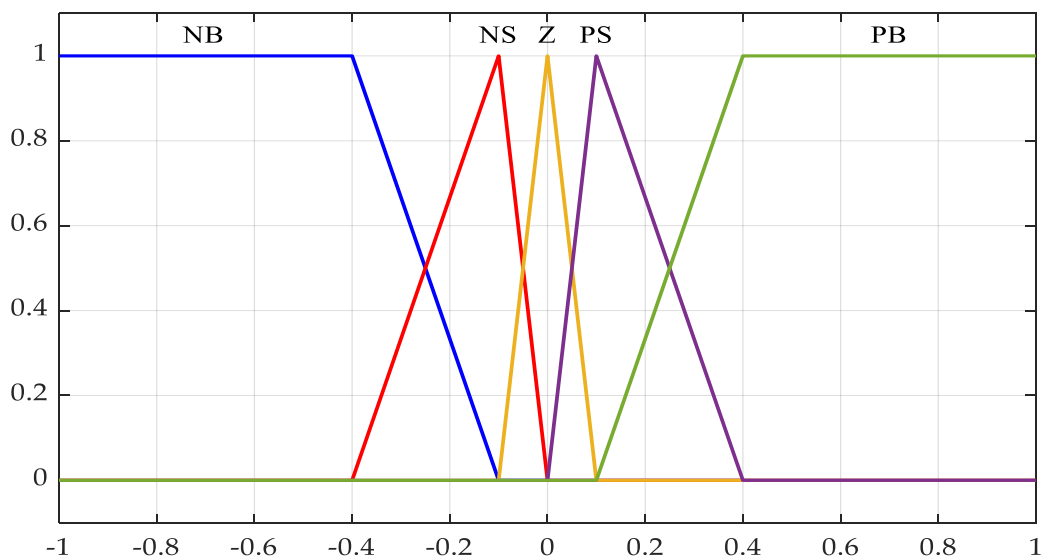


Figure 4.4. Membership functions of the two inputs and output.

Table 4.2. Fuzzy rule base of the proposed controller.

ΔF	ΔF				
	NB	NS	Z	PS	PB
NB	NB	NB	NB	NS	Z
NS	NB	NB	NS	Z	PS
Z	NB	NS	Z	PS	PB
PS	NS	Z	PS	PB	PB
PB	Z	PS	PB	PB	PB

4.3.2.3 Objective Functions

In the design of modern controllers and for any controlled system, stable performance and fast response are required. However, in practice, both requirements are never achievable simultaneously. Therefore, a compromise between quick response and excellent stability is considered when designing a controller, which is achievable by adequately selecting an appropriate controller and designing it by minimizing a properly selected cost/objective function with the aid of an optimization algorithm. The objective function used to tune the controller mainly relies on a performance criterion that considers the overall closed-loop response of the system. Many objective functions have been proposed in the control design, in which four kinds are the most often used for LFC. Because of their better performance compared to the other criteria [19], the Integral of Square Error (ISE) illustrated in Equation (4.3) and Integral Time Absolute Error (ITAE) expressed in Equation (4.4) are used in this work. Therefore, PID, FOPID and Fuzzy PIDF controllers are designed for the LFC of the GB power system by minimizing the defined objective functions with the help of the Bees Algorithm and other two techniques.

$$ISE = J = \int_0^{T_{sim}} (\Delta F)^2 \times dt \quad (4.3)$$

$$ITAE = J = \int_0^{T_{sim}} |\Delta F| \times t \times dt \quad (4.4)$$

It is proven that with ISE, large errors are more penalized than smaller ones. Thus, control systems designed by minimizing ISE are more most likely to eliminate large errors quickly. However, they have to tolerate small ones that are continuous for a long period of time. ITAE calculates the integration of the absolute error multiplied by the time over the simulation period. This criterion is based on weighing errors that occur after a long time more

largely than those that exist during the beginning of the response [20]. Control systems specified based on ITAE tuning tend to settle much more quickly than the ISE tuning methods.

4.3.3 Results and Discussion

This work was implemented in MATLAB (2019a) installed on Intell (R) Core(TM) i5-6600 CPU @ 3.30GHz computer, the BA, TLBO and PSO codes were programmed in (.m files), and the model of the GB power system was developed in the MATLAB Simulink environment (the .m MATLAB file (the code of the algorithm) is calling the Simulink file where the power system model is developed. The parameters of BA and PSO were set as depicted in Tables 4.3 and 4.4, respectively. With TLBO, the population size was set to 50, and the maximum number of iterations was taken as 40 for all algorithms.

It is worth mentioning that the computational time taken to obtain the optimal values of the FLC structures is slightly long. For example, the computational time of the BA tuning the parameters of the FLC takes longer than 36 hours. It is also observed that the used algorithms take a longer time in optimizing the parameters of the proposed fuzzy configurations when they are implemented in the two-area power system as they tune 12 parameters or more. This unenabled the author from providing several runs to observe the convergence of the cost function. However, the value of the cost function based on the optimal performance of each controller is provided.

Table 4.3. The BA parameters.

n	m	e	nep	nsp	ngh
30	12	6	11	7	0.011

Table 4.4. The PSO parameters.

No. Particles	W_{min}	W_{max}	C₁	C₂	CR
30	0.4	0.9	2	2	0.65

To study the dynamic performance of the GB power system, a step load perturbation of 0.03955 pu (at $t = 5$ s) represents a loss of generation unit equal to 1.32 GW (two of large generators, 660 MW) of the total generation power of the GB system used, which occurred in the GB system on 27th May 2008 [3].

ITAE and ISE are taken separately as objective functions to tune the parameters of the proposed controllers using the above-mentioned algorithms for LFC in the generalized GB power system model. Initially, the parameters of the PID controller are optimized; it is found

that the PID tuned by the proposed algorithms performs satisfactorily to damp out the drop in the frequency. However, a reduced drop in frequency with a slow response is achieved when ISE is considered as an objective function, while with ITAE, the drop in frequency worsened with the fast response obtained, bringing the frequency back to the nominal value in a shorter period of time. Then, the gains of FOPID are tuned; in this regard, it is worth highlighting that, in general, the FOPID tuned by BA designed via minimizing ITAE provides better results compared to the tuned PID. However, FOPID designed with ISE fails to bring the frequency back to its nominal value. Thereafter, Fuzzy PIDF parameters are tuned, where a significant improvement is achieved in comparison with PID and FOPID.

4.3.3.1 Classical Controllers

The gains of the conventional PID and FOPID controllers obtained using BA, TLBO and PSO optimization algorithms using the suggested objective functions are depicted in Table 4.5.

Table 4.5. Optimal gains of PID and FOPID with different algorithms for GB power system.

Proposed Controller	Optimization Algorithms/Controller Parameters			
	Parameters	BA	TLBO	PSO
PID-ISE	K_P	40	40	40
	K_I	18.61	18.6373	18.6347
	K_D	40	40	40
PID-ITAE	K_P	40	40	40
	K_I	2.3044	2.383	2.3129
	K_D	16.1483	14.523	15.1724
FOPID-ISE	K_P	40	40	40
	K_I	40	40	40
	K_D	40	40	40
	λ	0.5584	0.55805	0.5562
	μ	0.3441	0.3450	0.3439
FOPID-ITAE	K_P	40	40	40
	K_I	40	40	40
	K_D	40	40	40
	λ	0.89	0.872	0.8953
	μ	0.388	0.3184	0.236

Results obtained based on BA, TLBO and PSO tuning PID and FOPID are presented below. The undershoot (U_{sh} in Hz), overshoot (O_{sh} in Hz) and settling time (T_s in s) of the dynamic response of the simplified GB power system are shown in Tables 4.6 – 4.9. The changes in the frequency within the testbed power system following a disturbance with a magnitude of 0.03955 pu (at $t = 5$ s) when these controllers are used for LFC purposes are shown in Figures 4.5 – 4.8.

From Figure 4.5 and Table 4.6, it is clear that when the PID tuned using the proposed algorithms based on ISE as cost function almost identical responses are obtained. The used controller has brought back the frequency to its nominal values (steady state error = 0). However, the transient response of system is not good enough as the response is not quick and a significant overshoot/undershoot is resulted.

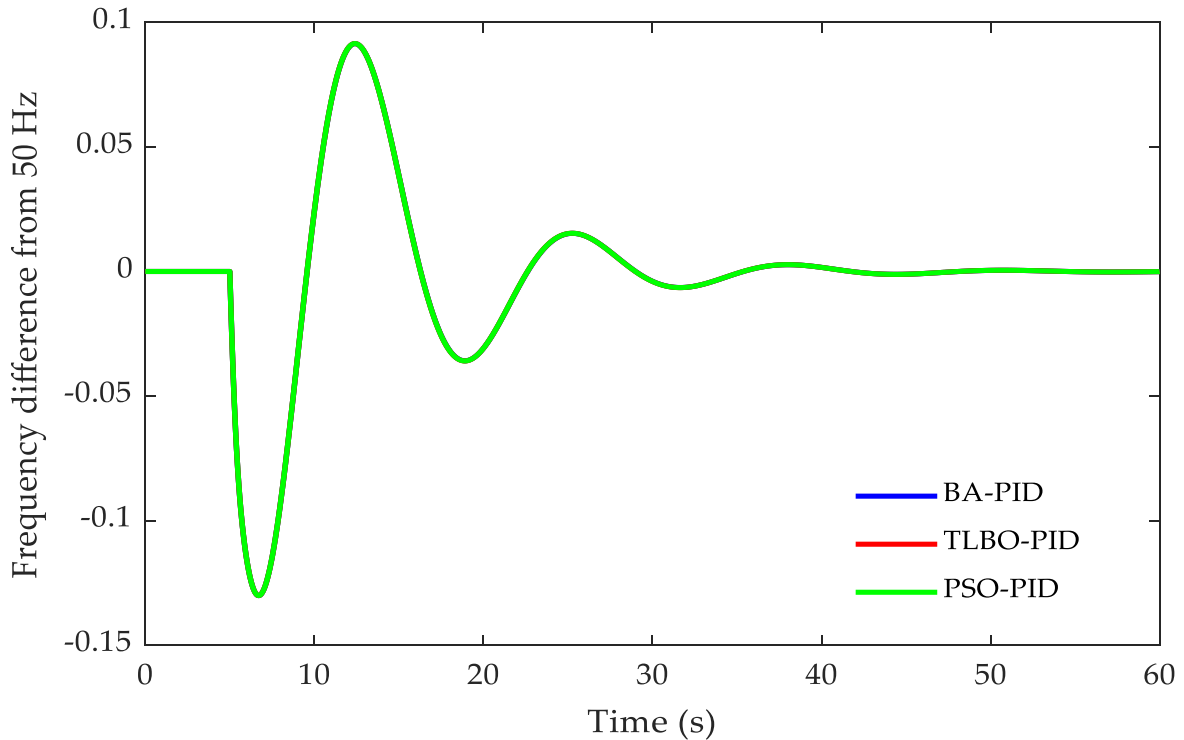


Figure 4.5. Change in frequency in the GB power system for 0.035 pu load disturbance with tuned PID-based ISE.

Table 4.6. Frequency response performances with PID tuned by different algorithms and designed by minimizing ISE.

Controller	U_{sh} in Hz	O_{sh} in Hz	T_s in s	Error	$ISE \times 10^{-5}$
BA-PID	-0.1301	0.09148	33.777	0	2.891
PSO-PID	-0.1301	0.09148	33.793	0	2.891
TLBO-PID	-0.1301	0.09143	33.794	0	2.891

On the other hand, when ITAE is used as an objective function to design the PID controller a slight further drop in the frequency with a very small overshoot and a quicker response is observed. As demonstrated in Figure 4.6 and Table 4.7, the drop in the frequency was -0.1840 Hz, -0.1859 Hz and -0.1870 Hz based on PID optimized by BA, PSO and TLBO, respectively. Furthermore, the transient response of the system has been slightly improved with a better settling time and less overshoot observed.

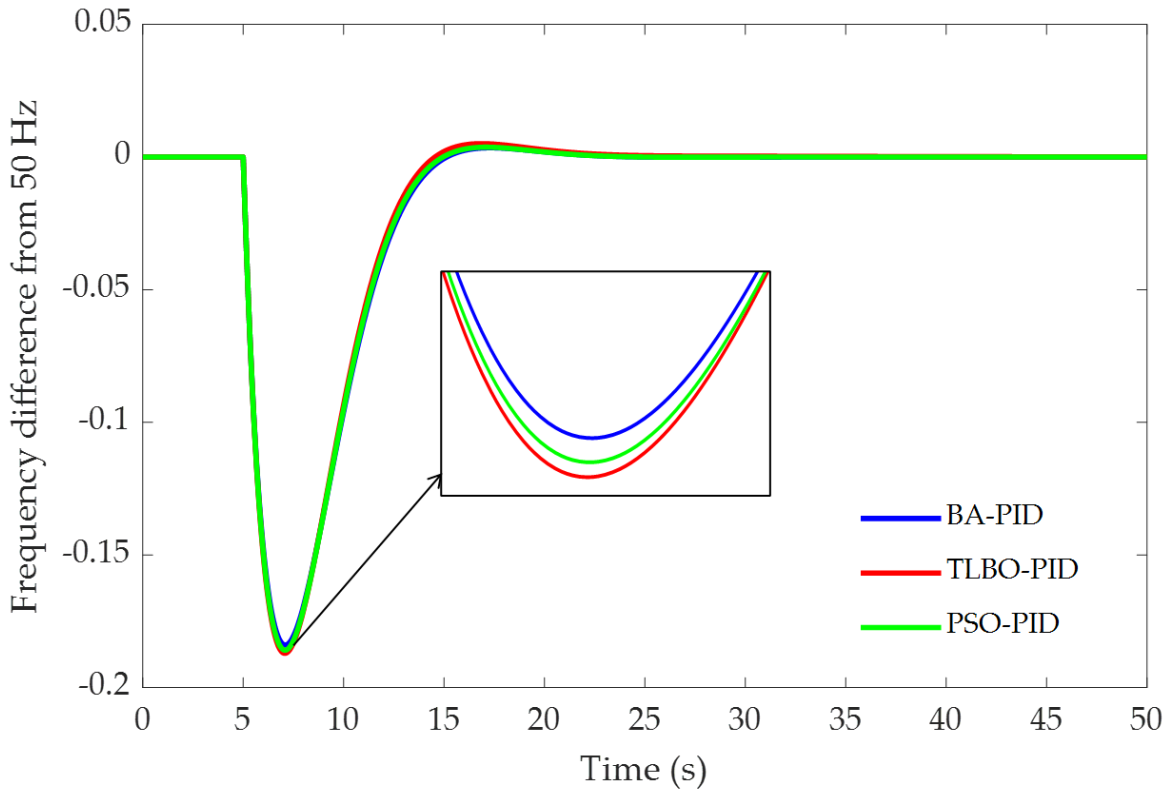


Figure 4.6. Change in frequency in the GB power system for 0.035 pu load disturbance with tuned PID-based ITAE.

Table 4.7. Frequency response performances with PID tuned by different algorithms and designed by minimizing ITAE.

Controller	U_{sh} in Hz	O_{sh} in Hz	T_s in s	Error	ITAE
BA-PID	-0.1840	3.51×10^{-3}	9.4256	0	0.1515
PSO-PID	-0.1859	3.71×10^{-3}	9.2792	0	0.1508
TLBO-PID	-0.1870	5×10^{-3}	13.8580	0	0.1553

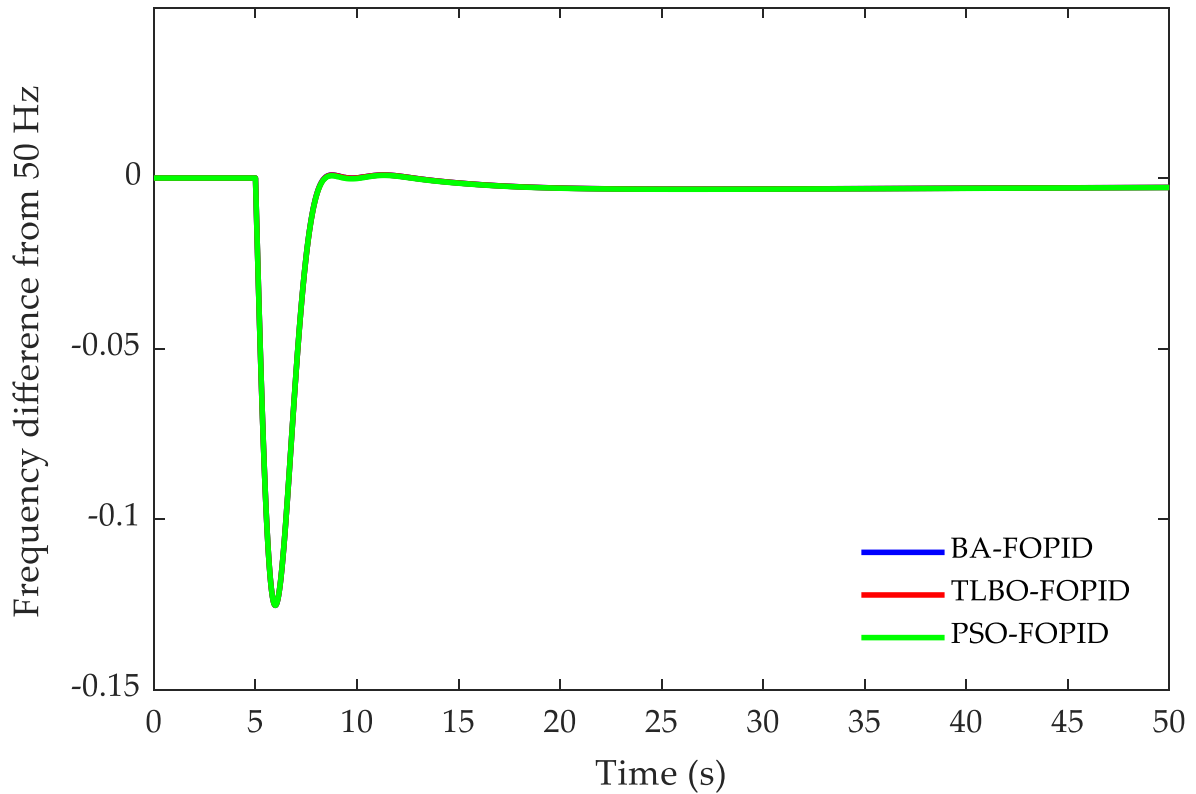


Figure 4.7. Change in frequency in the GB power system for 0.035 pu load disturbance with tuned FOPID-based ISE.

Table 4.8. Frequency response performances with FOPID tuned by different algorithms and designed by minimizing ISE.

Controller	U_{sh} in Hz	O_{sh} in Hz $\times 10^{-4}$	T_s in s	Error $\times 10^{-3}$	ISE $\times 10^{-6}$
BA-FOPID	-0.12	8.91	8.0145	2.72	7.8
PSO-FOPID	-0.12	7.8	7.9536	2.76	7.8
TLBO-FOPID	-0.12	8.82	8.0137	2.73	7.8

As shown in Figure 4.7 and Table 4.8, FOPID designed by minimizing ISE is found to be less effective in eliminating the steady-state error which made this technique less preferable option for this system. Furthermore, the performance of this controller as tuned by different optimization techniques is similar.

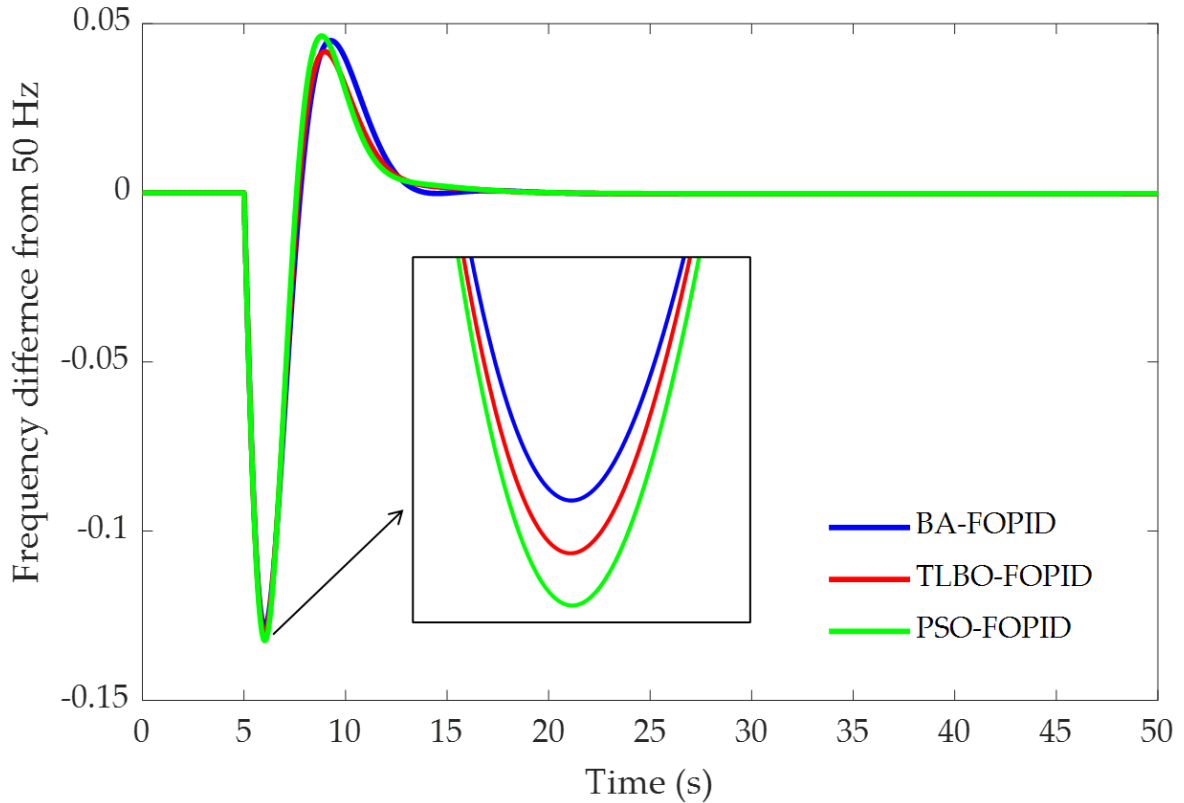


Figure 4.8. Change in frequency in the GB power system for 0.035 pu load disturbance with tuned FOPID-based ITAE.

Table 4.9. Frequency response performances with FOPID tuned by different algorithms and designed by minimizing ITAE.

Controller	U_{sh} in Hz	O_{sh} in Hz	T_s in s	Error	ITAE
BA-FOPID	-0.1282	0.045	8.045	0	0.0581
PSO-FOPID	-0.1324	0.0463	9.0826	0	0.0558
TLBO-FOPID	-0.1303	0.0417	8.7397	0	0.0566

Figure 4.8 and Table 4.9 prove that FOPID tuned by the proposed BA using ITAE as an objective function provides a slightly better performance in terms of undershoot and settling time in comparison with the same controller designed by minimizing the ISE objective function.

4.3.3.2 Fuzzy PIDF Controller

The optimal gains of the proposed Fuzzy PID with derivative filter obtained by the proposed BA, TLBO and PSO algorithms using the suggested objective functions are depicted in Table 4.10. Simulation results obtained with the BA are compared with those of TLBO and PSO, it is found to be an excellent tool and provides an improved performance in many aspects.

Table 4.10. Optimal gains of Fuzzy PIDF with different algorithms for GB power system.

Proposed Controller	Optimization Algorithms/Controller Parameters			
	Parameters	BA	TLBO	PSO
Fuzzy PIDF ISE	K_1	3.41	2.99	3.88
	K_2	40	40	29.72
	K_P	29.91	40	26.60
	K_I	18.59	39.99	17.82
	K_D	20.93	14.998	14.59
	K_F	40	40	40
Fuzzy PIDF ITAE	K_1	20.37	3.955	7.1590
	K_2	38.12	14.997	24.2973
	K_P	19.25	39.996	18.83
	K_I	38.14	40	7.68
	K_D	4.29	14.995	3.889
	K_F	40	40	40

Tables 4.11&4.12 and Figures 4.9 & 4.10 demonstrate the frequency response of the GB power system when the Fuzzy PIDF is optimized by different optimization algorithms implemented for LFC. It is observed that a significant improvement is achieved in comparison with classical controllers.

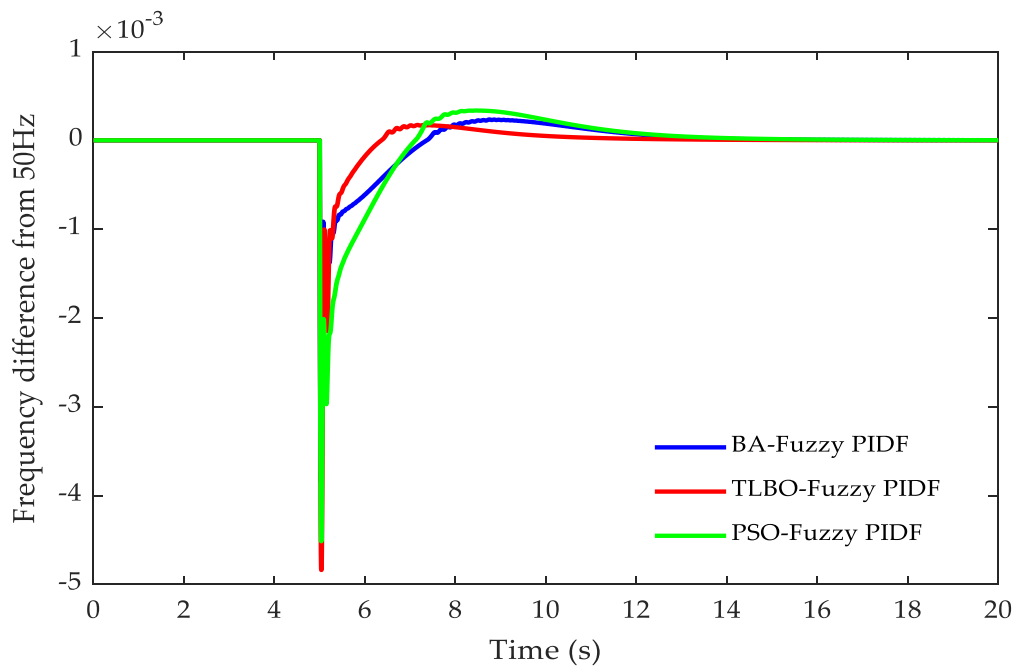


Figure 4.9. Change in frequency in the GB power system for 0.035 pu load disturbance with tuned Fuzzy PIDF-based ISE.

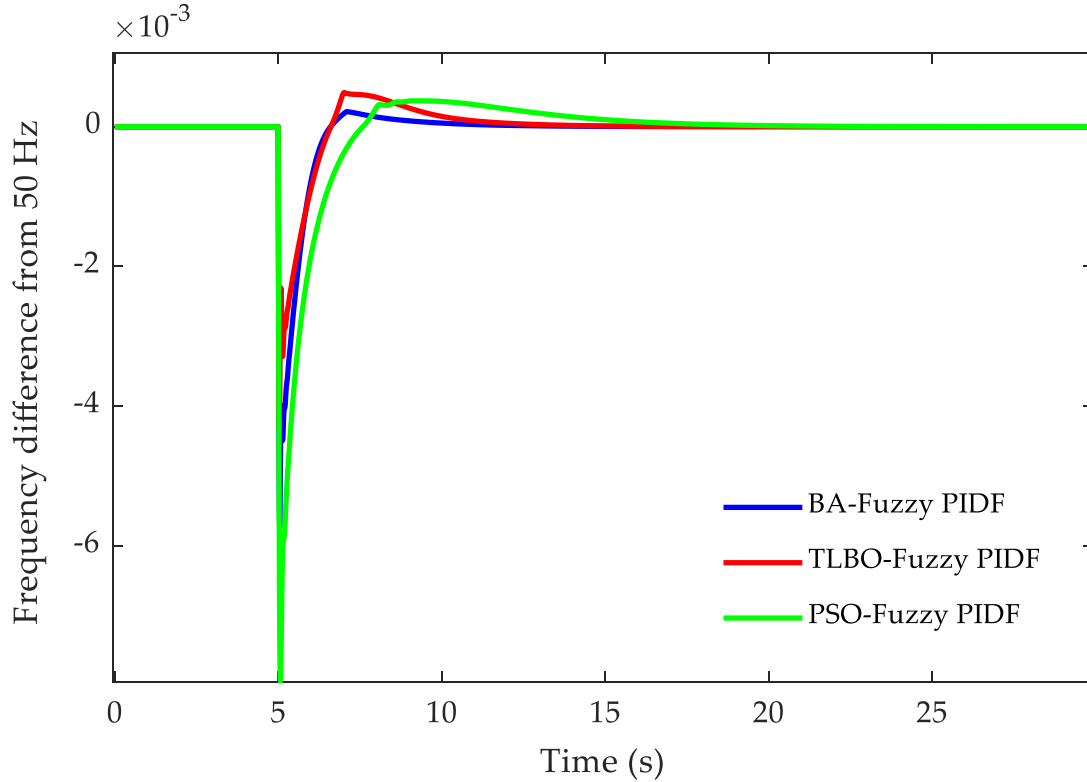


Figure 4.10. Change in frequency in the GB power system for 0.035 pu load disturbance with tuned Fuzzy PIDF-based ITAE.

Moreover, BA has proved to be a powerful technique to tune the Fuzzy PIDF as the results obtained from the proposed controller tuned by BA proved that the performance of the system witnessed a clear improvement in terms of undershoot and settling time. Regarding the error and overshoot, almost similar results are obtained based on all algorithms.

Table 4.11. Frequency response performance with Fuzzy PIDF controllers designed via ISE.

Controller	U_{sh} in Hz	O_{sh} in Hz	T_s in s	Error	$ISE \times 10^{-10}$
BA-Fuzzy PIDF	-0.0038	2.37×10^{-4}	11.7941	0	6.71
PSO-Fuzzy PIDF	-0.00451	3.36×10^{-4}	11.7689	0	15.2
TLBO-Fuzzy PIDF	-0.00483	1.75×10^{-4}	8.8523	0	6.88

Table 4.12. Frequency response performance with Fuzzy PIDF controllers designed via ITAE.

Controller	U_{sh} in Hz	O_{sh} in Hz	T_s in s	Error	ITAE
BA-Fuzzy PIDF	-0.0057	2.15×10^{-4}	8.3776	0	0.000391
PSO-Fuzzy PIDF	-0.00793	3.7×10^{-4}	13.6303	0	0.001065
TLBO-Fuzzy PIDF	-0.0043	4.9×10^{-4}	10.9389	0	0.000495

4.3.4 Robustness Analysis

4.3.4.1 Robustness Analysis against System Uncertainty

Parameters within the system, including the damping coefficient D , speed regulator R , system inertia coefficient H_{eq} and turbine governor time constant T_g , are subject to a continuous fluctuation, which can lead to a significant degradation in the performance of close-loop systems. There has been comparatively less focus in research on this issue within load frequency control; for example, the increase in the total system inertia will slow down the system response, while the frequency deviation decreases if the damping ratio increases, and if the governor time constant increases, the frequency deviation will increase. The impact of the variation in each parameter on the frequency response of the GB power system is provided in Appendix B. Therefore, investigations are carried out in order to study the consequences of parametric uncertainties in the system. For this, each parameter in the system is altered by $\pm 50\%$ from its nominal value. Two different scenarios of parameters' uncertainty, T_g , D , R and H_{eq} (listed in Table 4.13 and shown in Figure 4.11) are considered for the simplified GB power system model examination. In this sub-section, only controllers tuned by the proposed BA are examined. The optimal gains obtained during the normal condition will not be re-tuned when the model is subjected to variation in system parameters.

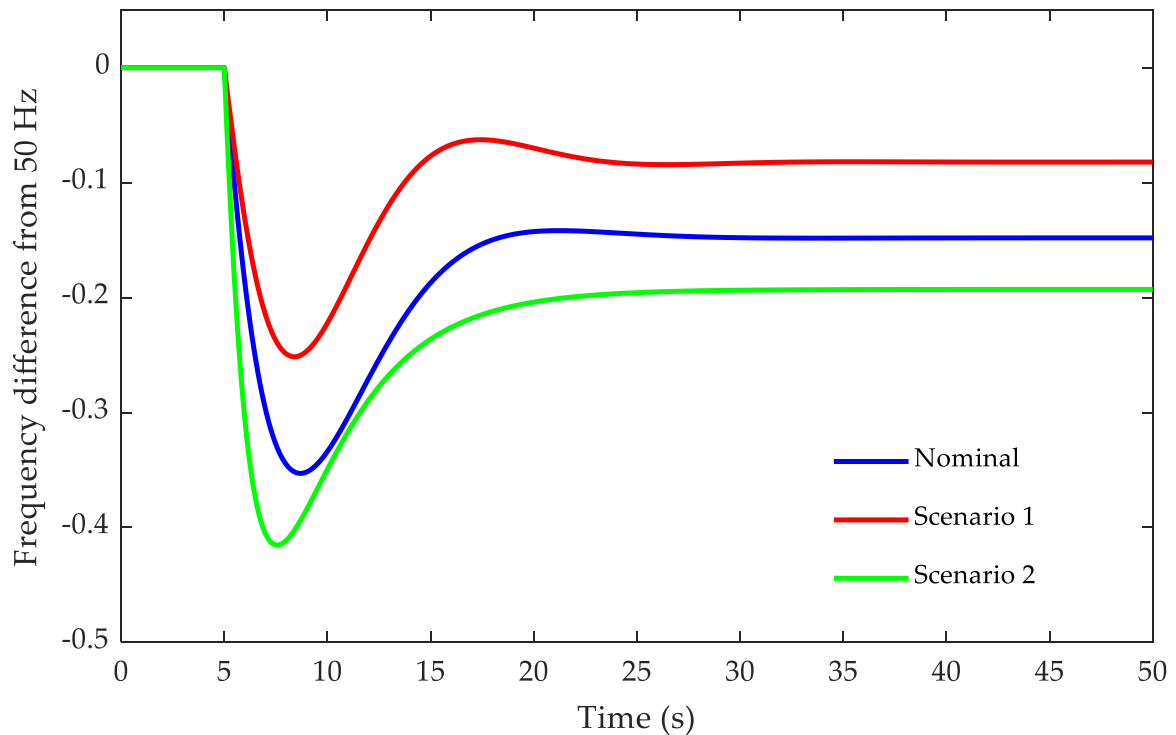


Figure 4.11. Comparison of the dynamic response of GB power model with parameter uncertainties of scenarios 1 and 2 with no secondary control loop.

Table 4.13. The variation range of the parameters in the two scenarios.

Scenarios	Parameters	Nominal Value	Variation Range	New Value
Scenario1	T_g	0.2	+50%	0.3
	H_{eq}	4.44	+50%	6.66
	D	1	-50%	0.5
	R	-0.09	-50%	-0.045
Scenario2	T_g	0.2	-50%	0.1
	H_{eq}	4.44	-50%	2.22
	D	1	+50%	1.5
	R	-0.09	+50%	-0.135

Furthermore, as shown in Figure 4.11, in the second scenario, the frequency response of the system is worse than the nominal case. Therefore, the second scenario only is investigated which also represents a possible decline in the total system inertia of the GB power system due to the increasing use of renewable energy resources.

Figures 4.12 and 4.13 show the frequency response of the GB power system under parametric uncertainties when different controllers tuned by BA are employed as the LFC system. From Figures 4.12 and 4.13, it is noted that Fuzzy PIDF controllers provide high stability while classical controllers show less robustness against system uncertainty, with the worst drop in frequency recorded at -0.178 Hz when PID is applied for LFC in scenario 2. The dynamic responses of the system with different BA-tuned controllers based on ISE and ITAE, respectively, are listed in Tables 4.14 and 4.15.

Table 4.14. Frequency response performances with different BA-tuned controllers designed via ISE for scenario 2.

Controller	U_{sh} in Hz	O_{sh} in Hz	T_s in s	Error	ISE
BA-Fuzzy PIDF	-0.0042	2.68×10^{-4}	12.61	0	6.77×10^{-10}
BA-FOPID	-0.141	0	9.40	-2.75×10^{-3}	0.0454
BA-PID	-0.126	0	22.09	0	0.1643

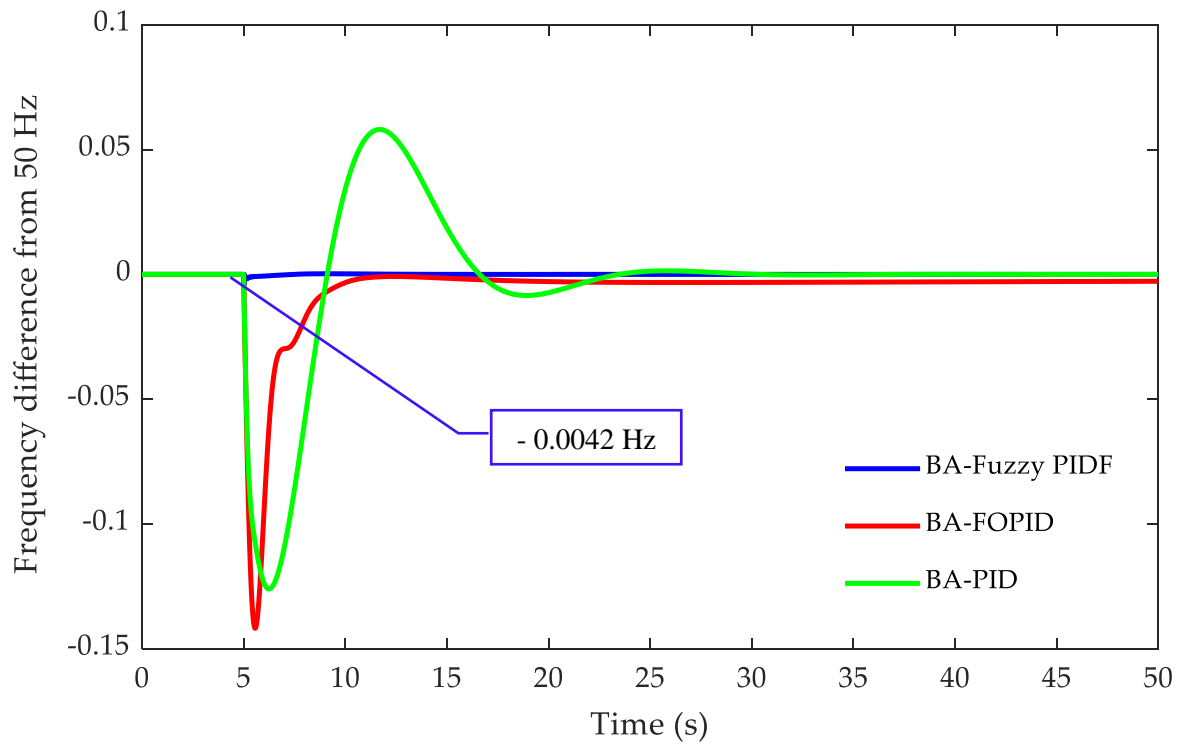


Figure 4.12. Comparison of three controllers tuned by BA based on ISE for scenario 2.

Table 4.15. Frequency response performance with different BA-tuned controllers designed via ITAE for scenario 2.

Controller	U_{sh} in Hz	O_{sh} in Hz	T_s in s	Error	ITAE
BA-Fuzzy PIDF	-0.0066	2.68×10^{-4}	8.22	0	0.0004
BA-FOPID	-0.143	0.020	15.16	0	0.0454
BA-PID	-0.178	0	20.75	-4×10^{-3}	0.1643

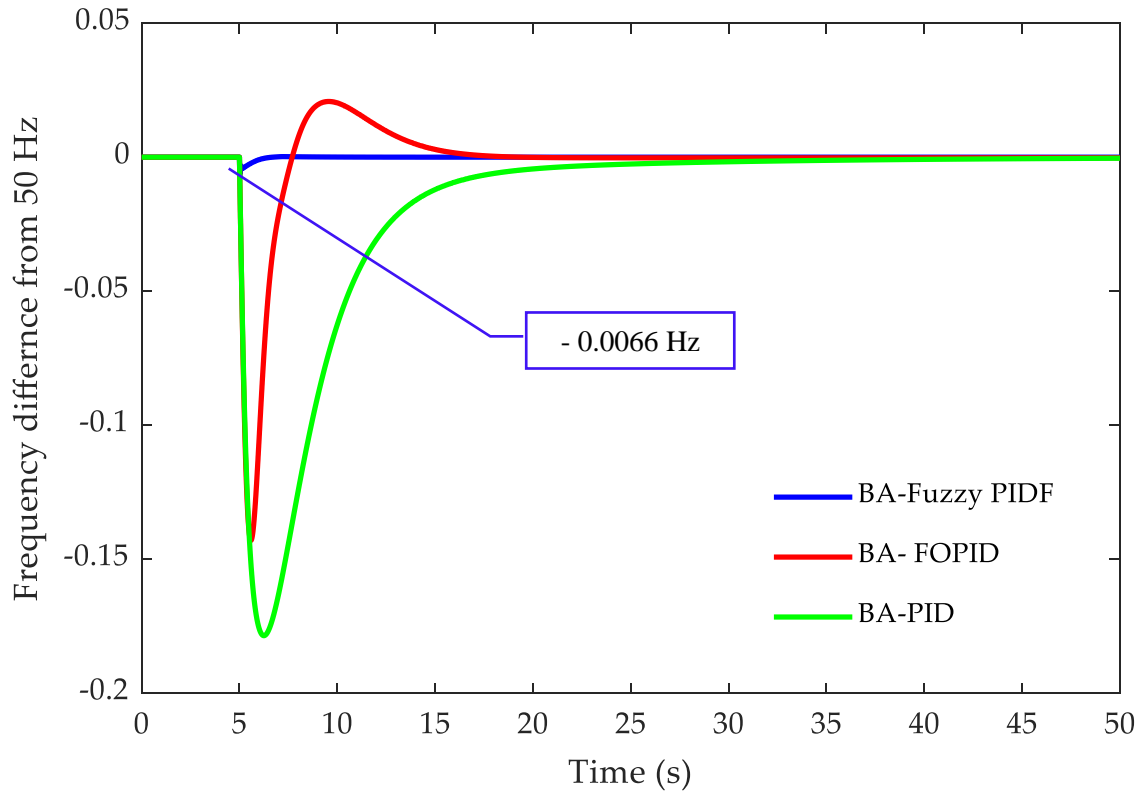


Figure 4.13. Comparison of three controllers tuned by BA based on ITAE for scenario 2.

4.3.4.2 Different Load Disturbances

To further investigate the robustness of Fuzzy PIDF, FOPID and PID tuned by BA, a loss of 1.8 GW (very large nuclear generator) in the generation unit representing around 0.053 pu is considered in this sub-section. The dynamic response of the GB power system with the new load disturbance is shown in Figure 4.14 and the frequency response performances are tabulated in Table 4.16. Furthermore, in order to further examine the robustness of the proposed techniques, parameter uncertainties from scenario 2 are considered when a power generation of 0.053pu is lost and the frequency response of the system in this case is given in Figure 4.15; the frequency response performances are depicted in Table 4.17, from which it is obvious that the proposed controller “Fuzzy PIDF” tuned by BA is robust and performs satisfactorily even when a larger generator is lost with parameter uncertainties. Note that only controllers tuned by BA based on minimizing the ITAE objective function are considered in this part.

Table 4.16. Frequency response performance with BA tuned different controllers designed via ITAE for scenario 2.

Controller	U_{sh} in Hz	O_{sh} in Hz	T_s in s	Error	ITAE
BA-Fuzzy PIDF	-0.0083	2.8×10^{-4}	8.22	0	0.00056
BA-FOPID	-0.171	0.0603	13.04	-3×10^{-4}	0.0779
BA-PID	-0.246	5×10^{-3}	14.42	0	0.203

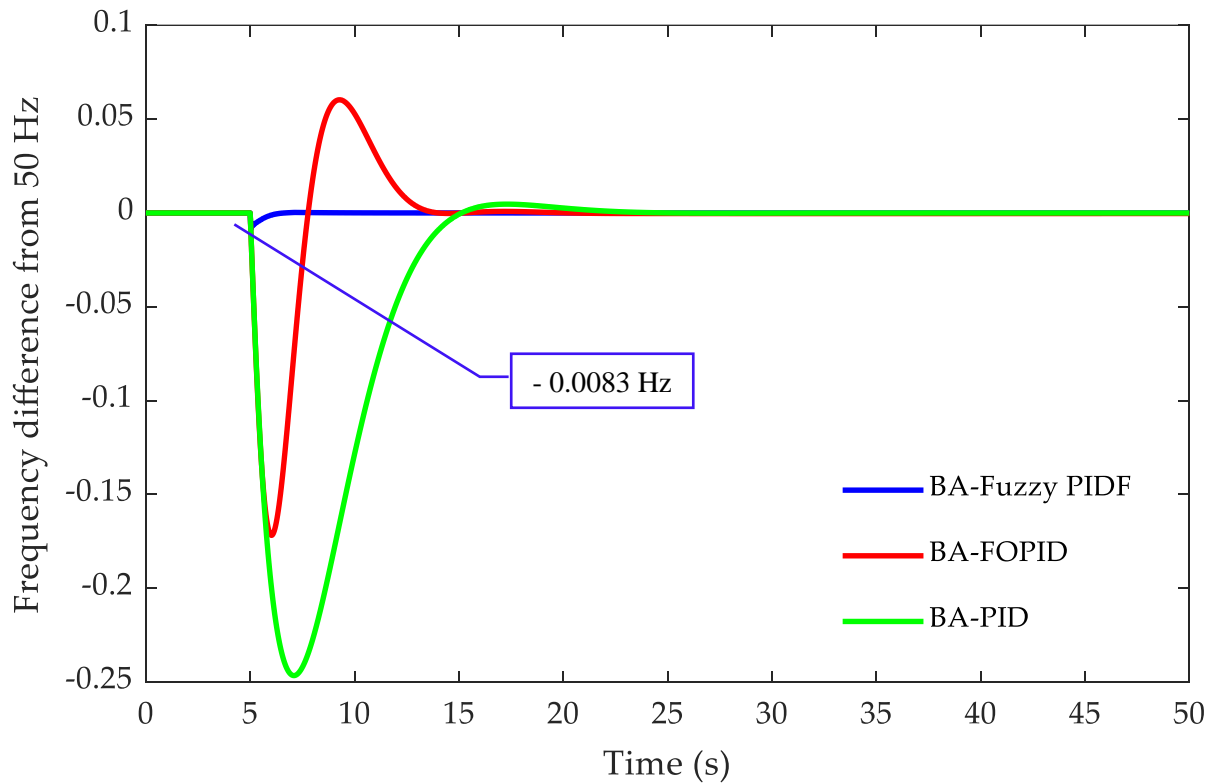


Figure 4.14. Comparison of three controllers tuned by BA based on ITAE for LFC of the GB system in the nominal scenario with 0.053 pu load disturbance.

Table 4.17. Frequency response performances with BA-tuned controllers designed via minimizing ITAE in scenario 2 with 0.053 pu load disturbance.

Controller	U_{sh} in Hz	O_{sh} in Hz	T_s in s	Error	ITAE
BA-Fuzzy PIDF	-0.0098	2.7×10^{-4}	8.021	0	0.00058
BA-FOPID	-0.191	0.028	15.16	-3.1×10^{-4}	0.06096
BA-PID	-0.239	0	20.75	-5.5×10^{-4}	0.22020

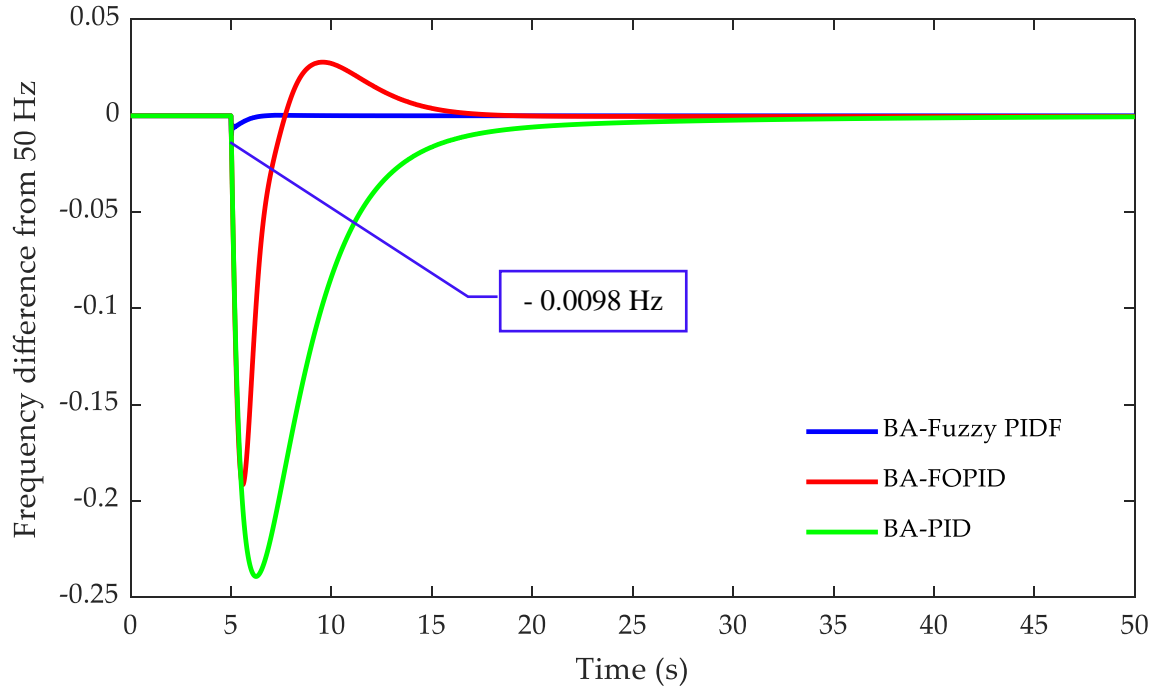


Figure 4.15. Comparison of three controllers tuned by BA based on ITAE for LFC of the GB system in scenario 2 with 0.053 pu load disturbance.

4.4 LFC Based Different Fuzzy Logic control Structures for Two-area Interconnected Power System.

This subsection implements the proposed Fuzzy Proportional Integral Derivative with Filtered derivative mode (Fuzzy PIDF) for Load Frequency Control (LFC) of a two-area interconnected power system. To attain the optimal values of the proposed structure's parameters which guarantees the best possible performance, the Bees Algorithm (BA) and other optimisation tools are used to accomplish this task. A Step Load Perturbation (SLP) of 0.2 pu is applied in area one to examine the dynamic performance of the system with the proposed controller employed as LFC system. The supremacy of Fuzzy PIDF is proven by comparing the results with those of previous studies for the same power system. Since the designed controller is required to provide reliable performance, this study is further extended to propose three different fuzzy control configurations that offer higher reliability. Moreover, an extensive examination of the robustness of these structures towards parametric uncertainties of the investigated power system considering thirteen cases is carried out. Simulation results indicate the contribution of the BA tuned the proposed fuzzy control structures in alleviating overshoot, undershoot and settling time of frequency in both areas and tie-line power oscillations. Based on the obtained results, it is revealed that the lowest drop of the frequency in area one is -0.0414 Hz which is achieved by the proposed Fuzzy

PIDF tuned by BA. It is also divulged that the proposed techniques have evidenced their performance to offer a good transient response, considerable capability of disturbance rejection and insensitivity toward parametric uncertainty of the controlled system. The objectives of the section can be concluded as follows:

- To propose a Fuzzy PIDF optimised by the BA and other two algorithms for load frequency control of a two-area power system and investigate its dynamic performance.
- To assess the supremacy of the proposed technique by comparing the results with those of previously published works based on TLBO tuned Fuzzy PID [7] and Lozi map- based Chaotic Optimisation Algorithm (LCOA) tuned PID [21].
- To investigate the robustness of the Fuzzy PIDF against a wide variation range in parametric uncertainties of the investigated system.
- Furthermore, from the comprehensive literature review, it is concluded that the proposed techniques based on different theories may provide the desired performance to overcome the problem of frequency deviation. However, most recent studies have not considered the reliability aspects in the design of the proposed schemes. This research gap has motivated the author to suggest fuzzy control configurations for LFC in power systems that offer different levels of reliability. Therefore, this study is then extended to propose three different fuzzy control structures, namely, Fuzzy Cascade PI-PD, Fuzzy PI+PD and Fuzzy PI plus Fuzzy PD. An extensive assessment of the robustness of these structures towards parametric uncertainties of the testbed system considering thirteen cases is conducted.

4.4.1 Two-area Power System-model Understudy

The investigated system in this section is an unequal dual area non-reheat interconnected power system shown in Figure 4.16. This system is widely investigated in literature to design and analysis LFC of interconnected power systems [7] [21]. For stable operation, if the load increases, the governor will decrease the speed, this means moving the turbine input valve to a more open state (this also means increasing the torque). The coefficient of speed regulation or the droop gain (R) represents the ratio of the frequency deviation to the generator output power variation. The relevant parameters of this model are given in Table 4.18.

Table 4.18. The parameter of the testbed system.

Parameters	Definition	Values in area 1	Values in area 2
1/R	Regulation constant	0.05 MW/Hz	0.0625 MW/Hz
B	Frequency bias	20.6 Hz/MW	16.9 Hz/MW
D	The ratio of change in load to change in frequency	0.6	0.9
H	System inertia time constant	5	4
T_g	Governor time constant	0.2 s	0.3 s
T_t	Turbine time constant	0.5 s	0.6 s
T	Synchronization coefficient	2	
F	Frequency of the system	60 Hz	
SLP	Step Load Perturbation	0.2 pu	

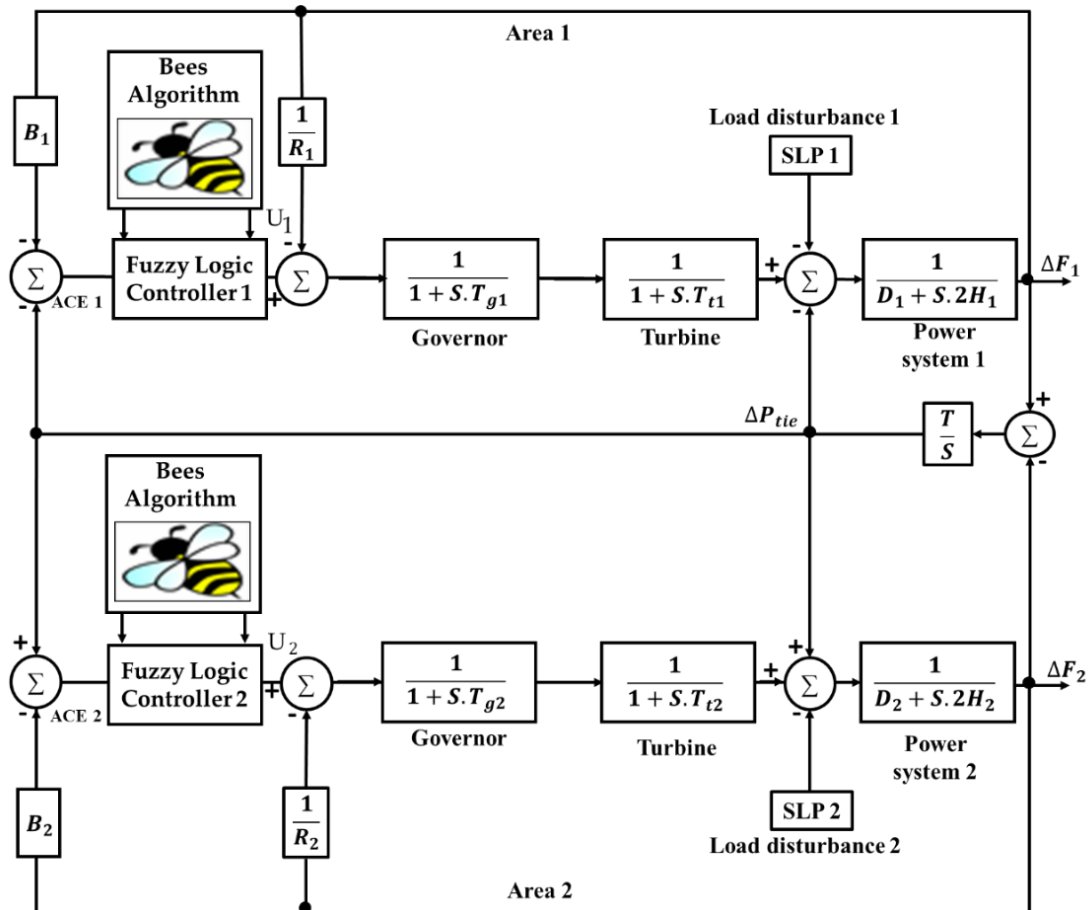


Figure 4.16. Transfer function model of the testbed system.

In this system, the generated mechanical power can be produced by gas, hydraulic and thermal turbines. The governor senses the generator speed variation and varies the mechanical output power of the turbine by adjusting the position of the turbine input valve, this response

is known as the primary frequency response. For stable operation, if the load increases, the governor will increase the speed; this means moving the turbine input valve to a more open state (this also means increasing the torque). The coefficient of the speed regulation or the droop gain (R) represents the ratio of the frequency deviation to the generator output power variation.

In order to accomplish the task of LFC, the term “Area Control Error (ACE)” is usually utilized. The ACE of each area is the input of the proposed fuzzy PIDF controller. Equations (4.5) and (4.6) express the ACEs of area one and area two, respectively. From control design aspect, the desired operation of large power systems is to maintain the frequency and tie-line power deviation fixed on prespecified values even in the case of load disturbance, this requires the term of ACE to be maintained at zero.

$$ACE_{\text{area 1}} = \Delta P_{12} + B_1 \Delta F_1 \quad (4.5)$$

$$ACE_{\text{area 2}} = \Delta P_{21} + B_2 \Delta F_2 \quad (4.6)$$

Where ΔF_1 , and ΔF_2 are the frequency deviation in areas one and two respectively, ΔP_{12} and ΔP_{21} are the power flow deviation in areas one and two, and B_1 , B_2 are frequency biases.

4.4.2 Fuzzy PIDF and Objective Function

The structural design of the proposed controller equipped in area one is explained in Figure 4.3. (the same control configuration used in the simplified GB power system). In this case, applying the controller in two-area power system, the two inputs of the controller are: ACE1 and derivative of ACE1 and one output. In this structure, K_1 and K_2 are the scaling factor gains of the input. While K_{P1} , K_{I1} , K_{D1} and K_{F1} which is the filter gain are the scaling factors of the output. A similar controller is also employed in area two with K_3 and K_4 as input scaling factors and K_{P2} , K_{I2} , K_{D2} and K_{F2} for the output scaling gains. Accordingly, twelve parameters are to be optimised to obtain the desired dynamic response of the investigated system. The rule bases of the controller are given in Table 4.2, while the membership functions are illustrated in Figure 4.4.

Prior to using the BA, TLBO, and PSO to achieve the best performance of the Fuzzy PIDF employed for load frequency control in the two-area power system, a proper cost function should be selected. In this section, the proposed Fuzzy PIDF is designed by minimizing the Integral Time Absolute Error (ITAE) cost function with the aid of the suggested algorithms. The used objective function is expressed in (4.7). The selection of this

cost function is because it was proven to reduce both the settling time and overshoot/undershoot.

$$\text{Objective Function} = \text{ITAE} = \int_0^t (|\Delta F_1| + |\Delta F_2| + |\Delta P_{\text{tie}}|).t. dt \quad (4.7)$$

4.4.3 Results and Discussions

The parameters of BA and PSO were set as shown in Table 4.19. Where C_1 & C_2 are the acceleration constants, w_{\min} & w_{\max} are the inertia weights, CR is the crossover rate and No. Par is the number of particles. The TLBO has two parameters to be set, namely, the population size and the number of iterations which were set as 50 and 40, respectively.

Table 4.19. The BA and PSO parameters.

Controller	Parameters					
BA	n	m	e	nep	nsp	ngh
	30	12	6	11	7	0.011
PSO	No. Par	w_{\min}	w_{\max}	C_1	C_2	CR
	30	0.4	0.9	2	2	0.65

A Step Load Perturbation (SLP) of 0.2 pu is applied in area one to study the dynamic performance of the system with the proposed Fuzzy PIDF. The optimum values of the Fuzzy PIDF parameters obtained by BA, TLBO and PSO are given in Table 4.20. The scaling factors of the proposed Fuzzy controller design are chosen in the limits of [0-2], and the filter coefficient K_F is constrained in the range from 0 to 100.

Moreover, as it is above mentioned, results obtained from the proposed fuzzy structure are compared with those of previously published studies for the same system investigated in [7] [21]. The optimum gains of PID tuned by LCOA proposed in [21] and TLBO optimized Fuzzy PID studied in [7] are given in Table 4.21.

Table 4.20. Gains of Fuzzy PIDF Controllers Tuned by BA, TLBO and PSO

Controller	Controller Gains of Area 1						Controller Gains of Area 2					
	K_1	K_2	K_{P1}	K_{I1}	K_{D1}	K_{F1}	K_3	K_4	K_{P2}	K_{I2}	K_{D2}	K_{F2}
Fuzzy PIDF-BA	0.403	2	2	2	2	98.484	0.2648	1.008	0.9133	1.9730	1.9889	93.892
Fuzzy PIDF-TLBO	0.035	1.9992	1.9986	1.9986	1.9995	99.060	1.9602	0.037	0.4435	1.3003	0.019	99.744
Fuzzy PIDF-PSO	0.02	2	2	2	2	100	2	2	2	0.015	1.4035	11.21

Table 4.21. Gains of Fuzzy PID tuned by TLBO and PID tuned by LCOA.

Controller	Controller Gains of Area 1			Controller Gains of Area 2				
	K_{P1}	K_{I1}	K_{D1}	K_{P2}	K_{I2}	K_{D2}		
PID-LCOA [21]	0.939	0.7998	0.5636	0.5208	0.4775	0.7088		
Fuzzy PID- TLBO [7]	K_1	K_2	K_3	K_4	K_5	K_6	K_7	K_8
	1.9857	1.9968	1.6870	1.9876	1.3469	1.5512	0.8098	0.5043

The frequency deviation in both areas ΔF_1 and ΔF_2 , following the implementation of 0.2 pu disturbance in area one is shown in Figures 4.17 and Figure 4.18, respectively. The tie-line power deviation is given in Figure 4.19.

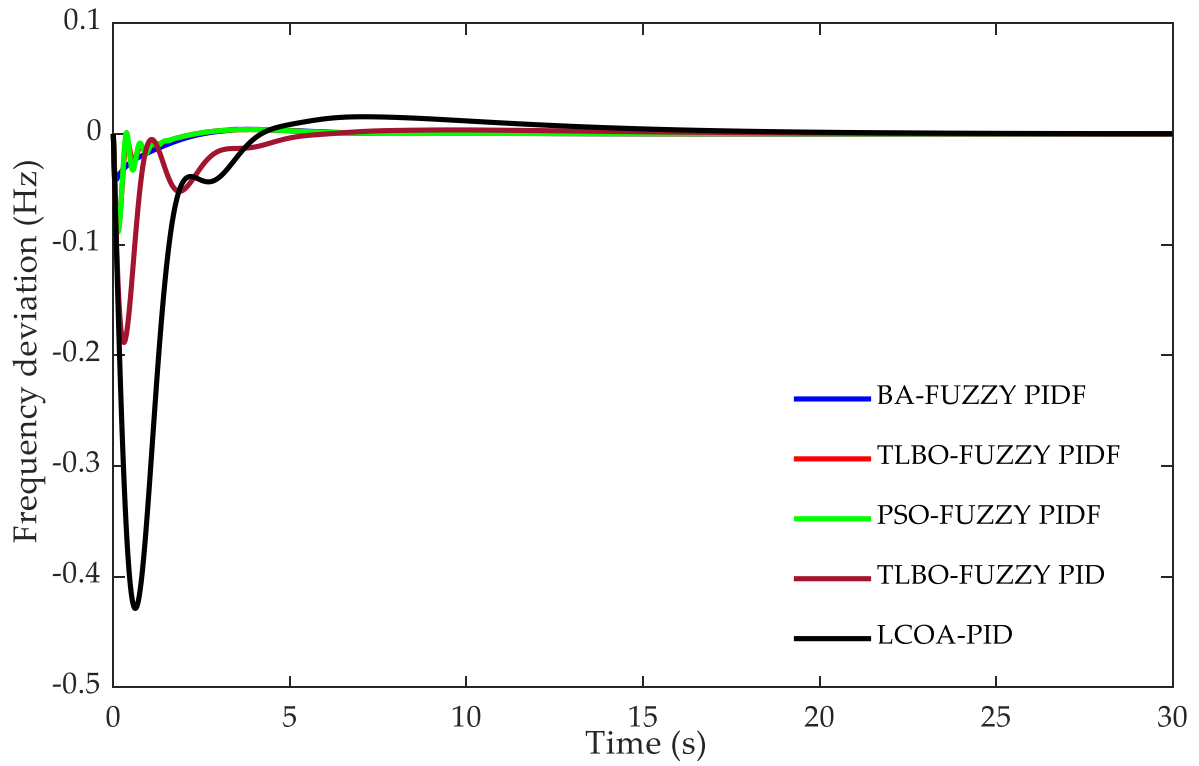


Figure 4.17. Frequency variation in area one (ΔF_1 in Hz).

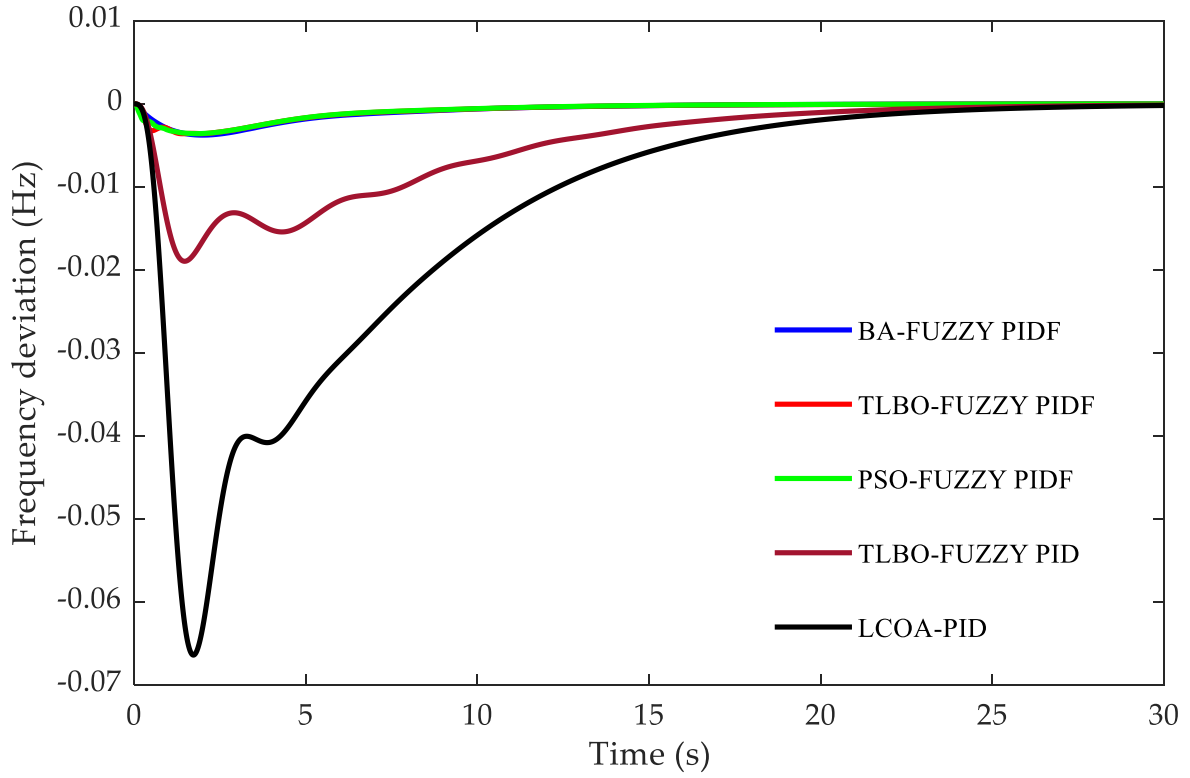


Figure 4.18. Frequency variation in area two (ΔF_2 in Hz).

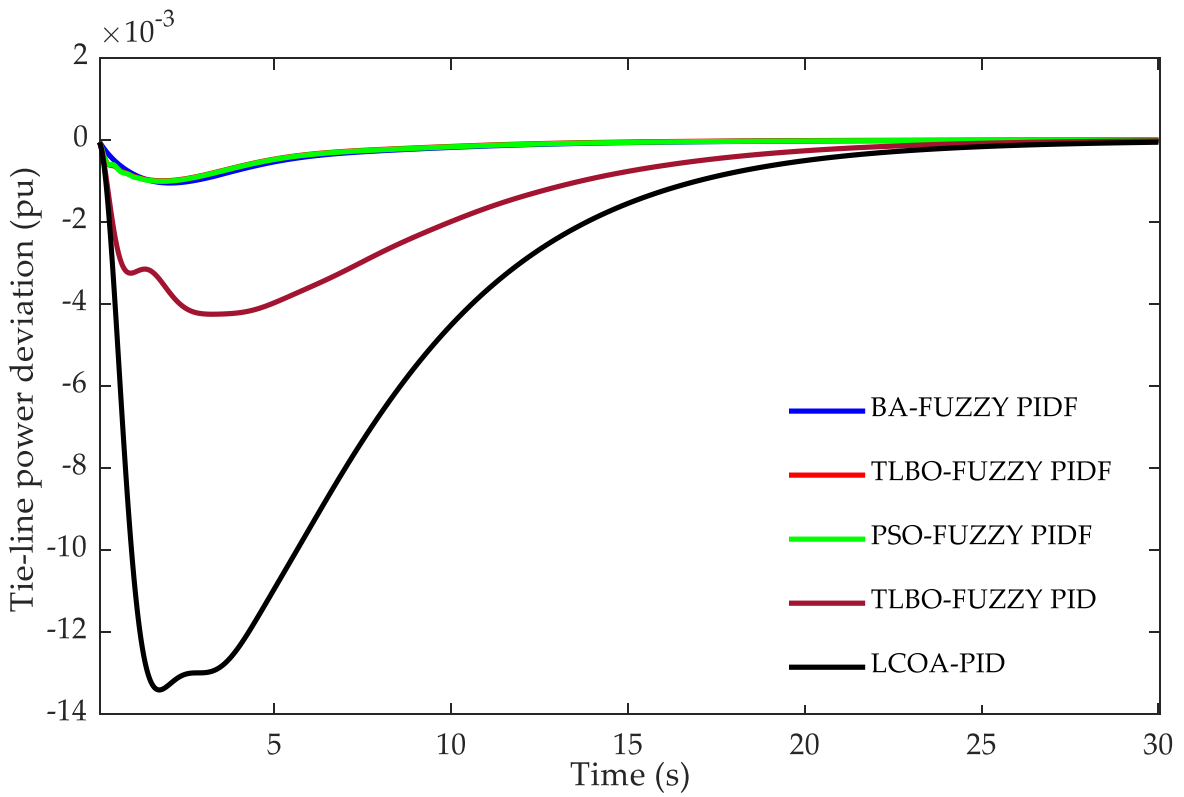


Figure 4.19. Tie line power variation (ΔP_{tie} in pu).

Figures. 4.17 - 4.19, summarize the main outcomes of the proposed Fuzzy PIDF, where it is obviously remarked that this controller has offered the best response among the investigated methods. Furthermore, in spite of the clear similarity in the dynamic response obtained by the proposed fuzzy structure tuned by BA, TLBO and PSO, it is observed that BA optimised the proposed fuzzy controller has provided the best result it terms of the drop in the frequency represented by peak undershoot occurred in area one after 0.2 pu disturbance enforcement. However, Fuzzy PIDF tuned by TLBO and PSO offered the best drop in frequency in area two. The dynamic performance of the system based Fuzzy PIDF tuned by the suggested algorithms, Fuzzy PID optimised by TLBO and PID controller tuned by LCOA represented by undershoot, peak overshoot, settling time in ΔF_1 , ΔF_2 and ΔP_{tie} is illustrated in Table 4.22; the value of the objective function based on each technique is also given.

Table 4.22. characteristics of the testbed system with several controllers.

Controller	Frequency variation in area 1			Frequency variation in area 2			Tie line power deviation			ITAE
	U_{sh} in Hz	O_{sh} in Hz	T_s in s	U_{sh} in Hz	O_{sh} in Hz	T_s in s	U_{sh} in pu	O_{sh} in pu	T_s in s	
BA- Fuzzy PIDF	-0.0414	0.0041	6.9401	-0.0038	0	19.2991	-0.0010	0	19.360	0.0361
TLBO- Fuzzy PIDF	-0.0868	0.0040	5.7544	-0.0036	0	19.3273	-0.00099	0	18.893	0.0304
PSO- Fuzzy PIDF	-0.0890	0.0040	5.7175	-0.0036	0	19.1020	-0.0010	0	19.154	0.0330
TLBO- Fuzzy [21]	-0.1885	0.0036	4.9936	-0.019	0	23.5188	-0.0042	0	23.937	0.3264
LCOA-PID [28]	-0.4288	0.0155	11.703	-0.0664	0	21.0698	-0.0134	0	21.978	0.7842

Table 4.22 gives further prove of the superiority of the suggested controller over those presented in previous studies. Percentage of improvement in undershoot (U_{sh}), settling time (T_s), and ITAE for the Fuzzy configuration optimized by different algorithms and Fuzzy PID proposed in [7] in comparison with LCOA based PID controller [21] are shown in Figure 4.20 (This figure is obtained by analyzing characteristics provided in Table 4.22). From Figure 4.20, it is noted that with the proposed Fuzzy PIDF controller optimized by the suggested algorithms, the overall performance of the system has witnessed a remarkable improvement.

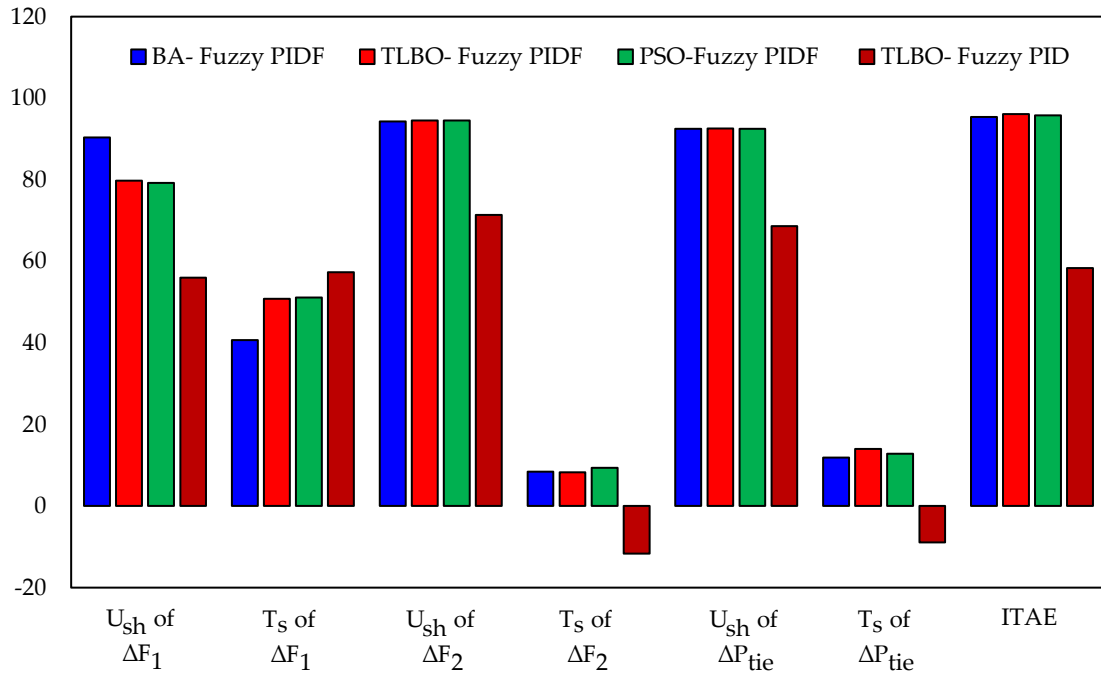


Figure 4.20. Percentage of improvement with different techniques.

In order to examine the robustness of Fuzzy PIDF towards parametric uncertainties of the controlled system, several parameters of the investigated testbed system are simultaneously altered from their nominal values. The parameters T_g , T_t and H in both areas are varied by +50 %, while the parameters B and D are varied by -50%. A step load perturbation of 0.2 pu is suddenly applied (at Time $t = 0$ s) in area one and the optimal gains of Fuzzy PIDF obtained in the normal condition are not to be re-tuned to verify the robustness of the proposed controller. Figures 4.21 - 4.23 and Table 4.23 show the dynamic performance of the two-area power system as it is exposed to a parametric deviation test with the recommended Fuzzy PIDF based BA, TLBO, and PSO employed for LFC.

Table 4.23. Frequency response performances with different controllers for parametric uncertainties analysis.

Controller	Frequency in area 1			Frequency in area 2			Tie line power deviation			ITAE
	U_{sh} in Hz	O_{sh} in Hz	T_s in s	U_{sh} in Hz	O_{sh} in Hz	T_s in s	U_{sh} in pu	O_{sh} in pu	T_s in s	
BA- Fuzzy PIDF	-0.1140	0.0131	5.9858	-0.0203	0	9.3781	-0.0026	0	10.453	0.03094
TLBO- Fuzzy PIDF	-0.1458	0.0111	5.4378	-0.0278	0.00183	14.818	-0.0026	0.000065	9.3769	0.0511
PSO- Fuzzy PIDF	-0.1465	0.0115	5.4468	-0.0175	0	10.269	-0.0024	0	10.421	0.02535

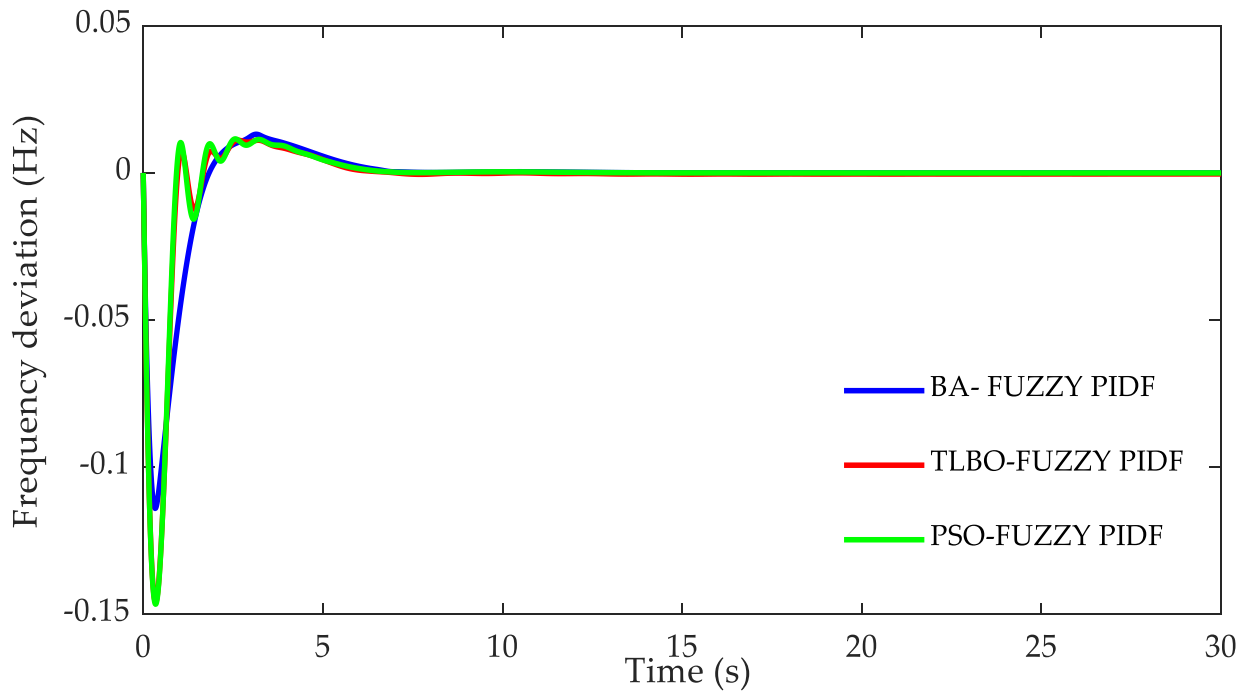


Figure 4.21. Frequency deviation in area one (ΔF_1 in Hz) under parametric uncertainties of the testbed system.

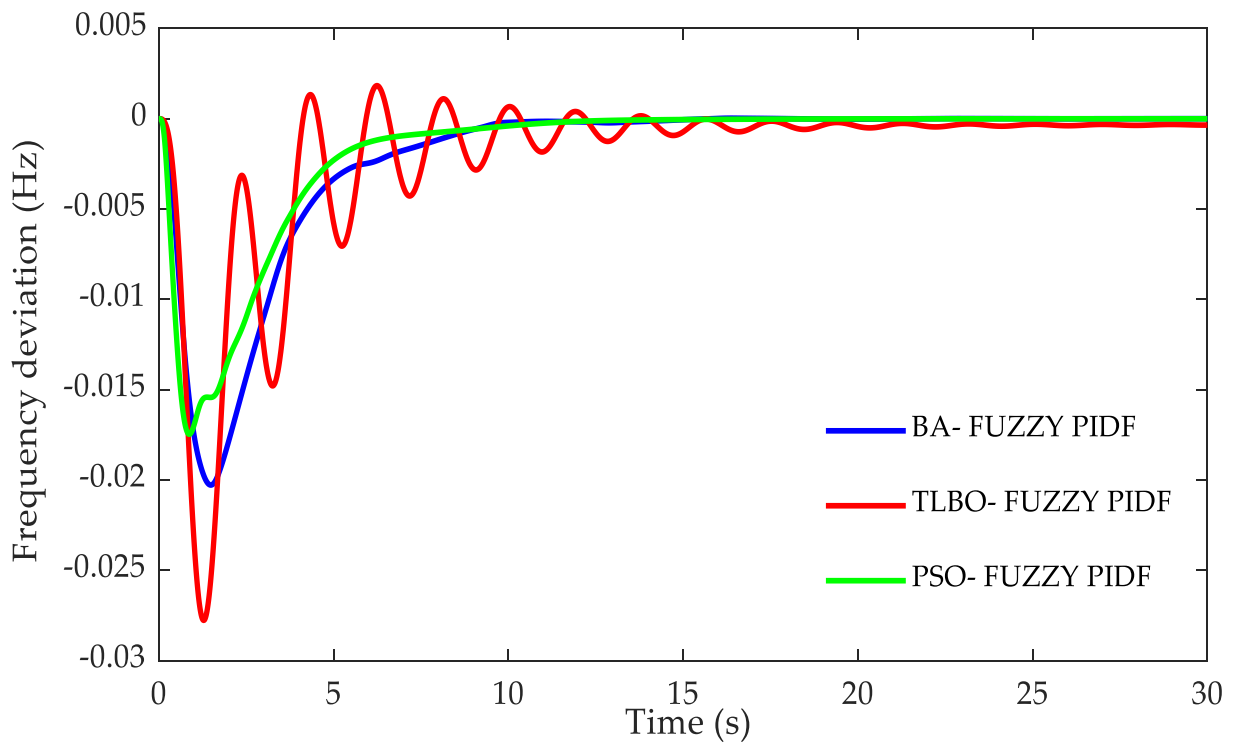


Figure 4.22. Frequency deviation in area two (ΔF_2 in Hz) under parametric uncertainties of the testbed system.

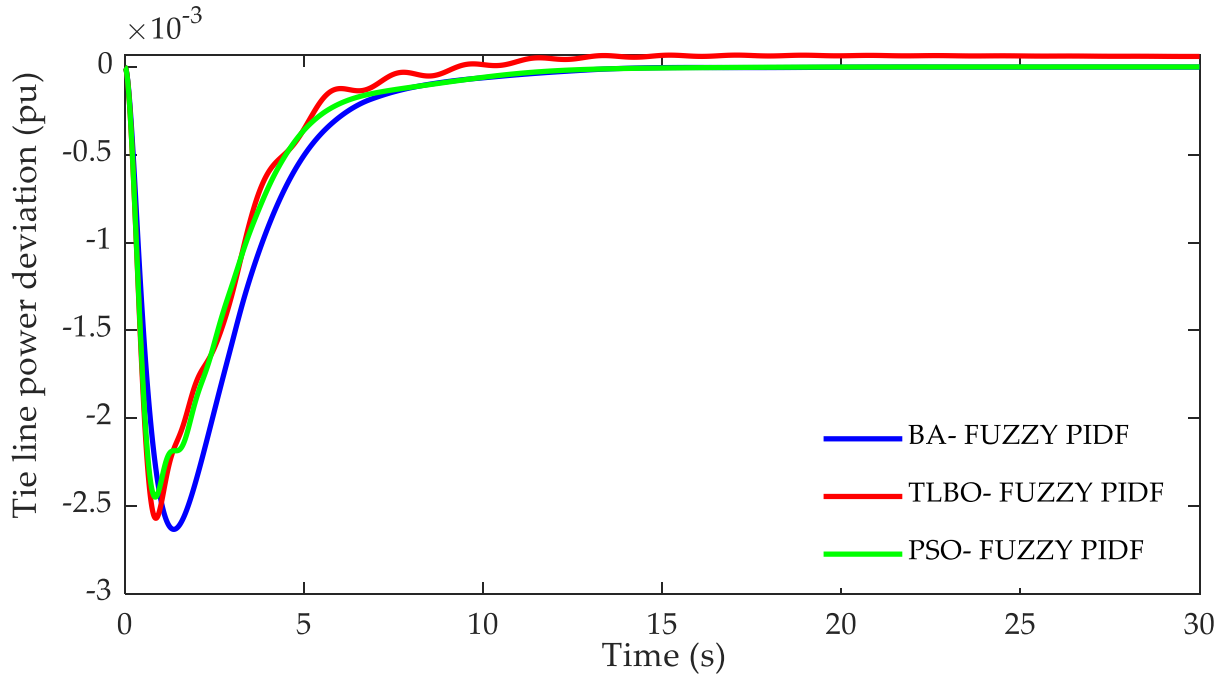


Figure 4.23. Tie line power deviation (ΔP_{tie} in pu) under parametric uncertainties of the testbed system.

Results obtained from robustness analysis demonstrate that the proposed Fuzzy structure equipped in the testbed system for LFC is robust towards the parametric variation of the controlled plant. It is also noticed that the same controller optimised by TLBO has shown less robustness as compared with the same controller tuned by BA and PSO.

Moreover, for further robustness examination of the proposed Fuzzy design at various load perturbations, a random disturbance is applied with different magnitude in area one, as demonstrated in Figure 4.24. The dynamic responses of the testbed system when it is exposed to different load disturbances are shown in Figures 4.25 – 4.27.

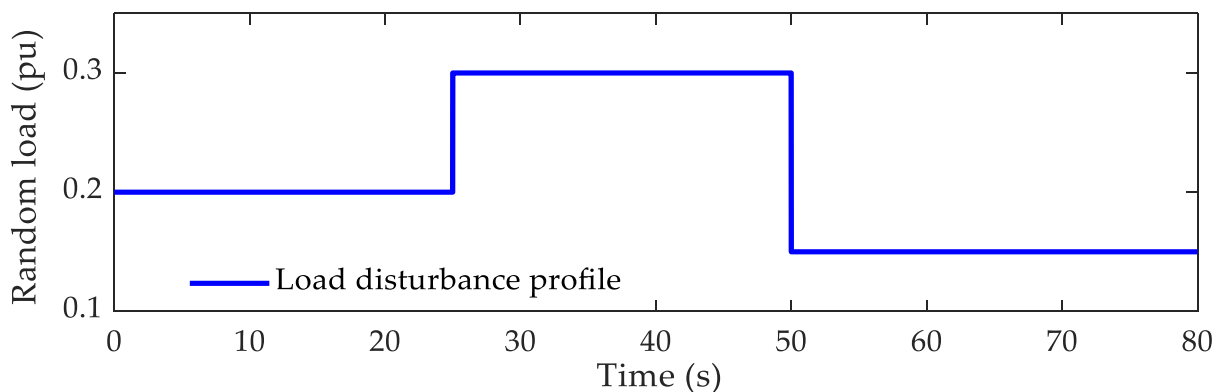


Figure 4.24. Random load profile.

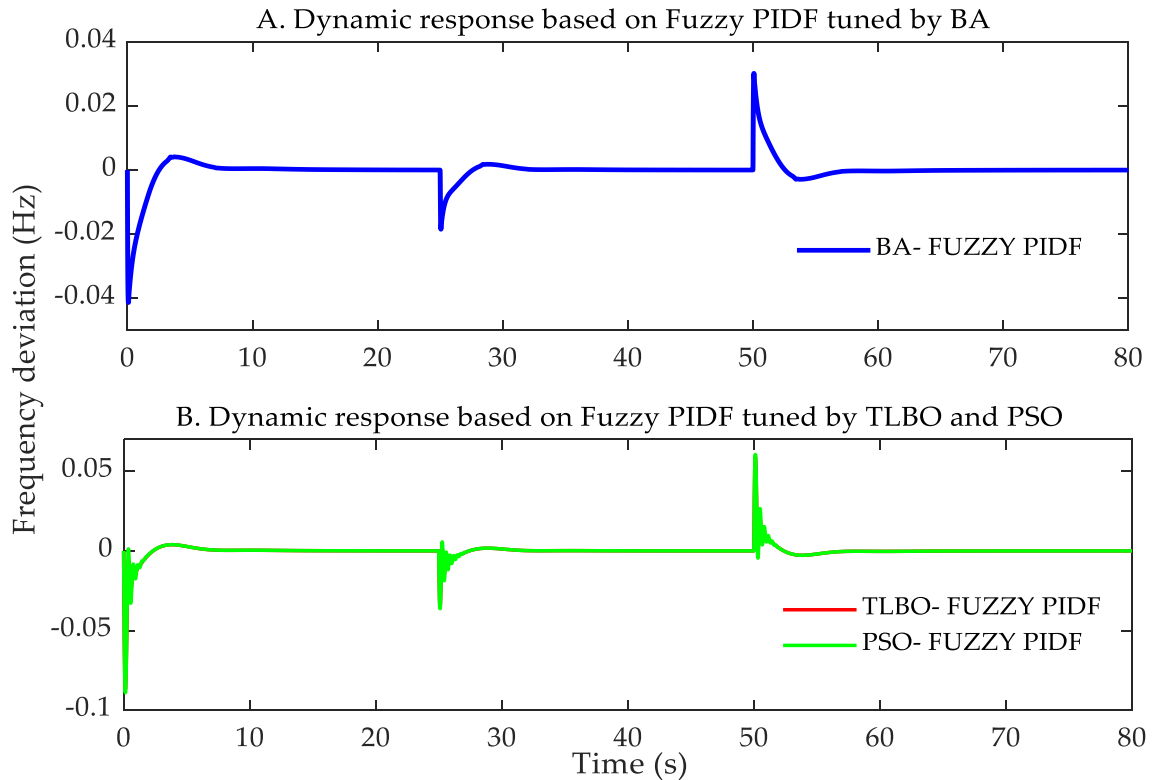


Figure 4.25. Frequency deviation in area one. (A) based on BA tuning; (B) based on TLBO and PSO tuning.

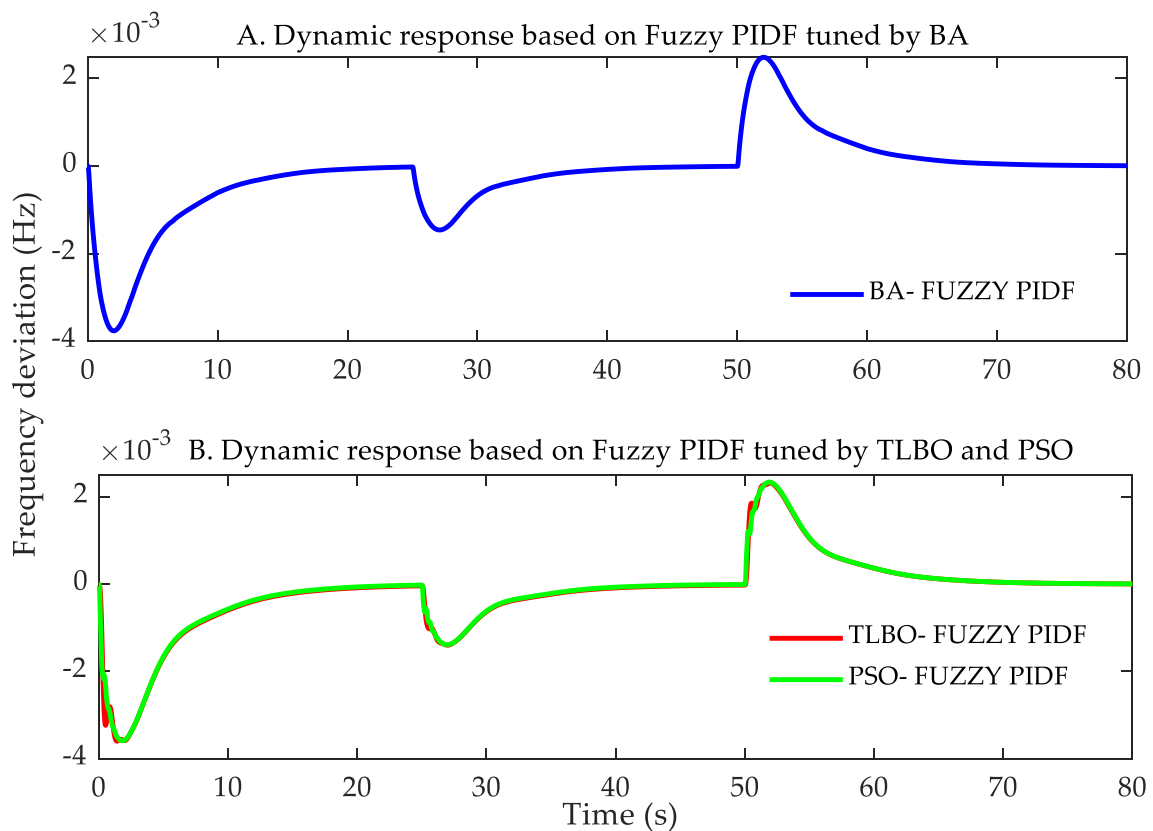


Figure 4.26. Frequency deviation in area two. (A) based on BA tuning; (B) based on TLBO and PSO tuning.

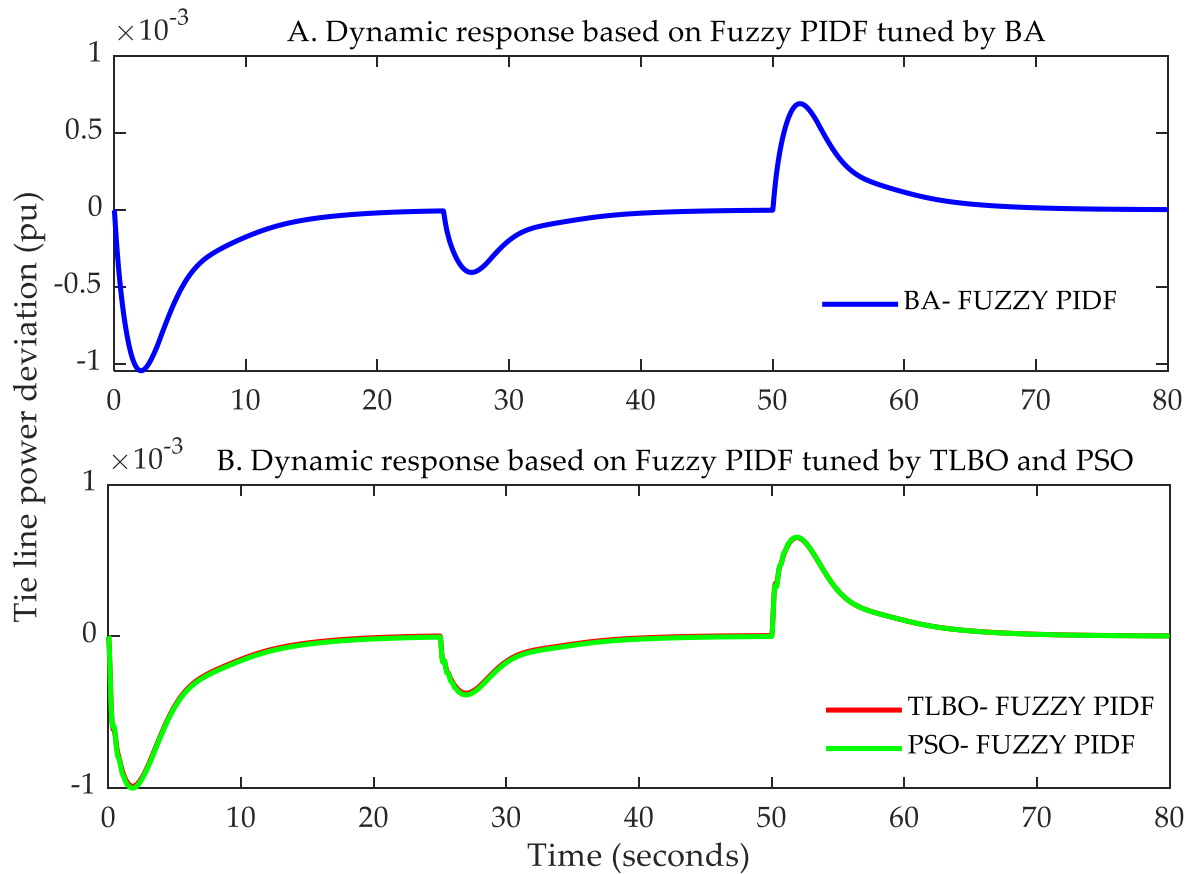


Figure 4.27. Tie line power deviation (ΔP_{tie} in pu). (A) based on BA tuning; (B) based on TLBO and PSO tuning.

From Figures 4.25 – 4.27, it is noticeable that the optimized fuzzy control structure continued to demonstrate its robustness even with random load disturbance applied in the system. Moreover, it is observed that Fuzzy PIDF based BA offers the best response as less peak undershoot and less oscillation is achieved in comparison with the same controller-based PSO and TLBO.

4.4.5 Different Configurations of Fuzzy Control Tuned by BA

It is revealed that the membership function selection and the setting of the rule base are vital in designing a fuzzy controller. However, it is also a significant matter to investigate the impact of the configuration of the fuzzy controller. This is to explore how different structures of the scaling factor gains influence on the performance of the controller. Based on this statement, this subsection proposes three different structures of fuzzy control employed as LFC system for the two-area power system shown in Figure 4.16. The same membership function used to design the Fuzzy PIDF are shown in Figure 4.4 is used with the proposed structures. Further, the rule bases required to generate the fuzzy output of the controller are tabulated in Table 4.2.

The three novel proposed structures are shown in Figures 4.28 – 4.30. Due to the superiority and robustness of the performance of cascading the fraction PI and fractional PD proposed in [22], it is possible to use this idea of cascading to gain further improvement on the performance of fuzzy controller by proposing a controller that benefits from the advantages of using fuzzy control and the merits of cascading PI and PD controllers. Accordingly, the configuration illustrated in Figure 28 is for the proposed Fuzzy Cascade PI-PD (Fuzzy C PI-PD) employed in area one. This controller has six scaling factor gains. Namely, K_1 & K_2 are the input gains of the fuzzy controller, K_{P11} & K_{I1} are the PI controller gains and K_{P12} & K_{D1} for the PD controller gains. Identical Fuzzy C PI-PD controller is employed in area two with the following scaling factor gains: K_3 , K_4 , K_{P21} , K_{I2} , K_{P22} and K_{D2} .

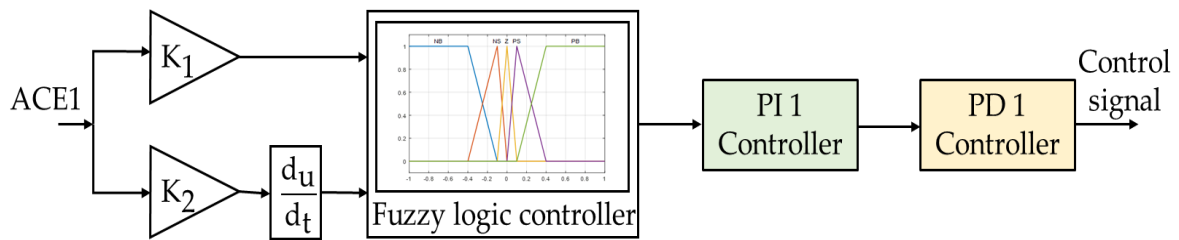


Figure 4.28. Block diagram of Fuzzy Cascade PI-PD controller configuration equipped in area one.

Figure 4.29 demonstrates the structural diagram of the proposed Fuzzy PI plus Fuzzy PD (Fuzzy PI + Fuzzy PD) controller employed in area one for LFC purposes. As it is obvious from the figure, two fuzzy controllers are equipped in each area. This hierarchal configuration should enhance the stability of the system and provide better reliability as any failure occurs in any part of this structure; the other part continues to provide its expected control action.

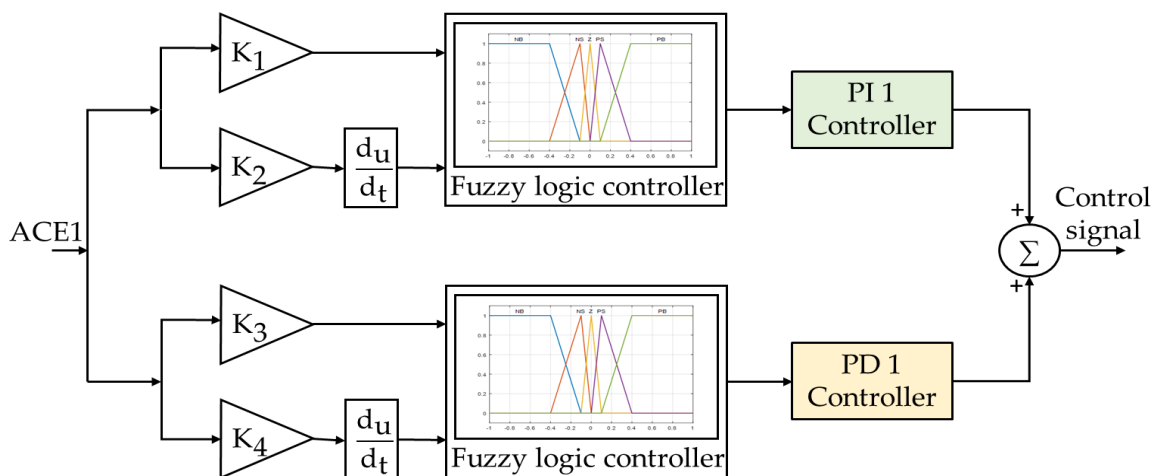


Figure 4.29. Block diagram of Fuzzy PI plus Fuzzy PD controller configuration equipped in area one.

This controller has eight scaling factor gains. Namely, K_1 & K_2 are the input gains of the Fuzzy PI controller, K_{P11} & K_{I1} are the PI controller gains, K_3 & K_4 are the input gains of the Fuzzy PD controller K_{P12} & K_{D1} for the PD controller gains. Identical Fuzzy PI + Fuzzy PD is employed in area two with the following parameters: K_5 , K_6 , K_{P21} , K_{I2} , K_7 , K_8 , K_{P22} and K_{D2} .

Due to the number of fuzzy rules needed to implement the Fuzzy PI + Fuzzy PD structure in each area $[(5 \times 5) + (5 \times 5) = 50]$ that requires a longer execution time which may result in slowing down the controller performance, it may be worth to propose another structure that reduces the execution time and guarantee a satisfactory level of reliability. In order to accomplish this, Fuzzy (PI + PD) shown in Figure 4.30 is suggested. This structure has less execution time $[5 \times 5 = 25]$ and still offer an acceptable range of reliability. This configuration has six scaling factor gains. Namely, K_1 & K_2 are the input gains of the fuzzy controller, K_{P11} & K_{I1} are the PI controller gains and K_{P12} & K_{D1} for the PD controller gains. A similar Fuzzy C PI-PD controller is employed in area two with the following scaling factor gains: K_3 , K_4 , K_{P21} , K_{I2} , K_{P22} and K_{D2} .

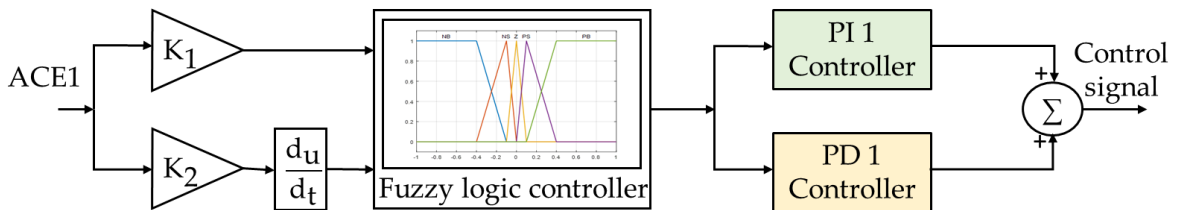


Figure 4.30. Block diagram of Fuzzy (PI + PD) controller configuration equipped in area one.

In order to achieve the best possible performance of the proposed fuzzy control configurations, the Bees Algorithm (BA) is used to concurrently find the optimal values of the proposed controllers' gains by minimising the ITAE of the frequency deviation in both areas and the tie-line power fluctuation. The optimum values of the suggested controllers' gains are illustrated in Table 4.24 and Table 4.25. The scaling factors of the proposed Fuzzy control configurations are chosen in the limits of [0-2].

Table 4.24. The optimum values of the proposed Fuzzy C PI-PD and Fuzzy (PI + PD) controllers obtained by the BA.

Controller	Controller Gains of Area 1						Controller Gains of Area 2					
	K_1	K_2	K_{P11}	K_{I1}	K_{P12}	K_{D1}	K_3	K_4	K_{P21}	K_{I2}	K_{P22}	K_{D2}
Fuzzy C PI-PD	0.0833	2	2	2	2	2	1.5307	0.0012	1.6472	0.012	0.9902	1.1494
Fuzzy (PI + PD)	0.0594	2	2	2	1.5673	2	2	0.0002	0.001	1.0716	0.4188	0.092

Table 4.25. The optimum Fuzzy PI + Fuzzy PD gains optimised by BA.

Controller	Parameters							
Fuzzy PI + Fuzzy PD	Controller gains of area 1							
	K_1	K_2	K_3	K_4	K_{P11}	K_{I1}	K_{P12}	K_{D1}
	0.0020	2	0.5981	2	2	2	2	2
	Controller gains of area 2							
	K_5	K_6	K_7	K_8	K_{P21}	K_{I2}	K_{P22}	K_{D2}
2	0.001	0.0004	0.0015	0.3429	0.7511	1.1997	2	

To investigate the performance of the proposed fuzzy control structures, a load disturbance with a magnitude of 0.2 pu is applied in area one at time $t = 0s$. The dynamic response of the system with the proposed controllers employed as LFC are demonstrated in Figures 4.31 - 4.33. The frequency deviation in area one ΔF_1 in (Hz) is given in Figure 4.31, the frequency deviation in area two ΔF_2 in (Hz) is given in Figure 4.32 and the tie-line power deviation ΔP_{tie} in (pu) is illustrated in Figure 4.33. Further, the characteristics of the dynamic response represented by the peak undershoot (U_{sh}), peak overshoot (O_{sh}), settling time (T_s) and the values of the objective function are exemplified in Table 4.26.

Table 4.26. Frequency response performances of different fuzzy structures tuned by BA.

Controller	Frequency in area 1			Frequency in area 2			Tie line power deviation			ITAE
	U_{sh} in Hz	O_{sh} in Hz	T_s in s	U_{sh} in Hz	O_{sh} in Hz	T_s in s	U_{sh} in pu	O_{sh} in pu	T_s in s	
Fuzzy C PI-PD	0.0431	0.00038	2.1873	0.00099	0	21.1703	0.00027	0	21.752 2	0.0135 1
Fuzzy PI + Fuzzy PD	0.0346	0.00089	7.0632	0.0024	0	20.5011	0.00064	0	20.815 3	0.0257 6
Fuzzy (PI + PD)	0.0792	0.00120	2.1384	0.0026	0	21.0681	0.00072	0	21.088 5	0.0310 4

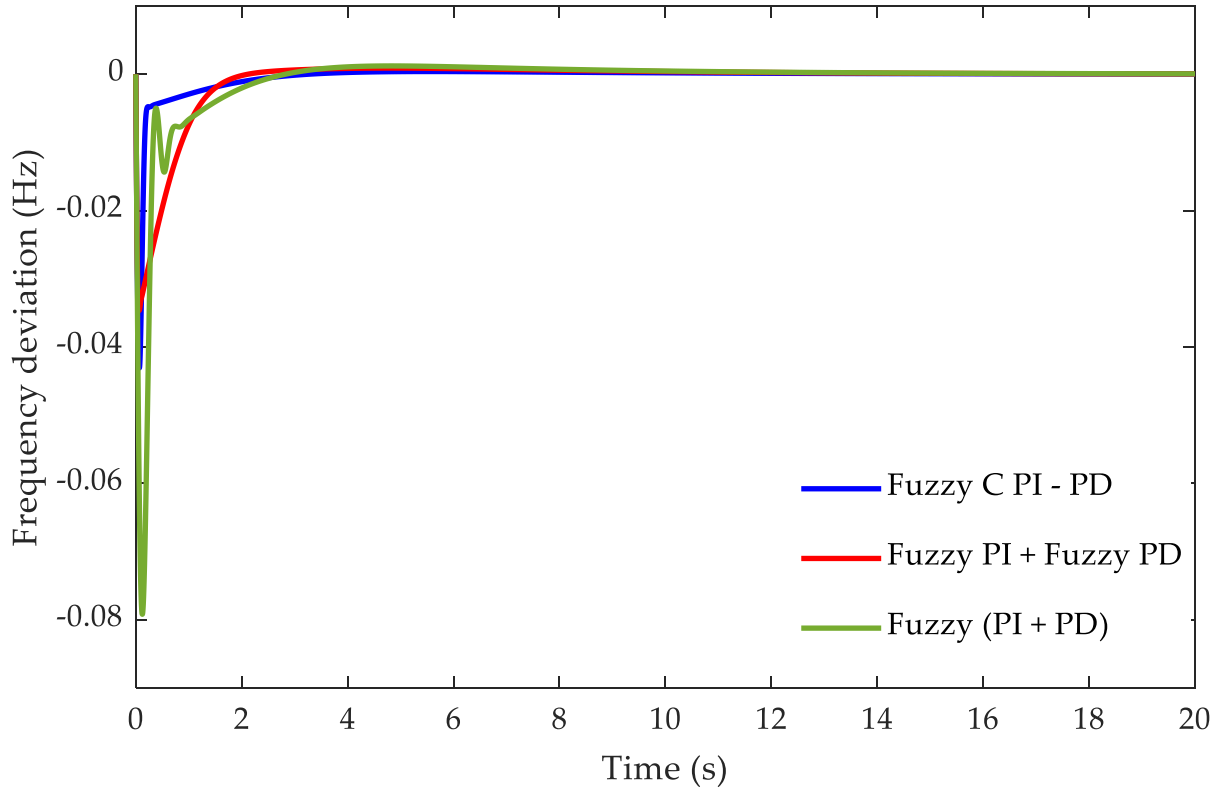


Figure 4.31. Frequency deviation in area one (ΔF_1 in Hz).

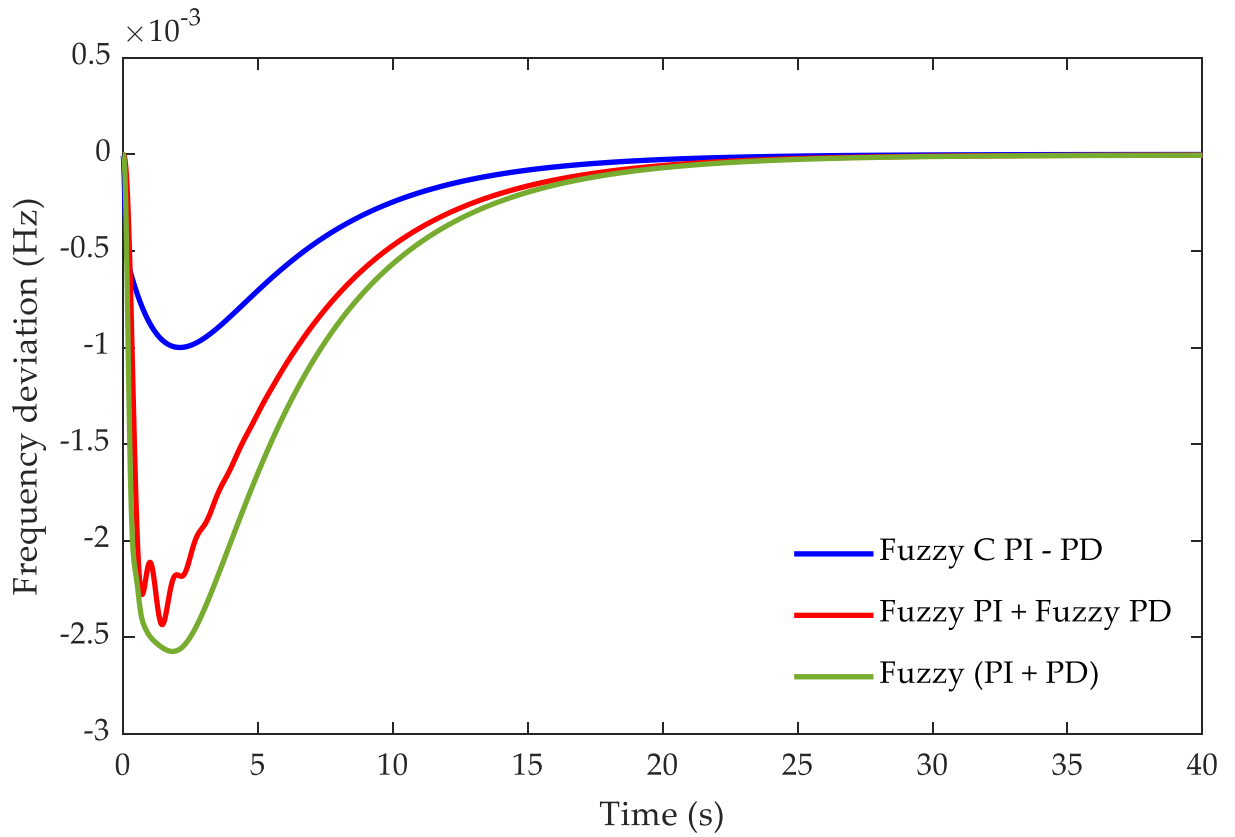


Figure 4.32. Frequency deviation in area two (ΔF_2 in Hz).

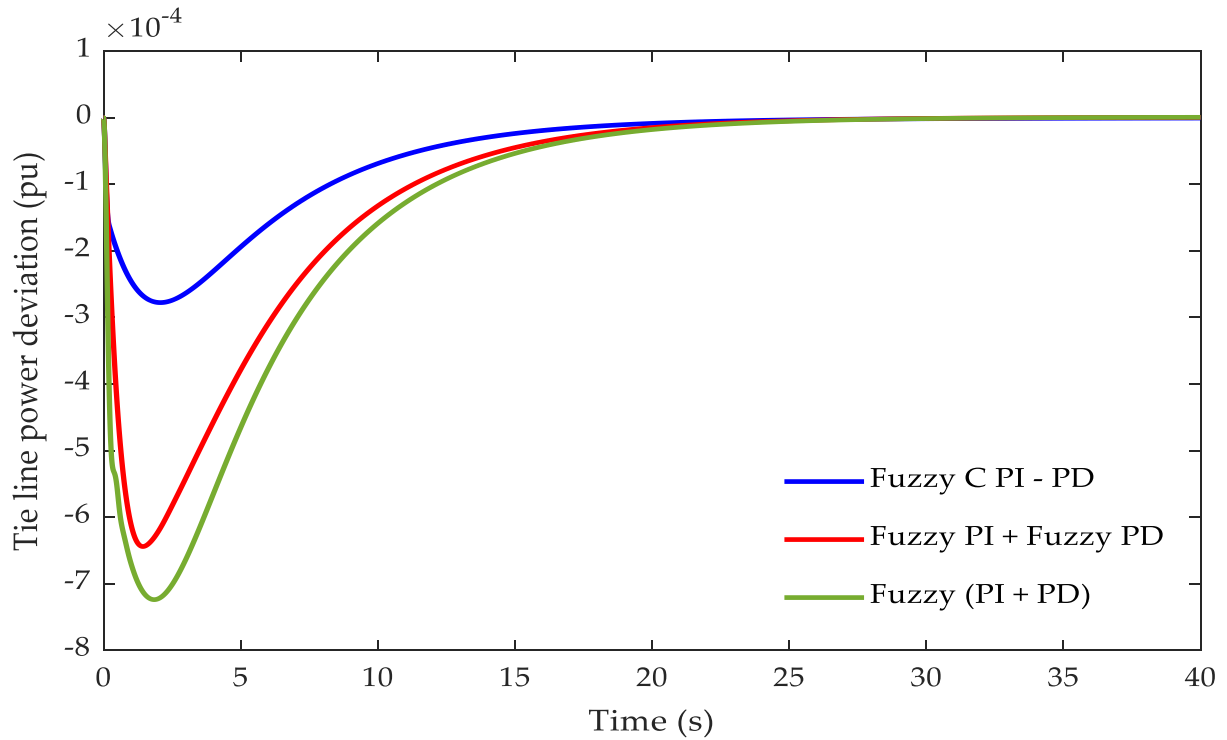


Figure 4.33. Tie line power deviation (ΔP_{tie} in pu).

The obtained simulation results show that the steady-state responses with the proposed controllers are similar as the frequency variation in both areas and the tie-line power deviation are ceased to zero. However, in terms of the transient response, the least drop in the frequency recorded in area one as a consequence of the implication of the load disturbance is -0.0346 Hz, this is achieved based on the proposed Fuzzy PI plus Fuzzy PD structure. Observably, this controller offered the slowest response for ΔF_1 with 7.0632 seconds settling time. Further, a negligible overshoot is observed in the dynamic response obtained based on the three suggested controllers. Regarding the drop in the frequency in area two, the proposed structures have provided satisfactory responses with a slight superiority of the Fuzzy C PI – PD over the other two structures. The tie-line power deviation of the system is illustrated in Figure 4.33 where the supremacy of the Fuzzy C PI-PD over the other controllers is observed. Moreover, the value of the ITAE is the smallest for the Fuzzy C PI- PD tuned by BA as compared with the other structures tuned by the same algorithm.

Based on the simulation results provided in Figures 4.31 – 4.33 and Table 4.26, it is evidenced that the proposed fuzzy configurations are evidenced to serve as effective solutions for the issue of LFC as they provide different advantages such as fast response with neglectable overshoot and zero steady-state error. Importantly, based on their structures, these controllers offer a wide range of reliability.

4.4.5.1 Robustness Investigation of Fuzzy Cascade PI-PD, Fuzzy PI+PD and Fuzzy PI plus Fuzzy PD

The investigated two-area power system has several parameters that may vary due to different operating conditions. This variation influences the stability of the system. For example, the increase in the governor time constant (T_g) results in an increase in the frequency deviation while decreasing the damping ratio (D) may lead to increasing the frequency deviation of the system which may bring about a possibility of system instability. Also, increasing the inertia time constant (H) can slow down the system. Therefore, the LFC system should have the required control action towards parametric uncertainties of the controlled system and provide an acceptable level of robustness.

Accordingly, to assess the robustness of the proposed fuzzy control configurations tuned by BA equipped as an LFC system in the dual-area interconnected power system, thirteen scenarios are assumed for parametric uncertainties of the testbed system as given in Table 4.27. This assessment begins with individually varying each parameter in the system by (+ and -) 50% from their nominal values. As it is understood, changing the parameters from their nominal values may have a positive impact on the overall system stability. Therefore, in order to make this analysis more credible, all parameters are simultaneously varied from their nominal values. Accordingly, in case thirteen, the negative impact of each parameter uncertainty and change them simultaneously has been considered. This guarantees to assess the robustness in the worst scenario that the system may experience during the operation time. A load disturbance of 0.2 pu is applied in area one to examine the effect of system parametric uncertainties on the behaviour of the Fuzzy C PI-PD, Fuzzy PI+PD and Fuzzy PI plus Fuzzy PD, a comparative study is given based on the obtained results. Fuzzy control robustness analysis can also be carried out in different ways as investigated in [23], [24].

From case 1 to case 12 in Table 4.27, only one parameter is changed at a time by +50% and -50 % from their nominal values. In case thirteen, the parameters T_g , T_t , H and R in both areas are varied by 50%. While the parameters B and D are varied by -50%. The dynamic response of the system with the proposed controllers under parametric uncertainty conditions are demonstrated in Figures 4.34 – 4.46. Moreover, the characteristics of the transient response are depicted in Table 4.28.

Table 4.27. Investigated scenarios of system parametric variations.

Case Number	Parameters	Nominal values		Variation range	New values	
		Area 1	Area 2		Area 1	Area 2
Case 1	H	5	4	+50%	7.5	6
Case 2	H	5	4	-50%	2.5	2
Case 3	T_t	0.5	0.6	+50%	0.75	0.9
Case 4	T_t	0.5	0.6	-50%	0.25	0.3
Case 5	B	20.6	16.9	+50%	30.9	25.35
Case 6	B	20.6	16.9	-50%	10.3	8.45
Case 7	D	0.6	0.9	+50%	0.9	1.35
Case 8	D	0.6	0.9	-50%	0.3	0.45
Case 9	T_g	0.2	0.3	+50%	0.3	0.45
Case 10	T_g	0.2	0.3	-50%	0.1	0.15
Case 11	R	0.05	0.0625	+50%	0.075	0.0937
Case 12	R	0.05	0.0625	-50%	0.025	0.0312
Case 13	B	20.6	16.9	-50%	10.3	8.45
	H	5	4	+50%	7.5	6
	R	0.05	0.0625	+50%	0.075	0.0937
	D	0.6	0.9	-50%	0.3	0.45
	T_t	0.5	0.6	+50%	0.75	0.9
	T_g	0.2	0.3	+50%	0.3	0.45

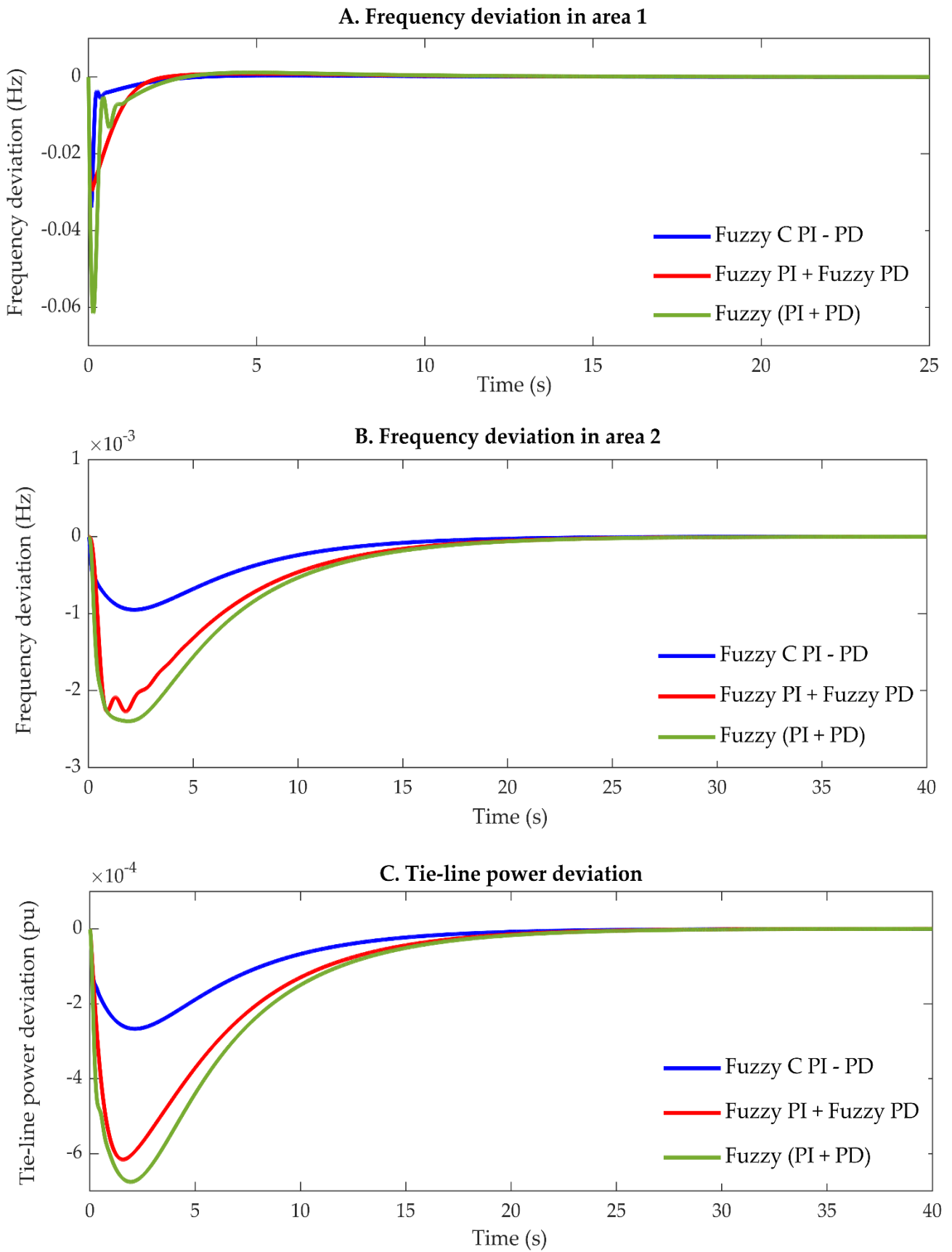


Figure 4.34. Dynamic response of the testbed power system based on different fuzzy controllers under parametric uncertainty condition, case 1. (A) Frequency variation in area 1; (B) Frequency variation in area 2; (C) Tie line power variation.

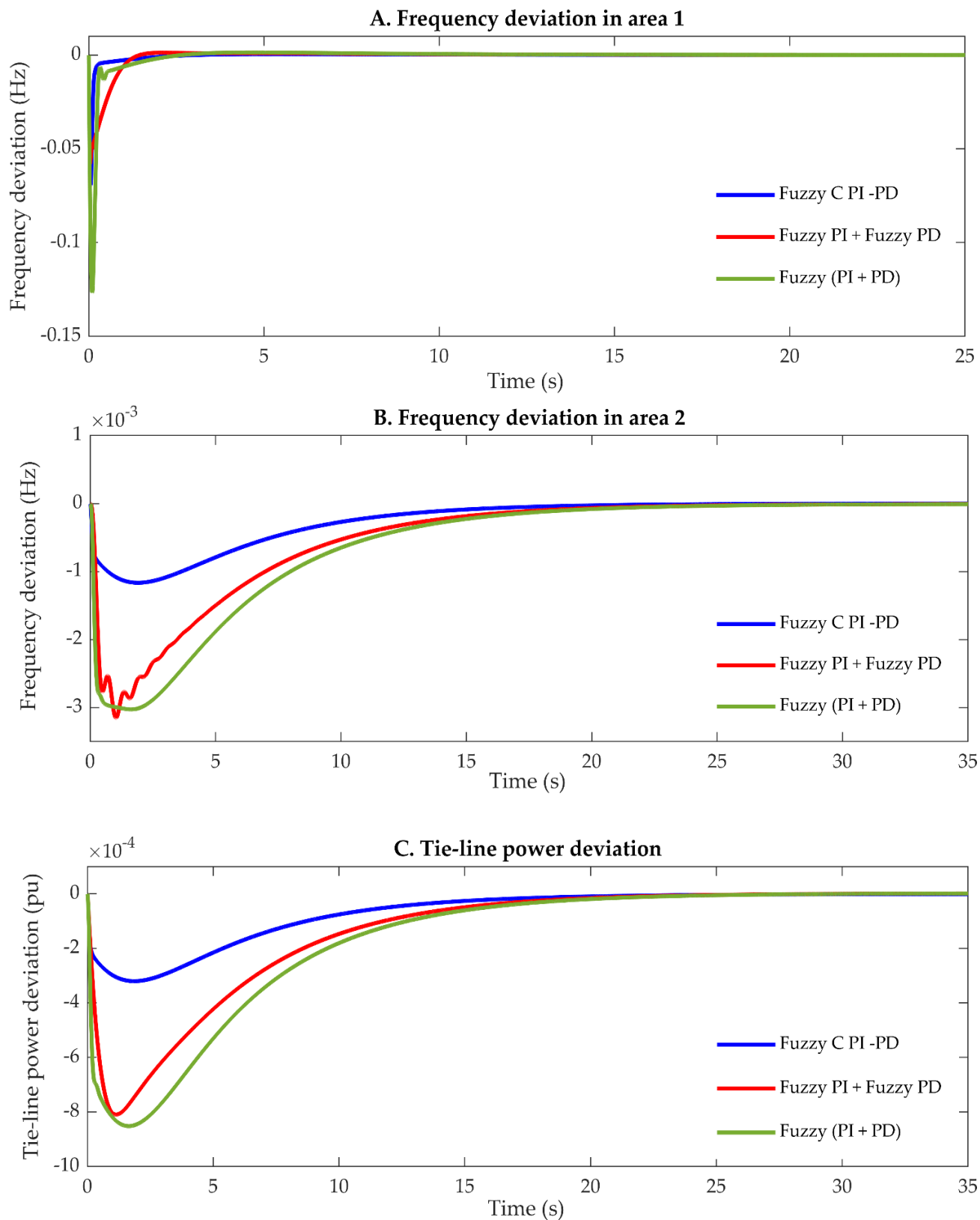


Figure 4.35. Dynamic response of the testbed power system based on different fuzzy controllers under parametric uncertainty condition, case 2. (A) Frequency variation in area 1; (B) Frequency variation in area 2; (C) Tie line power variation.

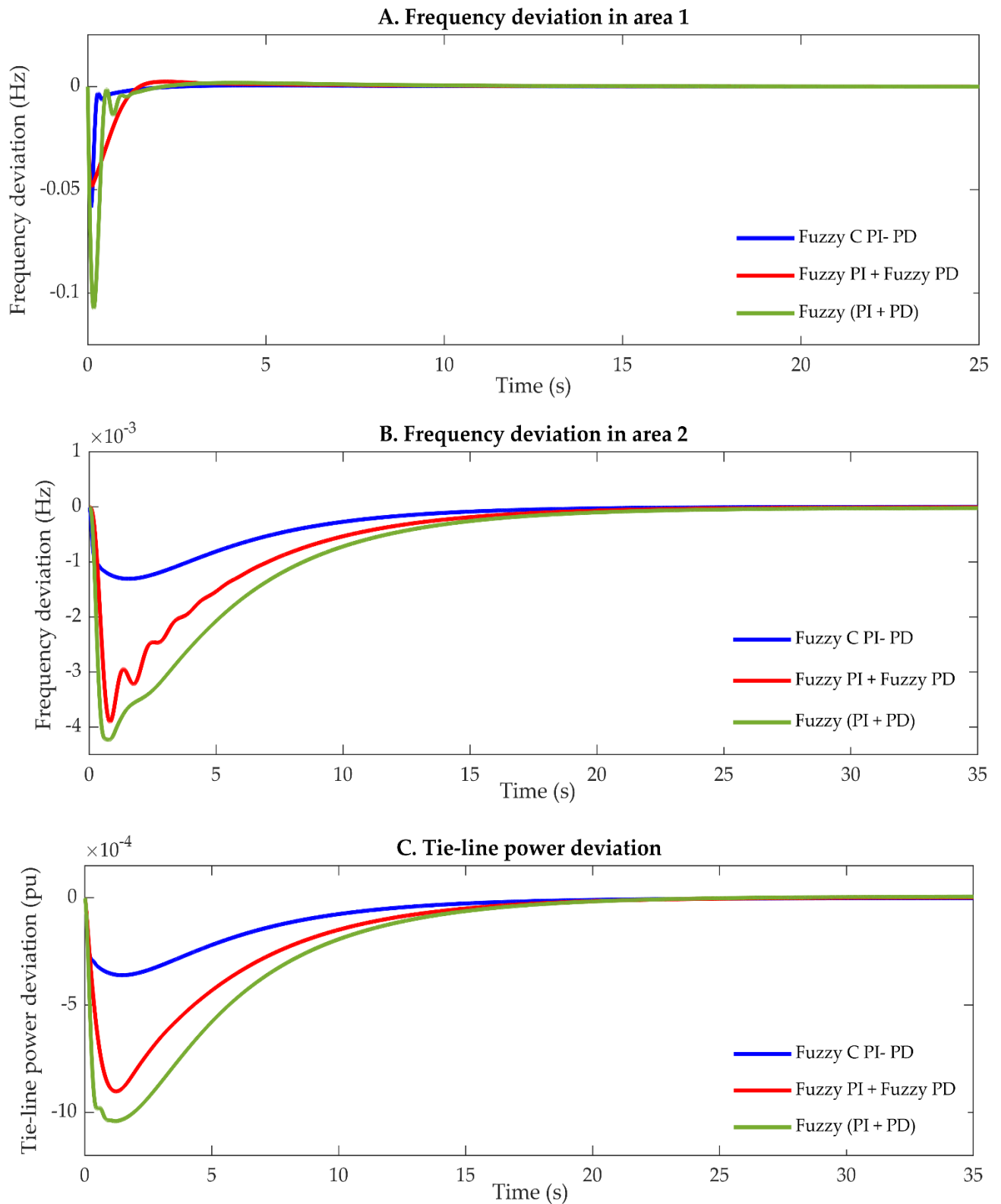


Figure 4.36. Dynamic response of the testbed power system based on different fuzzy controllers under parametric uncertainty condition, case 3. (A) Frequency variation in area 1; (B) Frequency variation in area 2; (C) Tie line power variation.

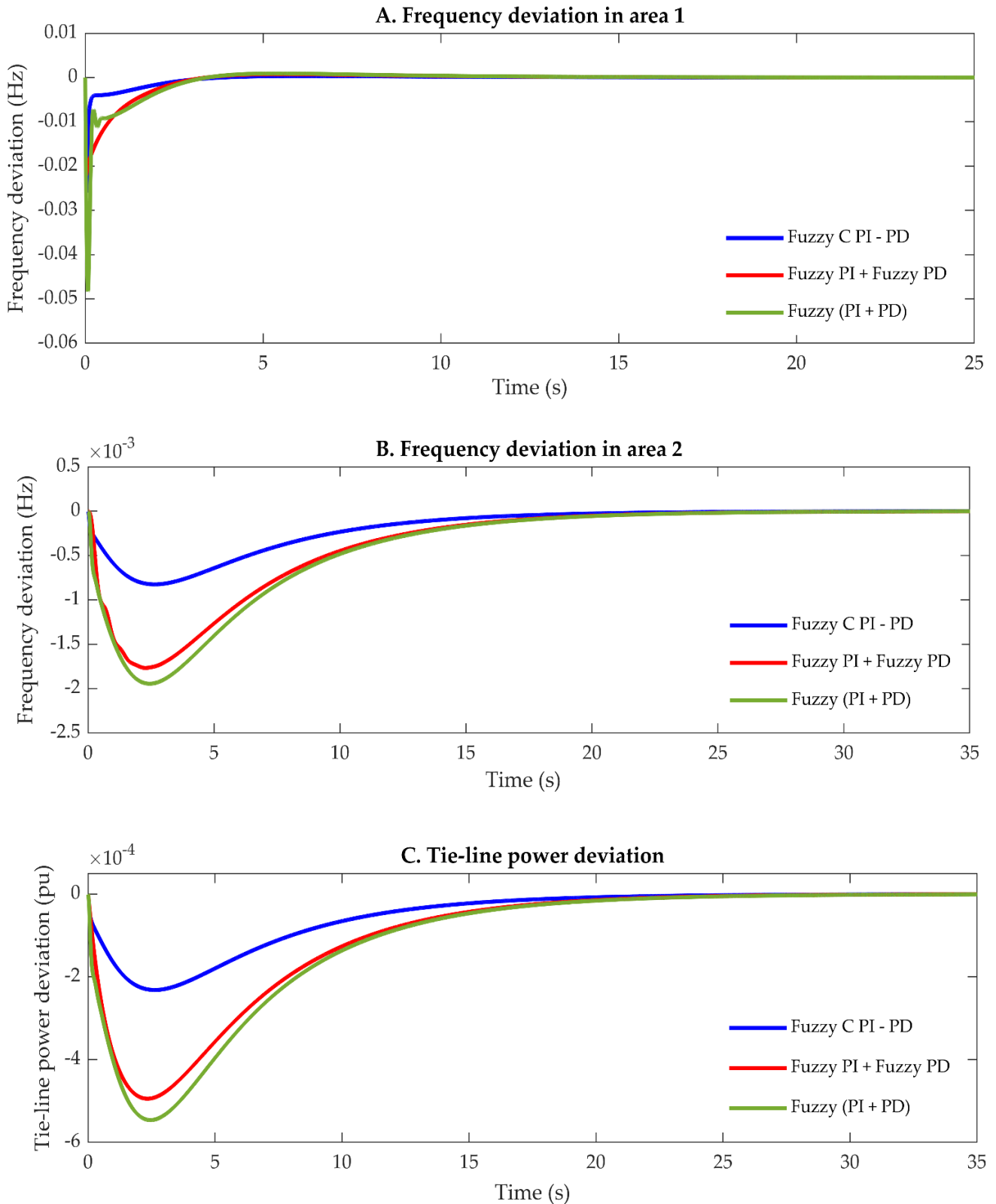


Figure 4.37. Dynamic response of the testbed power system based on different fuzzy controllers under parametric uncertainty condition, case 4. (A) Frequency variation in area 1; (B) Frequency variation in area 2; (C) Tie line power variation.

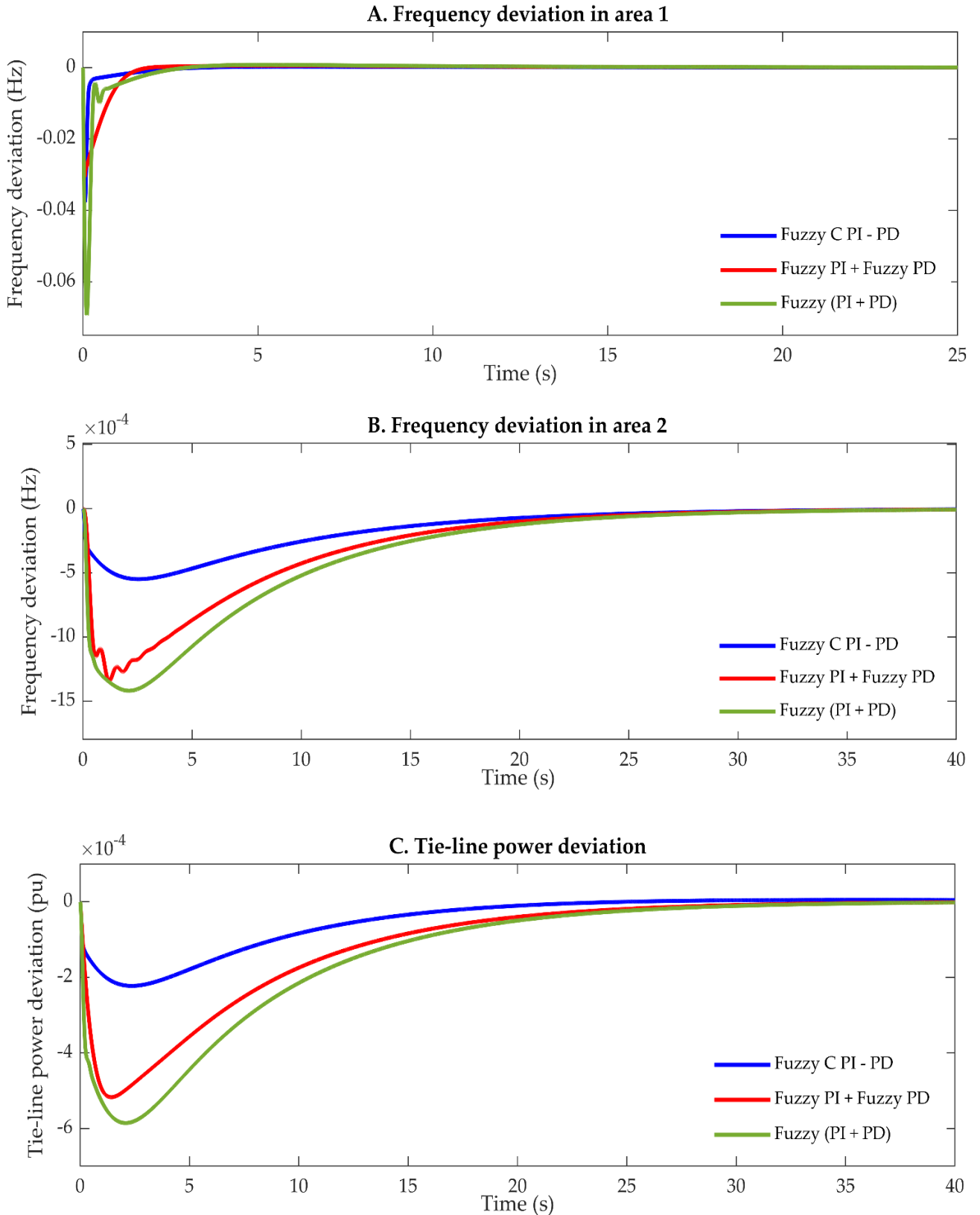


Figure 4.38. Dynamic response of the testbed power system based on different fuzzy controllers under parametric uncertainty condition, case 5. (A) Frequency variation in area 1; (B) Frequency variation in area 2; (C) Tie line power variation.

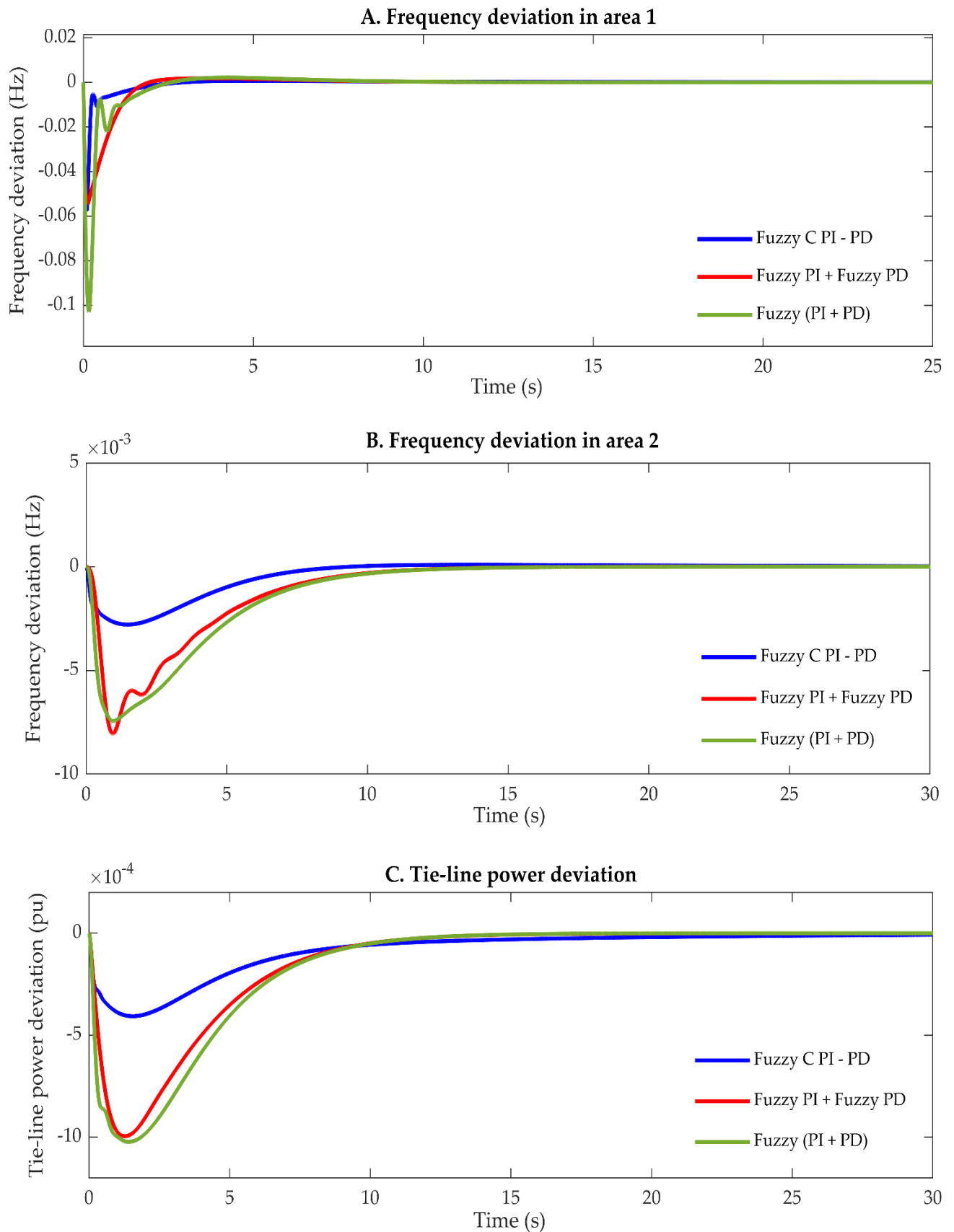


Figure 4.39. Dynamic response of the testbed power system based on different fuzzy controllers under parametric uncertainty condition, case 6. (A) Frequency variation in area 1; (B) Frequency variation in area 2; (C) Tie line power variation.

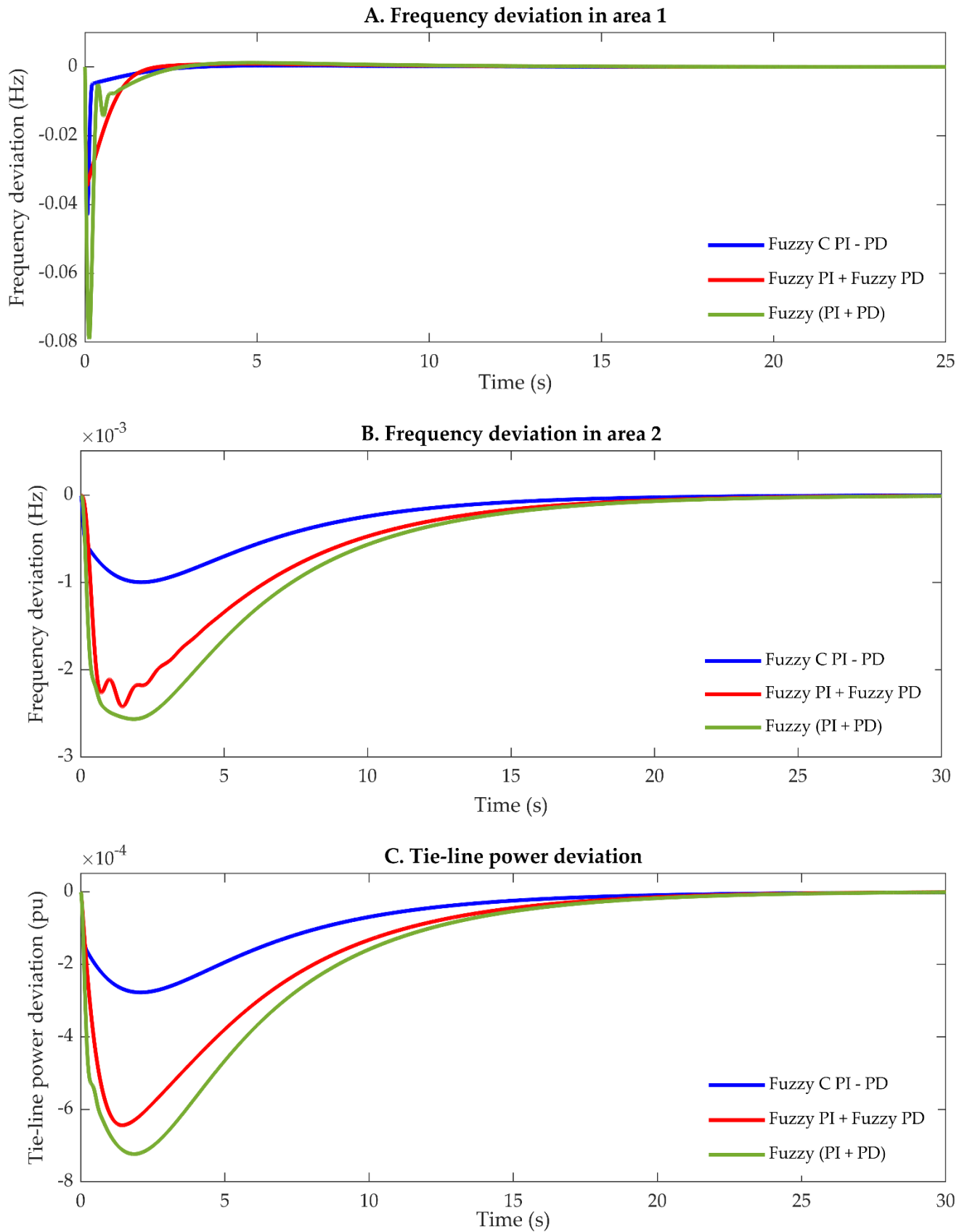


Figure 4.40. Dynamic response of the testbed power system based on different fuzzy controllers under parametric uncertainty condition, case 7. (A) Frequency variation in area 1; (B) Frequency variation in area 2; (C) Tie line power variation.

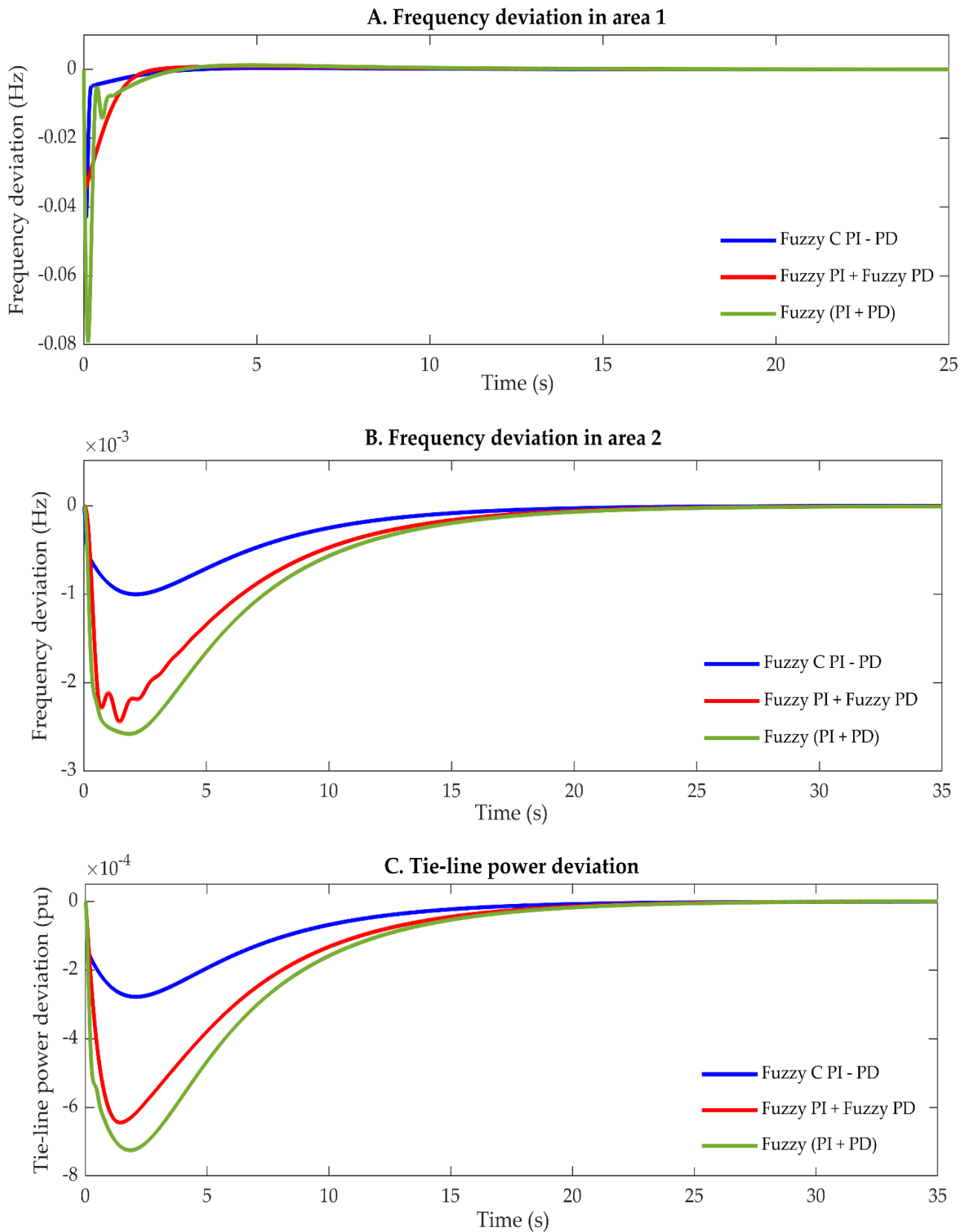


Figure 4.41. Dynamic response of the testbed power system based on different fuzzy controllers under parametric uncertainty condition, case 8. (A) Frequency variation in area 1; (B) Frequency variation in area 2; (C) Tie line power variation.

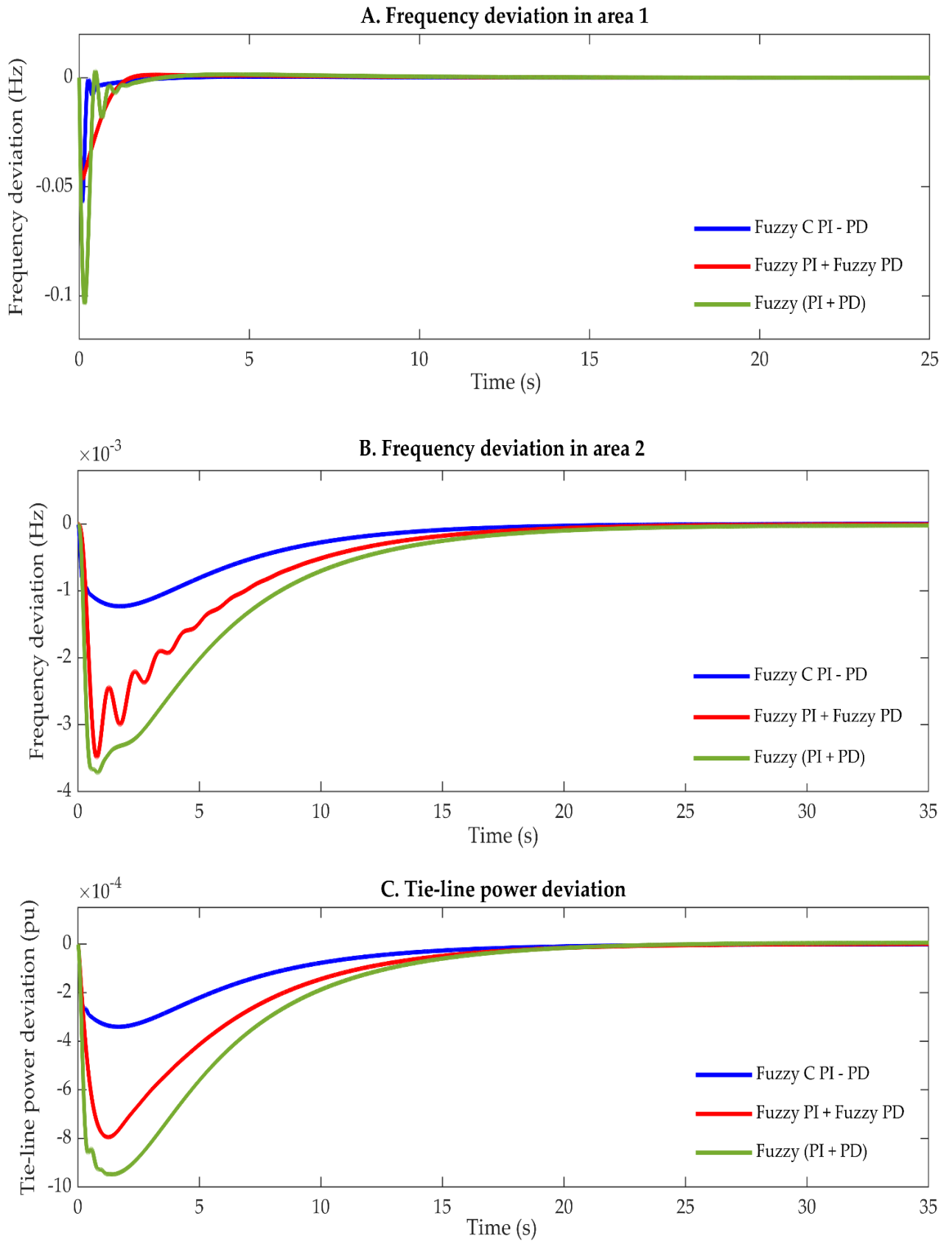


Figure 4.42. Dynamic response of the testbed power system based on different fuzzy controllers under parametric uncertainty condition, case 9. (A) Frequency variation in area 1; (B) Frequency variation in area 2; (C) Tie line power variation.

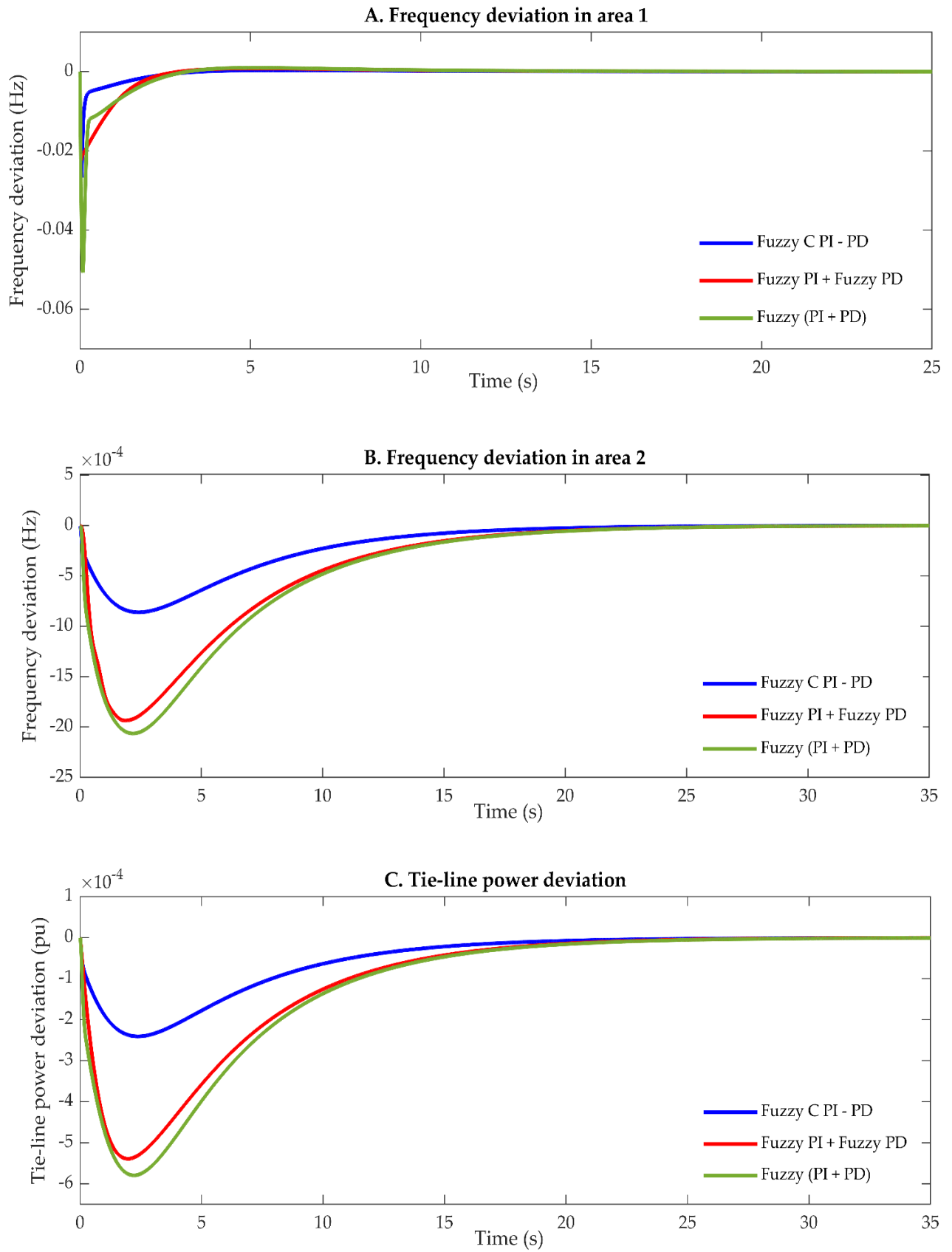


Figure 4.43. Dynamic response of the testbed power system based on different fuzzy controllers under parametric uncertainty condition, case 10. (A) Frequency variation in area 1; (B) Frequency variation in area 2; (C) Tie line power variation.

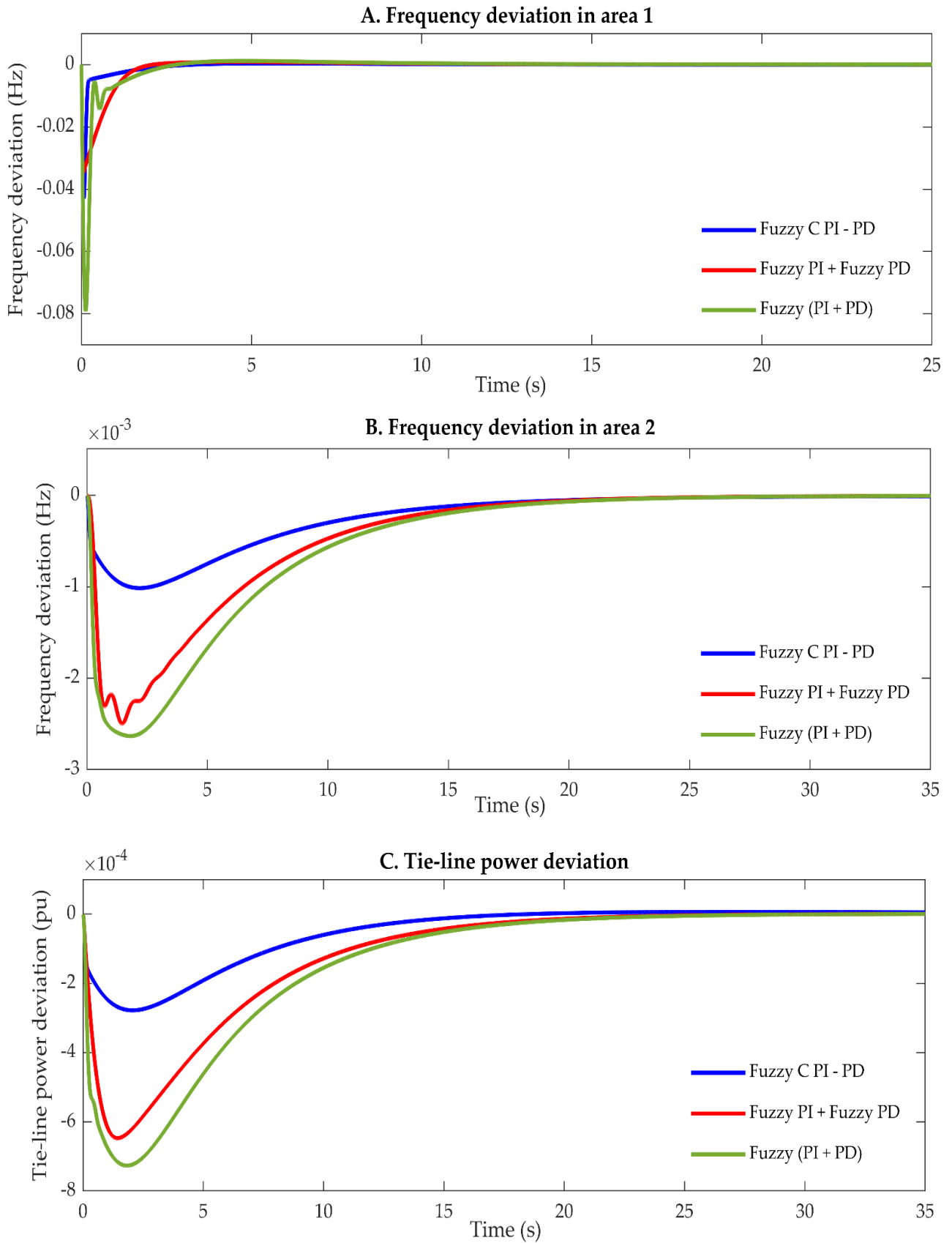


Figure 4.44. Dynamic response of the testbed power system based on different fuzzy controllers under parametric uncertainty condition, case 11. (A) Frequency variation in area 1; (B) Frequency variation in area 2; (C) Tie line power variation.

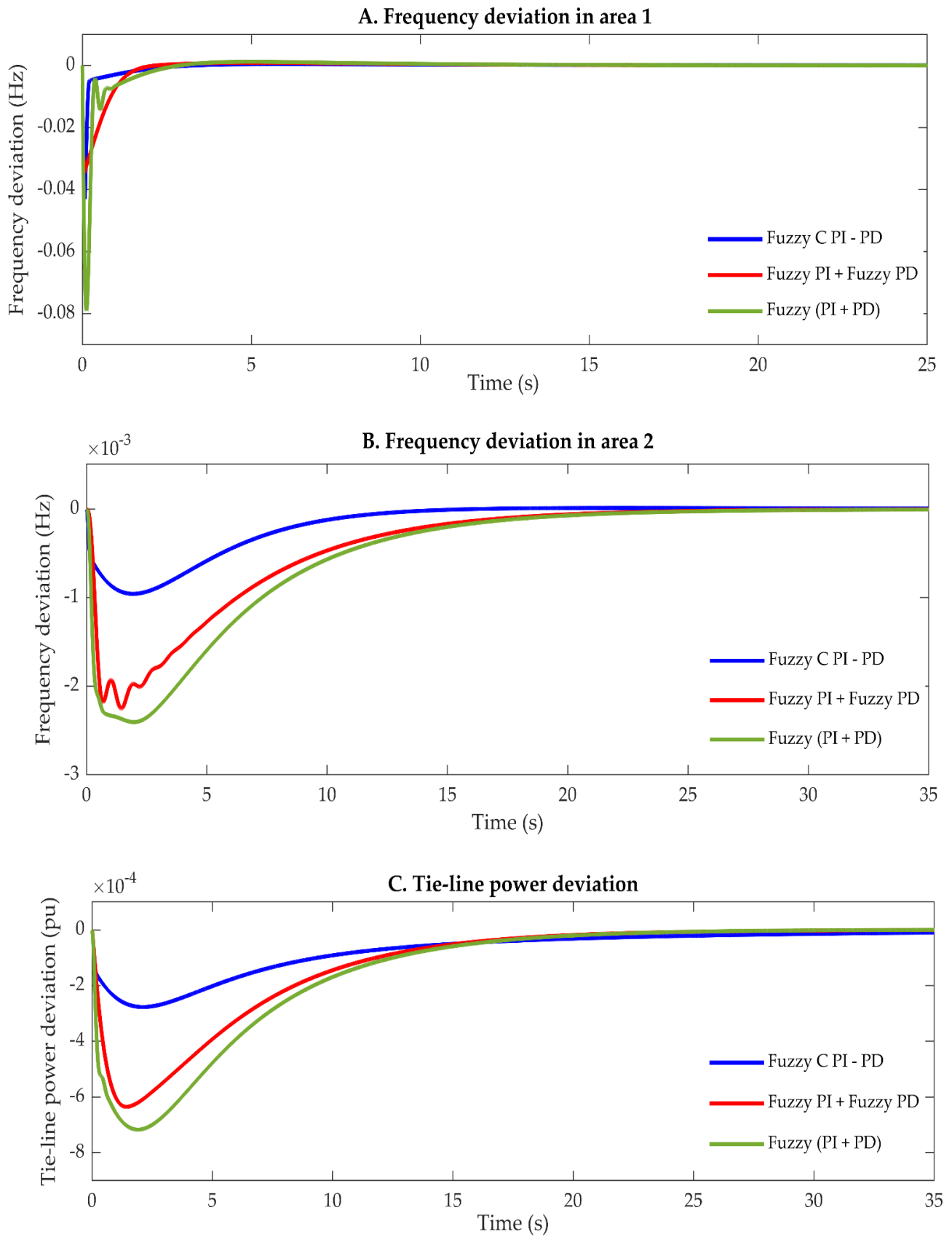


Figure 4.45. Dynamic response of the testbed power system based on different fuzzy controllers under parametric uncertainty condition, case 12. (A) Frequency variation in area 1; (B) Frequency variation in area 2; (C) Tie line power variation.

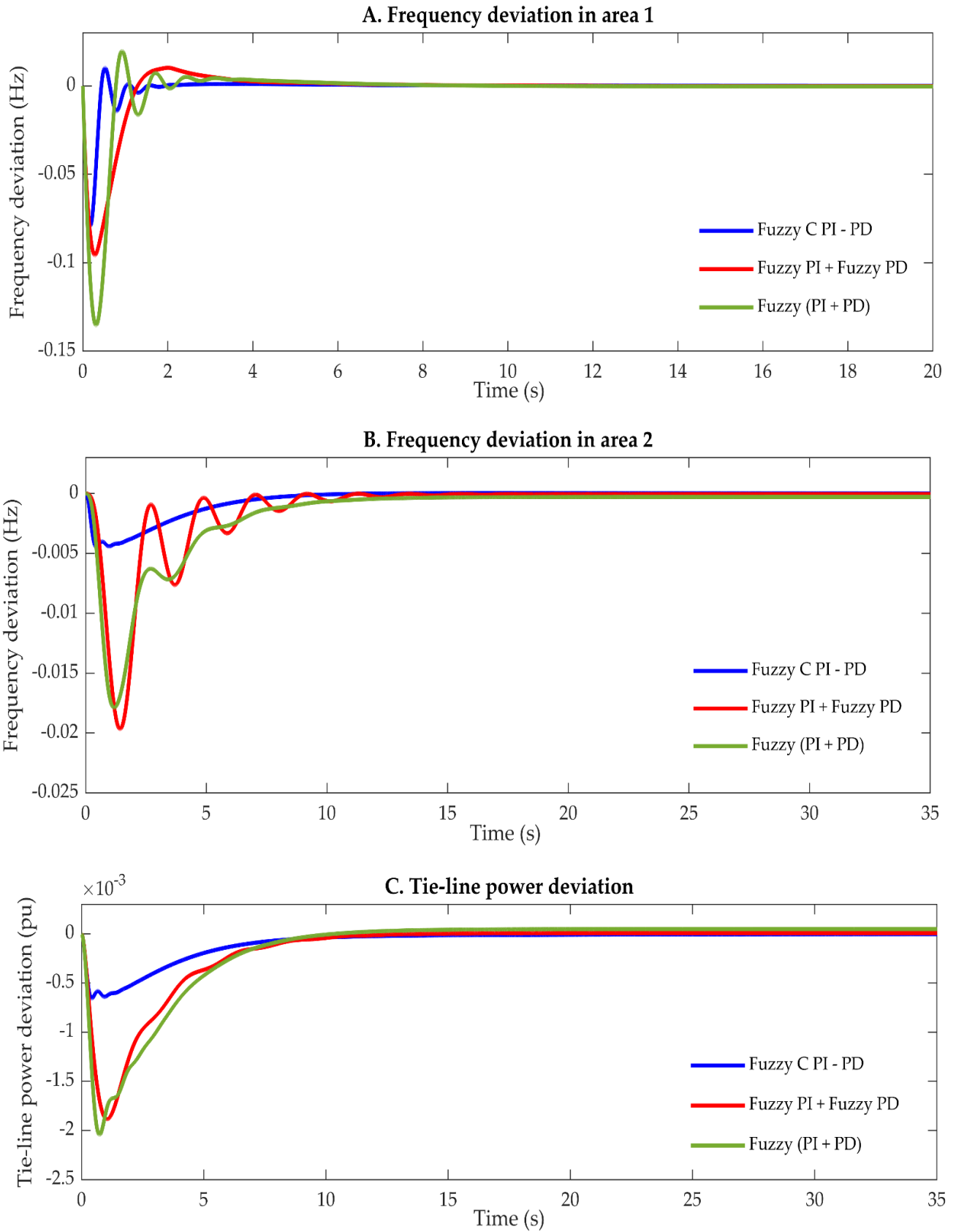


Figure 4.46. Dynamic response of the testbed power system based on different fuzzy controllers under parametric uncertainty condition, case 13. (A) Frequency variation in area 1; (B) Frequency variation in area 2; (C) Tie line power variation.

Table 4.28. Performance of the system under different scenarios with different controllers.

Case No	Controller	Frequency in area 1			Frequency in area 2			Tie line power deviation		
		U _{sh} in Hz	O _{sh} in Hz	T _s in s	U _{sh} in Hz	O _{sh} in Hz	T _s in s	U _{sh} in pu	O _{sh} in pu	T _s in s
Case 1	Fuzzy C PI-PD	-0.0339	0.00037	2.380	-0.00095	0	21.4962	-0.00026	0	21.697
	Fuzzy PI + Fuzzy PD	-0.0297	0.00087	7.768	-0.0023	0	20.7037	-0.00061	0	20.895
	Fuzzy (PI + PD)	-0.0615	0.0011	2.305	-0.0024	0	21.107	-0.00067	0	21.117
Case 2	Fuzzy C PI-PD	-0.0695	0.00044	1.713	-0.0012	0	20.714	-0.00032	0	21.688
	Fuzzy PI + Fuzzy PD	-0.0579	0.0012	2.455	-0.0032	0	19.835	-0.00080	0	20.300
	Fuzzy (PI + PD)	-0.1268	0.0010	1.765	-0.0030	0	20.947	-0.00085	0	20.972
Case 3	Fuzzy C PI-PD	-0.0585	0.0005	1.5501	-0.0013	0	20.157	-0.00036	0	21.119
	Fuzzy PI + Fuzzy PD	-0.0486	0.0023	6.0375	-0.0039	0	18.896	-0.00090	0	19.862
	Fuzzy (PI + PD)	-0.1074	0.0017	1.5144	-0.0042	0	19.826	-0.0010	0	20.445 7
Case 4	Fuzzy C PI-PD	-0.0260	0.00032	2.955	-0.00082	0	22.077	-0.00023	0	22.223
	Fuzzy PI + Fuzzy PD	-0.0220	0.00075	9.0899	-0.0018	0	21.720	-0.00049	0	21.757
	Fuzzy (PI + PD)	-0.0483	0.00092	2.851	-0.0019	0	21.611	-0.00054	0	21.633
Case 5	Fuzzy C PI-PD	-0.0377	0.00025	2.0857	-0.00054	0	31.659	-0.00022	0	25.188
	Fuzzy PI + Fuzzy PD	-0.0307	0.00056	1.6032	-0.0013	0	27.7717	-0.00051	0	28.143
	Fuzzy (PI + PD)	-0.0693	0.00077	2.1015	-0.0014	0	28.6358	-0.00058	0	28.660
Case 6	Fuzzy C PI-PD	-0.0577	0.00074	2.1637	-0.0028	0	19.4344	-0.00040	0	26.209
	Fuzzy PI + Fuzzy PD	-0.0546	0.0018	6.3768	-0.0080	0	11.6084	-0.00099	0	12.184
	Fuzzy (PI + PD)	-0.1029	0.0021	4.8285	-0.0074	0	11.8962	-0.0010	0	12.131
Case 7	Fuzzy C PI-PD	-0.0430	0.00038	2.1892	-0.00099	0	20.927	-0.00027	0	22.192
	Fuzzy PI + Fuzzy PD	-0.0346	0.00098	7.0758	-0.0024	0	20.531	-0.00064	0	20.837
	Fuzzy (PI + PD)	-0.0790	0.0012	2.141	-0.0026	0	21.084	-0.00072	0	21.104
Case 8	Fuzzy C PI-PD	-0.0431	0.00038	2.1854	-0.0010	0	21.418	-0.00027	0	21.325
	Fuzzy PI + Fuzzy PD	-0.0347	0.00089	7.0507	-0.0024	0	20.470	-0.00064	0	20.792
	Fuzzy (PI + PD)	-0.0794	0.0012	2.1359	-0.0026	0	20.052	-0.00072	0	21.072
Case 9	Fuzzy C PI-PD	-0.0573	0.00047	1.724	-0.0012	0	20.633	-0.00034	0	21.414
	Fuzzy PI + Fuzzy PD	-0.0468	0.0013	5.788	-0.0035	0	19.235	-0.00079	0	20.257
	Fuzzy (PI + PD)	-0.1038	0.0032	1.7013	-0.0037	0	20.298	-0.00094	0	20.738
Case 10	Fuzzy C PI-PD	-0.0267	0.00034	2.7138	-0.00086	0	21.6312	-0.00024	0	21.995
	Fuzzy PI + Fuzzy PD	-0.0224	0.0080	8.9968	-0.0019	0	21.285	-0.00053	0	21.362
	Fuzzy (PI + PD)	-0.0507	0.00098	2.5984	-0.0021	0	21.339	-0.00057	0	21.378
Case 11	Fuzzy C PI-PD	-0.0431	0.00038	2.1736	-0.001	0	24.738	-0.00027	0	17.791
	Fuzzy PI + Fuzzy PD	-0.0346	0.0089	6.953	-0.0025	0	20.2308	-0.00064	0	20.496
	Fuzzy (PI + PD)	-0.0792	0.0012	2.1284	-0.0026	0	20.848	-0.00072	0	20.863
Case 12	Fuzzy C PI-PD	-0.0430	0.00041	2.212	-0.00095	0	14.328	-0.00027	0	32.222
	Fuzzy PI + Fuzzy PD	-0.0346	0.00089	7.3773	-0.0023	0	21.268	-0.00063	0	21.710
	Fuzzy (PI + PD)	-0.0790	0.0011	2.1689	-0.0024	0	21.693	-0.00071	0	21.730
Case 13	Fuzzy C PI-PD	-0.0791	0.01027	1.435	-0.0045	0.00004	9.9188	-0.00065	0	14.922
	Fuzzy PI + Fuzzy PD	-0.0958	0.0103	5.1487	-0.0197	0	10.577	-0.00190	0.000007	10.393
	Fuzzy (PI + PD)	-0.1354	0.020	4.9656	-0.0179	0	10.1364	-0.0020	0.00004	10.681

Values that represent the best characteristics are indicated in bold.

Figure 4.34 illustrates the dynamic behaviour of the testbed system based on the proposed fuzzy control structures under parametric uncertainty case 1, where the inertia time constants in both areas are altered by +50% from their nominal values. It is noted that the increase in the inertia time constant has slowed the response of the system. For example, the settling time of the frequency in area one has increased from 2.1873 s, 7.0632 s and 2.1384 s to 2.380 s, 7.768 s and 2.305 s based on Fuzzy C PI-PD, Fuzzy PI plus Fuzzy PD and Fuzzy PI+PD, respectively. The settling time of ΔF_2 and ΔP_{tie} follows the same pattern where a slight increase is observed. Moreover, it is concluded that the increase in inertia time constant has led to a slight decrease in the drop of the frequency in both areas. Conversely, the decrease in the inertia time constant which is considered in case 2 brings about a further drop in the frequency and tie-line power deviation in the system. Also, it leads to a slight improvement in terms of the settling time in ΔF_1 , ΔF_2 and ΔP_{tie} . Figure 4.35 shows the dynamic performance of the system based on the proposed controllers under parametric uncertainty case 2.

The impact of uncertainty in the turbine time constant is investigated in case 3 and case 4. Figure 4.36 demonstrates the dynamic performance of the testbed system based on the proposed fuzzy configurations under parametric uncertainty case 3, where the turbine time constants in both areas are varied by +50% from their nominal values. From Figure 4.36 and Table 4.28, it is noticed that as a consequence of increasing the turbine time constants within the system the drop in the frequency in area one (ΔF_1) has jumped from -0.0431 Hz, -0.0346 Hz and -0.0792 Hz to -0.0585 Hz, -0.0486 Hz and -0.1074 Hz. While the drop of the frequency in area two (ΔF_2) increased from -0.00099 Hz, -0.0024 Hz and -0.0026 Hz to -0.0013 Hz, -0.0039 Hz and -0.0042 Hz based on Fuzzy C PI-PD, Fuzzy PI plus Fuzzy PD and Fuzzy PI+PD, respectively. It is also obvious that due to the increase of turbine time constant the settling time of the ΔF_1 , ΔF_2 and ΔP_{tie} has slightly decreased. Contrary, from Figure 4.37, the decline in the turbine time constant brings about a decrease in the frequency deviation and slightly slowed the system response.

Figure 4.38 indicates the dynamic response of the system under parametric uncertainty case 5. In this case, frequency bias in both areas is altered by +50%. It is noticed that the increase in frequency bias has marginally improved the dynamic response in terms of the drop in the frequency. Where the maximum undershoot of the frequency in area one (ΔF_1) has decreased from -0.0431 Hz, -0.0346 Hz and -0.0792 Hz to -0.0377 Hz, -0.0307 Hz and -0.0693 Hz. While the drop of the frequency in area two (ΔF_2) declined from -0.00099 Hz, -

0.0024 Hz and -0.0026 Hz to -0.00054 Hz, -0.0013 Hz and -0.0014 Hz based on Fuzzy C PI-PD, Fuzzy PI plus Fuzzy PD and Fuzzy PI+PD, respectively. In regard to the influence of decreasing the frequency bias on the stability of power systems which is considered in case 6 and illustrated in Figure 4.39, it is obvious that the decrease in the frequency bias has slightly worsened the dynamic response of the system in terms of the frequency variation. Where it is noted that the maximum undershoot of the frequency in area one has increased from -0.0431 Hz, -0.0346 Hz and -0.0792 Hz to -0.0577 Hz, -0.0546 Hz and -0.1029 Hz. While the drop of the frequency in area two (ΔF_2) increased from -0.00099 Hz, -0.0024 Hz and -0.0026 Hz to -0.0028 Hz, -0.0080 Hz and -0.0074 Hz based on Fuzzy C PI-PD, Fuzzy PI plus Fuzzy PD and Fuzzy PI+PD, respectively.

The influence of uncertainty in the damping constant (D) is investigated in cases 7 and 8. Figure 4.40 and Figure 4.41 demonstrate the dynamic performance of the testbed system based on the proposed fuzzy structures under parametric uncertainty conditions of cases 7 and 8, where the damping constant (D) in both areas are varied by +50% and -50% from their nominal values. Due to the change in this parameter, a negligible change in the dynamic performance of the system is observed based on these cases as compared with results obtained using in the nominal conditions.

The uncertainty in the governor time constant (T_g) has a similar impact of uncertainty in the turbine time constant on the stability of the system in terms of frequency variation and the speed of the response. Figure 4.42 reveals the dynamic performance of the dual-area power system when the proposed fuzzy structures are employed as LFC in the system with the consideration of parametric uncertainty case 9, where the governor time constants in both areas are varied by +50% from their nominal values. As a result of uncertainty in the governor time constants within the system, the drop in the frequency in area one (ΔF_1) has incremented from -0.0431 Hz, -0.0346 Hz and -0.0792 Hz to -0.0573 Hz, -0.0468 Hz and -0.1038 Hz. While the drop of the frequency in area two (ΔF_2) increased from -0.00099 Hz, -0.0024 Hz and -0.0026 Hz to -0.0012 Hz, -0.0035 Hz and -0.0037 Hz based on Fuzzy C PI-PD, Fuzzy PI+PD and Fuzzy PI plus Fuzzy PD, respectively. Moreover, the settling time of ΔF_1 decreased from 2.1873 s, 7.0632 s and 2.1384 s to 1.724 s, 5.788 s and 1.7013 s based on Fuzzy C PI-PD, Fuzzy PI plus Fuzzy PD and Fuzzy PI+PD, respectively. The dynamic response of the system under parametric uncertainty case 10 is illustrated in Figure 4.43. In this case of robustness analysis, the governor time constants in both areas are varied by -50% from their nominal values. Results obtained based on case 10 revealed that the decrease in

the governor time constant results in a clear decrease in the frequency variation and tie-line power deviation.

Figure 4.44 and Figure 4.45 show the dynamic response of the testbed system for parametric uncertainties case 11 and case 12, respectively. In case 11, the regulation constant in both areas is varied by +50% while it is altered by -50% in case 12. Obtained results based on cases 11 and 12 demonstrate that the uncertainty in the regulation constant has a small impact on the system stability when the proposed fuzzy controllers equipped in the system for load frequency control.

The worst drop in frequency in both areas (ΔF_1) and (ΔF_2) as well as in the tie-line power deviation (ΔP_{tie}) is recorded based on the results obtained from case 13 of the robustness analysis as shown in Figure 4.46, where the drop of the frequency in area one has increased from -0.0431 Hz, -0.0346 Hz and -0.0792 Hz to -0.0791 Hz, -0.0958 Hz and -0.1354 Hz. The drop of the frequency in area two increased from -0.00099 Hz, -0.0024 Hz and -0.0026 Hz to -0.0045 Hz, -0.0197 Hz and -0.0179 Hz. Whilst the maximum overshoot of the tie-line power deviation increased from -0.00027 pu, -0.00064 pu and -0.00072 pu to -0.00065 pu, -0.0019 pu and -0.0020 pu based on Fuzzy C PI-PD, Fuzzy PI plus Fuzzy PD and Fuzzy PI+PD, respectively.

From Figures 4.34 – 4.46 and Table 4.28, despite the wide range of parametric uncertainties of the investigated two-area system in the thirteen considered scenarios, the implementation of the three fuzzy control configurations tuned by BA suggested in this study have shown an excellent level of robustness which preserved the stability of the system within acceptable limits. Furthermore, although the similarity of the performance of the proposed configurations, it is obvious that the proposed Fuzzy C PI-PD and Fuzzy PI plus Fuzzy PD have out-performed the Fuzzy PI+PD in all aspects.

4.6 Summary

In this chapter different fuzzy control structures have been discussed. Fuzzy PID with filtered derivative mode (Fuzzy PIDF) was firstly designed and used as an LFC system for the simplified GB power system which its parameters are tuned using the BA and other algorithms. A comparative study based on simulation results was carried out where the dynamic performance of the Fuzzy PIDF was compared with those of Fractional Order PID (FOPID) and classical PID. The proposed Fuzzy PID has outperformed the other controllers.

An extensive robustness analysis of the controller against the parametric uncertainties of the GB power system was also conducted.

Fuzzy PIDF then was implemented in a two-area power system. This structure has evidenced its capability as an LFC system where the controller successfully kept the frequency within an acceptable limit following load disturbance applied in area one. Also, this configuration has illustrated its robustness against wide range of parametric variation of the investigated two area power system.

Furthermore, three other fuzzy configurations for LFC were proposed, namely, Fuzzy Cascade PI-PD (Fuzzy C PI-PD), Fuzzy PI plus Fuzzy PD (Fuzzy PI + Fuzzy PD) and Fuzzy (PI + PD). These configurations have shown several merits in their dynamic behaviors. These structures are designed not only to offer a robust performance but also a reliable action. Simulation results revealed the capability of the proposed fuzzy control structures as LFC systems.

In the following chapter, a new LFC system based on Sliding Mode Control is designed and implemented in the two testbed power systems. This is to study the effectiveness of different control theories for LFC purposes. Also, to further examine the BA as an optimization tool in tuning the parameters of different controllers.

4.7 References

- [1] A. Demiroren and E. Yesil, "Automatic generation control with fuzzy logic controllers in the power system including SMES units," *Int. J. Electr. Power Energy Syst.*, vol. 26, no. 4, pp. 291–305, May 2004, doi: 10.1016/j.ijepes.2003.10.016.
- [2] M. S. Salik, S. Priyal, N. Khokher, and N. Kumar, "Fuzzy Logic based Automatic Generation Control," in *2020 5th International Conference on Communication and Electronics Systems (ICCES)*, Jun. 2020, pp. 193–198, doi: 10.1109/ICCES48766.2020.9137953.
- [3] Z. A. Obaid, L. M. Cipcigan, and M. T. Muhssin, "Fuzzy hierarchal approach-based optimal frequency control in the Great Britain power system," *Electr. Power Syst. Res.*, vol. 141, pp. 529–537, Dec. 2016, doi: 10.1016/j.epsr.2016.08.032.
- [4] B. K. Sahu, T. K. Pati, J. R. Nayak, S. Panda, and S. K. Kar, "A novel hybrid LUS–TLBO optimized fuzzy-PID controller for load frequency control of multi-source power system," *Int. J. Electr. Power Energy Syst.*, vol. 74, pp. 58–69, Jan. 2016, doi: 10.1016/j.ijepes.2015.07.020.
- [5] R. K. Sahu, G. T. Chandra Sekhar, and S. Panda, "DE optimized fuzzy PID controller with

derivative filter for LFC of multi source power system in deregulated environment,” *Ain Shams Eng. J.*, vol. 6, no. 2, pp. 511–530, Jun. 2015, doi: 10.1016/j.asej.2014.12.009.

- [6] N. Jalali, H. Razmi, and H. Doagou-Mojarrad, “Optimized fuzzy self-tuning PID controller design based on Tribe-DE optimization algorithm and rule weight adjustment method for load frequency control of interconnected multi-area power systems,” *Appl. Soft Comput.*, vol. 93, p. 106424, Aug. 2020, doi: 10.1016/j.asoc.2020.106424.
- [7] B. K. Sahu, S. Pati, P. K. Mohanty, and S. Panda, “Teaching–learning based optimization algorithm based fuzzy-PID controller for automatic generation control of multi-area power system,” *Appl. Soft Comput.*, vol. 27, pp. 240–249, Feb. 2015, doi: 10.1016/j.asoc.2014.11.027.
- [8] R. K. Sahu, S. Panda, and N. K. Yegireddy, “A novel hybrid DEPS optimized fuzzy PI/PID controller for load frequency control of multi-area interconnected power systems,” *J. Process Control*, vol. 24, no. 10, pp. 1596–1608, Oct. 2014, doi: 10.1016/j.jprocont.2014.08.006.
- [9] M. M. Gulzar, M. Iqbal, S. Shahzad, H. A. Muqet, M. Shahzad, and M. M. Hussain, “Load Frequency Control (LFC) Strategies in Renewable Energy-Based Hybrid Power Systems: A Review,” *Energies*, vol. 15, no. 10, p. 3488, May 2022, doi: 10.3390/en15103488.
- [10] M. Ranjan and R. Shankar, “A literature survey on load frequency control considering renewable energy integration in power system: Recent trends and future prospects,” *J. Energy Storage*, vol. 45, p. 103717, Jan. 2022, doi: 10.1016/j.est.2021.103717.
- [11] N. El Yakine Kouba, M. Mena, M. Hasni, and M. Boudour, “Optimal load frequency control based on artificial bee colony optimization applied to single, two and multi-area interconnected power systems,” in *2015 3rd International Conference on Control, Engineering & Information Technology (CEIT)*, May 2015, pp. 1–6, doi: 10.1109/CEIT.2015.7233027.
- [12] H. Gozde, M. Cengiz Taplamacioglu, and İ. Kocaarslan, “Comparative performance analysis of Artificial Bee Colony algorithm in automatic generation control for interconnected reheat thermal power system,” *Int. J. Electr. Power Energy Syst.*, vol. 42, no. 1, pp. 167–178, Nov. 2012, doi: 10.1016/j.ijepes.2012.03.039.
- [13] H. Li, K. Liu, and X. Li, “A Comparative Study of Artificial Bee Colony, Bees Algorithms and Differential Evolution on Numerical Benchmark Problems,” 2010, pp. 198–207.
- [14] Y. Mu, J. Wu, J. Ekanayake, N. Jenkins, and H. Jia, “Primary Frequency Response From Electric Vehicles in the Great Britain Power System,” *IEEE Trans. Smart Grid*, vol. 4, no. 2, pp. 1142–1150, Jun. 2013, doi: 10.1109/TSG.2012.2220867.
- [15] J. B. Ekanayake, N. Jenkins, and G. Strbac, “Frequency Response from Wind Turbines,”

Wind Eng., vol. 32, no. 6, pp. 573–586, Dec. 2008, doi: 10.1260/030952408787548811.

- [16] P. Shah and S. Agashe, “Review of fractional PID controller,” *Mechatronics*, vol. 38, pp. 29–41, Sep. 2016, doi: 10.1016/j.mechatronics.2016.06.005.
- [17] P. K. Mohanty, B. K. Sahu, T. K. Pati, S. Panda, and S. K. Kar, “Design and analysis of fuzzy PID controller with derivative filter for AGC in multi-area interconnected power system,” *IET Gener. Transm. Distrib.*, vol. 10, no. 15, pp. 3764–3776, Nov. 2016, doi: 10.1049/iet-gtd.2016.0106.
- [18] G. T. Chandra Sekhar, R. K. Sahu, A. K. Baliarsingh, and S. Panda, “Load frequency control of power system under deregulated environment using optimal firefly algorithm,” *Int. J. Electr. Power Energy Syst.*, vol. 74, pp. 195–211, Jan. 2016, doi: 10.1016/j.ijepes.2015.07.025.
- [19] A. K. Barisal, “Comparative performance analysis of teaching learning based optimization for automatic load frequency control of multi-source power systems,” *Int. J. Electr. Power Energy Syst.*, vol. 66, pp. 67–77, Mar. 2015, doi: 10.1016/j.ijepes.2014.10.019.
- [20] B. Mohanty, S. Panda, and P. K. Hota, “Controller parameters tuning of differential evolution algorithm and its application to load frequency control of multi-source power system,” *Int. J. Electr. Power Energy Syst.*, vol. 54, pp. 77–85, Jan. 2014, doi: 10.1016/j.ijepes.2013.06.029.
- [21] S. Ganjefar, M. Alizadeh, and M. Farahani, “PID controller adjustment using chaotic optimisation algorithm for multi-area load frequency control,” *IET Control Theory Appl.*, vol. 6, no. 13, pp. 1984–1992, Sep. 2012, doi: 10.1049/iet-cta.2011.0405.
- [22] M. Shouran and A. M. Alsseid, “Cascade of Fractional Order PID based PSO Algorithm for LFC in Two-Area Power System,” in *2021 3rd International Conference on Electronics Representation and Algorithm (ICERA)*, Jul. 2021, pp. 1–6, doi: 10.1109/ICERA53111.2021.9538646.
- [23] D. Petrovic, M. Kalata, and J. Luo, “A fuzzy scenario-based optimisation of supply network cost, robustness and shortages,” *Comput. Ind. Eng.*, vol. 160, p. 107555, Oct. 2021, doi: 10.1016/j.cie.2021.107555.
- [24] J. Zhu and S. K. Nguang, “Fuzzy Model Predictive Control With Enhanced Robustness for Nonlinear System via a Discrete Disturbance Observer,” *IEEE Access*, vol. 8, pp. 220631–220645, 2020, doi: 10.1109/ACCESS.2020.3043359.

Chapter 5

LFC based Sliding Mode Control

5.1 Abstract

In this chapter, a new design of Sliding Mode Control (SMC) is modelled and implemented for LFC purposes in two different power systems. Firstly, the proposed design is derived based on the simplified Great Britain power system and implemented to maintain the frequency within acceptable limits under different load conditions. Then, the same technique is derived for LFC in a two-area power system. The Bees Algorithm (BA) is used to tune the parameters of the proposed controller in both power systems.

5.2 Introduction

The SMC comes under the family of Variable Structure Control (VSC). Since the first invention of this type in the early fifties from the last century, this controller has received considerable attention from researchers, with the aim of employing it on different applications and benefiting from its numerous advantages [1]. SMC has recently been successfully implemented in different areas; for example, robotic manipulator [2][3], process control [4][5], defence applications [6][7], as well as power electronics [8][9]. This is due to the broad spectrum of advantages offered by this approach, for example, robustness against parametric uncertainties and being an effective technique in non-linear systems. SMC was also considerably utilised to solve the problem of LFC in power systems. A design of sliding mode control for a single area power system is proposed in [10], this system comprises a wind turbine as a renewable energy resource. A discrete-SMC design for LFC in a four-area interconnected power system is presented in [11]. In [12], the authors have proposed SMC design for different power systems, the parameters of the controller are optimised by Particle Swarm Optimisation (PSO) and Grey Wolf Optimisation (GWO) algorithm. The author in [13] has proposed a new full order SMC method for LFC in three different power systems. Furthermore, a sliding mode controller tuned by TLBO is suggested in [14] for LFC in an unequal dual-area multi-source power system. A design of second-order integral sliding mode control employed for LFC in a two-area power system is introduced in [15]. In [16], a highly robust observer sliding mode is proposed for LFC in a three-area power integrated with two wind turbine plants. Second-order SMC combined with state estimator has recently been proposed for LFC in a two-area interconnected power system [17].

Many scholars have revealed in the literature that the SMC could solve the issue of LFC to a great extent. It is also verified that soft computing techniques could remarkably improve the performance of controllers. Therefore, in this chapter and in view of the above-said statement, a new SMC design is proposed to handle the problem of LFC in two different power systems, the mathematical model of the suggested SMC is derived based on the parameters of the investigated systems as detailed in the following sections.

5.3 Sliding Mode Control Optimised by the Bees Algorithm for LFC in the Great Britain Power System

A design of SMC is proposed in this section for LFC in the simplified Great Britain (GB) power system. The sliding surface of the proposed design has been identified to have five parameters. In order to guarantee the best usage of the proposed SMC design, the optimal gains of this controller are optimized by the Bees Algorithm (BA) and Particle Swarm Optimization (PSO); the optimizations are conducted by employing the Integral Time Absolute Error (ITAE) objective function. A step load perturbation is applied to study the dynamic response of the system. The supremacy of the proposed approach is proved by comparing the results obtained with that from Proportional Integral Derivative (PID) controller tuned by BA. The main objectives of this section are:

- Sliding mode control design with full mathematical deriving is proposed for a fourth-order system model which represents the simplified GB power system.
- To tune the parameters of the proposed controller using two different optimisation algorithms.
- To investigate the robustness of SMC tuned by BA against plant uncertainties and different load disturbances.

5.3.1 Simplified GB Power System Model

The simplified model shown in Figure 5.1 is developed to study the frequency response of the GB power system as well as for control design. The governor and turbine are modelled as first-order transfer function, a transient droop compensation is introduced between the governor and the turbine. The governor speed control is represented by an equivalent gain value, R . Also, the possible effect of frequency-dependent loads is lumped into a damping constant D . The total system inertia is represented as a time constant H_{eq} . The values of this simplified model are shown in Table 5.1. Where T_g : the governor time constant, T_t : turbine time constant, T_{ld} , T_{lg} : transient droop compensation time constants [18]–[20].

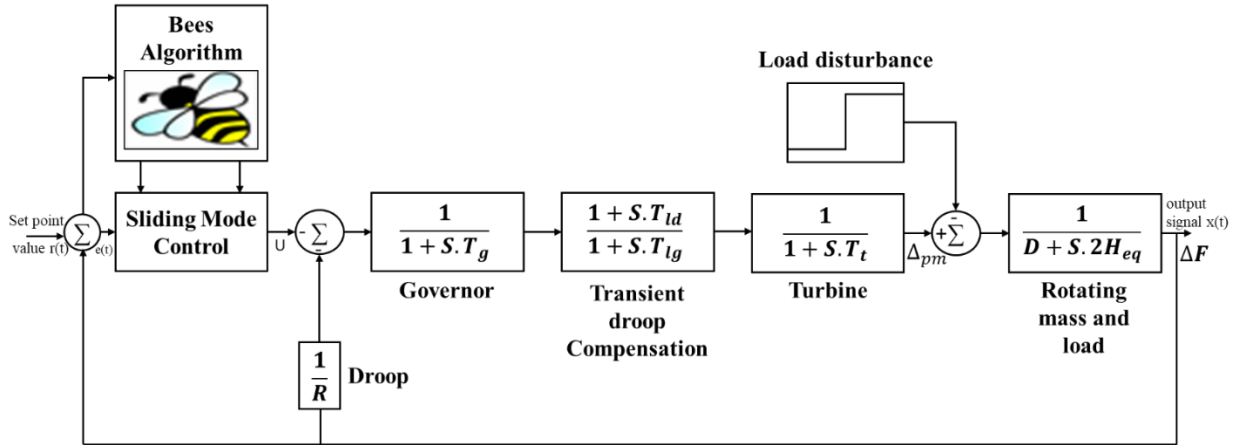


Figure. 5.1. GB simplified model with primary/ secondary control loops.

Table 5.1 The simplified GB power system parameters.

T_g	T_{ld}	T_{lg}	T_t	$2H_{eq}$	D	R
0.2 s	2 s	12 s	0.3 s	8.88 s	1 pu	-0.09 pu

5.3.2 SMC Design based GB power system parameters

In sliding mode control design, the sliding surface $s(t)$ is a key step to define the desired behavior of the investigated system. The function of SMC is to keep the state of the system as close as to this surface at all times. In this research work, the proposed sliding surface is given in Equation (5.1).

$$s(t) = K_1 \ddot{e}(t) + K_2 \dot{e}(t) + K_3 e(t) + K_4 \int e(t) dt \quad (5.1)$$

Where \dot{e} is the derivative of e ($\dot{e} = \frac{de}{dt}$). As in Equation (5.1), $e(t)$ reflects the tracking error, and the five parameters, namely, $K_1, K_2, K_3, K_4,$ and K_5 are proposed in this design to be tuned by the BA and PSO algorithms. The objective of this design is to ensure the tracking signal along with its derivatives are always zero, once $s(t)$ is achieved. Therefore, maintaining $s(t)$ at a constant value necessitates making its derivative equal to zero which is mathematically illustrated in Equation. (5.2).

$$\dot{s}(t) = 0 \quad (5.2)$$

Based on the conditions given in Equation (5.1) and (5.2), the control law $U(t)$ of the SMC design presented in Equation (5.3) is derived.

$$U(t) = U_C(t) + U_D(t) \quad (5.3)$$

Where, $U_C(t)$ is function of the output signal $x(t)$, the reference signal (setpoint value)

$r(t)$, and the tracking error $e(t)$ which is the difference between $r(t)$ and $x(t)$ as presented in Equation (5.4). The $U_D(t)$ is illustrated in Equation (5.5).

$$e(t) = r(t) - x(t) \quad (5.4)$$

$$U_D = K_D \frac{s(t)}{|s(t)| + \delta} \quad (5.5)$$

Here, the values of K_D and δ are to be tuned by the proposed algorithms. Therefore, in this design, seven parameters in total are to be calculated, namely, $K_1, K_2, K_3, K_4, K_5, K_D$ and δ . The fourth-order model considered in this design is represented in Equation (5.6).

$$\frac{X(s)}{U_c(s)} = \frac{(T_{ld}S+1)}{(T_{lg}S+1)(T_gS+1)(T_tS+1)(2H_{eq}S+1)} \quad (5.6)$$

From Table 5.1, and by considering $T_{ld}=2, T_{lg}=12, T_g=0.2, T_t=0.3$ and $(2*H_{eq}) = 8.88$, Equation (5.6) can be re-written as illustrated in Equation (5.7) which can also be represented in differential equation form as given in Equation (5.8).

$$\frac{X(s)}{U_c(s)} = \frac{1}{6.394 s^4 + 67.32 s^3 + 226.1 s^2 + 255.5 s + 43.76 + 2 s^{-1}} \quad (5.7)$$

$$U_c(t) = 6.394 \cdot \ddot{\ddot{x}}(t) + 67.32 \ddot{\ddot{x}}(t) + 226.1 \ddot{\ddot{x}}(t) + 255.5 \dot{\ddot{x}}(t) + 43.76 x(t) + 2 \int x(t) dt \quad (5.8)$$

Also, from Equation (5.1), Equation (5.2) can be re-written as

$$\dot{s}(t) = K_1 \cdot \ddot{\ddot{e}}(t) + K_2 \ddot{\ddot{e}}(t) + K_3 \ddot{\ddot{e}}(t) + K_4 \dot{\ddot{e}}(t) + K_5 e(t) = 0 \quad (5.9)$$

By solving Equation (5.8) for the fourth-order derivative of the variable $\ddot{\ddot{x}}(t)$, Equation (5.10) is obtained:

$$\begin{aligned} \ddot{\ddot{x}}(t) = \frac{1}{6.394} [& U_c(t) - 67.32 \ddot{\ddot{x}}(t) - 226.1 \ddot{\ddot{x}}(t) \\ & - 255.5 \dot{\ddot{x}}(t) - 43.76 x(t) - 2 \int x(t) dt] \end{aligned} \quad (5.10)$$

Analysing Equation (5.10) in conjunction with Equation (5.4) and substituting the

expression in Equation (5.9), we get:

$$\dot{s}(t) = \frac{K_1}{6.394} \left[-U_C(t) + 67.32 \ddot{x}(t) + 226.1 \dot{x}(t) + 255.5 \dot{x}(t) + 43.76 x(t) + 2 \int x(t) dt \right] - K_2 \ddot{x}(t) - K_3 \dot{x}(t) - K_4 \dot{x}(t) - K_5 x(t) \quad (5.11)$$

From Equation (5.11), the control law expression is as following:

$$U_C(t) = \left[67.32 - \frac{K_2}{K_1} * 6.394 \right] \ddot{x}(t) + \left[226.1 - \frac{K_3}{K_1} * 6.394 \right] \dot{x}(t) + \left[255.5 - \frac{K_4}{K_1} * 6.394 \right] \dot{x}(t) + \left[43.76 - \frac{K_5}{K_1} * 6.394 \right] x(t) + 2 \int x(t) dt \quad (5.12)$$

Finally, the SMC design is concluded as:

$$U(t) = U_C(t) + K_D \frac{s(t)}{|s(t)| + \delta} \quad (5.13)$$

The parameters of BA and PSO are set in this work as given in Table 5.2 and 5.3, respectively. Where, C_R is the crossover rate, w_{max} and w_{min} are the initial and final weights, whilst C_1 and C_2 are the acceleration coefficient.

Table 5.2. The BA parameters.

n	m	e	nep	nsp	ngb
30	10	5	10	7	0.01

Table 5.3. The PSO parameters.

No. Particles	w_{max}	w_{min}	C₁	C₂	C_R
30	10	6	1.2	1.2	0.65

5.3.3 Implementation, Results and Discussion

As it is above mentioned, in the proposed design of SMC, seven parameters are to be tuned using BA and PSO. The iteration number of each algorithm is set to 100. A step load change of 0.03955 pu represents a loss of two power generators with total power generated equals 1.32GW with about 33 GW base demand is applied to study the dynamic response of the system and to investigate the effectiveness of the proposed controller. The Integral Time Absolute Error (ITAE) expressed in Equation (5.14) is considered as an objective function due to its advantages in reducing the undershoot/ overshoot and the settling time [36].

$$ITAE = J = \int_0^{T_{sim}} (|\Delta F| \times t) dt \quad (5.14)$$

In this subsection, the implementation of the proposed design of SMC is conducted for LFC in the simplified GB power system. The overall transfer function of the system shown in Figure 5.1 without considering the secondary frequency control loop is given in Equation (5.15).

$$\frac{X(s)}{U_c(s)} = \frac{(T_{ld}S + 1)}{(T_{lg}S + 1)(T_gS + 1)(T_tS + 1)(2H_{eq}S + 1) + 1/R} \quad (5.15)$$

Accordingly, for the GB power system model presented in Equation (5.15), the control law of the SMC is as following:

$$U(t) = \left[67.32 - \frac{K_2}{K_1} * 6.394 \right] \ddot{x}(t) + \left[226.1 - \frac{K_3}{K_1} * 6.394 \right] \dot{x}(t) + \left[255.5 - \frac{K_4}{K_1} * 6.394 \right] x(t) + \left[32.76 - \frac{K_5}{K_1} * 6.394 \right] x(t) + 2 \int x(t) dt + K_D \frac{s(t)}{|s(t)| + \delta} \quad (5.16)$$

The optimal gains of the proposed SMC design obtained using the proposed BA and PSO algorithms by minimising ITAE objective function are depicted in Table 5.4. Convergence characteristics for BA and PSO algorithms with SMC are demonstrated in Figure 5.2. From Figure 5.2 it is observed that the Bees Algorithm is slightly better than PSO.

Table 5.4. The SMC optimum parameters obtained by BA and PSO.

Tuned parameters	Controller	
	BA- SMC	PSO- SMC
K ₁	20.796	31.4811
K ₂	15.175	5.0147
K ₃	10.1	2.3110
K ₄	40	38.195
K ₅	0.59	1.8896
K _D	0.4	0.4
δ	0.0018	0.0100

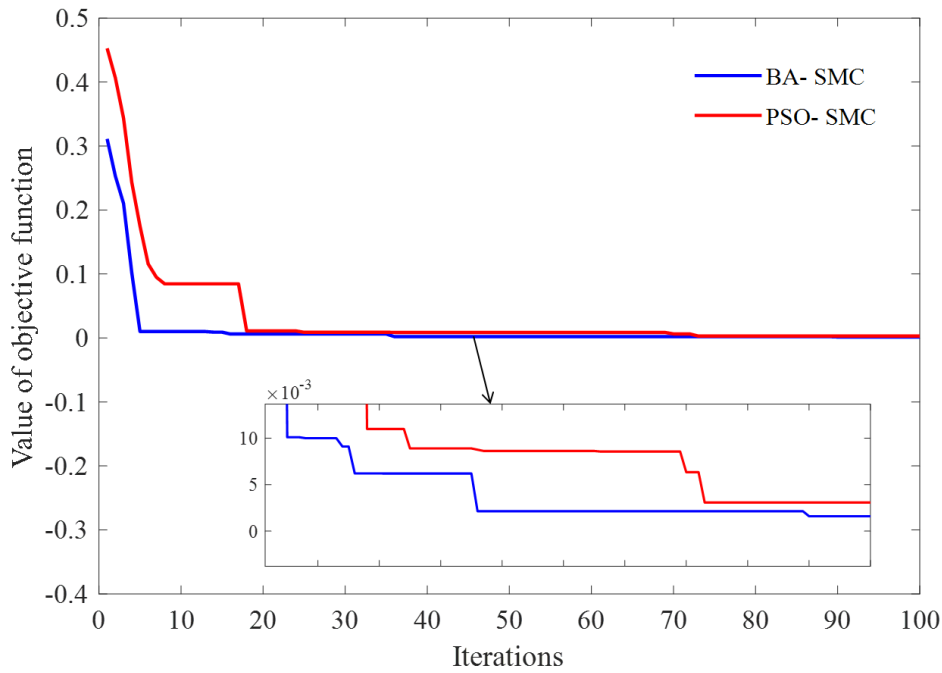


Figure. 5.2. Convergence characteristics of the BA and PSO tuned the proposed SMC design.

To show the supremacy of the proposed SMC design, the obtained results are compared with those obtained from applying PID controller tuned by BA where its optimal values are: $K_P = 40$, $K_I = 2.26$, and $K_D = 21.95$. The boundaries of the tuned parameters are chosen [0 - 40] in all cases. Figure 5.3 shows the dynamic response with PID controller employed for LFC and that without applying secondary control. Note that: the dynamic response obtained from applying SMC is better than the PID response. Therefore, plotting the responses based on PID and SMC in one graph does not help to clearly represent the SMC response.

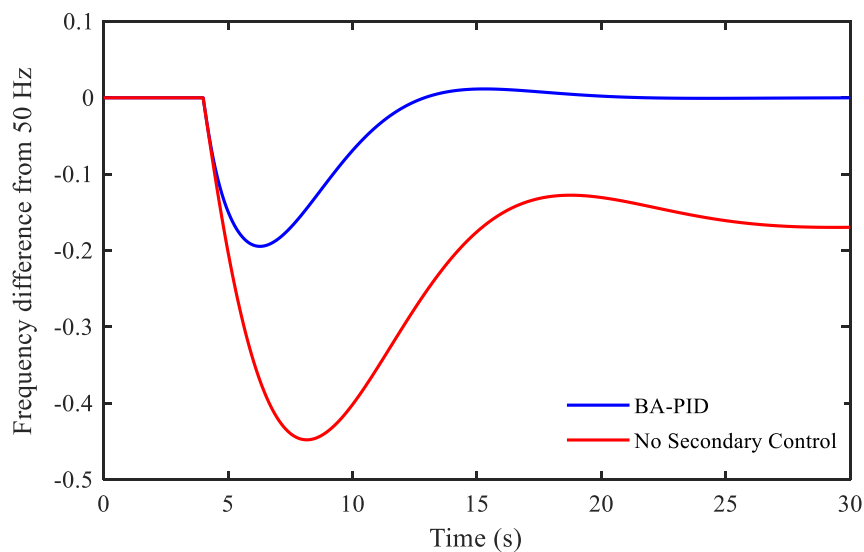


Figure. 5.3. The frequency deviation of the GB power system for 0.0395 pu load disturbance without LFC / with PID controller.

Figure 5.4 shows the dynamic response of the GB power system with SMC tuned by BA and PSO and the characteristics of the response are given in Table 5.5, where the values of undershoot, overshoot, settling time, ITAE, and the Integral time of the Square Error (ISE) are illustrated.

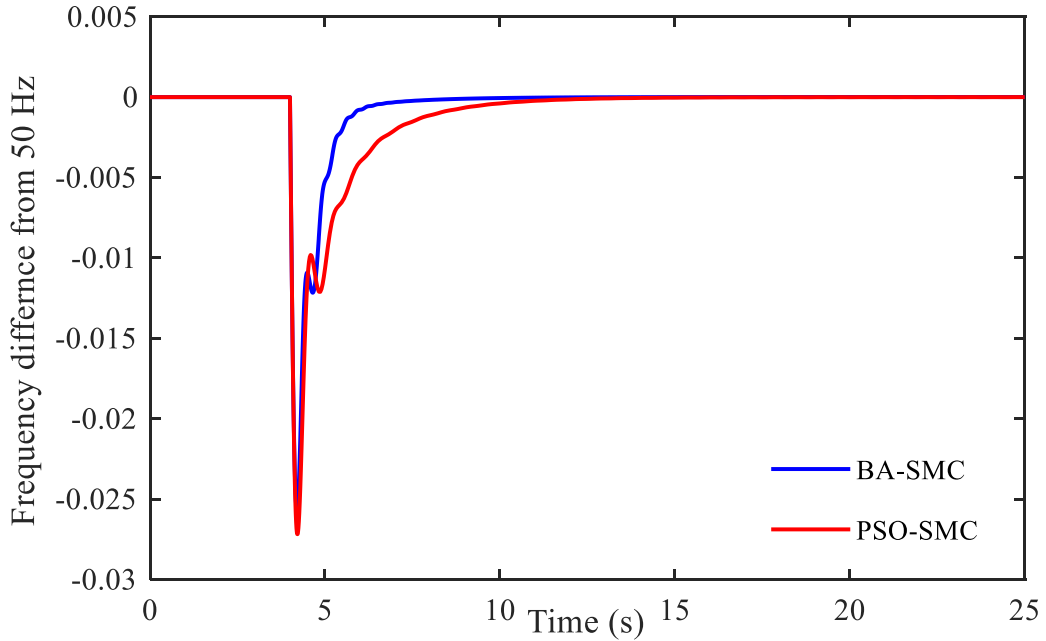


Figure. 5.4. The frequency deviation of the GB power system for 0.0395 pu load disturbance with the proposed SMC.

Table 5.5. Dynamic performance of the GB System with different controllers.

Controller	U_{sh} Hz	O_{sh} Hz	T_s s	ITAE	ISE
BA- SMC	-0.0257	0	6.401	0.00160	9.03×10^{-8}
PSO- SMC	-0.0272	0	9.364	0.003071	1.29×10^{-7}
BA- PID	-0.1945	0.0115	19.10	0.1545	5.24×10^{-5}

From Figure 5.4 and Table 5.5, an obvious improvement in the performance of the system is obtained when the proposed SMC is utilized. Moreover, it can be noted that SMC tuned by BA gives the best dynamic response in all aspects having a slightly smaller undershoot and less settling time in comparison with SMC tuned by PSO.

Percentage of improvement in overshoot, undershoot, settling time, ITAE, and ISE for SMC tuned by BA and PSO in comparison with PID optimised by BA is demonstrated in Table 5.6 and Figure 5.5. From Table 5.6, it is observed that with BA optimised SMC, undershoot, settling time, ITAE, and ISE are improved by 86.78%, 66.48%, 98.96% and

99.82% respectively, while with SMC tuned by PSO, these criteria are improved by 86.01%, 70.97%, 98.01% and 99.75% respectively.

Table 5.6. Improvement percentage in U_{sh} , O_{sh} , T_s , ITAE, and ISE with the proposed SMC.

Controller	U_{sh}	O_{sh}	T_s	ITAE	ISE
BA- SMC	86.78 %	100 %	66.48%	98.96%	99.82%
PSO- SMC	86.01%	100%	50.97%	98.01%	99.75%

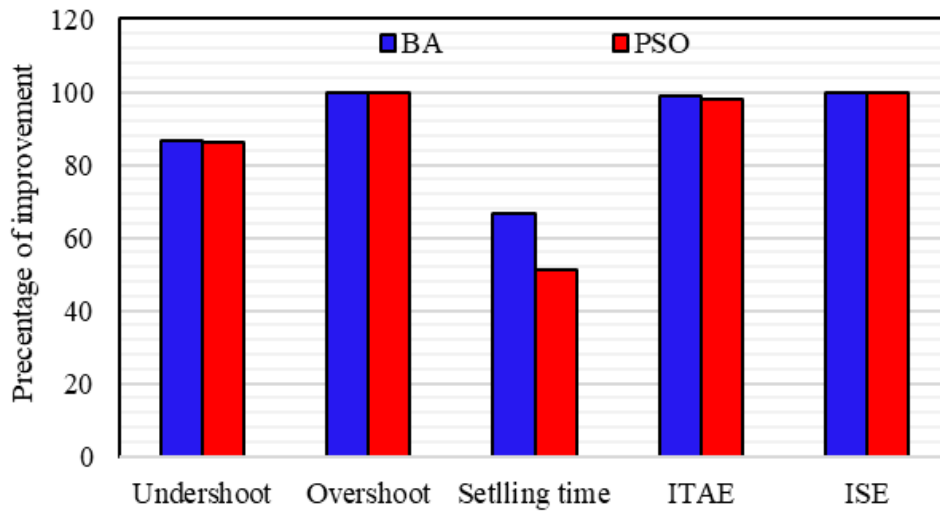


Figure. 5.5. Percentage of improvement in different criteria with SMC tuned by BA and PSO.

5.3.3.1 Robustness against system uncertainties and different load disturbances

The parameters of the GB power system are altered by $\pm 50\%$ in steps of 25%, namely, T_g , H_{eq} , D and R in order to examine the robustness of the system with SMC tuned by BA. A step load perturbation of 0.0395 pu is applied and the optimal SMC obtained with nominal conditions of the system are not re-tuned to verify the robustness. Different four cases of the system parametric uncertainties are given in Table 5.7 in which four parameters are varied simultaneously in each case. Figure 5.6 illustrates the dynamic response of the four cases along with the nominal case when no secondary control is applied.

It is obvious that case four represents the worst scenario of parametric uncertainties where the drop in the frequency is more than 0.5 Hz. Figure 5.7 and Table 5.8 show the dynamic performance of the GB power system when it is subjected to parametric deviation with the proposed SMC tuned by BA employed for LFC.

Table 5.7. The variation range of the parameters in the GB power system.

Parameters		Nominal value	Variation range	New value
Case 1	T_g	0.2	+25%	0.25
	H_{eq}	4.44	+25%	5.55
	D	1	-25%	0.75
	R	-0.09	-25%	-0.0675
Case 2	T_g	0.2	-25%	0.15
	H_{eq}	4.44	-25%	3.33
	D	1	+25%	1.25
	R	-0.09	+25%	-0.1125
Case 3	T_g	0.2	+50%	0.3
	H_{eq}	4.44	+50%	6.66
	D	1	-50%	0.5
	R	-0.09	-50%	-0.045
Case 4	T_g	0.2	+50%	0.3
	H_{eq}	4.44	-50%	2.22
	D	1	+50%	1.5
	R	-0.09	+50%	-0.135

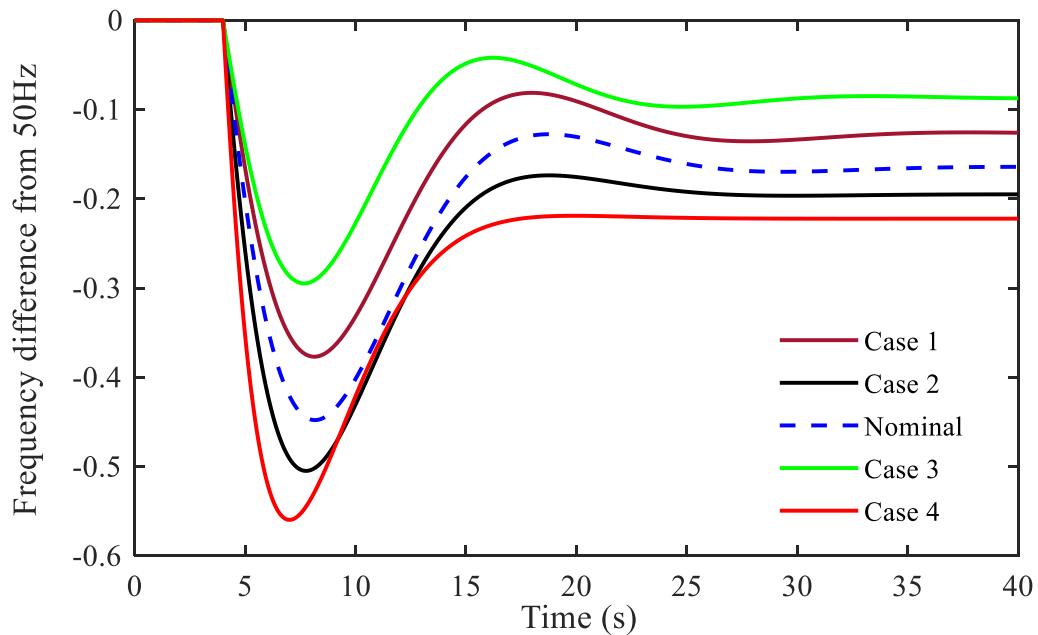


Figure. 5.6. Comparison of the dynamic response of GB power model with parameter uncertainties case 1, 2, nominal, 3, and 4 with no secondary control loop employed.

Table 5.8. The dynamic performance of the GB power system under parameter uncertainties conditions when BA-SMC is employed for LFC.

Case	U_{sh} Hz	O_{sh} Hz	T_s s	ITAE	ISE
Case 1	-0.0252	0	6.495	0.00163	9.3×10^{-8}
Case 2	-0.0262	0	6.363	0.00156	8.78×10^{-8}
Nominal	-0.0257	0	6.401	0.00160	9.03×10^{-8}
Case 3	-0.0249	0	6.517	0.00169	9.91×10^{-8}
Case 4	-0.0268	0	6.354	0.00155	8.29×10^{-8}

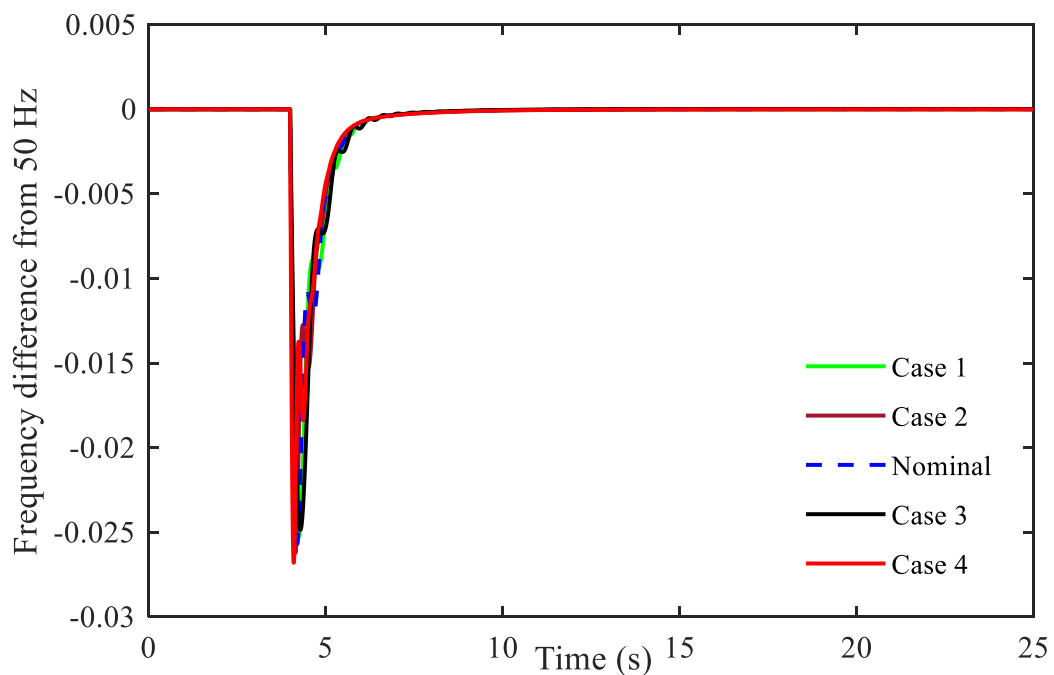


Figure. 5.7. The dynamic performance of the GB power system under parameter uncertainties conditions when BA-SMC is employed for LFC.

From Table 5.8 and Figure 5.7, it is observed that the proposed controller has shown high robustness against system parametric uncertainties although a wide range of variations have been considered.

As it is observed the highest drop in the frequency is recorded in case 4 in which the parameters of the system are varied by $\pm 50\%$. Therefore, to further examine the robustness of the proposed controller, load disturbance with 0.053 pu is considered in case 4 of parametric uncertainties of the GB power model. The dynamic response of the investigated system in this scenario is illustrated in Figure 5.8.

Figure 5.8 gives further proof of the robustness of the proposed sliding mode control tuned by the Bees Algorithm. It is noted that, although this part considers the worst case of parametric uncertainties with higher load disturbance equals 0.053 pu, only slightly further reduction in the frequency is resulted.

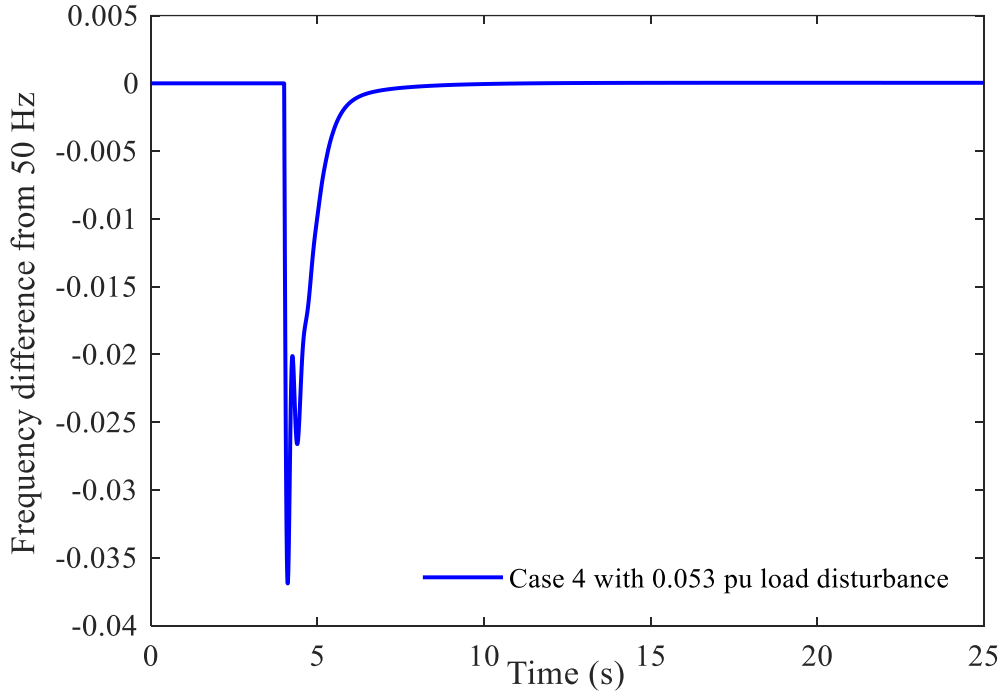


Figure. 5.8. The dynamic response of the GB power system under parametric uncertainties case 4 with SMC tuned by BA is employed for LFC when 0.053 pu load disturbance is applied.

5.4 The Bees Algorithm Tuned Sliding Mode Control for Load Frequency Control in Two-Area Power System

This section proposes a design of SMC for LFC in a two-area electrical power system. The mathematical model design of the SMC is derived based on the parameters of the investigated system. In order to achieve the optimal use of the proposed controller, the BA is suggested in to tune the parameters of the SMC. The dynamic performance of the power system with SMC employed for LFC is studied by applying a load disturbance of 0.2 pu in area one. To prove the supremacy of the proposed SMC based BA, the results obtained from applying the proposed SMC-based BA are compared with those of previously published works for the same system based on Fuzzy PID tuned by TLBO presented in [22] and traditional PID-based LCOA [21]. Furthermore, the robustness of SMC-based BA is examined against parametric uncertainties of the testbed power system by simultaneous changes in certain parameters of the testbed system with 40% of their nominal values. Simulation results prove

the superiority and the robustness of the proposed SMC as an LFC system for the investigated two-area interconnected power system.

A widely studied two-area interconnected power system [21] [22] is considered in this subsection as a testbed system to examine the potentiality of the SMC as an LFC system. Integral Time Absolute Error (ITAE) is taken as an objective function to find the optimal gains of the SMC by BA.

Concisely, the novelty of this section is in its proposal to apply the BA for tuning sliding mode control parameters implemented for load frequency control in a two-area power system. The SMC design used in this study is simple, understandable, and applicable. Additionally, to the best of the author's knowledge, no previous studies have compared the performance of SMC with Fuzzy Logic Control (FLC) for LFC. It is observed from the simulation results that the BA-optimised SMC has successfully performed as a robust LFC and affords the best dynamic performance in terms of peak undershoot with fast response as compared with the other controllers.

5.4.1 The Investigated Two-area Interconnected Power System

The testbed model considered in this subsection is shown in Figure 5.9. It is an extensively investigated system in literature to study the dynamic behaviour of different control concepts for LFC in power systems. Table 5.9 provides the associated parameters of this power system.

Table 5.9. The parameter of the testbed system [22].

Parameter	Definition	Values in Area 1	Values in Area 2
1/R	Regulation constant	0.05 MW/Hz	0.0625 MW/Hz
B	Frequency bias	20.6 Hz/MW	16.9 Hz/MW
D	The ratio of change in load to change in frequency	0.6	0.9
H	System inertia time constant	5	4
T_g	Governor time constant	0.2 s	0.3 s
T_t	Turbine time constant	0.5 s	0.6 s
T	Synchronization coefficient	2	
F	Frequency of the system	60 Hz	
SLP	Step Load Perturbation	0.2 pu	

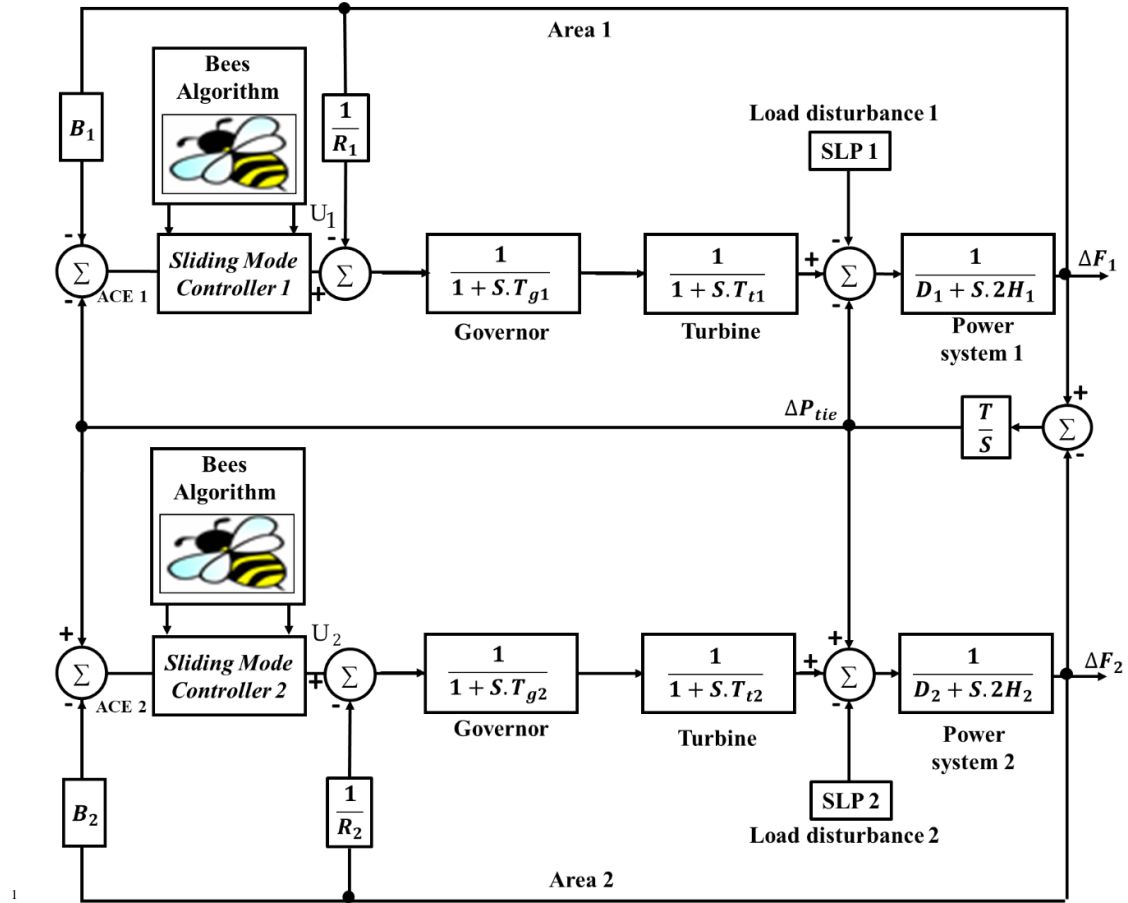


Figure 5.9. Transfer function model of the testbed system.

The term of Area Control Error (ACE) in each area is the input of the controller equipped in that area. For this system, the ACEs are represented in Equations (5.17) and (5.18).

$$ACE_{\text{area 1}} = \Delta P_{12} + B_1 \Delta F_1 \quad (5.17)$$

$$ACE_{\text{area 2}} = \Delta P_{21} + B_2 \Delta F_2 \quad (5.18)$$

where ΔF_1 and ΔF_2 are the frequency deviation in areas one and two, respectively, ΔP_{12} and ΔP_{21} are the power flow deviations, whilst B_1 and B_2 are frequency biases.

5.4.2 Design and Implementation of the Proposed SMC System

The first step in designing an SMC is to identify the required behaviour of the testbed system, represented by the sliding surface of the controller. In the current research, the sliding surface of the suggested SMC design is as expressed in Equation (5.19):

$$S(t) = K_1 \ddot{e}(t) + K_2 \dot{e}(t) + K_3 e(t) + K_4 \int e(t) \cdot dt \quad (5.19)$$

where $e(t)$ is the tracking error variable, K_1 , K_2 , K_3 and K_4 are the parameters that will be optimized via the Bees Algorithm. From a control perspective, it is essential to maintain

the tracking signal $e(t)$ and its derivatives equal to zero. Additionally, in order to keep $e(t)$ at a specified value, it is required to maintain its derivative equal to zero as illustrated in (5.20).

$$\dot{S}(t) = 0 \quad (5.20)$$

The control law of the proposed design illustrated in (5.21) is selected by taking into account the condition expressed in Equations (5.19) and (5.20).

$$U(t) = U_C(t) + U_D(t) \quad (5.21)$$

where $U_C(t) = F(x(t), r(t), e(t))$; in which $x(t)$ is the output signal, $r(t)$ is the reference signal, and $e(t)$ is the error signal. The term $U_D(t)$ can be expressed as in Equation (5.22).

$$U_D(t) = K_D \frac{S(t)}{|S(t)| + \delta} \quad (5.22)$$

where the gains K_D and δ are to be optimized by BA. Accordingly, the proposed SMC design comprises six parameters. The optimal values of these parameters are found by the BA via minimizing the integral time absolute error of the deviation in the frequency and exchanged power.

In the system shown in Figure 5.10, the transfer function of area one from the control signal U_1 to ΔF_1 with consideration of the droop characteristic R_1 can be demonstrated as in Equation (5.23).

$$G(s) = \frac{X(s)}{U_C(s)} = \frac{1}{(T_{g1}S + 1)(T_{t1}S + 1)(2H_1S + D_1) + 1/R_1} \quad (5.23)$$

By considering the values of the parameters tabulated in Table 5.9, Equation (5.23) can be re-written as follows:

$$G(s) = \frac{X(s)}{U_C(s)} = \frac{1}{S^3 + 7.06 S^2 + 10.42 S + 20.6} \quad (5.24)$$

Equation (5.24) can also be written in differential form as expressed in (5.25)

$$U_C(t) = \ddot{x}(t) + 7.06 \dot{x}(t) + 10.42 x(t) + 20.06 \quad (5.25)$$

From (5.19), Equation (5.20) can be re-written as follows:

$$\dot{S}(t) = K_1 \ddot{e}(t) + K_2 \dot{e}(t) + K_3 e(t) + K_4 e(t) = 0 \quad (5.26)$$

By solving Equation (25) for the third derivative order, Equation (5.27) is obtained.

$$\ddot{x}(t) = U_C(t) - 7.06 \ddot{x}(t) - 10.42 \dot{x}(t) - 20.06 \quad (5.27)$$

As the variable $e(t)$ is defined as the difference between the reference signal $r(t)$ and the control signal $x(t)$, this can be mathematically expressed as in (5.28).

$$e(t) = r(t) - x(t) \quad (5.28)$$

By analyzing Equation (5.27) based on (5.28) and substituting the expression in (5.26), Equation (5.29) is obtained.

$$\dot{S}(t) = \left[\begin{array}{l} K_1[-U_C(t) + 7.06 \ddot{x}(t) + 10.42 \dot{x}(t) + 20.06] \\ - K_2 \ddot{x}(t) - K_3 \dot{x}(t) - K_4 x(t) = 0 \end{array} \right] \quad (5.29)$$

The term $U_C(t)$ can be identified as follows:

$$U_C(t) = \ddot{x}(t) \left[7.06 - \frac{K_2}{K_1} \right] + \dot{x}(t) \left[10.42 - \frac{K_3}{K_1} \right] + x(t) \left[20.6 - \frac{K_4}{K_1} \right] \quad (5.30)$$

The control law of the controller employed in area one is expressed as in (5.31).

$$U(t) = \begin{aligned} & \ddot{x}(t) \left[7.06 - \frac{K_2}{K_1} \right] + \\ & \dot{x}(t) \left[10.42 - \frac{K_3}{K_1} \right] + \\ & x(t) \left[20.6 - \frac{K_4}{K_1} \right] + \\ & K_{D1} \left[\frac{-K_1 \ddot{x}(t) - K_2 \dot{x}(t) - K_3 x(t) - K_4 \int x(t) \cdot dt}{|-K_1 \ddot{x}(t) - K_2 \dot{x}(t) - K_3 x(t) - K_4 \int x(t) \cdot dt| + \delta_1} \right] \end{aligned} \quad (5.31)$$

Similarly, to derive the control law of the SMC equipped in area two, the same procedure is followed, this yields the equation expressed in (5.32).

$$U(t) = \begin{aligned} & \ddot{x}(t) \left[7.362 - 1.44 \times \frac{K_6}{K_5} \right] + \\ & \dot{x}(t) \left[8.810 - 1.44 \times \frac{K_7}{K_5} \right] + \\ & x(t) \left[16.90 - 1.44 \times \frac{K_8}{K_5} \right] + \\ & K_{D2} \left[\frac{-K_5 \ddot{x}(t) - K_6 \dot{x}(t) - K_7 x(t) - K_8 \int x(t) \cdot dt}{|-K_5 \ddot{x}(t) - K_6 \dot{x}(t) - K_7 x(t) - K_8 \int x(t) \cdot dt| + \delta_2} \right] \end{aligned} \quad (5.32)$$

In this section, the parameters of the BA are set as illustrated in Table 5.10. The number of iterations was set as 100.

Table 5.10. The parameters of the proposed BA.

n	m	e	nep	nsp	ngh
30	12	6	11	7	0.011

In this research, the parameters of SMC proposed for LFC in the dual-area power system is optimized using the BA by minimizing the Integral Time Absolute Error (ITAE) objective function expressed in Equation (5.32).

$$\text{Objective Function} = \text{ITAE} = \int_0^t (|\Delta F_1| + |\Delta F_2| + |\Delta P_{tie}|).t. dt \quad (5.32)$$

5.4.3 Results and Discussion

In this section, a step load disturbance of 0.2 pu is applied in area one to study the dynamic performance of the testbed system when the proposed SMC tuned by BA is equipped in the system for LFC. The BA is run for 100 iterations to obtain the optimal values of the SMC parameters and the restrains of the search space is set from [0 to 2]. The optimum gains of the SMC obtained by BA are shown in Table 5.11. Figure 5.10 shows the convergence characteristic curve of BA based on several runs. It is worth mentioning that running the algorithm for longer iterations may lead to a better performance. Also, choosing the proper setting of each parameter of the algorithm will enhance its behavior.

Table 5.11. The optimum SMC gains obtained by BA.

Controller	Parameters					
SMC	Controller gains of area 1					
	K_1	K_2	K_3	K_4	K_{D1}	δ_1
	1.4921	0.0309	0.1353	1.9007	1.7275	0.0029
	Controller gains of area 2					
	K_5	K_6	K_7	K_8	K_{D2}	δ_2
	1.8411	1.9269	0.8824	1.8353	0.0560	1.5275

Furthermore, in order to demonstrate the superiority of the SMC, the results obtained are compared with those from published articles based on TLBO tuned Fuzzy PID presented in [22] and LCOA tuned traditional PID presented in [21] employed for LFC in the same system. The optimum gains of these controllers are depicted in Table 5.12.

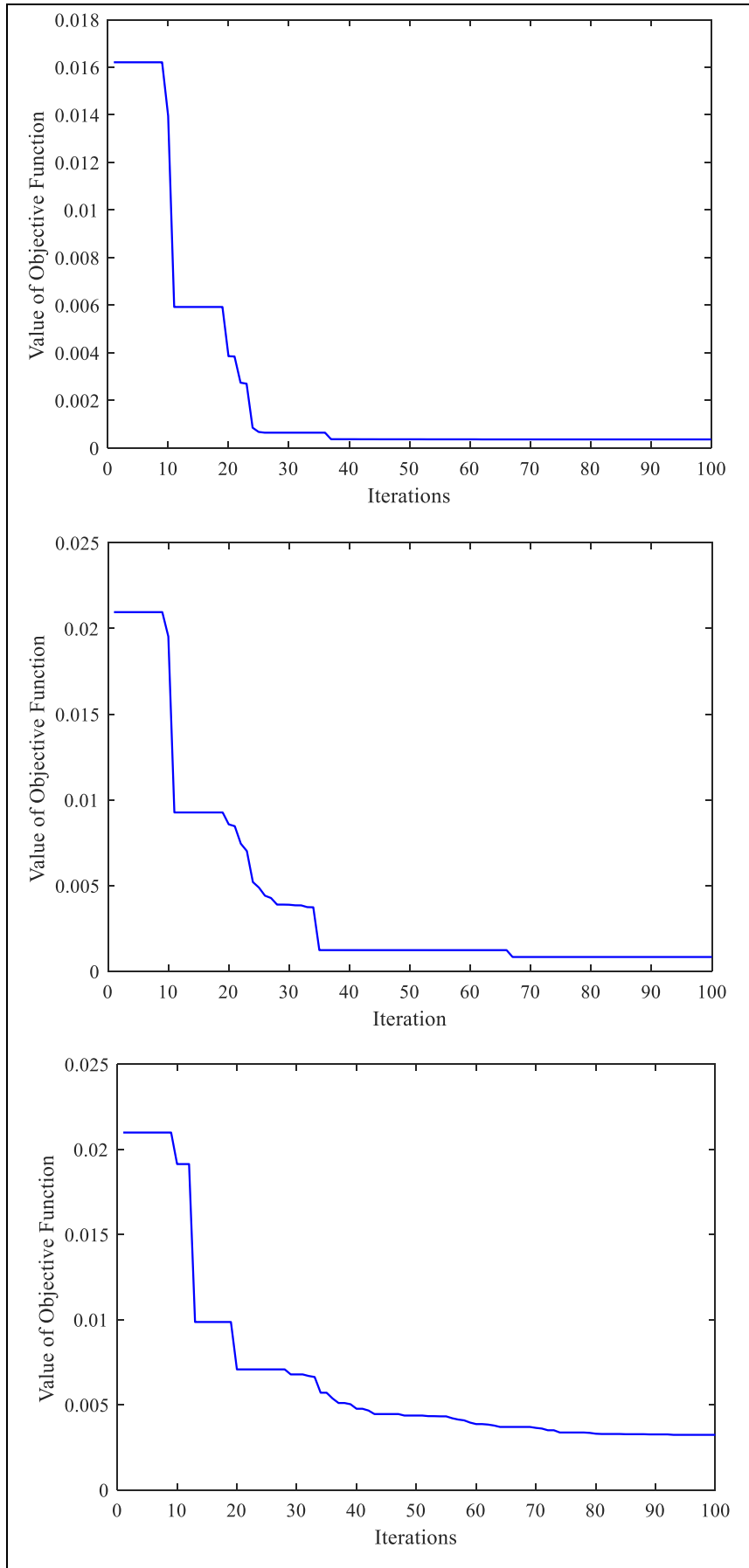


Figure 5.10. The convergence characteristic of BA algorithm based on several runs.

Table 5.12. The optimum gains of the controllers proposed in [21] and [22].

Controller	Controller Gains of Area 1				Controller Gains of Area 2			
	K ₁	K ₂	K ₃	K ₄	K ₅	K ₆	K ₇	K ₈
Fuzzy PID [14]	1.9857	1.9968	1.687	1.9876	1.3469	1.5512	0.809	0.5043
PID [7]	K _{P1}	K _{I1}	K _{D1}		K _{P2}	K _{I2}	K _{D2}	
	0.939	0.7998	0.5636		0.5208	0.4775	0.708	

The frequency variation in area one, frequency variation in area two, and tie-line power variation following the sudden 0.2 pu disturbance applied in area one are shown in Figures 5.11–5.13, respectively. From Figures 5.11 – 5.13, it is found that the SMC tuned by BA employed for LFC in the dual-area power system offers a better dynamic response compared with those provided in [21] [22]. The undershoot (U_{sh}), overshoot (O_{sh}), and settling time (T_s) of the frequency in both areas and tie-line power along with the values of the objective function are illustrated in Table 5.13.

Table 5.13. Frequency response performances with different controllers.

Controller	Frequency variation in Area 1			Frequency variation in Area 2			Tie Line Power Deviation			ITAE
	U_{sh} in Hz	O_{sh} in Hz	T_s in s	U_{sh} in Hz	O_{sh} in Hz	T_s in s	U_{sh} in pu	O_{sh} in pu	T_s in s	
SMC-BA	-0.0746	0.0495	2.323	-0.0016	0.0005	2.469	-0.0003	0.00005	2.0377	0.0003
Fuzzy PID-TLBO	-0.1885	0.0035	4.9849	-0.0190	0	25.0325	-0.0042	0	24.748	0.3305
PID-LCOA	-0.4288	0.0154	11.795	-0.0664	0	21.6623	-0.0134	0	22.689	0.7920

From Table 5.13, it is observed that the settling time and undershoot of ΔF_1 , ΔF_2 , and ΔP_{tie} is less when the proposed SMC tuned by BA is used as an LFC controller to study the dynamic behavior of the two-area power model as compared with the other techniques studied in [21] [22]. It is also evident that the value of the objective function (ITAE) is extremely less for BA-optimized SMC in comparison with the other controllers. However, a negligible increase in the overshoot is noticed.

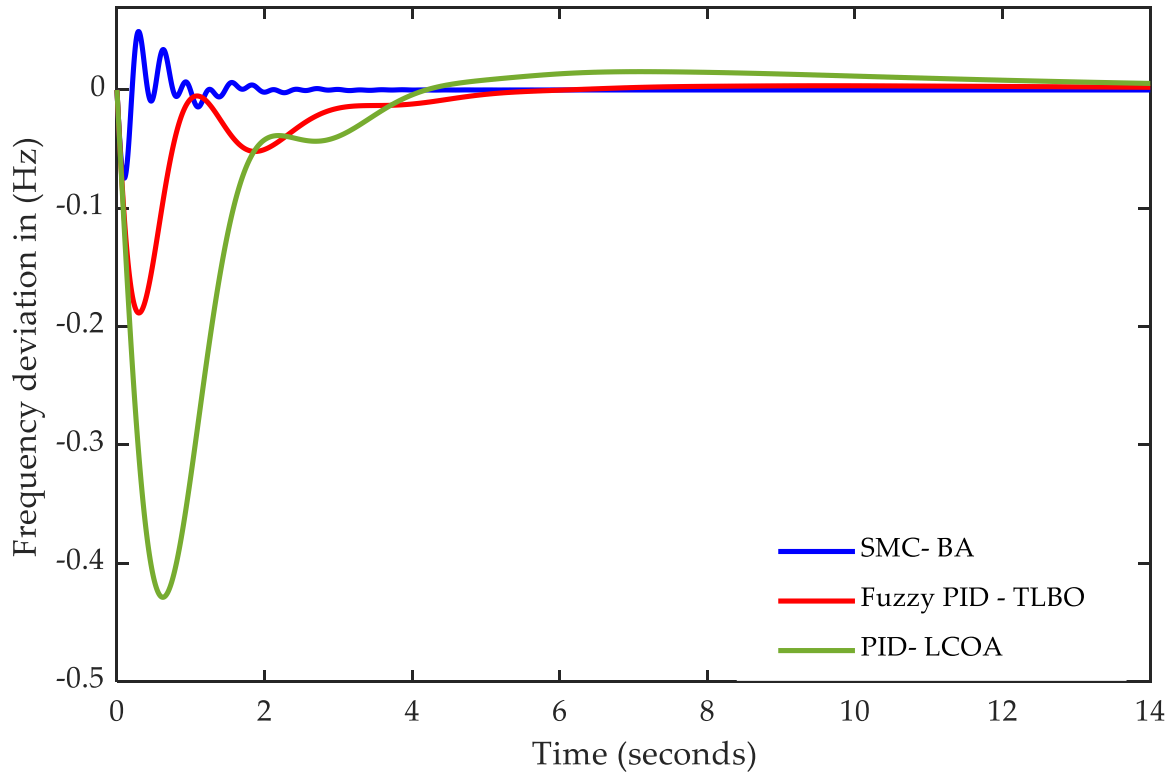


Figure 5.11. Frequency deviation in area one (ΔF_1 in Hz).

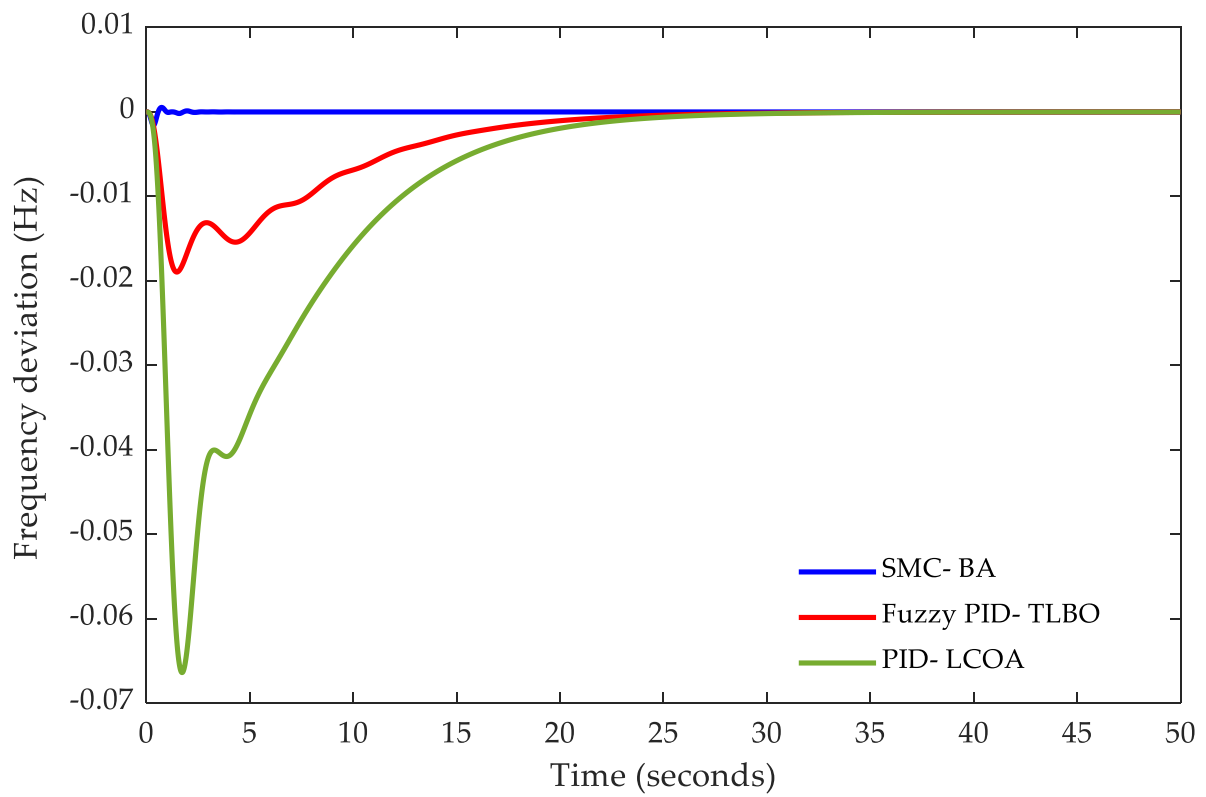


Figure 5.12. Frequency deviation in area two (ΔF_2 in Hz).

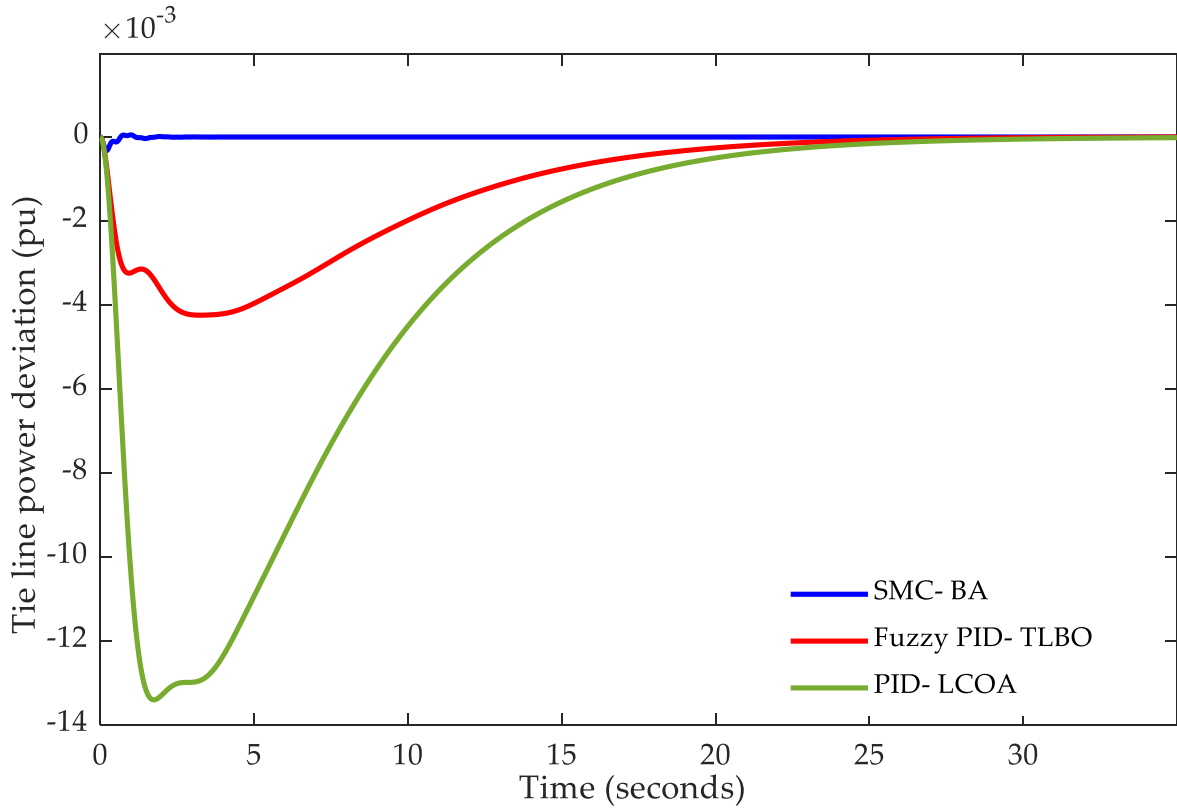


Figure 5.13. Tie line power deviation (ΔP_{tie} in pu).

Based on the characteristics provided in Table 5.13, the percentage of improvement in U_{sh} , T_s , and ITAE for the SMC proposed in this research and Fuzzy PID controllers [22] in comparison with the LCOA-based PID controller [21] is shown in Figure 5.14. From Figure 5.14, it is observed that with BA-optimized SMC, undershoot and settling time in the frequency deviation of area one (ΔF_1) are improved by 82.60% and 80.3055%, respectively. While in (ΔF_2), the undershoot and settling time in frequency deviation are improved by 97.59% and 88.606%, respectively, and in (ΔP_{tie}) they are improved by 97.76% and 91.01%, respectively. Based on the results shown in Figures 5.11–5.13 and Table 5.13, it is confirmed that the proposed SMC design offers the fastest response with the minimum undershoot, which in turn guarantees the best stability.

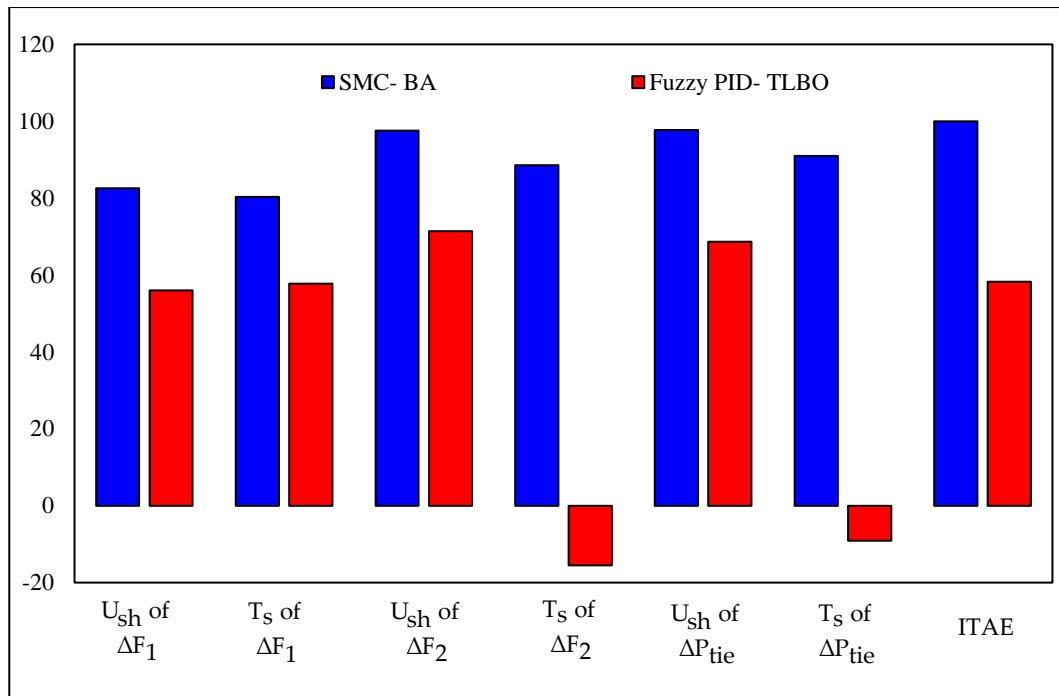


Figure 5.14. Percentage of improvement in undershoot, settling time and ITAE with different controllers

5.4.3.1 Robustness Investigation of SMC

An analysis of the parametric uncertainties in the two-area power system and its impact on the system stability is performed in this section by considering different scenarios. The testbed system has many parameters that may alter during the operating time, alternations in any parameter by increasing or decreasing will influence the overall system stability. For instance, increasing the value of the governor time constant T_g leads to an increase in the frequency fluctuation. While decreasing the damping ratio (D) could increase the frequency deviation which may result in a risk of system instability.

To verify the robustness of the proposed SMC optimised by BA employed in the two-area power model as an LFC system, several scenarios pertaining to the parametric uncertainties of the investigated system are considered as depicted in Table 5.14. Initially, each parameter of the testbed system has been varied individually. Subsequently, several parameters are simultaneously varied by (+ or -) 40% from their nominal values. A step load perturbation of 0.2 pu is applied in area one to observe the impact of the system parametric uncertainties on the performance of the SMC-LFC controller. Similar robustness investigation is carried out for the Fuzzy PID controller optimised by TLBO and the classical PID controller-based LCOA.

In cases 1 to 6 in Table 5.14, only one parameter is varied at a time. However, in order to make this investigation more realistic, more than one parameter is simultaneously varied from their nominal values. In case 7, the parameters T_g and D in areas one and two are varied by +40% and -40%, respectively. In case 8, the parameters T_t and B in both areas are varied by +40% and -40%, respectively. Furthermore, in case 9, T_g , T_t , and B are varied by +40%, -40% and -40%, respectively. Finally, in case 10, four parameters of the two-area power system are varied from their nominal values, namely, B , H , R and D . These different scenarios could represent the most common conditions of parametric uncertainties that the testbed system may experience in real-time operation.

The frequency variation in area one, frequency variation in area two and tie-line power variation following the implementation of the disturbance in area one under different scenarios of system parametric variations are shown in Figures 5.15 – 5.25. In Figures 5.15 – 5.25, subfigures (A) illustrate the frequency deviation in area one, subfigures (B) illustrate the frequency deviation in area two and subfigures (C) illustrate the tie line power deviation. Moreover, the dynamic response of the system represented by undershoot (U_{sh} in Hz), overshoot (O_{sh} in Hz) and settling time (T_s in s) in ΔF_1 , and ΔF_2 are presented in Table 1 (see Appendix C). Additionally, this table provides the undershoot (U_{sh} in pu), overshoot (O_{sh} in pu) and settling time (T_s in s) of ΔP_{tie} .

Table 5.14. Different investigated scenarios of system parametric uncertainties.

Case Number	Parameter s	Nominal Values		Variation Range	New Values	
		Area 1	Area 2		Area 1	Area 2
Case 1	H	5	4	+40%	7	5.6
Case 2	T_t	0.5	0.6	+40%	0.70	0.84
Case 3	B	20.6	16.9	-40%	12.36	10.14
Case 4	D	0.6	0.9	-40%	0.36	0.66
Case 5	T_g	0.2	0.3	+40%	0.28	0.42
Case 6	R	0.05	0.0625	+40%	0.07	0.0875
Case 7	T_g	0.2	0.3	+40%	0.28	0.42
	D	0.6	0.9	-40%	0.36	0.66
Case 8	T_t	0.5	0.6	+40%	0.70	0.84
	B	20.6	16.9	-40%	12.36	10.14
Case 9	T_g	0.2	0.3	+40%	0.28	0.42
	T_t	0.5	0.6	-40%	0.30	0.36
	B	20.6	16.9	-40%	12.36	10.14
Case 10	B	20.6	16.9	-40%	12.36	10.14
	H	5	4	+40%	7	5.6
	R	0.05	0.0625	-40%	0.03	0.0375
	D	0.6	0.9	-40%	0.36	0.66

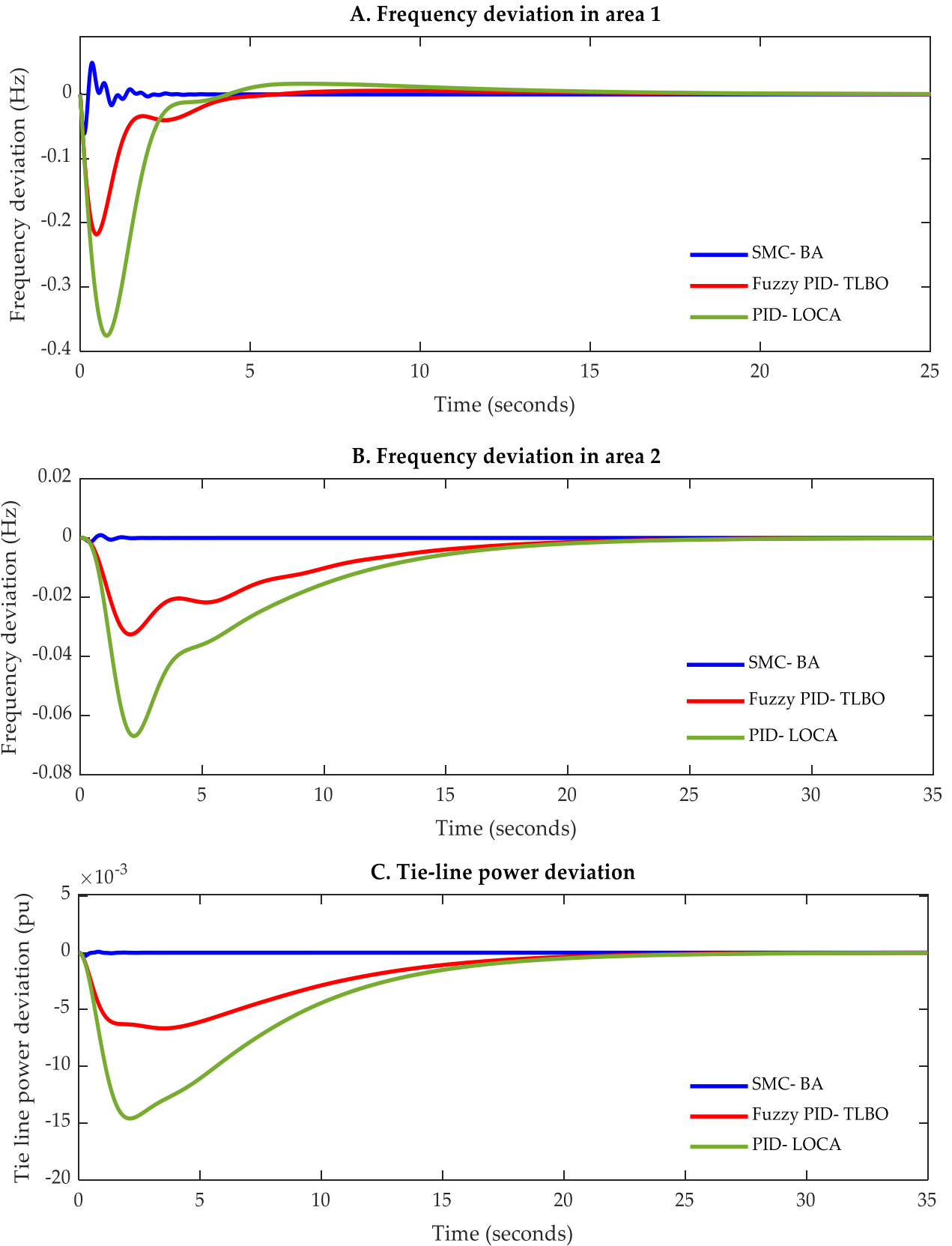


Figure 5.15. Dynamic response of the system with different controllers under parametric uncertainties, case 1. (A) Frequency deviation in area 1; (B) Frequency deviation in area 2; (C) Tie line power deviation.

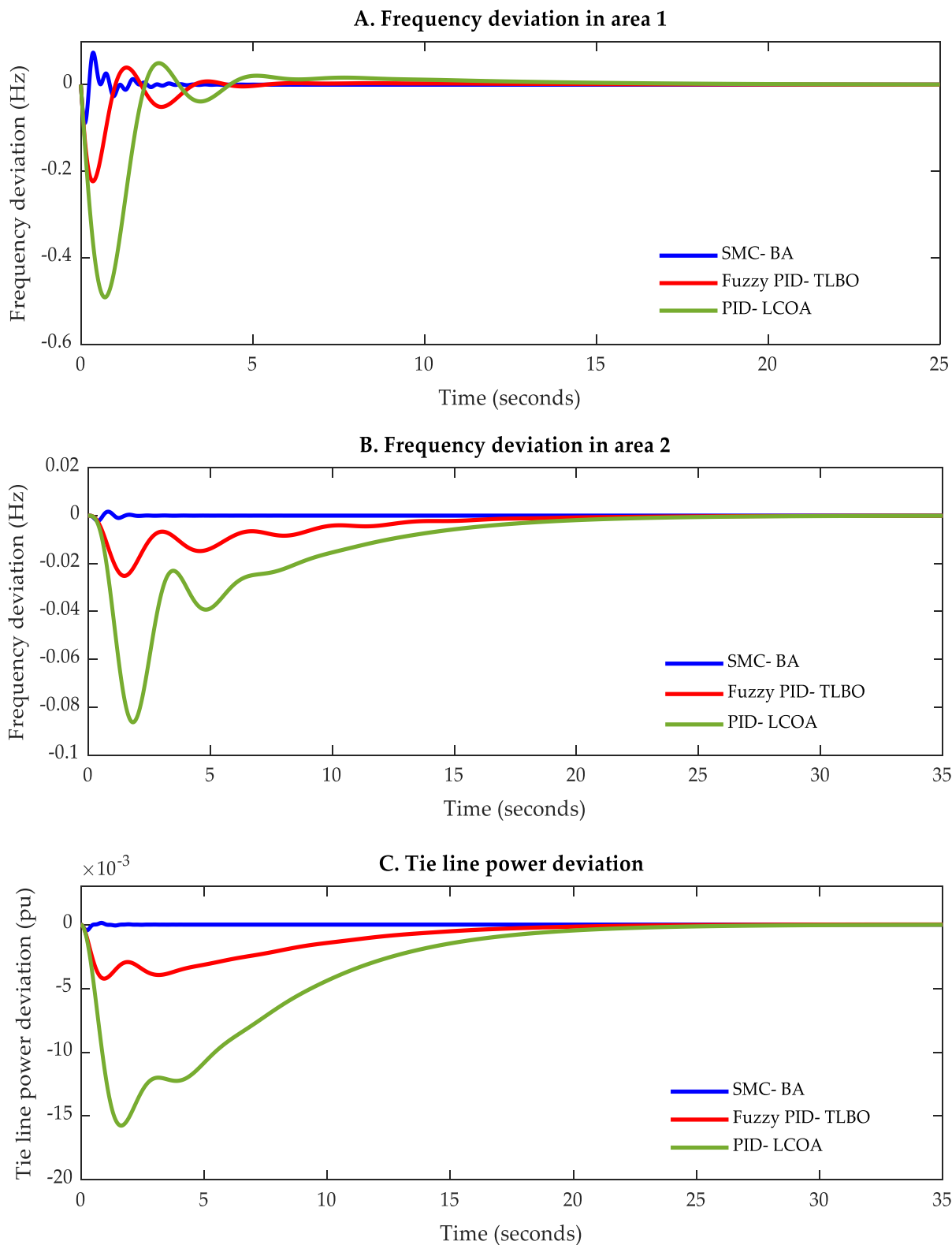


Figure 5.16. Dynamic response of the system with different controllers under parametric uncertainties, case 2. (A) Frequency deviation in area 1; (B) Frequency deviation in area 2; (C) Tie line power deviation.

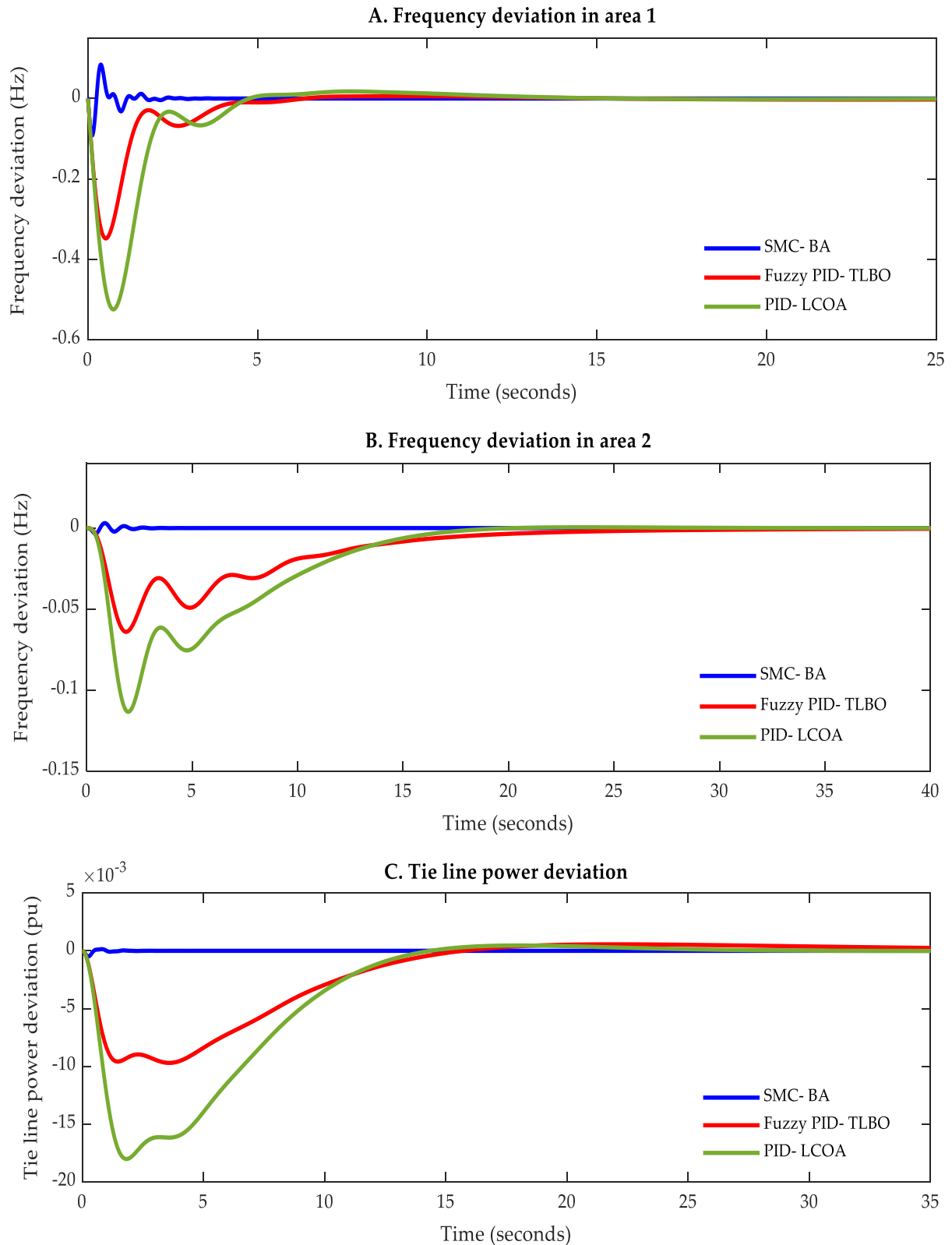


Figure 5.17. Dynamic response of the system with different controllers under parametric uncertainties, case 3. (A) Frequency deviation in area 1; (B) Frequency deviation in area 2; (C) Tie line power deviation.

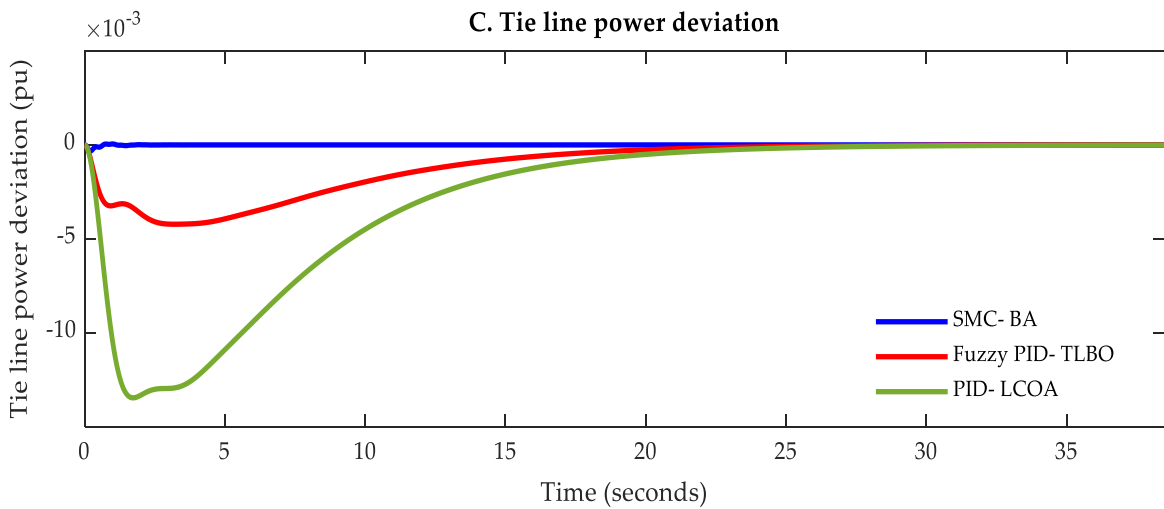
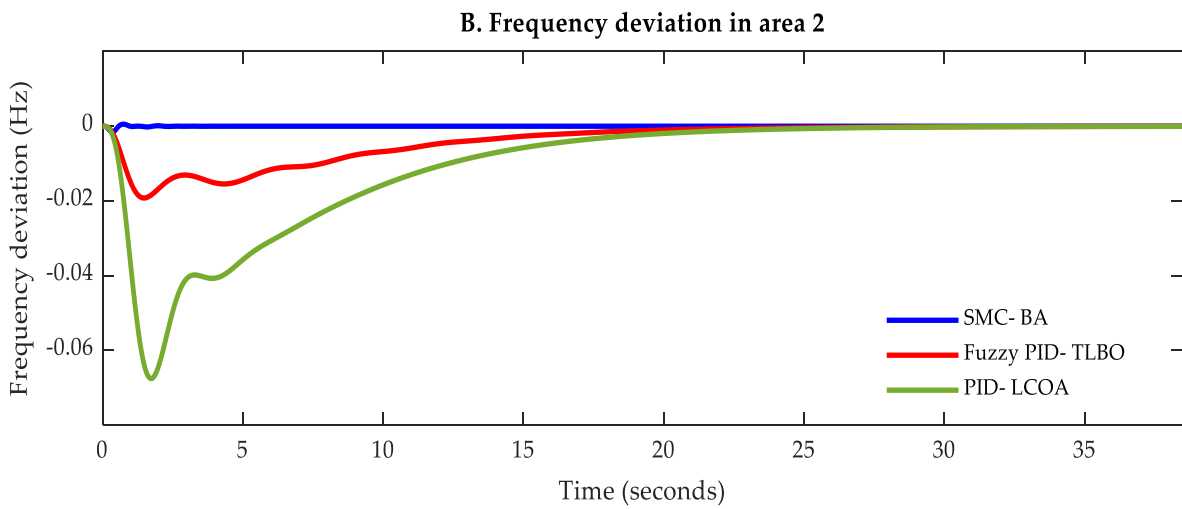
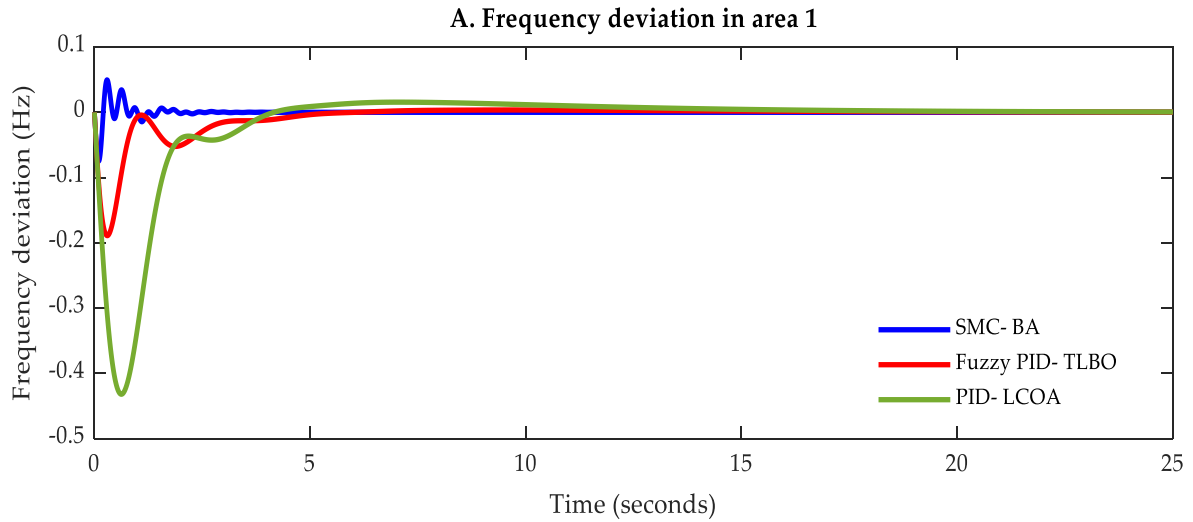


Figure 5.18. Dynamic response of the system with different controllers under parametric uncertainties, case 4. (A) Frequency deviation in area 1; (B) Frequency deviation in area 2; (C) Tie line power deviation.

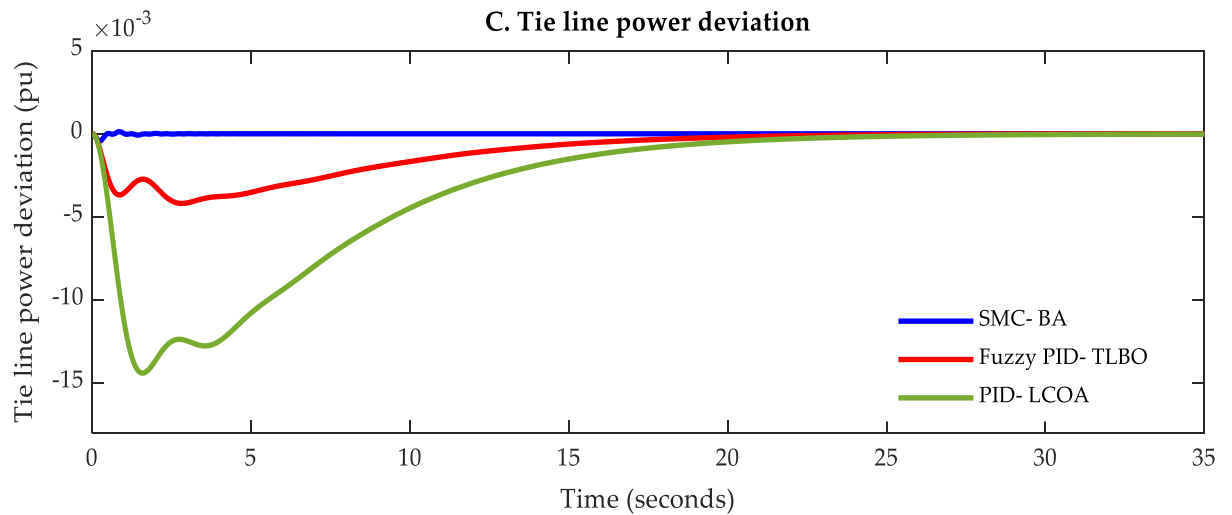
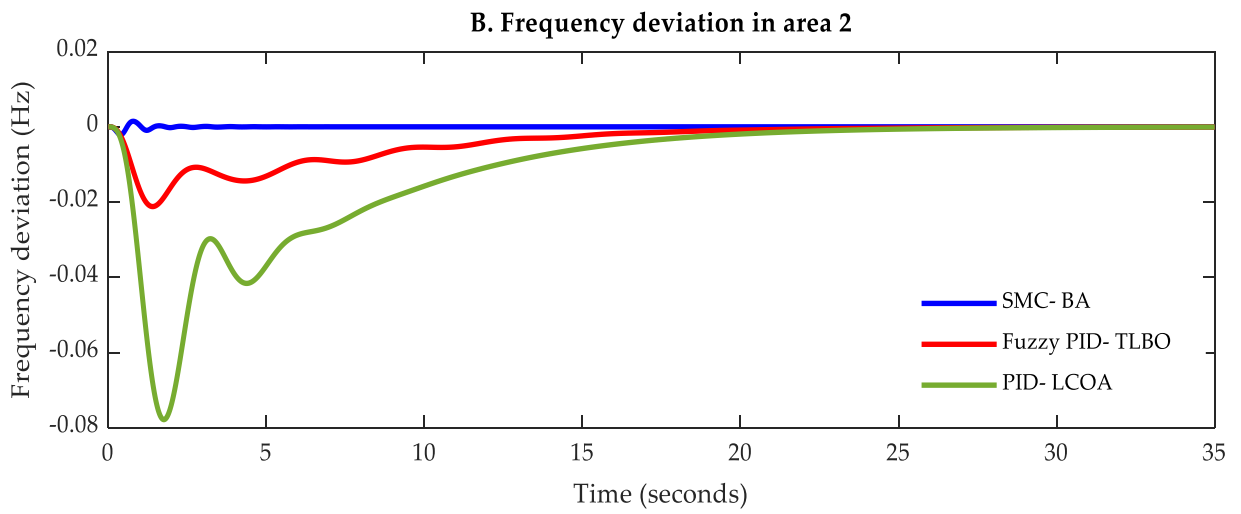
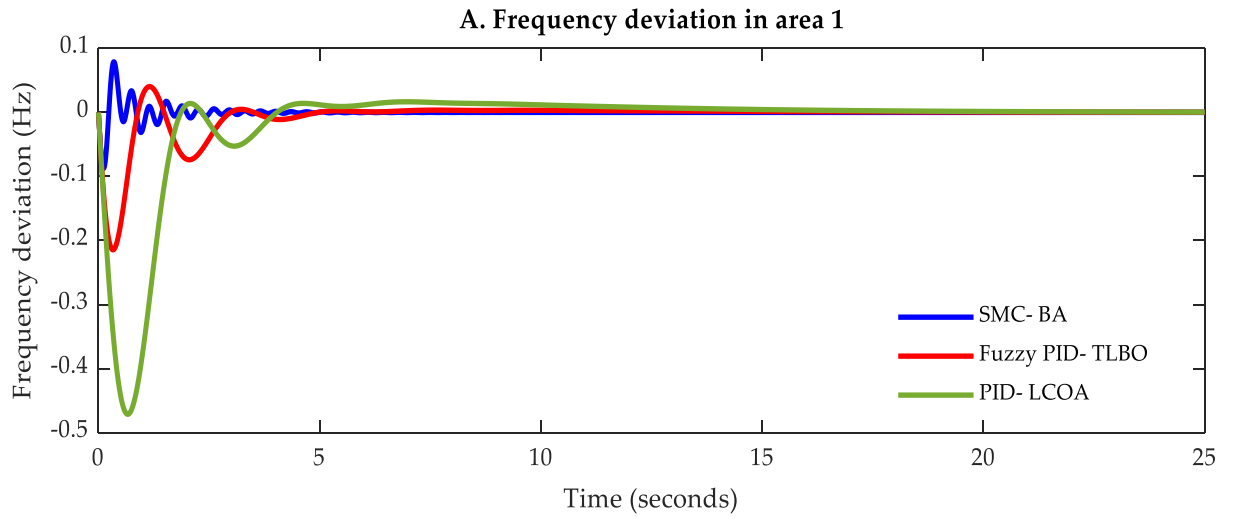


Figure 5.19. Dynamic response of the system with different controllers under parametric uncertainties, case 5. (A) Frequency deviation in area 1; (B) Frequency deviation in area 2; (C) Tie line power deviation.

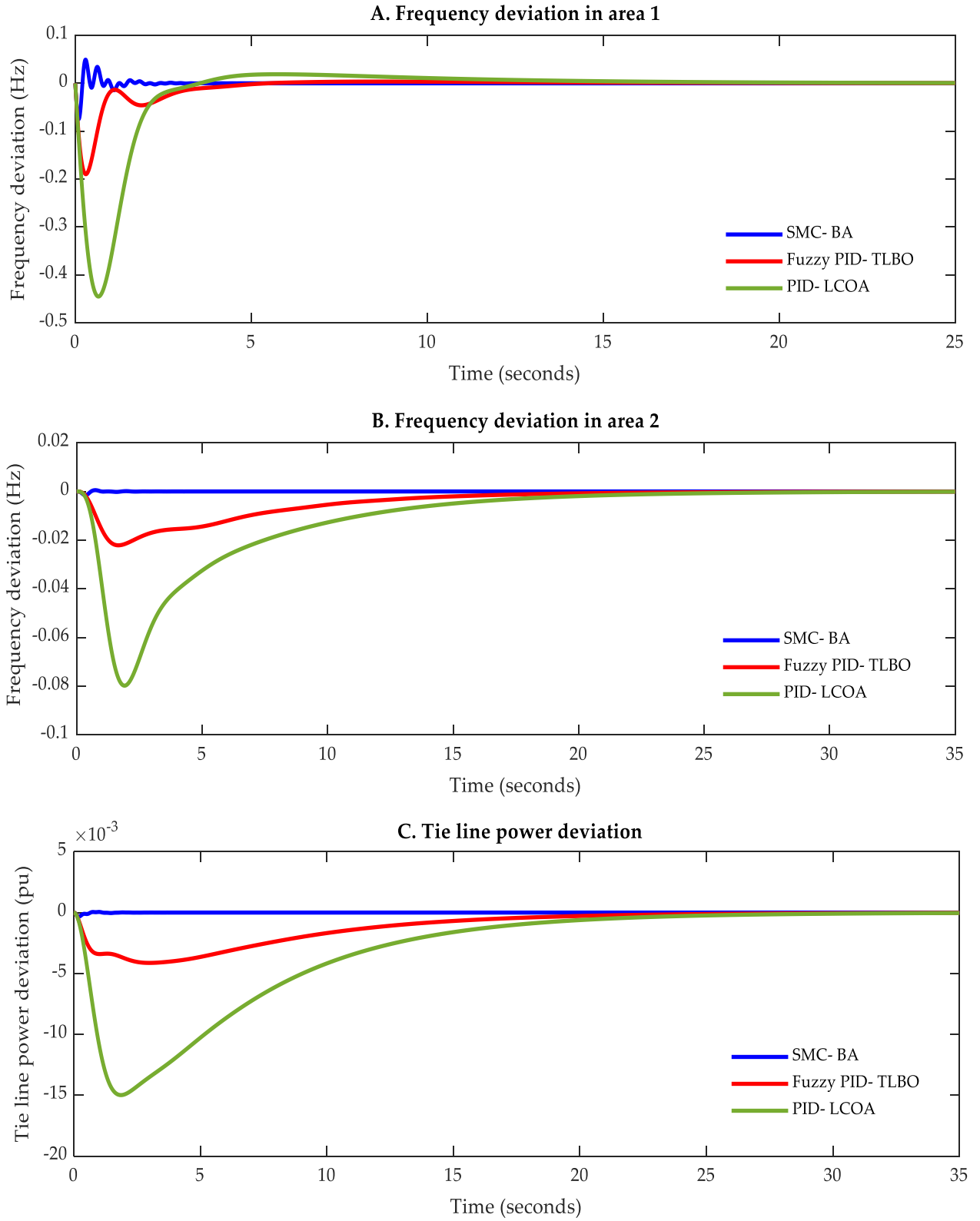


Figure 5.20. Dynamic response of the system with different controllers under parametric uncertainties, case 6. (A) Frequency deviation in area 1; (B) Frequency deviation in area 2; (C) Tie line power deviation.

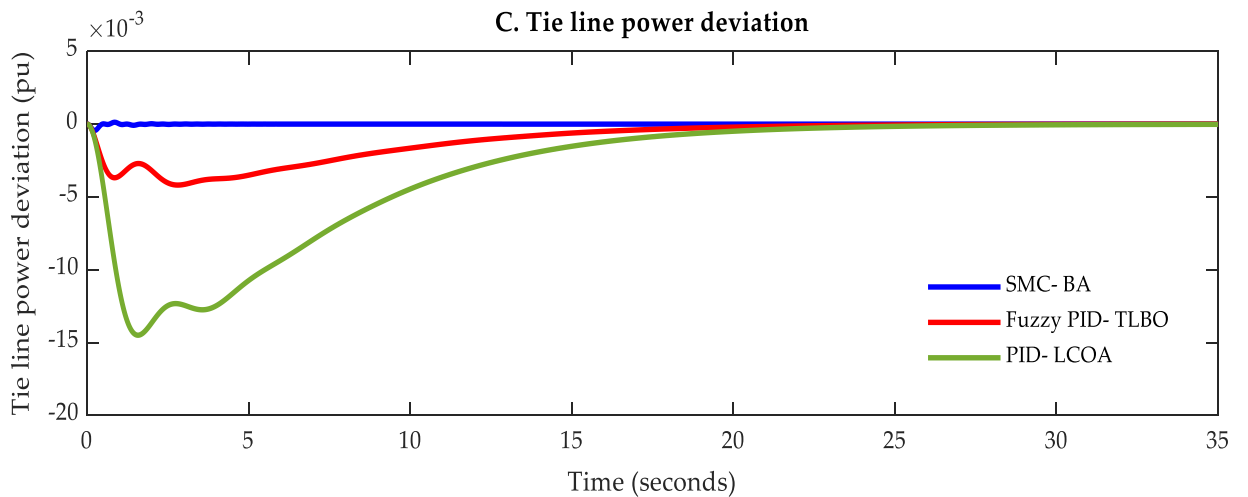
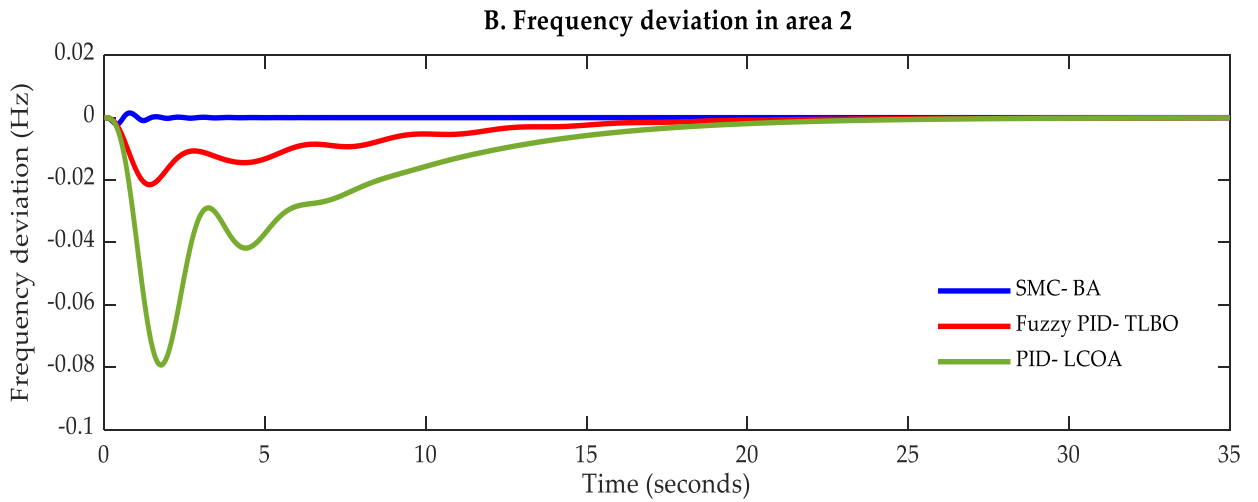
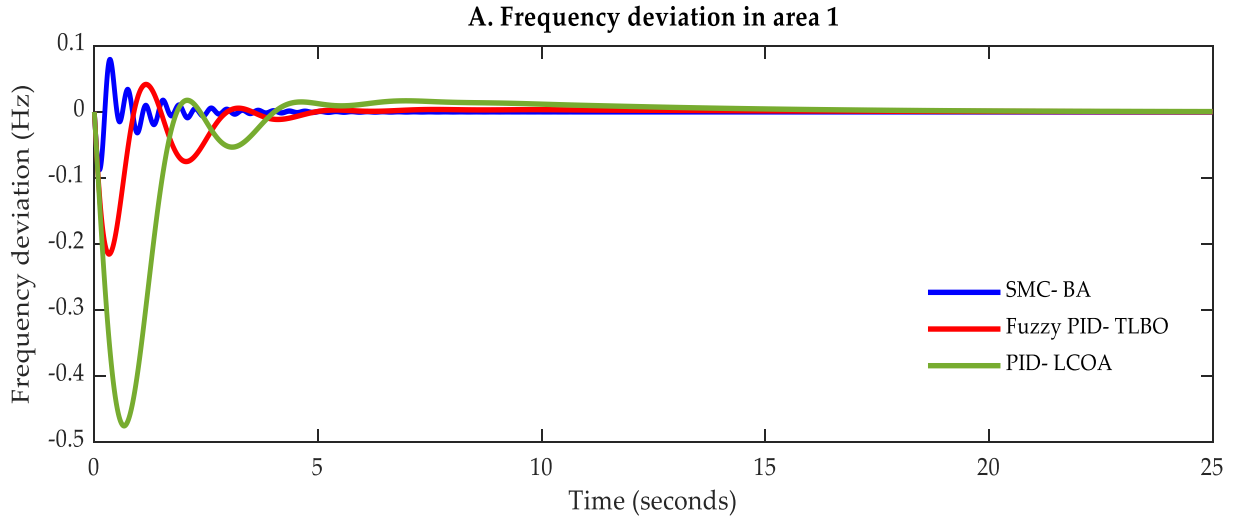


Figure 5.21. Dynamic response of the system with different controllers under parametric uncertainties, case 7. (A) Frequency deviation in area 1; (B) Frequency deviation in area 2; (C) Tie line power deviation.

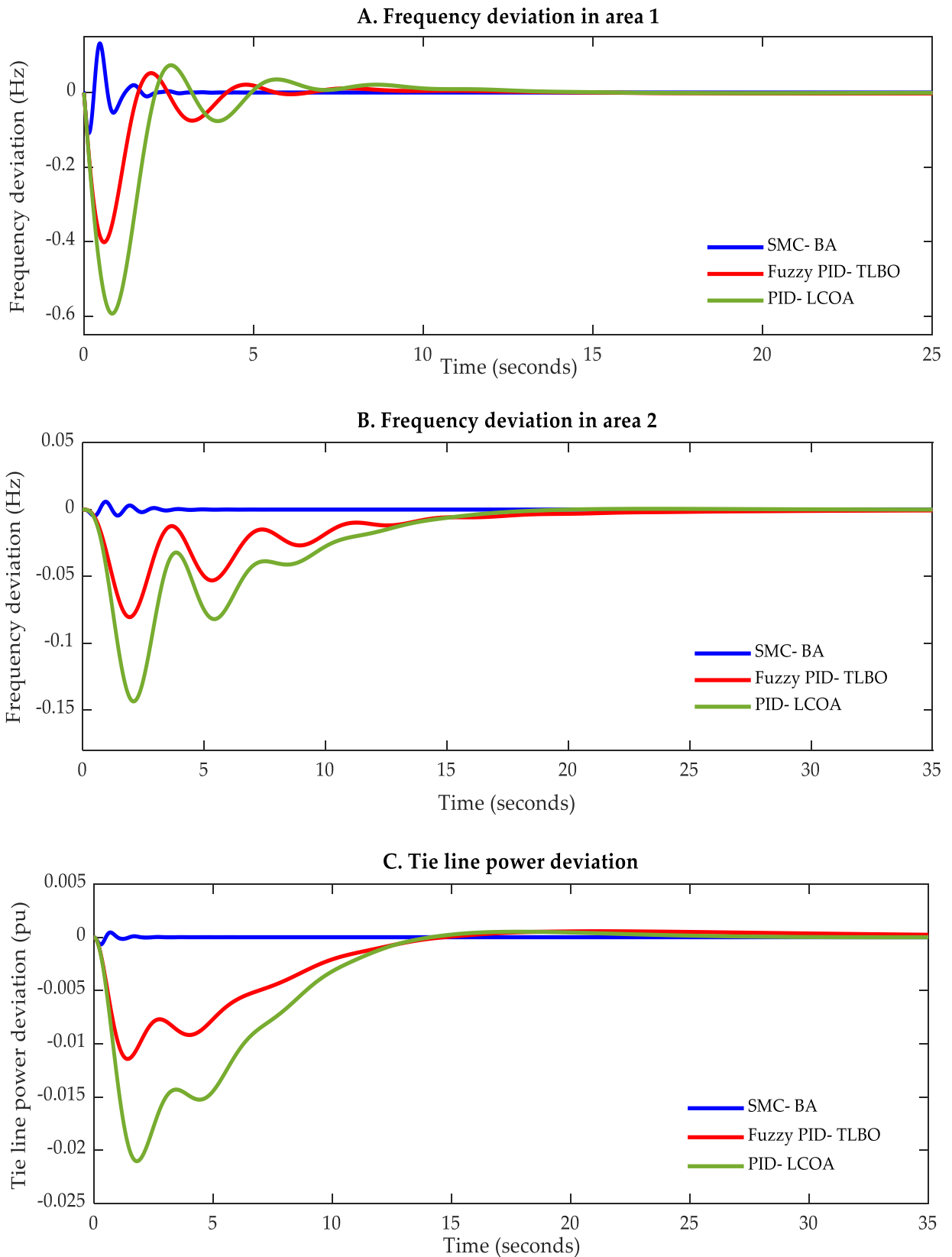


Figure 5.22. Dynamic response of the system with different controllers under parametric uncertainties, case 8. (A) Frequency deviation in area 1; (B) Frequency deviation in area 2; (C) Tie line power deviation.

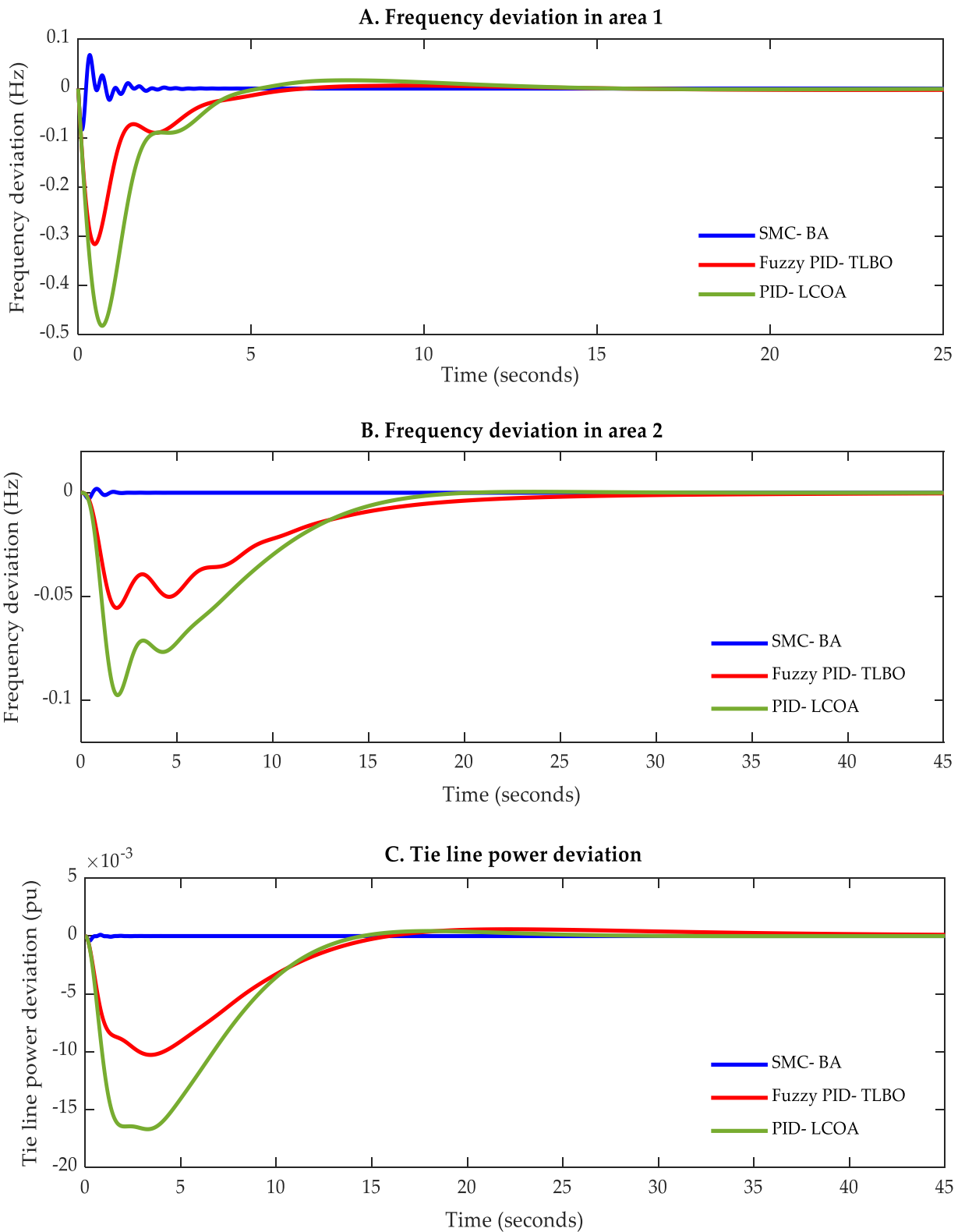


Figure 5.23. Dynamic response of the system with different controllers under parametric uncertainties, case 9. (A) Frequency deviation in area 1; (B) Frequency deviation in area 2; (C) Tie line power deviation.

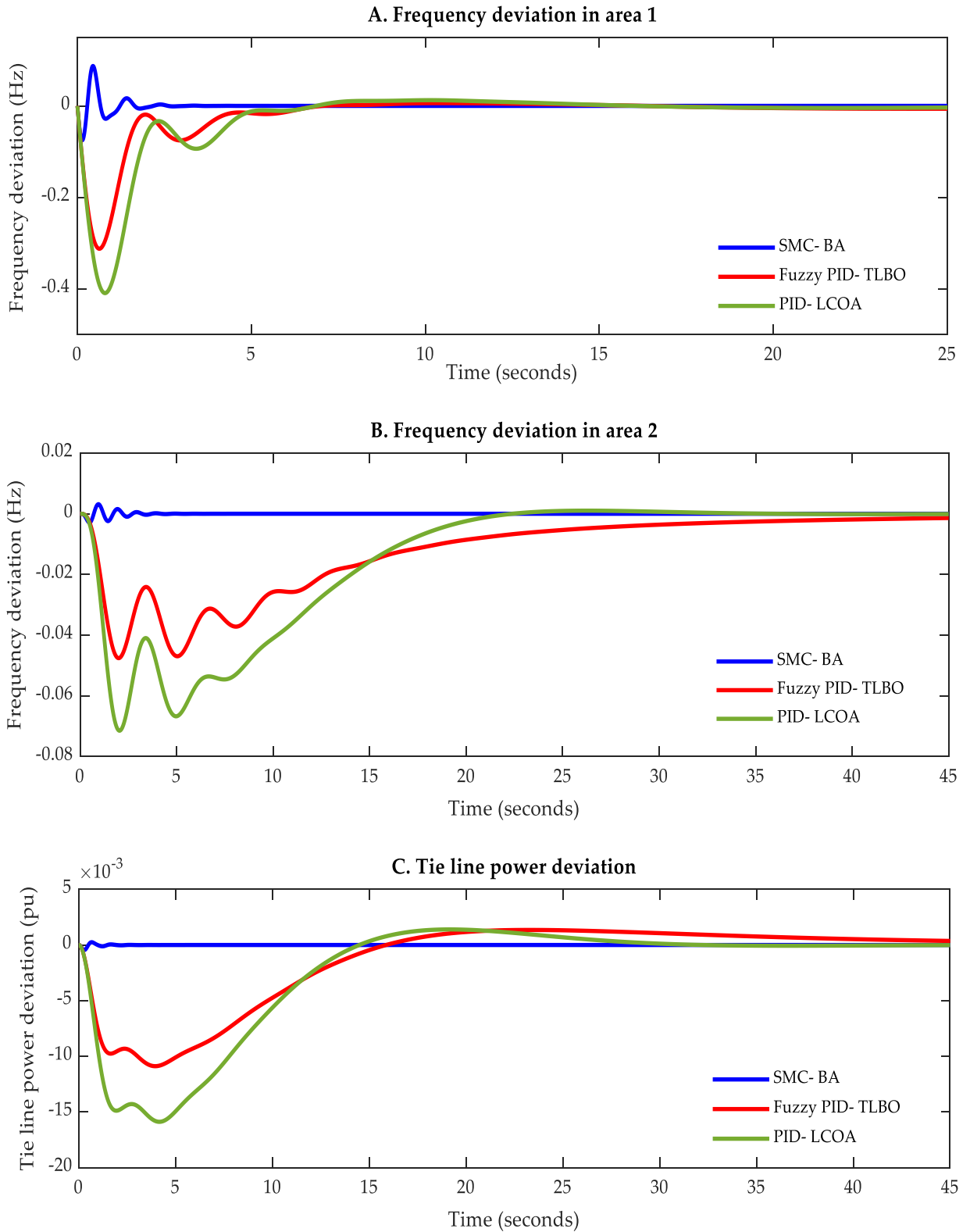


Figure 5.24. Dynamic response of the system with different controllers under parametric uncertainties, case 10. (A) Frequency deviation in area 1; (B) Frequency deviation in area 2; (C) Tie line power deviation.

Figure 5.15 shows the dynamic performance of the system based on SMC, Fuzzy PID, and the classical PID under parametric uncertainty case 1, where only the system inertia time constants in both areas are varied by 40% from their nominal values. It is observed that the proposed SMC provided the best performance in terms of undershoot and settling time in the frequency deviation in areas one and two as well as in the tie-line power deviation. Figure 5.16 indicates the response under parametric uncertainty case 2. In this case, the turbine time constants in both areas are altered by 40%. It is noticed that the increase in the turbine time constant worsened the dynamic response, it caused a further drop in the frequency in both areas. The dynamic response of the system with different controllers under parametric uncertainty case 3 is illustrated in Figure 5.17. In this case, the nominal values of the frequency bias constants in both areas are varied by -40% . As a result of this variation and based on the results obtained from the SMC tuned by BA, the drop in the frequency in areas one and two have increased from -0.0746 Hz and -0.0016 Hz to -0.0918 Hz and -0.0035 Hz, respectively. In case 4 of robustness analysis towards parametric uncertainty of the testbed system, the value of the coefficient D in both areas are varied by -40% . An extremely slight change in the dynamic performance of the system is observed as shown in Figure 5.18. However, based on the results obtained for case 5, where the governor time constants in both areas are increased by 40% from their nominal values, a slight increase in the drop in the frequency in both areas is observed as illustrated in Figure 5.19. In case 6 from the robustness investigation, no obvious change in the dynamic response is observed as shown in Figure 5.20.

In case 7, the values of T_g and D in both areas are varied by 40% and -40% , respectively. Although two parameters in areas one and two are varied, the proposed SMC-based BA still offering good performance and outperforms the other two controllers as demonstrated in Figure 5.21. The worst undershoot in the frequency in both areas as well as in the tie-line power deviation is recorded based on the results obtained from case 8 as shown in Figure 5.22, where the drop of the frequency in area one has increased from -0.0746 Hz to -0.1087 Hz, from -0.1885 Hz to -0.4015 Hz, and from -0.4288 Hz to -0.5931 Hz based on SMC, Fuzzy PID, and classical PID, respectively. Additionally, the drop of the frequency in area two has increased from -0.0016 Hz to -0.0047 Hz, from -0.0190 Hz to -0.0805 Hz, and from -0.0664 Hz to -0.1435 Hz based on SMC, Fuzzy PID, and classical PID, respectively. Whilst the undershoot in the tie-line power has increased from -0.0003 pu to 0.00067 pu, from -0.0042 pu to -0.0114 pu, and from -0.0134 pu to -0.0210 pu based on SMC, Fuzzy PID, and classical PID, respectively. The dynamic response of the system under parametric uncertainty case 9 is

demonstrated in Figure 5.23. In this case of robustness analysis, three different parameters are simultaneously varied. Namely, T_g and B in areas one and two are varied by -40% while the governor time constants T_g are altered by 40% . The notable observed change in the dynamic performance of the system is the slight increase in the drop in the frequency in both areas. Finally, in case 10, four different parameters are varied, the dynamic response of the testbed system under parametric uncertainty case 10 based on SMC, Fuzzy PID and the traditional PID is given in Figure 5.24.

From Figures 5.15 – 5.24, in spite of the wide range of parametric uncertainties of the testbed system in the ten investigated scenarios, the implementation of the proposed SMC design tuned by BA has provided a robust performance which has maintained the system stability within acceptable limits. Furthermore, this controller has outperformed the Fuzzy PID and the traditional PID in terms of the peak undershoot and settling time regardless of the negligible increase in the overshoot noted in certain cases.

Moreover, to further assess the performance of the SMC controller, a random load disturbance is applied in area one under the parametric uncertainties of the system case 10 as shown in Figure 5.25. A. The frequency deviation in area one is shown in Figure 5.25. B, the frequency deviation in area two is shown in Figure 5.25. C and Figure 5.25. D shows the tie line power deviation.

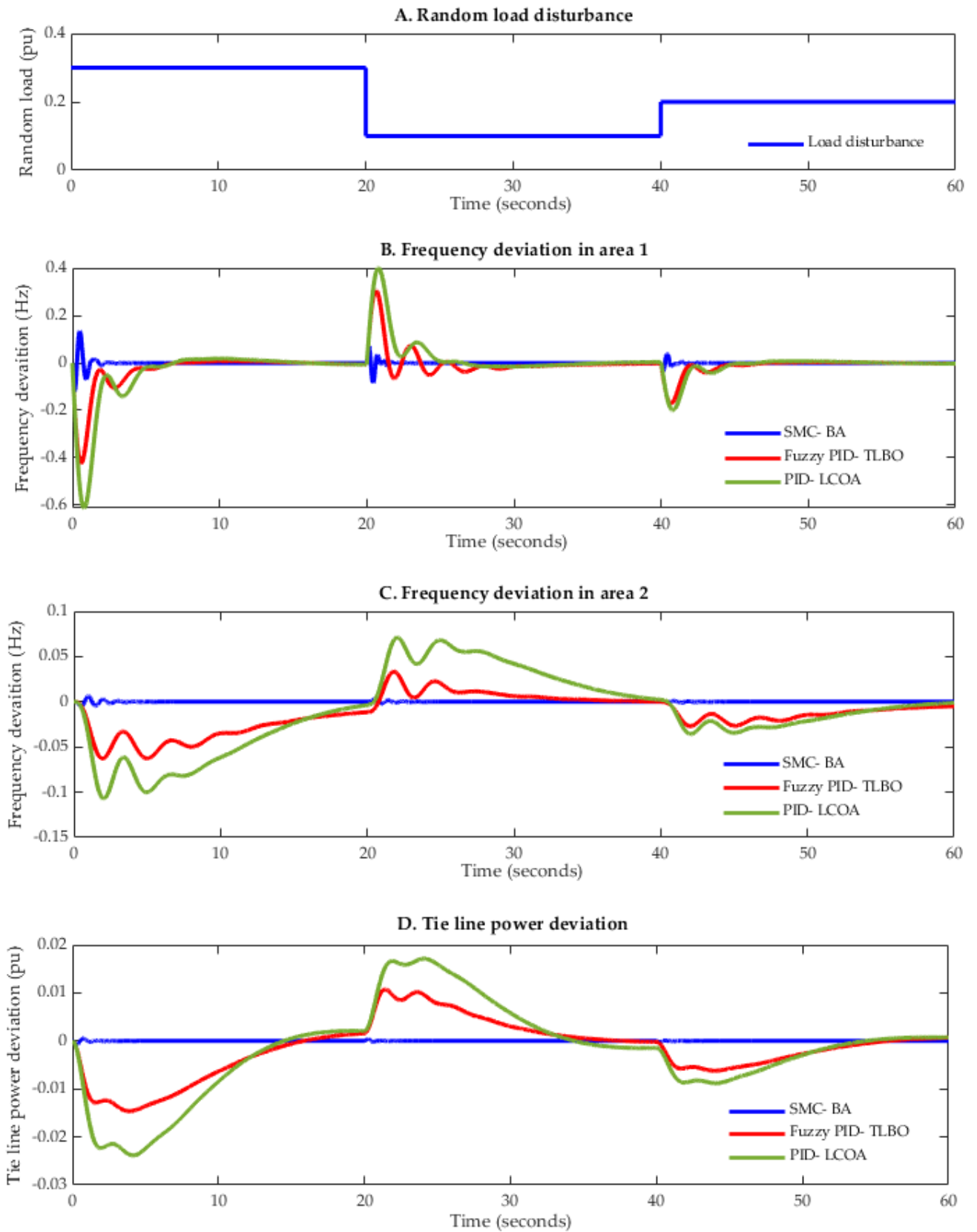


Figure 5.25. Dynamic response of the system with different controllers under parametric uncertainties, case 10 with a random load disturbance applied in area one. (A) Random load disturbance; (B) Frequency deviation in area 1; (C) Frequency deviation in area 2; (D) Tie line power deviation.

From Figure 5.25, it is understandable that the proposed SMC-BA controller continues to offer the best dynamic response for frequency variation in area one, frequency variation in area two and tie-line power deviation even with the presence of load disturbance changes every twenty seconds. Additionally, this controller has guaranteed the fastest response with the best-damped oscillation in comparison with Fuzzy PID controller-based TLBO and PID controller tuned by LCOA.

It is observed that the SMC design proposed for LFC in the two-area power system has outperformed the other two controllers. The logical reason for the good performance of the proposed SMC over the other techniques is as it is perceived as a robust control tool for complex systems under the effect of parametric uncertainties and external perturbations. SMC design approaches to the key issues like compensation of the effect of unstructured dynamics and adaptability in the uncertain system. Therefore, in general, the wide use of SMC as a control system for various applications is due to the better performance for nonlinear systems, suitability to multiple input multiple output systems and also it acknowledges that it is applicable to discrete-time systems with appropriate design. However, it is worth mentioning the importance of improving the performance of the proposed SMC design in terms of the resulted overshoot in most cases.

5.5 Summary

Sliding Mode Control (SMC) was designed and implemented in two different power systems. Firstly, a fourth order modelling of an SMC system is investigated for the simplified Great Britain power system. Then, the suggested BA was utilised to optimise the parameters of the SMC. A comparison between BA based SMC and other techniques was conducted. Also, the robustness of the proposed controllers towards parametric uncertainties of the GB power system was also carried out. Simulation results evidenced that the proposed BA based SMC implemented in the testbed system is robust and successfully solved the problem of frequency variation under different operation conditions.

Similarly, BA based SMC was used as an LFC system in two area interconnected power system. In this part, the mathematical model design of the controller is derived based on the parameters of the investigated two area power system. Simulation results prove the superiority and the robustness of the proposed SMC as an LFC system.

5.6 References:

- [1] S. J. Gambhire, D. R. Kishore, P. S. Londhe, and S. N. Pawar, "Review of sliding mode based

- control techniques for control system applications,” *Int. J. Dyn. Control*, vol. 9, no. 1, pp. 363–378, Mar. 2021, doi: 10.1007/s40435-020-00638-7.
- [2] C.-I. Huang, K.-Y. Lian, C.-S. Chiu, and L.-C. Fu, “Smooth sliding mode control for constrained manipulator with joint flexibility,” *IFAC Proc. Vol.*, vol. 38, no. 1, pp. 91–96, 2005, doi: 10.3182/20050703-6-CZ-1902.01285.
- [3] Y. Wang and L. Sun, “On the Optimized Continuous Nonsingular Terminal Sliding Mode Control of Flexible Manipulators,” in *2014 Fourth International Conference on Instrumentation and Measurement, Computer, Communication and Control*, Sep. 2014, pp. 324–329, doi: 10.1109/IMCCC.2014.74.
- [4] H.-Y. Chen and S.-J. Huang, “Adaptive fuzzy sliding-mode control for the Ti6Al4V laser alloying process,” *Int. J. Adv. Manuf. Technol.*, vol. 24, no. 9–10, pp. 667–674, Nov. 2004, doi: 10.1007/s00170-003-1742-7.
- [5] B. M. Patre, P. S. Londhe, and R. M. Nagarale, “Fuzzy Sliding Mode Control for Spatial Control of Large Nuclear Reactor,” *IEEE Trans. Nucl. Sci.*, vol. 62, no. 5, pp. 2255–2265, Oct. 2015, doi: 10.1109/TNS.2015.2464677.
- [6] R. R. Nair and L. Behera, “Robust adaptive gain nonsingular fast terminal sliding mode control for spacecraft formation flying,” in *2015 54th IEEE Conference on Decision and Control (CDC)*, Dec. 2015, pp. 5314–5319, doi: 10.1109/CDC.2015.7403051.
- [7] S. S.-D. Xu, C.-C. Chen, and Z.-L. Wu, “Study of Nonsingular Fast Terminal Sliding-Mode Fault-Tolerant Control,” *IEEE Trans. Ind. Electron.*, pp. 1–1, 2015, doi: 10.1109/TIE.2015.2399397.
- [8] G. D. Hemke and S. Daingade, “Fast Terminal Sliding Mode based DC-DC Buck converter,” in *2016 IEEE 1st International Conference on Power Electronics, Intelligent Control and Energy Systems (ICPEICES)*, Jul. 2016, pp. 1–4, doi: 10.1109/ICPEICES.2016.7853612.
- [9] M. Defoort, F. Nollet, T. Floquet, and W. Perruquetti, “A Third-Order Sliding-Mode Controller for a Stepper Motor,” *IEEE Trans. Ind. Electron.*, vol. 56, no. 9, pp. 3337–3346, Sep. 2009, doi: 10.1109/TIE.2009.2026378.
- [10] Y. Mi, Y. Fu, D. Li, C. Wang, P. C. Loh, and P. Wang, “The sliding mode load frequency control for hybrid power system based on disturbance observer,” *Int. J. Electr. Power Energy Syst.*, vol. 74, pp. 446–452, Jan. 2016, doi: 10.1016/j.ijepes.2015.07.014.

- [11] K. Vrdoljak, N. Perić, and I. Petrović, “Sliding mode based load-frequency control in power systems,” *Electr. Power Syst. Res.*, vol. 80, no. 5, pp. 514–527, May 2010, doi: 10.1016/j.epsr.2009.10.026.
- [12] A. Kumar, M. N. Anwar, and S. Kumar, “Sliding mode controller design for frequency regulation in an interconnected power system,” *Prot. Control Mod. Power Syst.*, vol. 6, no. 1, p. 6, Dec. 2021, doi: 10.1186/s41601-021-00183-1.
- [13] J. Guo, “Application of full order sliding mode control based on different areas power system with load frequency control,” *ISA Trans.*, vol. 92, pp. 23–34, Sep. 2019, doi: 10.1016/j.isatra.2019.01.036.
- [14] B. Mohanty, “TLBO optimized sliding mode controller for multi-area multi-source nonlinear interconnected AGC system,” *Int. J. Electr. Power Energy Syst.*, vol. 73, pp. 872–881, Dec. 2015, doi: 10.1016/j.ijepes.2015.06.013.
- [15] V. Van Huynh *et al.*, “New Second-Order Sliding Mode Control Design for Load Frequency Control of a Power System,” *Energies*, vol. 13, no. 24, p. 6509, Dec. 2020, doi: 10.3390/en13246509.
- [16] V. Van Huynh, B. L. N. Minh, E. N. Amaefule, A.-T. Tran, and P. T. Tran, “Highly Robust Observer Sliding Mode Based Frequency Control for Multi Area Power Systems with Renewable Power Plants,” *Electronics*, vol. 10, no. 3, p. 274, Jan. 2021, doi: 10.3390/electronics10030274.
- [17] A.-T. Tran *et al.*, “Load Frequency Regulator in Interconnected Power System Using Second-Order Sliding Mode Control Combined with State Estimator,” *Energies*, vol. 14, no. 4, p. 863, Feb. 2021, doi: 10.3390/en14040863.
- [18] Y. Mu, J. Wu, J. Ekanayake, N. Jenkins, and H. Jia, “Primary Frequency Response From Electric Vehicles in the Great Britain Power System,” *IEEE Trans. Smart Grid*, vol. 4, no. 2, pp. 1142–1150, Jun. 2013, doi: 10.1109/TSG.2012.2220867.
- [19] Z. A. Obaid, L. M. Cipcigan, and M. T. Muhssin, “Fuzzy hierarchal approach-based optimal frequency control in the Great Britain power system,” *Electr. Power Syst. Res.*, vol. 141, pp. 529–537, Dec. 2016, doi: 10.1016/j.epsr.2016.08.032.
- [20] M. Cheng *et al.*, “Power System Frequency Response From the Control of Bitumen Tanks,” *IEEE Trans. Power Syst.*, vol. 31, no. 3, pp. 1769–1778, May 2016, doi:

10.1109/TPWRS.2015.2440336.

- [21] S. Ganjefar, M. Alizadeh, and M. Farahani, “PID controller adjustment using chaotic optimisation algorithm for multi-area load frequency control,” *IET Control Theory Appl.*, vol. 6, no. 13, pp. 1984–1992, Sep. 2012, doi: 10.1049/iet-cta.2011.0405.
- [22] B. K. Sahu, S. Pati, P. K. Mohanty, and S. Panda, “Teaching–learning based optimization algorithm based fuzzy-PID controller for automatic generation control of multi-area power system,” *Appl. Soft Comput.*, vol. 27, pp. 240–249, Feb. 2015, doi: 10.1016/j.asoc.2014.11.027.

Chapter 6

Conclusions and Recommendations for Future Work

6.1. Conclusions

Several secondary frequency controls were designed based on different theories to maintain the frequency within its normal ranges in two different testbed systems. In order to achieve the best possible dynamic performance, the Bees Algorithm and other optimisation technique were utilised to find the optimum values of the proposed controller. The following points are concluded:

1. Fuzzy PIDF based LFC in the Simplified GB Power System:

It was evident from the results that the BA-tuned FOPID designed by minimizing ITAE offered the best performance among the investigated classical controllers. In terms of applying the proposed Fuzzy PIDF, an obvious improvement in the performance of the system was achieved, and the obtained results from this controller based on BA, TLBO and PSO were somewhat similar, with the lowest drop in frequency equal to -0.0028 Hz when BA was used. Furthermore, it was demonstrated that the Fuzzy PIDF tuned by BA is robust against system uncertainties and different load disturbances.

2. Fuzzy PIDF based LFC in the two-area power system:

Obtained results revealed that Fuzzy PIDF provides excellent dynamic performance as it gives the best objective function values, less undershoot for frequency and tie-line power in comparison with other controllers proposed in previous studies. For example, based on Fuzzy PIDF tuned by BA results as compared with results based on the classical PID tuned by LCOA reported in a previous study, the peak undershoot and settling time of the frequency deviation in area one have been improved by 90.345% and 40.698%, respectively, while the same characteristics of the frequency deviation in area two are improved by 94.277% and 8.403%, respectively. Furthermore, notwithstanding considering a wide range of variations in the power system parameters and implementing a random load disturbance, it is proven that the Fuzzy PIDF is robust and has successfully kept the system stable. It is also concluded that the BA, PSO, and TLBO have demonstrated to be effective techniques for soft computing (TLBO to a lesser extent as the LFC system with Fuzzy PIDF based TLBO is less robust against the system parametric uncertainties in comparison with Fuzzy PIDF tuned by BA and PSO).

3. Different Fuzzy Structures Based LFC in the Two-area Power System

Three further fuzzy configurations for LFC were proposed, namely, Fuzzy Cascade PI-PD (Fuzzy C PI-PD), Fuzzy PI plus Fuzzy PD (Fuzzy PI + Fuzzy PD) and Fuzzy (PI + PD). These configurations have shown several strengths in their performance. For example, in addition to offering a robust control action with a quick response, they guarantee a higher range of reliability as compared with other structures. The Bees Algorithm has been employed to find the optimum values of the scaling factor gains of the suggested configurations. An extensive examination of the impact of parametric uncertainties of the testbed system on the performance of the proposed fuzzy control structures has been conducted considering different scenarios that the system may experience in real-time operation. The obtained results based on these three structures have shown that the lowest drop of the frequency in area one following 0.2 pu load disturbance is -0.0431 Hz which is achieved by the proposed Fuzzy PI + Fuzzy PD, while the lowest drop of frequency in area two is -0.00099 Hz which is obtained by employing Fuzzy C PI-PD. Simulation results revealed that the proposed fuzzy controllers have shown a high level of robustness towards parametric uncertainties of the two-area power system (Fuzzy (PI + PD) to a less extent).

4. SMC Based LFC in the Simplified GB Power System

A design of a Sliding Mode Controller (SMC) is proposed for a fourth-order system and implemented for LFC in the simplified GB power system. The BA and PSO algorithms have been used to obtain the optimal values of the SMC controller parameters. Considering ITAE as an objective function, a step load perturbation of 0.0395 pu is applied to study the dynamic response of the testbed system. The robustness of the proposed SMC design has been verified towards a wide range of parametric uncertainties and different load disturbances. The results obtained from SMC tuned by BA and PSO are compared with that based on BA optimized PID controller and it has been revealed that SMC tuned by BA provides superior dynamic performance. Finally, the proposed SMC design tuned by BA has proved its robustness and stability against a wide variation of the GB power system parameters.

5. SMC Based LFC in the Two-area Power System

Simulation results demonstrated that the SMC tuned by BA performs better than the other reported methods; the peak under-shoot and settling time of the frequency deviation in area one has been improved by 82.60% and 80.3055%, respectively, while the same characteristics of the frequency deviation in area two are improved by 97.59% and 88.606%,

respectively, as compared with results based on the classical PID tuned by LCOA. Furthermore, the robustness examination of the proposed controller tuned by BA towards a wide range of parametric uncertainties of the investigated system was also performed by considering ten different scenarios. Based on the results obtained from this research, it is revealed that the performance of the proposed SMC design used as LFC in the two-area power system is robust and superior; it provides satisfactory performance in different aspects such as undershoot and settling time regardless of the slight and negligible increase in the overshoot noticed in particular cases.

The only possible limitation of the proposed SMC design is the probability of complexity linked with the mathematical modelling of the controller if the controlled system comprises multi-sources.

6.2. Recommendations for Future Work

This research may be further extended in future work in the following directions:

1. To assess the validity of the proposed controllers as LFC in power systems that comprise Renewable Energy Resources (RESs) Energy Storage Systems (ESSs). Also, to test the impact of time delay and some nonlinear elements within the system such as Governor Dead Band (GDB) and Generation Rate Constraint (GRC) on the performance of the suggested controllers. Furthermore, considering the AVR loop in the LFC model to complete the LFC aim and considering the cross-coupling of LFC with AVR.
2. It is worth testing other versions of the Bees Algorithm in tuning the proposed controllers and evaluating the possible improvement in the dynamic performance of these controllers. Also, using other recent optimization techniques to optimize the proposed controllers is another way to further enhance the performance of these LFC systems.
3. Further investigation in the design of the fuzzy controllers in which the membership functions are also optimized by an optimization technique, this will improve the overall performance of fuzzy logic controllers.
4. Considering the Fractional Order PID controller as a hybrid controller with the fuzzy controller is a topic that needs further investigation in the sake of improving the performance of the proposed fuzzy configurations.
5. Due to the quick response offered by the proposed SMC, further investigations might be conducted to test the stability of the system under different operation conditions as it is known that a very quick response has a risk of system oscillations.

6. Demand Side Frequency Response (DSFR) is another effective way which can be further investigated to control the frequency within the power system. Therefore, studying more in this topic and providing new solutions is a good pathway in frequency control.

Appendixes

Appendix A

Electrical vehicle's gain effect.

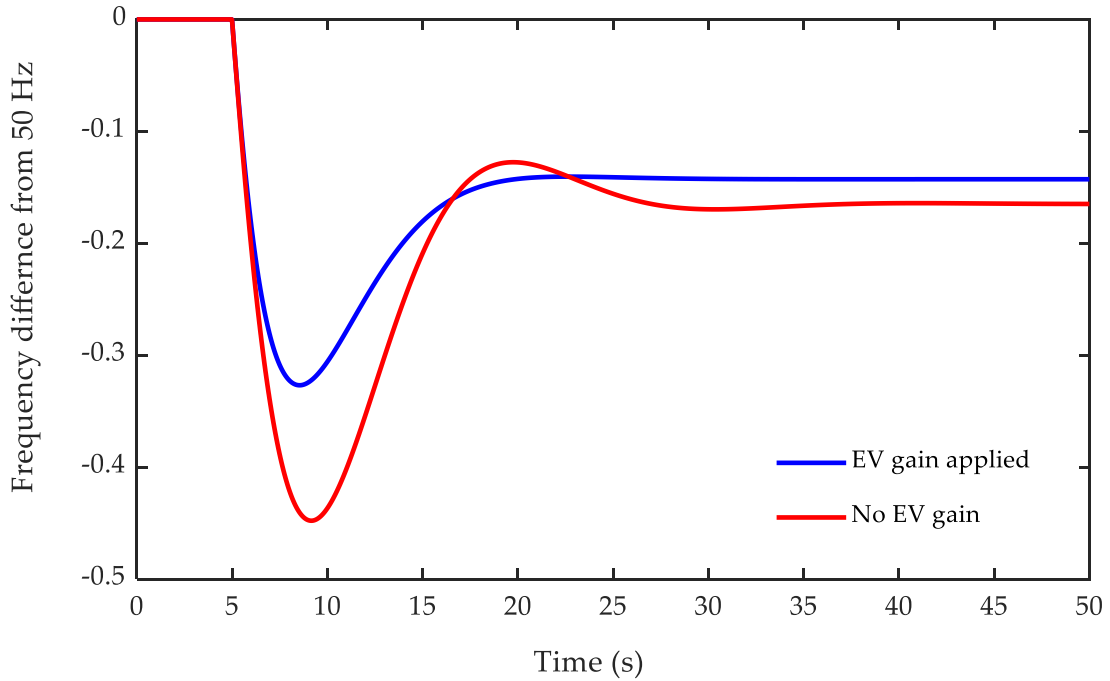


Figure A1.1 The primary frequency response of GB power system with and without the feedback gain of electrical vehicles.

Appendix B

The effect of parametric uncertainties on the frequency response of the GB power system.

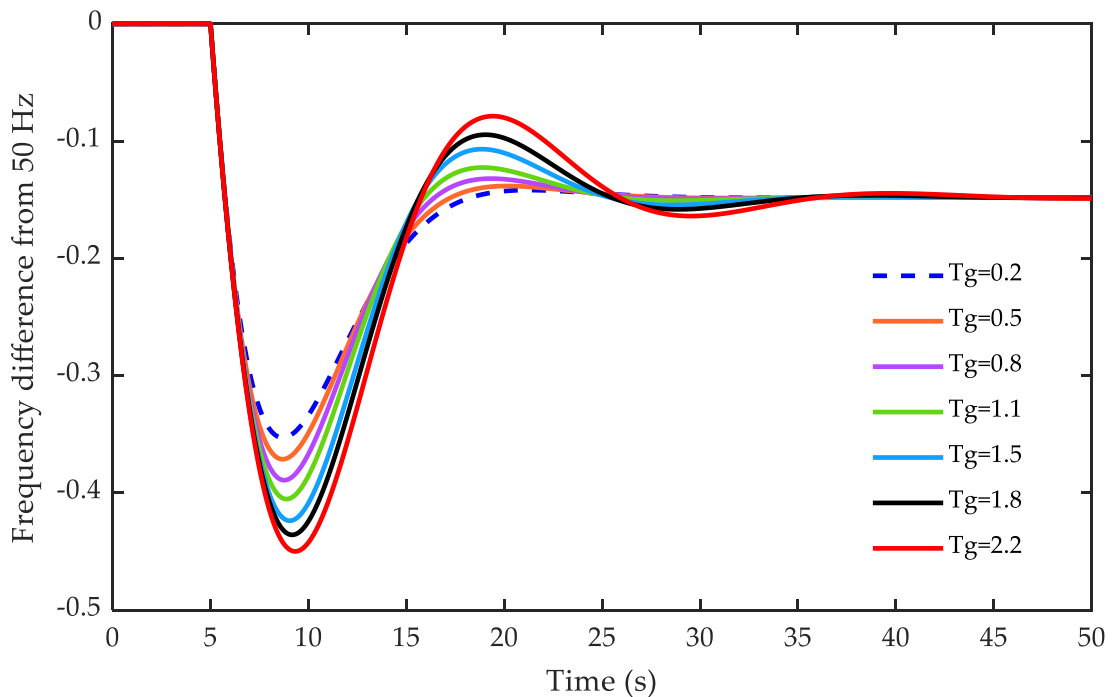


Figure B.1 The primary frequency response of GB system with various values of T_g .

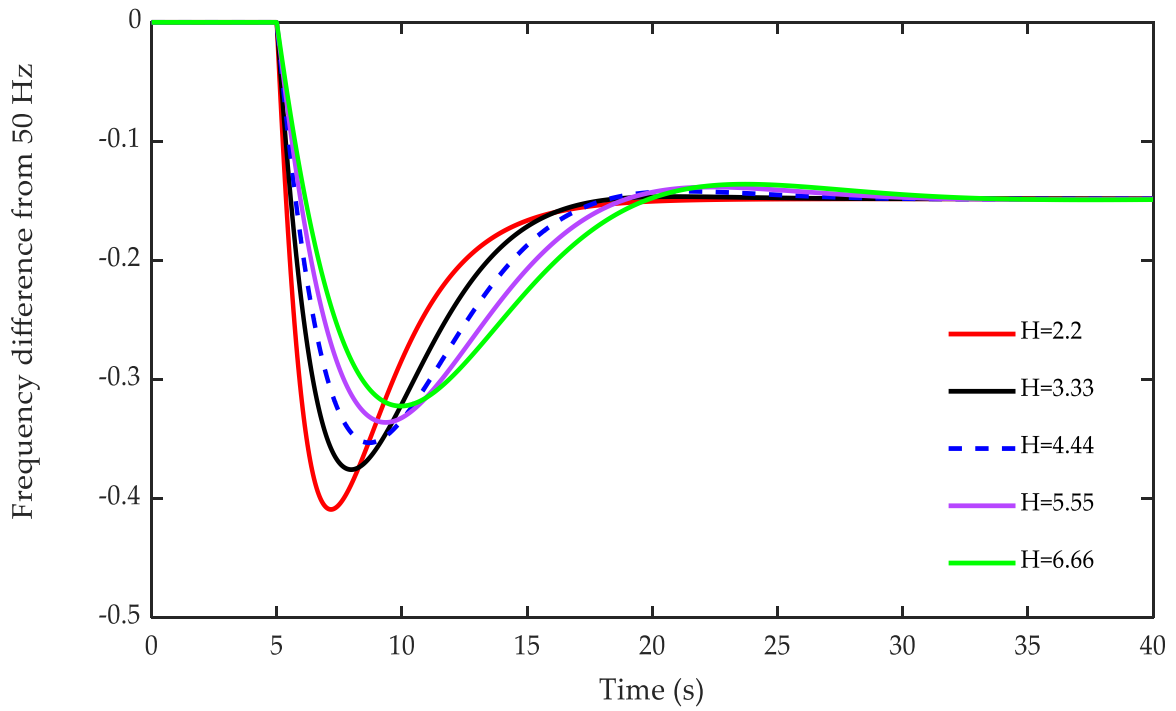


Figure B.2 The primary frequency response of GB system with various values of H.

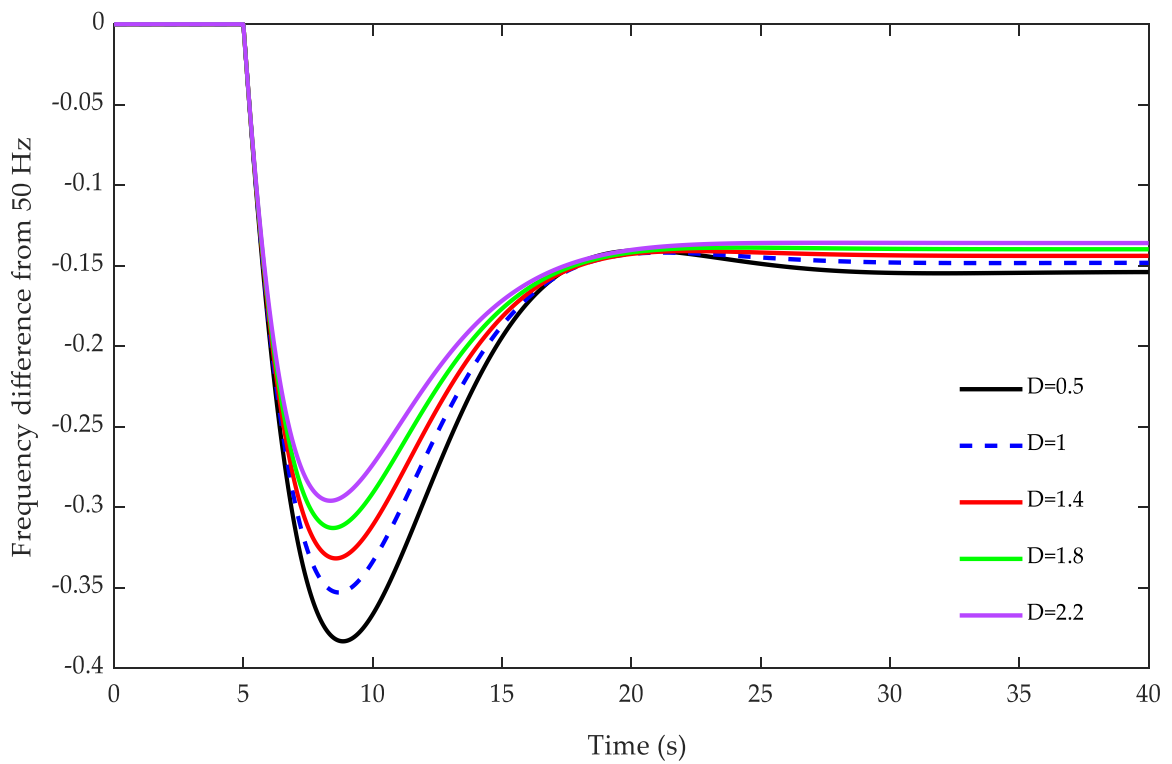


Figure B.3 The primary frequency response of GB system with various values of D.

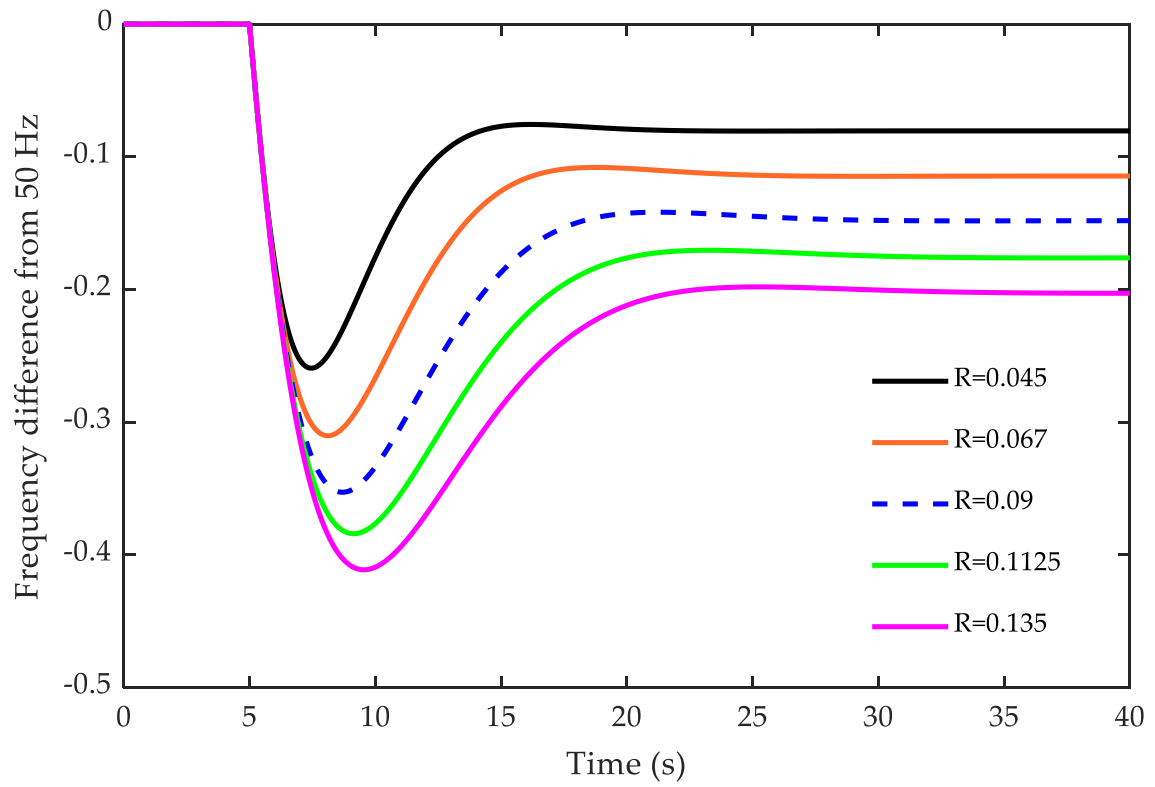


Figure B.4 The primary frequency response of GB system with various values of R.

Appendix C

Table C.1. Dynamic response of the system under different parametric uncertainties scenarios.

Case Number	Controller	Frequency in Area 1			Frequency in Area 2			Tie Line Power Deviation		
		U_{sh} in Hz	O_{sh} in Hz	T_s in s	U_{sh} in Hz	O_{sh} in Hz	T_s in s	U_{sh} in pu	O_{sh} in pu	T_s in s
Case 1	SMC-BA	-0.0613	0.0491	2.5551	-0.0014	0.0094	2.3499	-0.0003	0.00008	2.5182
	Fuzzy PID-TLBO	-0.2180	0.0056	12.213	-0.0326	0	23.914	-0.0067	0	24.501
	PID-LCOA	-0.3758	0.0165	12.408	-0.0669	0	21.545	-0.0146	0	22.428
Case 2	SMC-BA	-0.0885	0.0740	2.6330	-0.0022	0.0016	3.1974	-0.0004	0.0001	2.5101
	Fuzzy PID-TLBO	-0.2234	0.0390	4.0000	-0.0252	0	22.329	-0.0042	0	22.469
	PID-LCOA	-0.4917	0.0491	11.007	-0.0863	0	20.3628	-0.0157	0	21.552
Case 3	SMC-BA	-0.0918	0.0840	2.4372	-0.0035	0.0030	3.5679	-0.0004	0.00014	2.3491
	Fuzzy PID-TLBO	-0.3476	0.0057	5.6151	-0.0640	0	26.840	-0.0097	0.00056	34.459
	PID-LCOA	-0.5240	0.0176	10.730	-0.1133	0.0005	17.187	-0.0180	0.00046	20.744
Case 4	SMC-BA	-0.0747	0.0496	2.3248	-0.0016	0.0005	2.4699	-0.0003	0.00005	2.0371
	Fuzzy PID-TLBO	-0.1890	0.0035	4.9709	-0.0192	0	24.814	-0.0042	0	24.933
	PID-LCOA	-0.4319	0.0155	11.743	-0.0675	0	21.596	-0.0135	0	22.753
Case 5	SMC-BA	-0.0874	0.0788	3.6971	-0.0021	0.0014	3.9541	-0.00043	0.00012	3.0577
	Fuzzy PID-TLBO	-0.2146	0.0403	4.6644	-0.0212	0	23.693	-0.0041	0	23.645
	PID-LCOA	-0.4714	0.0165	11.247	-0.0778	0	20.910	-0.0144	0	22.188
Case 6	SMC-BA	-0.0746	0.0492	2.3229	-0.0016	0.0005	2.4716	-0.00032	0.00005	2.0446
	Fuzzy PID-TLBO	-0.1897	0.0036	4.6915	-0.0221	0	23.011	-0.0042	0	26.826
	PID-LCOA	-0.4450	0.0188	11.133	-0.0798	0	20.904	-0.0150	0	23.725
Case 7	SMC-BA	-0.0875	0.0792	3.7032	-0.0021	0.0015	3.9606	-0.00043	0.00012	3.0666
	Fuzzy PID-TLBO	-0.2152	0.0415	4.6671	-0.0215	0	23.395	-0.0042	0	23.753
	PID-LCOA	-0.4750	0.0175	11.183	-0.0793	0	20.832	-0.0145	0	22.242
Case 8	SMC-BA	-0.1087	0.1316	2.5614	-0.0047	0.0059	5.0311	-0.00067	0.00044	2.8036
	Fuzzy PID-TLBO	-0.4015	0.0520	8.5691	-0.0805	0	24.406	-0.0114	0.00056	32.293
	PID-LCOA	-0.5931	0.0730	9.8592	-0.1435	0.0005	16.687	-0.0210	0.00051	20.342
Case 9	SMC-BA	-0.0835	0.0681	2.5323	-0.0029	0.0018	2.28390	-0.00039	0.0001	2.4348
	Fuzzy PID-TLBO	-0.3161	0.0060	10.054	-0.0555	0	28.4522	-0.01030	0.0005	34.399
	PID-LCOA	-0.4820	0.0165	11.008	-0.0975	0.0004	17.5005	-0.01670	0.0004	20.884
Case 10	SMC-BA	-0.0750	0.0872	2.5095	-0.0029	0.0031	4.58160	-0.00045	0.00024	2.4077
	Fuzzy PID-TLBO	-0.3125	0.0060	12.6461	-0.0476	0	39.4405	-0.01090	0.00135	41.302
	PID-LCOA	-0.4094	0.0124	12.4555	-0.0715	0.0010	20.7551	-0.01590	0.00140	27.769

Values that represent the best performance are indicated in bold.